01 Nov 1973

Local and overall buckling of cold-formed compression members

John T. DeWolf

George Winter

Teoman Peköz

CCFSS LIBRARY DeWolf, J. T., Winter, G.,
22 1 * 220 Pekoz, T. LOCAL AND OVERALL
c2 BUCKLING OF COLD-FORMED
COMPRESSION MEMBERS

DATE	ISSUED TO

Department of Structural Engineering
School of Civil and Environmental Engineering
Cornell University

Report No. 354

LOCAL AND OVERALL BUCKLING OF COLD-FORMED COMPRESSION MEMBERS

by
John T. DeWolf
Research Assistant

George Winter
Teoman Pekoz
Project Directors

A research project sponsored by the
American Iron and Steel Institute

Ithaca, New York November 1973

PREFACE

This report is a modification of a thesis presented to the Faculty of the Graduate School of Cornell University for the degree of Doctor of Philosophy.

The research project covered by this report was sponsored by the American Iron and Steel Institute.

The author wishes to express his thanks and gratitude to Professors George Winter and Teoman Pekoz, Project Directors. Their suggestions, criticism, and guidance have been invaluable.

The cooperation of the Sheet Committees of the American Iron and Steel Institute is gratefully acknowledged.

TABLE OF CONTENTS

ABSTRACT

The objective of this investigation has been to develop information on the interaction between local plate buckling and overall column buckling in cold-formed compression members with a view toward possible improvement of those provisions in the American Iron and Steel Institute Specification for the Design of Cold-Formed Steel Structural Members concerned with column design.

Two types of compression members were tested: two channels connected flange-to-flange to form a box section, and two channels connected back-to-back to form an I-section. For both of these shapes, the stress at which local buckling occurs and the postbuckling strength were varied by varying the width-thickness ratios of the elements, and the overall column buckling strength was varied by varying the slenderness ratio. From a total 37 full scale concentric column tests, the behavior of a wide variety of column shapes subject to local and overall buckling can be deduced.

Two significant findings have resulted from comparison of the test data with the present Specification: (1) Sections made primarily of unstiffened elements (elements with only one edge connected to an adjoining element) with width-thickness ratios up to at least 30 are overly conservative as treated by the Specification. (2) For sections made of stiffened elements (with both edges connected to adjoining elements), as the element width-thickness ratios increase, the Specification gives

increasingly unconservative results for those slenderness ratios which are in the range of interaction between local and overall column buckling.

An analytical approach based on applying rigorous theory to treat the plate behavior, considering both large deflections and plasticity, has been used to study the box sections. The results when compared with the tests are not satisfactory, which is primarily attributable to shortcomings in the analytical treatment when applied to sections with large postbuckling strengths.

A semi-empirical approach has been developed based on treating the plate behavior by using an effective width expression developed by Winter to consider the postbuckling behavior of stiffened elements. The expression has been expanded to also encompass unstiffened elements, and the results are shown to be in good agreement with the tests.

Using this semi-empirical approach, it is shown that: (1) The full postbuckling strength can be utilized not only in sections composed of stiffened elements, but also of unstiffened elements at least with width-thickness ratios up to 30. (2) The stiffness of the section must be reduced in proportion to the loss in ability of the locally buckled plates to resist longitudinal shortening. This approach has proved satisfactory when compared to the test data in this investigation and to that in other investigations reported in the pertinent literature.

Major changes have been suggested to the present Specification, based on findings from the semi-empirical approach and

the test data, which correct the above mentioned shortcomings.

On the basis of the test results and comparisons with the analytical approaches, it has been shown that: (1) The strength of cold-formed columns can be considerably reduced by local plate buckling. (2) Column capacities calculated on the basis of the local plate buckling stress considerably underestimate the actual column strengths, and therefore, the consideration of the postbuckling strength of the plates can yield substantial economies in design. (3) The behavior of columns subject to a combination of plate buckling and overall column buckling can be reasonably accurately predicted analytically.

Chapter 1

INTRODUCTION

1.1 General

Cold-formed sections have widespread use in the building industries. In contrast to hot-rolled sections, they are used where the loads are not large, and thus where light members will suffice, achieving substantial economies. They are also used where requirements on the shape exclude hot-rolled members. In addition, they are more easily fabricated, with a greater variety of shapes possible, and may be formed in small machine shops which are widely available.

Cold-formed sections are formed from flat sheet, either by brake forming or by roll forming. In contrast to hot-rolled members which are subject to residual stresses, they are subject to strain hardening at points of bending, which significantly affects the structural performance. Even more important, while the width-thickness ratios of the component plate elements are limited in hot-rolled sections due to the manufacturing processes, the cold-forming process allows for practically unlimited width-thickness ratios. With large width-thickness ratios, local plate buckling occurs prior to attainment of the maximum strength, which can be significantly decreased. This represents a primary difference between cold-formed and hot-rolled sections.

1.2 Behavior of a Section Subject to Local and Overall Buckling

Provided that a concentrically compressed section is nei-

ther subject to torsional-flexural buckling nor to torsional buckling, and that local plate buckling occurs prior to yield of the material, the behavior as the section is loaded to failure follows one of three patterns, depending on the member's slenderness ratio: (1) local plate buckling, followed by development of postbuckling strength to resist further loading until the compressive strength of the component plates is reached; (2) local plate buckling, followed by failure of the column due to overall, or flexural, buckling; (3) failure due to overall buckling of the column, with no prior local plate buckling. Members with low slenderness ratios behave in the first way, those with moderate slenderness ratios behave in the second way, and those with large slenderness ratios behave in the third way.

When local bifurcation buckling occurs in one or more of the component plates, the plate distorts into a number of waves. The amplitudes of these waves are small when the plate first buckles, and may not even be visible. The load at which the plate first buckles is by no means the maximum load that the plate will carry. The compressive load may be increased further, often to more than two or three times the load at which local buckling first occurs. As the load is increased, the shape of the buckled pattern in the plate may change, and the amplitudes of the waves, or deformations, increase. This range of loading beyond the local buckling load is known as the postbuckling range.

For members subject to local buckling with a moderate

slenderness ratio, the prior local plate buckling lowers the point at which overall buckling, and thus failure, occurs, though as pointed out, the local plate buckling is by no means an indication of impending failure. The postbuckling range, which is often substantial in sections subject to local and overall buckling, may be used to achieve significant economies in design.

1.3 Purpose of the Investigation

The procedure for predicting the ultimate load of a column subject to local buckling in the "Specification for the Design of Cold-Formed Steel Structural Members"[1]* utilizes a form factor to account for local buckling in conjunction with a column formula to account for overall buckling. This procedure was adopted for the first edition of the Specification in 1946 and has remained unchanged through the 1968 edition now in use. It has proved to give satisfactory results for design use, and no significant problems have resulted from its use.

Recent work in the field of the interaction of local and overall buckling, however, has indicated that the procedure may be excessively conservative in some situations and unconservative in others. Uribe and Winter[2] concluded that the Specification method for computing the form factor of sections composed mainly of unstiffened elements, elements stiffened on only one edge parallel to the direction of stress by another element, is often excessively conservative. However, for sections

---

* Superscripts designate entries in the list of references.

composed mainly of stiffened elements, elements stiffened on both edges parallel to the direction of stress by other elements, they found that the method gave good results. Johnson [3] and Wang[4] at Cornell and Graves Smith[5] in England have also indicated that the Specification can lead to conservative results, though their work involved stainless steel and aluminum. Klöppel and Schubert[6] in Germany conducted a series of tests on aluminum box-shaped columns; their results indicate that the Specification method can lead to unconservative results.

The purpose of this investigation has been to study the interaction between local buckling and overall buckling in steel cold-formed sections and to develop information for use in the Specification, either to modify the present approach or to replace it with a new one. This has been done through both experimental investigation and analytical study of columns subject to local and overall buckling.

1.4 Scope of the Investigation

The chapters which follow contain the results of this investigation, i.e. a detailed study of cold-formed columns subject to local and overall buckling.

Chapter 2 contains a brief survey of the pertinent literature, both experimental and analytical. Some of the problems that have prevented a more thorough study of the subject are also mentioned, and a discussion of the possible analytical approaches for treatment of sections subject to local and overall buckling is presented.

The experimental work is presented in Chapter 3. This includes the results of two series of tests, comprising 37 columns. One series involved stiffened elements and another series unstiffened elements. Both series cover the range of column lengths for which local buckling has an effect on the column strength, and they include sections with a variety of width-thickness ratios, so that the local buckling loads and postbuckling strengths are varied.

Chapter 4 contains the basis of the present Specification concerning sections subject to local and overall buckling, with the theory behind the Specification approach. The results of the column tests are compared to the Specification approach, defining the areas in which improvement of the Specification is needed.

An analytical approach based on applying rigorous theory to treat the plate behavior in the sections composed of stiffened elements is given in Chapter 5. The test results are compared with this approach and conclusions are given to explain the considerable variation between the test results and the analytical treatment.

Chapter 6 contains a semi-empirical approach, referred to as the effective width approach, for analyzing columns subject to local and overall buckling. Comparisons of the effective width approach with the tests conducted in this investigation, as well as with tests from other investigations, are given. The analytical treatment is shown to yield reasonably good results. Conclusions are also given which are applicable to the

Specification, and the necessary changes are outlined.

A design approach which is conceptually simple and which follows the approach in the present Specification for the treatment of stiffened sections, with a change in the calculation of the radius of gyration, is given in Chapter 7. The design approach considers both stiffened and unstiffened sections.

The final chapter, Chapter 8, presents the general conclusions of this investigation. This writer has presented an approach for design that can be used to obtain fairly accurate ultimate strength predictions for concentrically compressed members subject to local and overall buckling and has shown how it might be applied to design specifications.

Chapter 2

LITERATURE SURVEY

2.1 General

The interaction of local plate buckling with overall column buckling is complex and is difficult to treat analytically. However, it is a common phenomenon in cold-formed, thin-walled structures, and it is thus surprising that little research has been devoted to the study of it.

Many researchers have investigated local plate buckling and a number have studied the postbuckling range. Overall column buckling has been extensively investigated. However, only a small number of researchers have studied the interaction of these two phenomena. Part of the problem has been the lack of information concerning the postbuckling behavior of plates, particularly the behavior in the later stages of postbuckling, where relatively large plate deflections interact with nonlinear material behavior.

This investigation is concerned with concentrically compressed members which are not subject to torsional-flexural buckling or torsional buckling, and thus the pertinent literature is considerably limited since many researchers have devoted themselves to eccentrically loaded columns and shapes subject to torsional-flexural buckling such as single channels. Also, this investigation is concerned primarily with carbon and low alloy steels, either sharp yielding or gradual yielding with a proportional limit not lower than about 70 percent of

the specified minimum yield point, as is implied in the American Iron and Steel Institute Specification[1]. However, some of the work on the interaction effects with aluminum and stainless steel is pertinent and mentioned in this survey.

Before discussing the literature pertaining to the interaction of local buckling and overall column buckling, column buckling and local buckling are discussed separately. Research concerning the analytical treatment of interaction is generally based on the two phenomena, each considered separately and then combined to obtain the interaction analytical approach, and it is thus necessary to present some of the background for each separately. Therefore, a few of the references with general backgrounds of overall column buckling and local buckling and the more significant conclusions are presented; this is brief and by no means complete.

Following the discussions of column buckling and local buckling separately, research pertaining to the interaction is given more completely. This includes both experimental and analytical research.

2.2 Column Buckling

The evolution of a column formula to predict the maximum compressive load on columns in both the elastic and inelastic ranges is presented by Johnston[7]. A more thorough coverage of the theory along with the evolution of the column formula is given by Timoshenko and Gere[8].

The tangent-modulus formula has been shown to represent the bifurcation stress for an initially straight, concentrically

compressed column in both the elastic and inelastic ranges; for the elastic range, the formula is equivalent to Euler's formula. This was first presented and explained by Shanley[9] and further developed by Duberg and Wilder[10]. Once bifurcation occurs, some additional postbuckling strength is available, though this is quite small for steel columns[11]. The tangent-modulus stress is thus used to determine the maximum stress for a column in present design specifications. It has remained in use for a couple of decades now and has proved to represent well the failure of columns by overall, or flexural, buckling.

2.3 Local Buckling

The literature pertaining to local buckling is vast, both concerning the prediction when local plate buckling occurs and concerning the behavior of plates after the occurrence of local plate buckling, that is in the range of postbuckling behavior. It is well known that once a plate buckles, added strength exists; it is in this postbuckling range that failure of the column subject to local and overall buckling occurs. This discussion is limited to the postbuckling behavior of plates.

As mentioned in Section 2.1, the behavior of a plate in the postbuckling range is rather complex, particularly in the later postbuckling stages where large deflections interact with nonlinear material behavior. As a result of these complications, a large number of researchers have resorted to empirical means to treat the postbuckling behavior. This discussion refers to two general approaches for considering the postbuckling behavior, the rigorous approach, based on theory, and the em-

pirical approach, based on using test results to account for some of the variables.

Koiter[12] presents a good discussion of postbuckling behavior, including the problems one is faced with in extending a theoretical analysis into the later stages of postbuckling, mainly in the area of inelasticity. He also includes a review of some of the work done by researchers in applying theoretical approaches to the problem, though all of these were concerned with the elastic case only. Bulson[13] reviews the literature concerning the postbuckling behavior of plates, both by rigorous theoretical approaches and by empirical approaches. He also presents some of the results from various investigations.

Very few researchers have included plasticity, which is an important factor in the later stages of postbuckling, partly due to uncertainties in plastic theories and partly due to the complexity involved in applying plastic analysis. However, a few researchers have considered plasticity in the postbuckling range; among these are Stowell[14], Mayers and Budiansky[15], Graves Smith[5], and Qureshi[16].

Empirical approaches usually involve some type of effective width approach. This involves replacing the actual plate with a hypothetical width that is related to the total compressive load on the plate. This is discussed in more detail in the following chapters. In empirical approaches or semi-empirical approaches, the effective width is based on experimental work rather than explicitly on theoretical considerations. Jombock and Clark[17] present a variety of effective width

formulas that have been proposed and compare them. Koiter[12], Timoshenko and Gere[8], Winter[18], and Wang[4] have general discussions of the effective width approach as applied to post-buckling behavior. These references also contain good bibliographies listing much of the research that has been done.

More information pertaining to the rigorous theoretical approach by Graves Smith is given in Chapter 5. The effective width concept with its applications to cold-formed sections is discussed in Chapters 5 and 6.

2.4 Interaction of Local and Overall Buckling

With all of the problems and shortage of research pertaining to the behavior of plates in the postbuckling range, it is not surprising that the amount of research conducted on the interaction of local buckling and overall buckling is limited. A brief survey of references that apply to concentrically compressed columns which are not subject to torsional-flexural buckling or torsional buckling and which are subject to local buckling is given here. Both analytical and experimental work are reviewed.

Bijlaard and Fisher[19] have studied the interaction of local plate buckling and overall column buckling for a column in which the theoretical local buckling stress is equal to the theoretical overall, or flexural, buckling stress. They wanted to find out if buckling in such a column occurred at a value below either of these two theoretical values considered separately. Both theoretical and experimental results are given. The theoretical part is based on the small deflection theory

and does not include the postbuckling range. On the basis of the theoretical investigation and test results for square aluminum tubes, it is concluded that the reduction in the stress at which buckling occurs under the above conditions is negligible for all but sections in which torsional instability is an important factor.

In another paper, Bijlaard and Fisher[20] have presented the results of a study on the postbuckling strength of columns subject to local and overall buckling. They include both theoretical and analytical work. The theoretical part is based on purely elastic conditions and is thus limited to the higher slenderness ratio portion of the interaction range where the material does not become plastic before failure. Essentially they propose breaking the column curve, column load vs. slenderness ratio, into three parts. The part with the highest slenderness ratios is governed by Euler's buckling stress; the part with moderate slenderness ratios, the part in which elastic interaction occurs, is represented by an equation they give; the part with the low slenderness ratios, in which the behavior of the plate elements become plastic, is represented by a Johnson parabola, with the maximum strength equivalent to the crushing strength of the section. This is in contrast to the American Iron and Steel Institute Specification which uses a Johnson parabola for the range of low and moderate slenderness ratios of steel members. According to the authors, based on their experimental work on aluminum 'H'-shaped sections and square tubes, their approach gives better results than the

Specification approach. This is not surprising since the Specification is written for steel but not for aluminum members.

Scidenfaden[21], also discussed in some detail by Pflugger[22], has studied channel sections subject to local and overall buckling. His work is based on purely elastic behavior, and includes torsional instability in addition to local and overall buckling. He came to the conclusion that preceding local buckling reduces the column buckling load only by a negligible amount, based on the sections studied. Pflugger[22] conducted tests with aluminum angle sections to check this theory and did not obtain good comparisons. Pfugger claims that the differences are due to inaccuracies in the shape of the specimens and not to the fact that local buckling can significantly reduce the column strength in the region in which local and overall buckling interact.

Jombock and Clark[17] have proposed an approach to consider the effect of local buckling on overall buckling. They use an effective width approach to consider the postbuckling behavior of the plate elements and from this obtain a stiffness for the whole column. This is then used in the Euler column formula to obtain the failure load for the column. The results of this approach are compared with tests of square aluminum tubular stub columns with reasonable results. They have not compared their approach with test results for slenderness ratios in the range of interaction.

One of the more significant contributions to the study of the interaction of local and overall buckling has been made by

Graves Smith[5], also summarized in two other papers[23,24]. He has developed a theoretical approach for rectangular tubes that considers both the large deflections that occur in the plate elements in the postbuckling range and plasticity of the plate elements. The approach uses the large deflection equations of von Kármán and the Rayleigh-Ritz method to define the behavior of the plate elements. An experimental investigation with square aluminum tubes was also conducted and gave good results when compared with his theoretical approach. This is discussed more fully in Chapter 5 where an approach modified from his is used to study some of the sections in this investigation.

Bulson[25] gives an empirical equation to account for the interaction of local and overall buckling, and gives references to a large number of tests on aluminum sections to show the validity of this equation. He also presents an elastic theory to cover the region of transition from local to overall column buckling. It is rather limited since the wavelengths of the local plate buckles are considered equal to the wavelength of the overall column once it has buckled; this is the case only for very short columns.

Uribe[2,26] at Cornell has studied the effect of cold-forming on thin-walled steel columns subject to local and overall buckling. The work reported is both experimental and analytical, and involves columns made of two types of plate elements, those stiffened on one side by another plate element and free on the other side, and those stiffened on both sides.

This is significant in that the results can be applied to a more general range of columns than the results of previous investigations, which have been limited to one column shape. Uribe's columns did not have a very large postbuckling range, that is, local buckling did not occur much before failure and thus did not always have a very great effect on the failure of the column in the range of interaction. He treats the columns analytically by using an effective width approach to account for the local buckling and applying this to the tangent-modulus equation to account for overall buckling of the column. This approach is discussed in more detail in Chapter 6.

An experimental investigation into the interaction of local plate buckling with overall column buckling is presented by Skaloud and Zörnerová[28]. They decided to investigate the interaction experimentally because of the lack of a suitable plastic deflection theory. They give a detailed description of the behavior until failure of steel tubular columns made of two hat sections connected along the lips. They also give an empirical method to determine the ultimate strength of the columns tested which is based on two coefficients determined from the stub column tests. Reference is also given in this paper to the previous work done by Skaloud relating to the interaction of local and overall buckling and which was used as a basis for some of the work in the present paper.

Klöppel and Schubert[6], based on the work done by Klöppel, Schmied, and Schubert[29,30], present an approach to calculate the carrying capacity of thin-walled box sections loaded

with either a concentric or eccentric load. They have studied the plate behavior in the postbuckling range by obtaining solutions to the von Kármán large deflection equations. Their work does not include inelastic behavior as Graves Smith's work does. They use these results to obtain the theoretical effective widths in plate elements, rather than effective widths based on tests. In computing the stress at which overall buckling occurs, they reduce the column stiffness using the effective widths. They say that reducing the stress only, as is done in the American Iron and Steel Institute Specification, is not correct and leads to allowable stresses that are too high.

Deliege, Baar, and Hick[31] have studied closed tubes made of two hat-shaped sections. Their investigation has included a comparison of a design method by Massonnet and one by Winter, on which the present Specification is based. They also give the results of a fairly extensive series of tests of steel columns made of two hat-shaped sections. The results of their comparison of the two design methods indicate little difference between them, with Massonnet's method giving slightly higher results. The tests indicate that Winter's method is either on the conservative side or only very slightly on the unconservative side, though the longest columns tested had slenderness ratios of only 100. It is obvious from the tests that the range of interaction extends to slenderness ratios well in excess of 100 and that they have therefore not covered the entire range of interaction.

A subsequent report by Hick[32] involves the study of rec-

tangular tubular sections subject to eccentric loading and also contains a comparison of the work in the preceding paper with the work of Klöppel[6]. One of the major differences between these two approaches is that while Klöppel considers only part of the section as effective in resisting overall buckling, the work reported in the preceding paper considers the gross section effective in resisting overall buckling. The results of this comparison show that while Klöppel's approach gives failure loads on rectangular tubular columns subject to interaction higher than experimental values with a maximum difference of 7 percent, the work reported in the preceding paper gives failure loads always lower than experimental values with a maximum difference of 15 percent. The second part of this paper deals with applying the theory to design specifications and considers analytically a number of different sections.

2.5 Summary and Conclusions

(1) The tangent-mosulus formula gives a very good estimation of the failure stress of a column that fails by overall, or flexural, buckling.

(2) The postbuckling behavior of plates is complex, particularly in the later stages of postbuckling, and the theoretical treatment of the postbuckling behavior has not been extensively developed.

(3) Semi-theoretical approaches for treating the postbuckling behavior of plates, usually based on determining effective widths, have been rather extensively investigated, and some of the approaches produce good results for the prediction

of the plate behavior throughout the postbuckling range.

(4) Because of the complexities in the behavior of plates in the postbuckling range, little work has been applied to the theoretical treatment of columns in the range of interaction of local and overall buckling. The work of Graves Smith is thought to be the most complete, rigorous theoretical approach, and thus the best starting point to extend the theoretical treatment to other column shapes.

(5) The semi-theoretical treatments of columns subject to the interaction of local and overall buckling are limited and most have not covered varied column shapes, each with a broad range of slenderness ratios in order to very the overall buckling strength and with a broad range of plate dimensions in order to vary the ratio of the loading range before local buckling to the postbuckling range. However, Uribe has worked along these lines, and his work is thought to be the best starting point for a semi-theoretical investigation for columns of larger postbuckling ranges than considered by Uribe.

Chapter 3

EXPERIMENTAL INVESTIGATION

3.1 General

This chapter includes the preparation, test procedure, and results of two series of 37 full-scale column tests. The two series, one involving tubular sections and one involving 'H' shaped sections, are designed so that the ratio of the strength at local buckling to the postbuckling strength is varied systematically. In this way, a broad range of columns subject to the interaction of local and overall buckling are studied, with the effects of the interaction clearly illustrated.

3.2 Material

The material used for all test specimens came from twelve 16 gage sheets of carbon steel of structural quality. One tensile coupon from each sheet was tested and no significant differences were found for any of the sheets.

The initial portion of the stress-strain curve for the sheets in shown in Fig. 3.1. This is a measured curve for one of the specimens which best represents the average behavior for the 12 coupons. The average tensile yield stress is 41.9 ksi, with extremes of 40.1 ksi and 43.5 ksi. The average tensile ultimate stress is 53.8 ksi, with extremes of 51.7 ksi and 55.0 ksi. Strain hardening occurs at an average strain of 0.014 in/in, and the average percentage of elongation of a two-inch gauge length at rupture is 37 percent.

3.3 Choice of Sections

Thin-walled columns are usually made of two types of plate elements. Stiffened elements are flat elements with both edges parallel to the direction of stress stiffened by a web, flange or other stiffener that meets certain stiffness requirements. Unstiffened elements are flat elements with only one edge stiffened and the other edge free.

The only other type of flat element is one with one edge stiffened by a flange or web and the other edge stiffened by a small stiffener that does not meet minimum stiffness requirements, that is, a small lip of low width to thickness ratio. Minimum stiffness requirements for stiffeners are discussed in the Commentary to the American Iron and Steel Institute Specification[18]. The Specification[1] does not allow stiffeners that do not meet certain requirements, and in practice such stiffeners would either be avoided or the stiffener would not be relied on to furnish any stiffness to the plate element. Such an element stiffened by a stiffener that does not meet the requirements would be conservatively considered as an unstiffened element.

Only the first two types of elements mentioned, stiffened and unstiffened elements, are of interest in this investigation. Two different sections have been chosen in order to study each of these element types separately.

The first section, which is referred to as the stiffened section and is designated with a 'S', consists entirely of stiffened elements. It is made of two channels connected at

the flanges to form a closed tube as shown in Fig. 3.2(a), with dimensions and properties given in Table 3.1(a). The axis about which overall buckling occurs is the weak axis, or horizontal axis in the figure. The two sides parallel to the weak axis are referred to as the flanges and are designed so that local buckling occurs prior to material yielding. The width-thickness ratios of these flanges are chosen so that the American Iron and Steel Institute Specification Q-values, as defined in Chapter 4, cover the range of approximately 0.5 to 0.9. This range is felt to encompass those sections of practical application which are made of stiffened elements and which are subject to local buckling. The two sides perpendicular to the weak axis are referred to as the webs and are designed so that local buckling does not occur prior to column failure. Four sections with varying flange widths, and therefore varying load levels at which local buckling occurs, were fabricated.

The second section, which is referred to as the unstiffened section and is designated with a 'U', consists of two channels connected back-to-back along the webs to form an 'H' shaped section as shown in Fig. 3.2(b), with dimensions and properties given in Table 3.1(b). The axis about which overall buckling occurs is the weak axis, or horizontal axis in the figure. The unstiffened flanges are designed so local buckling occurs prior to material yielding, based on the American Iron and Steel Institute Specification. The width-thickness ratios of these flanges are chosen so that the Specification Q-values, as defined in Chapter 4, cover the range of approximately 0.5

to 0.9. As for stiffened sections, this range is thought to cover sections which are of practical application and which are made of elements which are subject to local buckling. The web, or horizontal element in the figure, is designed so that local buckling does not occur prior to column failure. Four sections with varying flange widths, and therefore varying load levels at which local buckling occurs, were fabricated.

Both sections are bisymmetrical and not subject to torsional-flexural buckling. Column lengths have been chosen to cover the region in which the American Iron and Steel Institute Specification indicates that local buckling affects the overall column strength. Stub column lengths were based on the recommendations in the Appendix on Compression Testing in the Specification. In addition to the stub columns, three preliminary lengths were chosen. The first had a slenderness ratio so that the elastic buckling load as determined, using Euler's equation, equaled the ultimate load for a stub column determined from the American Iron and Steel Institute Specification. The second had a column length of from 0.5 to 0.7 times the length of the first column. The third column had a length greater than those above, but smaller than the length for which the Euler buckling stress equals the local buckling stress. Some modifications in these lengths were made as necessary during the experimental investigation. The lengths for the columns tested are given in Tables 3.2 and 3.3

3.4 Fabrication

3.4.1 Fabrication of Channel Sections

The sections were cut and press brake formed; a sharp punch was used so that the inside radius of the corners was extremely small, considered as negligible in all subsequent calculations. The quality of the work was excellent. The specified dimensions were met with no significant variations.

Flatness of the plate elements was randomly checked and the out-of-plane distortions within the plane elements were small. They were less than a tenth of the plate thickness and less than a tenth of one percent of the element width for the stiffened elements subject to local buckling. For the unstiffened elements, the out-of-plane distortions were less than a tenth of the plate thickness and less than half of one percent of the element width. For the stiffened and unstiffened elements, the influence of the out-of-plane distortions is discussed in Section 3.7. Also, the influence is discussed in Chapter 5 for the unstiffened elements.

3.4.2 Fabrication of Column Specimens from the Channel Sections

Each specimen was made from two channel sections cut from the same sheet of steel. The channels were cut slightly longer than specified for the final test specimen. Holes were drilled in the channel flanges for the stiffened sections as shown in Fig. 3.3(a) and in the channel webs for the unstiffened sections as shown in Fig. 3.3(b). The spacing of the holes is discussed in Section 3.5. The surfaces to be joined were then cleaned with a solvent. An epoxy compound, Epon 907, was then

applied, 0.0014 inch diameter wire spacers were placed at approximately a four inch spacing to prevent all of the epoxy from being squeezed out, and the sections were then connected together with screws or rivets. The screws or rivets were used to hold the channels together during the drying period and to give further connection strength during the testing if necessary. When the specimens had dried, the ends were ground to assure uniform bearing against the testing apparatus.

3.5 Method of Connection

All stub columns were screwed together after the epoxy was applied. Six screws were used for each channel flange for the stiffened sections, following the pattern shown in Fig. 3.3(a); two screws were placed at each end and two at mid-height. Five screws were used to connect the channel webs for the unstiffened sections, following the pattern shown in Fig. 3.3(b); two screws were placed at each end and one at mid-height in the middle of the web.

No failure was observed in the epoxy during the stub column tests, even at failure. The strain on the column was increased following failure, and it was during this portion of the test that the epoxy in the region between the screws failed. This was accompanied by a cracking noise with a definite separation of the joints.

Following the stub column tests, columns S-1 - 69.1, S-2 - 102.0, S-3 - 109.8 and S-4 - 116.0 (the third figure is the slenderness ratio) were fabricated. Screws at approximately nine inch spacings were used in the connections, with epoxy and

spacers as specified in the previous section. Column S-3 was then tested and the ultimate load was below that predicted with the American Iron and Steel Institute Specification approach excluding safety factors.

It thus appeared, in view of the conservative results shown in Uribe's work[2], that either the test apparatus was not satisfactory or the connection between the channels was not adequate. Since the load was concentric, as determined from the strain gages (this is discussed in the next section), it was thought that the epoxy in the region between the screws had failed, causing the two channels to act separately and resulting in a reduced flexural buckling load.

Another column was then made up identical to the first, but with screws at a two inch spacing. The ultimate load was nearly identical to the first. Since the channel flanges were two inches wide, it was thought that failure in the epoxy between the screws may have occurred again. A one inch spacing was then chosen for another specimen of identical dimensions.

Since the application of screws is time consuming and the drying time for the epoxy is not sufficient for the number of screws necessary for a one inch spacing, it was decided to use cold-rivets, which were put in with an air gun. The third column behaved as the previous two, with a nearly identical ultimate load. It was then assumed that the epoxy was not failing prior to attainment of ultimate load, but that the ultimate load indicated by the American Iron and Steel Institute Specification was on the unconservative side for this particular

column.

For all further tests, cold-rivets were used at a spacing of one inch, with the exception of the longest columns which had rivets spaced up to two inches. No epoxy failures were observed to have occurred. It is interesting to note that all three of the above columns had ultimate loads within less than four percent of the mean.

3.6 Testing of Column Specimens

3.6.1 General

Hydraulic testing machines were used. The strain was increased slowly in increments and then varied to maintain the desired load while dial and strain gage readings were taken.

3.6.2 Stub Columns

The test set-up for the stub columns was based on the Stub Column Test Procedure in the Column Research Council Guide[7]. The ground ends of the stub columns were set against ground bearing plates. A thin layer of hydrostone was spread between the bearing plates and the testing machine table and heads as shown in Fig. 3.4. For stub columns U-3, S-1 and S-2, hydrostone was used only between the table and bottom ground plate since the head of the testing machine was able to rotate. It was decided after these tests that it would be better to use hydrostone between the top ground plate and head, and not rely on the rotation potential of the head. Uniform strain distributions on the stub column cross-sections were obtained, indicating that the load was concentric.

SR-4 strain gages, one inch long, were placed at the mid-height of the stub columns as shown in Fig. 3.2. On the cross-section, gages were located on both sides of the plate elements at the points of maximum out-of-plane distortions. These gages were used to obtain an indication of local buckling. More important, the strain gages were the best means for determining if the load applied on the stub column was concentric during the beginning of the loading.

Dial gages were also used to measure head movement for overall vertical shortening of the stub columns. For the first test, an unstiffened section, two dial gages were placed, one at the center of each flange as near as possible to the specimen. For all other stub column tests, four dial gages were placed, one at each corner of the specimen, to measure the vertical shortening. It was hoped that an overall stress-strain curve for the section could be obtained with these dial gages. However, they gave varied results for the columns; the overall modulus of elasticity varied from 19,800 ksi to 34,800 ksi. This variation existed partially because of poor accuracy since the range of shortening was small in relation to the dial divisions and partially because the seating of the stub columns against the base plates during the initial stages of loading was not always perfect, due to variances in the grinding of the stub column ends.

The load was applied in two to three kip increments, with ultimate loads of over twenty kips for all of the stub columns. The stub columns were first loaded to about twenty percent of

the predicted ultimate load, so that local buckling and resulting permanent deformations in the plate elements did not occur, and then unloaded to one kip. This process was repeated as necessary, until it was ascertained that the load was concentric. If the load was not concentric, the hydrostone was replaced.

3.6.3 Longer Columns

All of the remaining columns were tested with pinned ends. This was achieved by adapting end fixtures developed at Cornell for previous pinned-end column tests[33]. The columns, after grinding the ends, were welded to base plates and set against ground plates in the end fixtures. Figure 3.5 contains sections drawn through the end fixtures. Figure 3.6 is a picture of one of the longer columns in the test set-up and Fig. 3.7 is a closeup of the lower end fixture with the column set in it.

The end fixtures allowed for all adjustments necessary for alignment of the columns to obtain a concentric load. The columns were held in an end box by two bolts on each of the four sides. These bolts could be adjusted as necessary to move the ends of the columns horizontally in either direction. The boxes could also be rotated about an axis perpendicular to the knife edges by adjusting the lower sets of bolts shown in Fig. 3.5(a). This adjustment ensured that a good fit existed between the column and end boxes. With both of these adjustments, concentric loads were obtained, with three exceptions discussed in the end of this section.

SR-4 strain gages, one inch long, were placed at the mid-

height of all columns at the same locations on the cross-sections as for the stub columns. The locations are shown in Figs. 3.2(a) and 3.2(b). These were used to obtain an approximate stress distribution across the mid-height cross-section and, more important, to determine when local buckling occurred. It was not necessary to have the gages located at the point of maximum amplitude.

Dial gages were also used to measure overall lateral deflections of the column. The location of the dial gages is shown in Fig. 3.8 for the stiffened sections and in Fig. 3.9 for the unstiffened sections. One gage was also used at each end fixture to check for any movement of the fixture with respect to the testing machine as shown.

In addition to the above, the out-of-plane distortions of the flanges were measured for the unstiffened sections. As is discussed in Chapter 4, the magnitude of the out-of-plane distortions is one basis for determining the maximum allowable or service stress in unstiffened elements. For member U-2 - 85.6, the magnitudes of the out-of-plane distortions were determined by measuring the distance from the outer edge of one flange to the outer edge of the opposite flange, parallel to the web. This was done at points at half inch spacings as close to the central area of the column as possible. Measurements were not possible at the very center because the strain gages were in the way.

For the other unstiffened columns, excepting the stub columns, the out-of-plane distortions were measured with the de-

vice shown in Fig. 3.10. This was slid along the edge of the flange to the location that gave the maximum reading, which was then considered as the maximum amplitude in the buckle.

Two problems existed with this device. One was that the strain gages at the middle interfered so that it was not possible to slide the device, or to slide it more than an inch or two. Nevertheless, it gave an indication of when out-of-plane distortions started to become noticeable and what their magnitudes were. The results are discussed in the next section.

The columns were loaded and unloaded one or more times to approximately twenty percent of the expected ultimate load, depending on when local buckling was expected. Adjustments in the end fixtures were made during these initial load applications to obtain a concentric load. For the first test, S-2 - 102.0, strain readings were taken for all of the strain gages, and the increments were then checked to see whether they were all of equal magnitude as necessary to assure concentric loading. At first the load was found to be concentric, but when further load was applied, some eccentricity started to become noticeable. As in previous column tests at Cornell, it was determined that the strain gages were not the best means of determining whether the column loading was concentric, especially for the longest columns. The distribution of the strain at the midpoint of the column was not necessarily an indication of the distribution along the entire column length, and therefore the distribution could not be used effectively as a means of determining whether the load was concentric.

For all of the columns following S-2 - 102.0, the deflections as read by the dial gages were used to check if the load was concentric during the initial loadings. This was found satisfactory for most of the columns, with the exception of some of the shorter ones which are discussed in the next paragraph. The dial gages at the center were read for both directions so any bending, and thus eccentricity in the loading, would be noticeable about either axis, and the dial gages at the top and bottom were also checked.

For a few of the shorter columns, the dial gages were not a good indication of bending due to a very small range of overall lateral deflection. The strain increments were also taken for these columns, and using these jointly with the dial gage readings, a good indication of whether the load was concentric or not was obtained. In spite of this, bending, if any, did not always become clear until the final stages of the loading. At this point it was not thought appropriate to stop and unload since permanent deformations might have occurred in the flanges due to prior local buckling.

Nevertheless, the results of most tests indicated that the load was concentric. The columns which did not have concentric loads were U-1 - 62.1, U-3 - 50.1 and U-4 - 71.0. In these, bending occurred from the start of loading, indicating either imperfections in the column or eccentric loading. Since in some tests imperfections in the seating of the column against the base plate in the end fixtures occurred, it was not possible to ascertain until the later stages whether this or bending

was the cause of the lateral deflections. If seating imperfections were the cause, the problem was corrected after a few load increments while if bending was occurring, the lateral deflections continued to increase through failure. These three columns with eccentric loading are therefore excluded from consideration in the following discussion and the results are not given in any of the figures containing test results.

For a few of the columns, some bending about the strong axis was noticed; this was in the earlier stages of loading only, and stopped after a couple of load increments. This was most likely due to lack of fit of column in the test apparatus, though adjustments for this were attempted. Since the problem corrected itself before the later stages of loading, it is not felt that it is of any significance.

3.7 Test Results

A picture of two of the shorter columns tested in the pinned-end apparatus is given in Fig. 3.11. The local buckles as well as the overall buckling of the columns are clearly visible in both the unstiffened column and the stiffened column.

The ultimate loads and effective lengths are given for the stiffened sections in Table 3.2 and for the unstiffened sections in Table 3.3. The stub columns are those with the shortest lengths.

The column lengths shown in Tables 3.2 and 3.3 have been modified for both the stub columns and the longer columns to put them in terms of pinned-end columns. The stub columns were tested in a fix-end apparatus, with no end rotation allowed.

The actual length of the stub columns was multiplied by 0.65, as recommended in the American Iron and Steel Institute Commentary[20] to get a reasonable value for the effective column length for determining the slenderness ratio. For the stub columns, this is sufficient for locating the test point in the column curves used in subsequent chapters.

The length of the longer columns, those tested in the pinned-end apparatus, also needed modification since the end fixtures increased the actual column length. This was accomplished using a procedure given by Graves Smith[5]. The end fixtures were assumed infinitely stiff and the shape of the buckled curve was assumed as a sine curve. It was found that little difference exists between the total length between fixtures, including the length of the box holding the column, and the modified column length, and for all practical purposes the total length between fixtures could have been used.

Differences in the type of failure between the two types of columns, stiffened and unstiffened, were noticed. The stiffened columns started to deflect laterally at about four-fifths of the ultimate load and the deflection continued to increase with increasing load until failure. The unstiffened columns, however, remained practically straight until failure and then failed quite suddenly. While the stiffened columns gave some indication of impending failure during the testing, the unstiffened columns gave none.

The strain gages placed opposite each other on both sides of the plate elements subject to local buckling gave a good in-

dication of the effects of initial imperfections in the plate elements. Initial imperfections would cause differences in the slope in the curve of load vs. strain for the two gages, since the initial imperfections would cause bending in the plate element from the beginning of loading. These differences were small and usually not noticeable, indicating that the behavior of the sections was not significantly affected by imperfections in the plate elements.

The results of the out-of-plane distortion measurements for the unstiffened sections show that for all columns tested, except the stub columns where these measurements were not taken, the amount of out-of-plane distortions was negligible up to the last load increment before failure. The flanges were not observed to show any noticeable out-of-plane distortions from their initial position, more than a few thousandths of an inch, until the last load increment had begun, and often not until failure. This is further indication that the initial imperfections were not significant; otherwise, out-of-plane distortions would have been noticeable much earlier in the loading stages.

Results of the column tests are plotted in column curves, showing average stress vs. slenderness ratio, in the following chapters. The stress used is the average stress, that is, the ultimate load divided by the full area of the column cross-section. The slenderness ratio is based on an effective length factor of 1.0, for perfectly pinned-ends. This is reasonable for the test apparatus.

Results of the determination of when local buckling oc-

curred in the test specimens are given in Chapter 6.

3.8 Conclusions

1) The test columns were accurately fabricated, with negligibly small imperfections.

2) The test apparatus for the stub columns with fixed-ends functioned so that for all practical purposes, concentric loading was maintained.

3) The test apparatus for the longer columns with pinned-ends also functioned so that effectively concentric loading was maintained for practically all columns. Where concentric loading was not maintained, data collected during the test was sufficient to indicate that the load was not concentric.

4) The ultimate loads obtained from the tests which were concentric are felt to be reliable. This is substantiated in the case of column S-3 where all three columns of identical lengths, but with different connector spacings, failed at nearly the same load. It is also demonstrated for column section U-2 where two identical stub columns had nearly identical failure loads. Also, when all of the test results for each type of column are compared with each other and when the results for different types of columns are compared, the patterns are consistent with no striking variations, further indicating reliability. This is seen more clearly in the column curves in the following chapters where the test results are compared with various analytical approaches.

5) Out-of-plane distortions for the unstiffened elements were negligible until the last increment of loading, indicating

that local deformations in the plate elements are not significant for the sections tested.

Chapter 4

AMERICAN IRON AND STEEL INSTITUTE SPECIFICATION APPROACH AND COMPARISON WITH TESTS

4.1 General

A brief background of the American Iron and Steel Institute Specification[1], referred to in this chapter as the AISI Specification, is given. This is followed with a comparison of the test results with the predicted ultimate loads from the AISI Specification. Safety factors are not of interest here and will not be discussed or included in the formulas from the AISI Specification.

The discussion that follows in Section 4.2 is divided into two parts: overall or flexural buckling of the column and the influence of local buckling on the overall buckling.

4.2 Background of the AISI Specification

4.2.1 Flexural Buckling

The flexural buckling stress at failure for a perfect column not subject to torsional-flexural buckling is based on the tangent-modulus equation which gives the stress at failure as:

$$\sigma = \frac{\pi^2 E_t}{(\frac{KL}{r})^2} \qquad 4\text{-}1$$

where E_t is the tangent-modulus of the material, K is the effective length factor for the column, L is the column length, and r is the radius of gyration of the column. If the slenderness ratio, $\frac{KL}{r}$, is large enough, E_t is equal to the modulus of elasticity, E, of the material, and Eq. 4-1 is then equivalent

to the Euler critical stress equation:

$$\sigma = \frac{\pi^2 E}{(\frac{KL}{r})^2} \qquad 4\text{-}2$$

where the variables are defined as above. This equation is used in the AISI Specification for the higher range of slenderness ratios.

For columns with small or moderate slenderness ratios, σ is above the effective proportional limit of the material and it is therefore necessary to calculate E_t from the material stress-strain curve. Since this involves an iteration procedure, a simpler procedure is adopted in the AISI Specification for columns with small or moderate slenderness ratios. The tangent-modulus equation is approximated in the range of low and moderate slenderness ratios by the so-called CRC equation:

$$\sigma = F_y - (\frac{F_y^2}{4\pi^2 E})(\frac{KL}{r})^2 \qquad 4\text{-}3$$

where F_y is the material yield stress and the other variables are as defined above.

The limiting slenderness ratio which divides the two regions in which Eqs. 4-2 and 4-3 are used may be obtained by equating the right sides and solving. Thus,

$$(\frac{KL}{r})_{lim} = \pi\sqrt{\frac{2E}{F_y}} \qquad 4\text{-}4$$

where $(\frac{KL}{r})_{lim}$ is the limiting slenderness ratio and the other variables are as defined above. For slenderness ratios below Eq. 4-4, the flexural buckling stress is calculated from Eq. 4-3 and for values above Eq. 4-4 from Eq. 4-2. The ultimate

load is obtained by multiplying the stress by the total column area.

4.2.2 Local Buckling

4.2.2.1 General

Local buckling reduces the strength of the column and its effect is treated in the AISI Specification by use of a form factor Q which is equal to one if local buckling is not expected to occur prior to yielding of the material, and is less than one if local buckling is expected prior to yielding.

Local buckling is assumed to affect the column strength for only the low and moderate slenderness ratios where Eq. 4-3 applies. Its effect is included in Eq. 4-3, using Q as follows:

$$\sigma = QF_y - \left(\frac{QF_y}{4\pi^2 E}\right)\left(\frac{KL}{r}\right)^2 \qquad 4\text{-}5$$

For large slenderness ratios, the stress at which the column buckles is assumed to be below the stress at which local buckling occurs, and thus Eq. 4-2 applies. The limiting slenderness ratio, above which Eq. 4-2 governs and below which Eq. 4-5 governs, then becomes:

$$\left(\frac{KL}{r}\right)_{lim} = \pi\sqrt{\frac{2E}{QF_y}} \qquad 4\text{-}6$$

where the variables are as defined above.

The determination of Q is considered in Section 4.2.2.2 for columns composed of stiffened elements, in Section 4.2.2.3 for columns composed of unstiffened elements, and in Section 4.2.2.4 for columns composed of both stiffened and unstiffened

elements.

4.2.2.2 Columns Composed Entirely of Stiffened Elements

A stiffened element is an element with both edges stiffened by a web, flange or stiffener. The ultimate capacity for this type of element is based on the maximum strength, utilizing the full postbuckling capacity. An effective width approach is used with the element strength equal to the element edge stress times the effective area. The effective width approach used in the AISI Specification assumes that elements are simply supported along the edges parallel to the direction of loading and that the edge stress equals the material yield stress at maximum strength.

To calculate the form factor Q for a member composed entirely of stiffened elements, the effective area A_{eff} is the sum of the effective areas of the elements. Then Q is given by:

$$Q_{stif} = \frac{A_{eff}}{A} \qquad 4\text{-}7$$

where A is the full area of the column cross-section and the other variables are as defined above.

4.2.2.3 Columns Composed Entirely of Unstiffened Elements

An unstiffened element is an element with only one edge stiffened by a web, flange or stiffener. The ultimate capacity of an unstiffened element is based on its theoretical buckling strength, rather than on an effective width approach utilizing the postbuckling strength. This is done to insure that excessive local distortions of the unstiffened elements do not oc-

cur. The approach assumes that the unstiffened elements have very little edge fixidity, being nearly simply supported.

To calculate the form factor Q for a member composed entirely of unstiffened elements, the allowable compressive stress, based on the theoretical local buckling stress, is found for each of the elements. The lowest allowable compressive stress F_c is used as the maximum stress in the section and Q is given by:

$$Q_{unstif} = \frac{F_c}{F} \qquad 4\text{-}8$$

where F is the maximum allowable stress if local buckling does not occur and the other variables are as defined above. Omitting safety factors, the maximum allowable stress F is equivalent to the material yield stress.

4.2.2.4 Columns Composed of Both Stiffened and Unstiffened Elements

The form factor Q for columns composed of a combination of stiffened and unstiffened elements is given by:

$$Q = (Q_s)(Q_a) \qquad 4\text{-}9$$

where $Q_s = Q_{unstif}$ computed according to Section 4.2.2.3 and $Q_a = Q_{stif}$ computed according to Section 4.2.2.2, with the edge stress used in computing A_{eff} equal to F_c used in computing Q_{unstif}.

4.3 Comparison of Test Results to Results Predicted by the AISI Specification

4.3.1 General

The section referred to as a stiffened section is composed entirely of stiffened elements. The two webs, or the shorter elements which are perpendicular to the axis of buckling, are fully effective up to yield, with the other two sides having effective widths below the full width in the higher load levels due to local plate buckling.

The section referred to as an unstiffened section is composed of a web which is a stiffened element and four flange elements which are unstiffened elements. The web is fully effective and thus in computing Q, Q_a equals 1.0. Q for the member is then computed as for columns composed entirely of unstiffened elements.

4.3.2 Comparison of Q-Values

The Q-values computed according to the AISI Specification are given in Table 4.1. Q-values based on the stub column tests are also given. These are computed using:

$$Q_{test} = \frac{P_{ult}}{AF_y} \qquad 4\text{-}10$$

where F_y is the yield strength of the material, P_{ult} is the ultimate load of the stub column, and A is the full area of the column cross-section. The two sets of values of Q are also plotted in Figs. 4.1(a) and 4.1(b) for the stiffened and unstiffened sections, respectively.

The experimental Q-values for the stiffened sections are

somewhat higher than those predicted by the AISI Specification, with a maximum variation of about fourteen percent of the Specification value. The discrepancy between the two sets of values is consistent with the edge conditions for the stiffened elements that are not fully effective. The AISI Specification approach is based on stiffened elements having simply supported edges, while the test specimens had edges that were largely restrained against rotation by the narrower and thicker adjoining elements. It appears that the effective width approach is reasonable for the stiffened stub columns, allowing for this discrepancy in the edge conditions. Similar results are shown in Uribe's work[2].

The experimental Q-values for the unstiffened sections are seen to be considerably above those predicted by the AISI Specification, up to ninety-six percent higher. The test value of Q for U-1, equal to 1.05, indicates the presence of strain hardening effects. It should be remembered that the AISI Specification for unstiffened elements is based on limiting the useable strength to a stress less than the ultimate stress in order to prevent excessive local distortions; this accounts for a large portion of the difference between the test and the Specification values. Also, as for the stiffened sections, the longitudinal edges of the unstiffened elements are largely restrained against rotation in the test specimens, while the Specification assumes that the edges of the elements are nearly simply supported; this accounts for some more of the discrepancy between the AISI Specification and the test results.

Since the observed out-of-plane distortions for the unstiffened elements were negligible up to the last load increment before failure, as discussed in Chapter 3, it appears that the AISI Specification approach of limiting distortions in the elements is excessively conservative and not necessary, at least for the range of elements tested. Thus, the range of postbuckling strength, while only partially accounted for in the Specification, should be fully considered in the design of unstiffened elements to achieve substantial economies over the present approach.

4.3.3 Column Curves

4.3.3.1 General

The test results are compared with the AISI Specification approach in Figs. 4.2 through 4.5 for the four stiffened sections, and in Figs. 4.6 through 4.9 for the four unstiffened sections. These figures contain column curves, slenderness ratio vs. ultimate stress, and as mentioned, the ultimate stress equals the ultimate load divided by the total cross-section area of the column. Tables 4.2 and 4.3 contain the numerical values for these comparisons.

In Figs. 4.2 through 4.9, the curve based on the AISI Specification approach is given as the solid line and is based on the Q-value as determined from the Specification. In addition, the maximum column strength, if local buckling were not to occur and the column were to remain elastic until yield, is represented by the dashed lines. These lines represent the Euler buckling curve, which is the curve of stress vs. slender-

ness ratio for buckling in perfect, elastic columns and the yield stress, which is the maximum stress for a column, excluding strain hardening.

Since, as has been pointed out, the Q-values as determined from the AISI Specification do not consider the fixity of the edge conditions of the plate elements, and in the case of the unstiffened columns do not fully consider the postbuckling strength, an attempt is made to consider these factors using the Q-values as determined from the stub column tests with the AISI Specification approach. The resulting curve is given as the curve labeled AISI Spec. with Q based on the tests as given in Table 4.1 with the exception of U-1, where 1.00 was used instead of 1.05. These were calculated based on the tests, and are an approximate method of considering more realistic edge conditions and the postbuckling strength.

The comparison of the test results with the AISI Specification approach and the modified AISI Specification approach, based on the Q-values from the stub column tests, is discussed in the next two sections for the stiffened columns and unsitffened columns, respectively.

4.3.3.2 Stiffened Columns

For the stiffened columns, comparing the test results to the Euler and yield curves, the effects of local buckling and inelasticity are seen to be significant, becoming greater as the width-thickness ratios for the stiffened elements subject to local buckling become greater. It is important to note that if local buckling were not present, the stub column would reach

yield strength, regardless of the effects of prior inelasticity, assuming a concentrically loaded, perfect column. Thus the range between the ultimate stub column strength and the material yield stress is one indication of the effects of local buckling, and as is seen, local buckling has a great effect on the column strength.

a) From the comparison between the test results and the results using Q computed according to the AISI Specification, it is seen that the Specification gives results that are somewhat conservative for the lower slenderness ratios for all four of the stiffened columns. It should be remembered that the Specification assumes hinged-edge conditions for the plate elements, while the test columns had more rigid edge conditions as discussed in Section 4.3.2. This accounts for a large part of the difference between the tests and the Specification approach in the range of lower slenderness ratios.

In the range of moderate slenderness ratios, that is, the range of slenderness ratios just below the range in which failure occurs by Euler buckling, it is seen that the AISI Specification becomes increasingly unconservative as Q decreases. In the case of S-4, the column with the elements of largest width-thickness ratios and therefore the lowest Q-value, for the largest slenderness ratio the value predicted by the AISI Specification is approximately one and a half times the test value. This tendency is quite clear when the four different column specimens are compared. For large slenderness ratios, a definite relationship is indicated between the increase in width-

thickness ratios and corresponding decrease in Q-values, and the increase in the degree of unconservative prediction of the AISI Specification approach for stiffened elements.

b) Comparing the tests with the curves obtained by using the AISI Specification approach with Q-values computed from the stub column tests, it is seen that the only improvement over the approach using the Specification Q-values is for the low range of slenderness ratios. The degree of unconservatism in the range of moderate slenderness ratios is even greater if the Q-values from the tests are used than if the Q-values from the Specification are used. Thus, accounting for the difference in edge conditions by using Q-values from the tests rather than those from the Specification does not lead to more accurate treatment of stiffened columns in the range of moderate slenderness ratios, except perhaps for columns in which local buckling does not have a large effect on the column strength, that is, where the element width-thickness ratios are high and the Q-values are thus near one, which is the case for column section S-1.

4.3.3.3 Unstiffened Columns

For the unstiffened columns in the covered range of width-thickness ratios, the effects of inelasticity and local buckling, more notably the second, were not as great as for the stiffened columns. The stub columns for the sections U-1 and U-2 failed at approximately the yield strength, indicating that local buckling was not of much consequence.

From the comparison between the test results and the re-

sults from the AISI Specification, it is seen that the Specification approach gives ultimate strengths far below the test results. Since the AISI Specification is based in point on limiting distortions in unstiffened plate elements, the difference between the ultimate strengths predicted by the Specification and those from the tests is not surprising. Also, since the AISI Specification assumes hinged edge conditions and since the elements in the test columns were partially fixed, some discrepancy can be accounted for.

It is interesting to look at the curves obtained by the AISI Specification approach, but using Q-values based on the tests rather than directly on the Specification approach for determining the Q-values. For columns U-1 and U-2, using Q = 1.00 as per the stub column tests, reasonable results are obtained when compared with the test ultimate strengths. This indicates that local buckling did not significantly affect the column behavior for all slenderness ratios for these two columns, with width-thickness ratios equal to 16.2 and 20.5.

For column sections U-3 and U-4, the results using Q based on the tests with the Specification approach are also very good when compared to the tests. This is expected since the Q from the tests accounts for both the actual edge conditions and the postbuckling strength of the plate elements. Also, the columns U-3 and U-4, with width-thickness ratios equal to 24.8 and 29.1, behaved similarly to column S-1 in that they have stub column strengths close to the yield stress, indicating that local buckling was not as significant as for columns S-2, S-3 and

S-4. Therefore, on the basis of these three columns, S-1, U-3 and U-4, the AISI Specification using Q based on the stub column tests seems satisfactory for predicting the ultimate loads. However, on the basis of columns S-2, S-3 and S-4, where local buckling is quite significant, the Specification approach, even modified to consider the actual edge conditions by using Q based on the stub column tests, does not produce satisfactory ultimate loads in the range of the interaction of local and overall buckling.

4.4 Conclusions

1) The stiffened sections tested with width-thickness ratios up to 151.8 covered a broader range of local buckling stresses and thus a broader range of postbuckling strengths than the unstiffened sections with width-thickness ratios up to 29.1. Correspondingly, the stiffened stub columns with the larger width-thickness ratios had ultimate strengths that were considerably below the material yield stress, while for unstiffened sections, even those with the largest width-thickness ratios had ultimate loads much closer to the yield stress.

2) The stiffened sections tested are slightly conservative as treated in the AISI Specification for the stub columns. For higher slenderness ratios up to approximately 100 for S-1 and to approximately 50 for the other stiffened sections, the Specification gives results that are conservative and close to the test results. As Q decreases below about 0.75, however, in the range of slenderness ratios above 50 but below approximately 140 at which Euler buckling controls, the Specification gives

results that are unconservative, by an amount up to about 30 percent of the calculated Specification value.

3) For unstiffened sections, the AISI Specification gives strengths that are quite conservative, down to values as low as approximately half of the test values, which is expected since the strength is based largely on limiting out-of-plane distortions. This does not seem necessary since the minute out-of-plane distortions measured during the testing does not justify a reduction in the allowable loads.

4) Using the Q-value determined from the stub column tests in the Specification approach, the ultimate loads for the stiffened section S-1 (with the AISI Q-value = 0.87) and for all of the unstiffened sections are very good. This is because this method accounts for the actual plate edge conditions and in the case of the unstiffened sections, it takes account of the full postbuckling strength rather than placing limits on the stress to prevent excessive out-of-plane distortions. However, for the stiffened sections other than S-1, with Q-values below 0.75, this method is more unconservative than when using the Q-values calculated by the AISI Specification.

5) From this total evidence it follows that modification of the AISI Specification approach, or possible replacement with a new approach, primarily for columns in which local buckling has a large effect on the ultimate column strength, appears not only justified but necessary.

Chapter 5

"RIGOROUS" ANALYTICAL APPROACH

5.1 General

A "rigorous" analytical treatment of columns subject to the interaction of local and overall buckling would hoepfully be more reliable than the various empirical and semi-empirical approaches including the AISI Specification method, and would eliminate the necessity of relying largely on testing. Thus, for example, it would not be necessary to derive effective width formulas empirically.

As discussed in previous chapters, such an approach, one that is rigorous and reasonably exact, would have to be quite complex since it would have to deal with the more advanced postbuckling stages within the plate elements and combine the plate behavior with the behavior of the column as a whole. It would have to include both large deflections in the plate and the effects of inelasticity.

5.2 Basis of the "Rigorous" Analytical Approach

5.2.1 General

As discussed in Chapter 2, the approach of Graves Smith [5], also discussed in two other papers by the same author [23, 24], considers the interaction of local and overall column buckling for rectangular tubular columns and includes both the effects of large plate deflections and inelasticity within the plate elements. This is the most complete analytical treatment known to this writer and it has been chosen as a basis for the

analytical approach developed for the tubular sections in this investigation.

Section 5.2.2 contains a summary of that portion of the Graves Smith approach used in this investigation. The additional analysis developed for this investigation is then given in Section 5.2.3.

5.2.2 Graves Smith's Approach

Graves Smith's approach is divided into two parts. The first, called the 'Compression Analysis', considers a short column subject to axial loading only. It deals with the local buckling of the plates and the complete postbuckling range. The second part, called the 'Interaction Analysis', considers columns subject to flexural buckling. It deals with the relation between the column load and the slenderness ratio at which flexural buckling occurs, using the Compression Analysis to account for the effect of local buckling on flexural buckling. Because the present investigation uses only Graves Smith's Compression Analysis, only this is discussed.

The Compression Analysis is based on the assumption that local buckling occurs entirely elastically, which is a reasonable assumption for materials with a fairly sharp yielding stress-strain curve, such as that considered in this investigation. Until local buckling occurs in the plate elements, the compressive stress in the plates is uniform and is equal to the strain multiplied by the modulus of elasticity; once local buckling occurs, the stress distribution is no longer uniform. The stress distribution is a function of the strain distribu-

tion, which is found once the the deflected shape of the plate is known. The Compression Analysis is used to define the deflected shape, including the amplitude, for each plate element.

What follows is taken from Graves Smith's work and is given in more detail in any of the above mentioned references.

The tubular column section with the local buckles is shown in Fig. 5.1(a). The deflected shapes of the plate elements are found by solving the well known von Karman large deflection equations:

$$\nabla^4 F = E\{(\frac{\partial^2 \omega}{\partial x \partial y})^2 - \frac{\partial^2 \omega}{\partial x^2} \cdot \frac{\partial^2 \omega}{\partial y^2}\} \qquad 5\text{-}1$$

$$\nabla^4 \omega = \frac{t}{D}\{\frac{\partial^2 F}{\partial x^2} \cdot \frac{\partial^2 \omega}{\partial y^2} + \frac{\partial^2 F}{\partial y^2} \cdot \frac{\partial^2 \omega}{\partial x^2} - 2\frac{\partial^2 F}{\partial x \partial y} \cdot \frac{\partial^2 \omega}{\partial x \partial y}\} \qquad 5\text{-}2$$

$$\sigma_{xm} = \frac{\partial^2 F}{\partial y^2}, \quad \sigma_{ym} = \frac{\partial^2 F}{\partial x^2}, \quad \tau_{xym} = -\frac{\partial^2 F}{\partial x \partial y} \qquad 5\text{-}3, 4, 5$$

where F is the stress function, ω is the out-of-plane deflection, σ_{xm} and σ_{ym} are the membrane stresses in the x and y directions, respectively, and τ_{xym} is the shear membrane stress. ω and F are found by solution of these equations subject to the boundary conditions.

The boundary conditions are: at $y = L_b/2$ in Fig. 5.1(a):

$$\omega = \frac{\partial^2 \omega}{\partial y^2} = 0 \qquad 5\text{-}6, 7$$

$$\frac{\partial^2 F}{\partial x \partial y} = 0 \qquad 5\text{-}8$$

At $x_f = -a/2$ and $x_w = b/2$:

$$\omega_f = \omega_w = 0 \qquad 5\text{-}9, 10$$

$$\frac{\partial \omega_f}{\partial x} = \frac{\partial \omega_w}{\partial x}, \qquad \frac{h^3 \partial^2 \omega_f}{\partial x^2} = \frac{k^3 \partial^2 \omega_w}{\partial x^2} \qquad 5\text{-}11,\ 12$$

$$\frac{\partial^2 F_f}{\partial y^2} = \frac{\partial^2 F_w}{\partial y^2} = 0 \qquad 5\text{-}13,\ 14$$

$$h\frac{\partial^2 F}{\partial x \partial y} = k\frac{\partial^2 F}{\partial x \partial y}, \qquad v_f = v_w \qquad 5\text{-}15,\ 16$$

where h and k are the plate thicknesses for the flange and web, respectively, and v represents the displacements in the y direction and is determined from the strain applied to the column. At $y = L_b/2$:

$$v = -\frac{SL_b}{2} \qquad 5\text{-}17$$

where S is the strain applied to the column and L_b the length of one buckle.

Using the boundary conditions, the out-of-plane deflections for the flange and web can be shown to be:

$$\omega_f = \delta_f(A_f \cosh\alpha_f x + B_f \cos\beta_f x)\cos\gamma y \qquad 5\text{-}18$$

$$\omega_w = \delta_w(A_w \cosh\alpha_w x + B_w \cos\beta_w x)\cos\gamma y \qquad 5\text{-}19$$

where:

$$A_f + B_f = A_w + B_w = 1 \qquad 5\text{-}20,\ 21$$

$$\begin{matrix}\alpha_f^2 \\ \beta_f^2\end{matrix} = \left[\begin{matrix}+ \\ -\end{matrix}\gamma^2 + \left(\sigma_{cr}\frac{h\gamma^2}{D_f}\right)^{\frac{1}{2}}\right] \qquad 5\text{-}22$$

$$\begin{matrix}\alpha_w^2 \\ \beta_w^2\end{matrix} = \left[\begin{matrix}+ \\ -\end{matrix}\gamma^2 + \left(\sigma_{cr}\frac{k\gamma^2}{D_w}\right)^{\frac{1}{2}}\right] \qquad 5\text{-}23$$

In these equations δ is the amplitude of the out-of-plane deflections, A and B are constants, $\gamma = \pi/L_b$, σ_{cr} is the critical

plate buckling stress and D is the flexural rigidity:

$$D = \frac{Et^3}{12(1 - \nu^2)} \qquad 5\text{-}24$$

The values of A_f, A_w, δ_f/δ_w and σ_{cr} are found from the boundary conditions for an assumed L_b. By minimizing σ_{cr}, the value of L_b that governs is found.

Using boundary conditions and the large deflection equations, Eqs. 5-1 and 5-2, and the relations for the strains given below, the in-plane displacements in the x and y directions can be found. The strain relations are:

$$\varepsilon_{xm} = \frac{\partial u}{\partial x} + \frac{1}{2}\left(\frac{\partial \omega}{\partial x}\right)^2 = \frac{1}{E}\left[\frac{\partial^2 F}{\partial y^2} - \nu\frac{\partial^2 F}{\partial x^2}\right] \qquad 5\text{-}25$$

$$\varepsilon_{ym} = \frac{\partial v}{\partial y} + \frac{1}{2}\left(\frac{\partial \omega}{\partial y}\right)^2 = \frac{1}{E}\left[\frac{\partial^2 F}{\partial x^2} - \nu\frac{\partial^2 F}{\partial y^2}\right] \qquad 5\text{-}26$$

$$\gamma_{xym} = \frac{\partial u}{\partial y} + \frac{\partial v}{\partial x} + \frac{\partial \omega}{\partial x}\cdot\frac{\partial \omega}{\partial y} = -2\frac{(1 + \nu)}{E}\frac{\partial^2 F}{\partial x \partial y} \qquad 5\text{-}27$$

where ε_{xm} and ε_{ym} are the membrane strains in the x and y directions and γ_{xym} is the membrane shear strain.

The resulting expressions for the displacements in the x and y directions, u and v, are:

$$u = -\frac{2\gamma(1+\nu)}{E}\left\{H_1 \sinh 2\gamma x + H_2\left(x\cosh 2\gamma x - \frac{(1-\nu)\sinh 2\gamma x}{2\gamma(1+\nu)}\right)\right\}\cos 2\gamma y$$
$$- \frac{1}{E}\left\{4\gamma^2\int\psi(x)dx + \nu\frac{d}{dx}\psi(x) + \int\frac{E}{4}\left(\frac{dw}{dx}\right)^2 dx\right\}\cos 2\gamma y$$
$$- \frac{\nu}{E}\int 2C_1 x + \frac{d}{dx}\chi(x) + \frac{1}{\nu}\int\frac{E}{4}\left(\frac{dw}{dx}\right)^2 dx\Big\} + f(y) \qquad 5\text{-}28$$

$$v = \frac{2\gamma(1+\nu)}{E}\left\{H_1\cosh 2\gamma x + H_2\left(x\sinh 2\gamma x + \frac{\cosh 2\gamma x}{\gamma(1+\nu)}\right)\right\}\sin 2\gamma y$$
$$+ \frac{1}{2E\gamma}\left\{\nu 4\gamma^2\psi(x) + \frac{d^2}{dx^2}\psi(x) + \frac{E}{4}\gamma^2 w^2\right\}\sin 2\gamma y \qquad \text{(contd.)}$$

$$+ \frac{1}{E}\{2C_1+\frac{d^2}{dx^2}\chi(x)-\frac{E}{4}\gamma^2w^2\}y+g(x) \qquad 5\text{-}29$$

where H_1, H_2, C_1, $f(y)$, $g(x)$ and $\chi(x)$ are found by satisfying the boundary conditions. w is equal to $\omega/\cos\gamma y$ and $\psi(x)$ is:

$$\psi(x) = \delta^2 \frac{E\gamma^2}{2}\{\frac{A^2\alpha^2}{16\gamma^4} - \frac{B^2\beta^2}{16\gamma^4} + R_e\frac{AB\cosh(\alpha + i\beta)x}{(\alpha - i\beta)^2}\} \qquad 5\text{-}30$$

Once the displacements in the plate are known, the membrane strains are found using Eqs. 5-25 through 5-27 and the bending strains are:

$$\epsilon_{xb} = -t\frac{\partial^2\omega}{\partial x^2} \qquad 5\text{-}31$$

$$\epsilon_{yb} = -t\frac{\partial^2\omega}{\partial y^2} \qquad 5\text{-}32$$

$$\gamma_{xyb} = -2t\frac{\partial^2\omega}{\partial x\partial y} \qquad 5\text{-}33$$

where t represents the plate thickness.

Plasticity is checked for at individual points in the plate using von Mises' Criterion for plane stress:

$$\sigma_x^2 + \sigma_y^2 - \sigma_x\sigma_y + 3\tau_{xy}^2 = \sigma_y^2 \qquad 5\text{-}34$$

where σ_y is the material yield stress. The material is assumed elastic-perfectly plastic. The plate thickness is divided into elastic and plastic zones. In the plastic zones, the stress increments are given by:

$$\Delta\sigma_x = \frac{E}{(1 - \nu^2)}(\Delta\epsilon_x + \nu\Delta\epsilon_y - \{\frac{\Delta W}{2k^2}\}(s_x + \nu s_y)) \qquad 5\text{-}35$$

$$\Delta\sigma_y = \frac{E}{(1 - \nu^2)}(\Delta\epsilon_y + \nu\Delta\epsilon_x - \{\frac{\Delta W}{2k^2}\}(s_y + \nu s_x)) \qquad 5\text{-}36$$

$$\Delta\tau_{xy} = G(\Delta\gamma_{xy} - 2\{\frac{\Delta W}{2k^2}\}\tau_{xy}) \qquad 5\text{-}37$$

where Δ refers to increments, s_x and s_y are the stress deviators, G is the shear modulus and:

$$\{\frac{\Delta W}{2k^2}\} = \frac{s_x(\Delta\varepsilon_x+\nu\Delta\varepsilon_y)+s_y(\Delta\varepsilon_y+\nu\Delta\varepsilon_x)+(1-\nu)\Delta\gamma_{xy}\tau_{xy}}{s_x(s_x+\nu s_y)+s_y(s_y+\nu s_x)+2(1-\nu)\tau_{xy}^2} \qquad 5\text{-}38$$

The strain energy for the plate elements, which is a function of the unknown maximum displacement δ_f, is then minimized to find δ_f. The strain energy in the elastic portions of the plate is:

$$U_{e/\text{unit.vol.}} = \frac{\sigma_x\varepsilon_x}{2} + \frac{\sigma_y\varepsilon_y}{2} + \frac{\tau_{xy}\gamma_{xy}}{2} \qquad 5\text{-}39$$

where the stresses and the strains are the totals of the membrane and bending components. In the plastic regions, the change in the strain energy is:

$$\Delta U_{p/\text{unit area}} = \pm t\int_e^{1/2}\{\sum_{x,y,xy}(\sigma_x + \frac{\Delta\sigma_x}{2})\Delta\varepsilon_x\}d(\frac{z}{t}) \qquad 5\text{-}40$$

where z is the distance from the mid-plane to a point in the plate thickness and e·t is the distance from the mid-plane to the boundary between the elastic and plastic regions. The positive and negative signs refer to the top and bottom portions of the plate, respectively.

Once δ_f is found from the minimization of the strain energy, the behavior in the flange and web plate elements is fully defined and the stresses at all points in the elastic regions are:

$$\sigma_x = \frac{E}{1-\nu^2}[\varepsilon_{xm} + \nu\varepsilon_{ym} + \frac{z}{t}(\varepsilon_{xb} + \nu\varepsilon_{yb})] \qquad 5\text{-}41$$

$$\sigma_y = \frac{E}{1 - \nu^2}[\varepsilon_{ym} + \nu\varepsilon_{xm} + \frac{z}{t}(\varepsilon_{yb} + \nu\varepsilon_{xb})] \qquad 5\text{-}42$$

$$\tau_{xy} = G[\gamma_{xym} + \frac{z}{t}\gamma_{xyb}] \qquad 5\text{-}43$$

In the plastic regions it is necessary to add the stress increments given by Eqs. 5-35 through 5-37 to the stresses from the previous loading.

The axial load on the column is obtained as:

$$P = \frac{2}{L_b} \cdot \frac{\partial U}{\partial S} \qquad 5\text{-}44$$

where L_b is the length of the local buckle and $\partial U/\partial S$ is the partial derivative of the strain energy with respect to the strain S applied to the column.

Graves Smith's Interaction Analysis, which is not used in the present investigation, is based on finding the length of the column at which overall, or flexural, buckling occurs, given the average stress for the selected strain from the Compression Analysis. The stiffness of the column is found by applying infinitesimal increments of strain and repeating the same type of procedure for the Compression Analysis. The plate deflected shapes are assumed based on the shape of the column cross-section just after the occurrences of overall buckling. The column stiffness, EI, is obtained using the Rayleigh-Ritz technique in a manner similar to that in the Compression Analysis and the length at which the column fails is then found using this stiffness in Euler's formula.

The general approach, which yields the column curve of average stress vs. the slenderness ratio, is based on starting

with a compressive strain below that which causes local buckling and then increasing the strain in small increments so the effects of plate buckling and plasticity are accounted for as they occur. For each strain, the average stress and the length of the column at which overall buckling occurs are found.

5.2.3 Modification of Graves Smith's Approach

Only the Compression Analysis from Graves Smith's approach is used for the "rigorous" analytical treatment for this investigation. The equations and the calculation of the strain energy for the Interaction Analysis is even more involved than that for the Compression Analysis and since one of the initial interests in this investigation was the application of the rigorous approach to other cross-sections, particularly the unstiffened sections being investigated, a simpler procedure which could be readily adapted to other sections was desired to treat the effect of overall buckling. Also, something more in line with an effective width approach such as that used in the AISI Specification was desired. Modeling the approach after that in the Specification, but based on a rigorous theory, would hopefully produce a better understanding of the Specification and indicate what changes might be necessary.

The Compression Analysis, discussed in the previous section, yields the stresses at all points in the plate elements in the column. These are then used to obtain effective widths for each of the plate elements. The section through the maximum out-of-plane distortion, denoted by line F-F for the flange and by line W-W for the web in Fig. 5.1(a), is selected as the

basis for the effective width determination. The stress distribution and resulting effective width representation are shown in Fig. 5.1(b). The effective width for the flange is given by:

$$b = \frac{2}{\sigma_{edge}} \int_0^{a/2} \sigma_y(x)dx \qquad 5\text{-}45$$

where b is the effective width, σ_{edge} is the average edge stress or corner stress across the plate thickness, a is the plate width and $\sigma_y(x)$ is the average stress across the plate thickness in the y-direction at the distance x, obtained from Eq. 5-42. The effective width for the web is calculated in the same manner.

Once the effective widths are known for each of the four plate elements in the tubular section, the length at which overall, or flexural, buckling occurs, assuming pinned ends, is found using Euler's formula for flexural buckling:

$$\sigma = \frac{\pi^2 E}{(\frac{KL}{r})^2} \qquad 5\text{-}46$$

where L is the column length and r is the radius of gyration. The assumption that the column behaves entirely elastically so that Euler's formula applies is consistent with the assumption that the material is elastic-perfectly plastic.

In order to consider the effects of local buckling, the radius of gyration and the stress are based on an effective section, i.e. the section composed of the effective portions of the plate elements. Since for the tested specimens, the webs, or shorter elements of double thickness, of the tubular section

are, for all practical purposes, fully effective due to their much greater stiffness than that of the other two elements, the effective section and the stress distribution are shown in Fig. 5.2. The portion indicated by the cross-hatched area comprises the effective section.

The radius of gyration is then given by:

$$r = \sqrt{\frac{I_{eff}}{A_{eff}}} \qquad 5\text{-}47$$

where I_{eff} is the moment of inertia of the effective section about its neutral axis and A_{eff} is the area of the effective section. Then the stress is that on the effective section, which is equal to the stress at the corners of the real section. Thus the compressive load on the column is given by:

$$P = \sigma A_{eff} \qquad 5\text{-}48$$

where σ is the stress given by Eq. 5-46, using Eq. 5-47 for the radius of gyration and 5-45 to determine the effective section.

For K equal to 1.0, Eq. 5-46 is then written in terms of the length as:

$$L = \sqrt{\frac{\pi^2 E I_{eff}}{P}} \qquad 5\text{-}49$$

The solution of Eq. 5-49 to obtain a column curve of average stress vs. slenderness ratio involves the following steps: (1) select a uniform longitudinal compressive strain ε; (2) from the Compression Analysis, compute the axial load on the column given by Eq. 5-44 and the average stress $\sigma_{avg} = P/A$; (3) compute the stress distribution on each plate element in the y

direction using Eq. 5-42; (4) compute the effective width of each plate element using Eq. 5-45; (5) compute the effective moment of inertia I_{eff} based on the effective portions of the separate plate elements; (6) solve Eq. 5-49 for the length L at which overall column buckling occurs for the particular average stress σ; (7) increase the strain ε and repeat the above process. The strain is increased until the load as computed from the Compression Analysis starts to decrease, indicating that the maximum possible short column strength has been reached. For lengths below the length at which this maximum strength is reached, the maximum strength of the column no longer is governed by overall buckling but is equal to the maximum strength determined from the Compression Analysis. This corresponds to Graves Smith's approach.

Thus to account for the effect of local buckling on the column behavior, the stiffness of the section is reduced using an effective section. This is equivalent to the original Graves Smith approach and also to the work of Klöppel[6]. The reduction of the section to an effective section is also used in the effective width approach discussed in the following chapter.

The computer program based on the above for treating the stiffened, or tubular, sections of this investigation required approximately 6 minutes on an IBM 360/65 machine for a specific column section. The large capacity needed, the large number of iterations needed per column section analyzed and the complexity of the program, particularly when portions of the plate ele-

ments become plastic in the later stages of postbuckling, all contribute to the expense of the analysis.

5.3 Results from the "Rigorous" Analytical Approach

5.3.1 Graves Smith's Examples

In order to check the compression part of the program, which is modeled after Graves Smith's approach, and to compare the results of the approach developed in this investigation to account for overall buckling with his interaction analysis, the program was first run with two of Graves Smith's examples. Both are based on an elastic-perfectly plastic material with a modulus of elasticity of 29,500 ksi and a yield strength of 52.8 ksi. The ultimate column loads were not compared with tests.

The first example is a square tubular column with dimensions shown in Fig. 5.3(a). The column curves for Graves Smith's approach and the modified approach used in this investigation are given in Fig. 5.3(b). The second example is a rectangular tubular column with the dimensions shown in Fig. 5.4(a) and with column curves shown in Fig. 5.4(b). Numerical results including the effective widths at each load level are presented in Table 5.1 for the square column and 5.2 for the rectangular column. For the first example, the width-thickness ratio, based on the clear width between the adjacent elements, is 56.8 and for the second, the maximum ratio is 65.0.

Since the compression analysis in this investigation is identical to that of Graves Smith, both approaches give identical ultimate strengths for short columns. However, since the

analysis for determining the column lengths which results in failure by overall buckling for a given load level differs for the two approaches, some differences are expected in the column curves in the range of interaction. For a given load level the approach used in this investigation gives a greater length, and thus higher slenderness ratio, than Graves Smith's approach and this difference is greater for the rectangular column than for the square column. For the rectangular column, the maximum difference in the ultimate load for the two approaches at a given slenderness ratio amounts to approximately 18 percent of the value from Graves Smith's approach though for the majority of the range in which interaction occurs, the difference is not nearly as great. For the square column, the maximum difference is less than 5 percent. The interaction ranges are, respectively, 16 percent and 26 percent of the failure loads for the shortest columns. Since the whole interaction range in both examples is short, the question arises whether or not this discrepancy, even though tolerable for the examples, will be larger for larger width-thickness ratios. This is discussed in the following sections where the results of the "rigorous" analytical approach are applied to the columns of the present investigation.

5.3.2 Stiffened Columns Under Investigation

For the four stiffened sections, the test results and the column curves according to the modified Graves Smith approach are given in Figs. 5.5 through 5.8. In order to compare the approach with the test results, the stresses shown are the col-

umn loads divided by the total unreduced section area, and the radius of gyration in the slenderness ratios are also those of the full cross-section, not of the effective section. The local buckling stress determined by the theory is shown dashed and to show the effects of local buckling on the column strength, the Euler stress curve with a cutoff at yield is also shown dashed. The numerical values for the test ultimate loads and the theory ultimate loads are presented and compared in Table 5.3. Tables 5.4 through 5.6 contain the effective widths at increasing load levels for sections S-2, S-3 and S-4. Section S-1 is fully effective at all load levels as discussed below.

With the program, it was not possible to model the columns exactly, taking into consideration the corners ocrrectly. All columns were considered with outside dimensions identical to the actual columns, flange thickness equal to the plate thickness and web thickness equal to twice the plate thickness. With this modeling, the corners were considered as perfectly square, which when compared with the actual conditions as indicated in Fig. 3.2(a), results in more rigid edge conditions. More discussion on this aspect is given in the next seciton. Column section S-1, according to the "rigorous" analytical approach, should not buckle locally prior to reaching yield stress. Thus, since the theory considers the column as a concentrically compressed, perfect member with an elastic-perfectly plastic material stress-strain curve and square corners, failure of the column should occur at the Euler buckling stress

but not higher than the yield stress. The results are not in good agreement since the theory overestimates the tests by as much as 20.5 percent of the test results.

According to the "rigorous" analytical approach, the three column sections S-2, S-3 and S-4 are all subject to local buckling prior to reaching yield and thus are subject to the interaction of local buckling and overall buckling. The results obtained with the theory are obviously not very good, being considerably higher than the test results, up to 57% for S-4 with a slenderness ratio of 65.5. For nearly all columns tested, the theory is so unconservative as to make it useless for either predicting the strength or obtaining any further insight into the behavior of columns subject to the interaction of local and overall buckling.

Both the stresses, which are determined from the Compression Analysis of Graves Smith, and the lengths, which are determined on the basis of effective widths determined from the Compression Analysis, are high. For the low slenderness ratios, where the columns are not subject to interaction, the strengths predicted by the "rigorous" analytical approach are high, 25 percent above the stub column test load in the case of S-4. If in the range of interaction, the original Graves Smith Interaction Analysis were used instead of the approach developed for this investigation, the resulting lengths and thus slenderness ratios would have been lower for a given column load, as is indicated in the test examples. Thus, some improvement would have resulted for the column curve in the range

of interaction. However, since the stresses obtained from the Compression Analysis used in this investigation are higher than the tests, the discrepancy between the "rigorous" analytical approach and the tests would still be large. Thus, the problem cannot all be attributed to the modification of the Graves Smith theory used in this investigation to account for column failure by overall buckling.

As a further comparison, the effective widths as determined by Eq. 5-45 are compared in Table 5.7 with those determined by the effective width expression, Eq. 6-7, in Chapter 6. With k = 4.00, theoretically the minimum possible value, this reduces to the effective width expression used in the AISI Specification for stiffened elements. The maximum possible k is 6.97 and the value of k in Table 6.1 is determined from the stub column tests. This is all discussed more fully in the effective width approach discussed in Chapter 6 and is only presented here to show the large variation in effective widths for the two methods. These methods are basically identical with the exception of the effective width determination and the fact that for the effective width approach it is not necessary to approximate the material as elastic-perfectly plastic.

It is seen that the variation in effective widths is large, from 11.6% to 49% if k = 4.0 and from 5.9% to 29.8% if k is determined on the basis of the stub column tests. It is thus further concluded that the "rigorous" analytical approach does not adequately treat the postbuckling range for the columns in this investigation.

The following section contains a discussion of the shortcomings of the analytical approach as applied to the stiffened sections in this investigation.

5.3.3 Sources of Error in Application of the "Rigorous" Analytical Approach to the Stiffened Sections in this Investigation

A number of factors have contributed to the "rigorous" analytical approach's overestimation of the maximum column strength for the sections tested. The main sources of error are now discussed.

The primary source of error is related to the extent of the postbuckling range, which is large for the column sections in this investigation. The test results when compared with the local buckling stresses for sections S-2, S-3 and S-4 indicate quite sizable postbuckling ranges, that is, the range between the stress at which local buckling occurs and the short-column ultimate stress. The postbuckling ranges were 31 percent of the short-column ultimate strength for S-2, 62 percent for S-3 and 76 percent for S-4. The postbuckling ranges for the two Graves Smith steel examples with an elastic-perfectly plastic stress-strain curve were 16% and 26%. For the aluminum column tests he conducted which gave good comparison with the theory, the postbuckling ranges were 29 and 42 percent of the short-column ultimate stress. This cannot really be used for comparison with the present investigation, however, since the two materials were not the same. If the width-thickness ratios of the separate plate elements for the three sections in this in-

vestigation, S-2, S-3 and S-4, with width-thickness ratios from 83 to 152, are comapred with those of the steel examples of Graves Smith, 57 and 65, it is seen that his are smaller than those in this investigation, particularly for S-3 and S-4. The width-thickness ratio is related to the stress at which local buckling occurs, with higher ratios resulting in lower local buckling stresses. With local buckling occurring earlier in the loading to failure, the postbuckling range becomes greater.

Since the approach of Graves Smith and the approach used in this investigation involve choosing plate displacement functions to define the shape of the locally buckled plate immediately after local buckling takes place, and since these functions, given in Eqs. 5-18 and 5-19, are used throughout the postbuckling range, some discrepancy will occur as the postbuckling range becomes greater. It is known that the shape of the plate does not remain constant, but flattens out in the central portions of the local buckles, as the compressive load is increased. Thus the assumption that the plates retain the same deflected shape throughout the postbuckling range with only the amplitude changing, while satisfactory for plates with small postbuckling ranges such as the steel examples of Graves Smith, results in significant discrepancies for plates with large postbuckling ranges such as those which make up the column sections in this investigation. Graves Smith referred to this possible discrepancy, though it was not known how great it would be.

Another source of error related to the postbuckling range

concerns the incremental procedure necessary for analyzing the column. The larger the postbuckling range, the greater the number of increments needed and thus the greater the error that might result since during each increment, the magnitude of the deflected shape, as well as other variables, is held constant. Each increment therefore results in some error and a greater number of increments can lead to a large error in the final ultimate strength. Also, it has been found that the increments cannot be made smaller and smaller to overcome the errors that result when certain variables are held constant because numerical problems then occur in the necessary minimization procedures.

Another source of error which has already been mentioned is the modeling of the corners. Since the program is based on rectangular columns with perfectly square corners, the actual corner conditions of the two channels connected to form the tube are not correctly modeled. The flange and corner are of single thickness, with the web of double thickness. It is also not possible to establish that the epoxy connecting the two plate elements is sufficiently strong to cause the two elements to act fully as one element between screws. Excessive deformation and even some separation of the epoxy in the region of the column corners is possible.

In order to check the magnitude of the error that might result by assuming square corners with double thickness webs framing into the corners, the program was run for section S-1 with the web thickness equal to the flange thickness, and thus

with single thickness corners, more nearly like those in the actual specimen. The resulting column curve was an improvement over the column curve for the double thickness web, but the improvement was not nearly as large as the discrepancy between the test results and the analytical approach based on double thickness webs. The local buckling stress was only slightly below the yield stress, approximately 8 percent, and thus the effects of interaction were not very significant. For Section S-4, the same procedure was followed, with the web thickness equal to the flange thickness. Though the results were partially improved in the region of moderate slenderness ratio where the buckling range is small, that is, where the failure load is not far above the local buckling load, it was not possible to tell when the peak was reached in the Compression Analysis. This was a problem for columns with low local buckling loads, since as the postbuckling range increased, the peak in the Compression Analysis results became less pronounced.

The approach used in this investigation assumes that the column is geometrically perfect and concentrically compressed, which can lead to some error since perfect conditions are not obtained in the laboratory. Imperfections can and do exist, both in the overall columns and in the plate elements making up the column. Since concentric loads, or nearly concentric loads, with no significant effects on the overall behavior of the column are indicated in the test results, the first type of imperfection does not seem to be a contributing factor to the discrepancy between the tests and the analytical approach. The

test results indicated that bending in the columns was negligible during the early and even middle stages of loading, which would not have been the case had initial overall imperfections of shape existed in the columns.

The other factor, local imperfections in the plate elements, is also not thought to be a very significant factor causing error between the test results and the analytical approach. The amount of local imperfections measured and discussed in Chapter 3, less than a tenth of one percent of the plate widths for the plate elements in the stiffened sections, compares with the smallest imperfections Graves Smith considered. His calculations show that such imperfections affect the maximum strength of columns by only a few percent, based on the ultimate short-column loads. Thus the imperfections in the plate elements are not thought to account for much of the discrepancy between the test results and the results of the "rigorous" analytical approach.

5.4 Conclusions

1) The modified analytical approach, when applied to the sections in this investigation, did not produce good predictions of the ultimate column strengths for the range of slenderness ratios in which local buckling occurred prior to column failure. For section S-1, with a width-thickness ratio of 57, the stress at which local buckling occurs according to the analytical approach was 23 percent greater than the yield stress, though as shown in Chapter 4, local buckling did occur slightly below yield. For sections S-2, S-3 and S-4, with width-thick-

ness ratios ranging from 83 to 152, the results from the analytical approach were always above the test results. The stub column results from the analysis were as much as 25 percent higher than the test results, and the results in the range of interaction, with slenderness ratios greater than those of the stub columns but smaller than those at which Euler buckling controls, were as much as 57 percent higher than the rest results.

2) The modified analytical approach and that of Graves Smith on which it is based are limited to columns in which local buckling occurs at a high enough stress so that the postbuckling range is not very large, less than 30 percent of the total range. It is also limited to sections which can be easily modeled, while the sections in this investigation had corners unlike the rectangular tubes assumed in the analysis.

3) What is needed is a more complete theory that can consider the full range of postbuckling behavior of plates, regardless of the extent of the postbuckling range, and that can consider sections of more general shape such as those in this investigation.

Chapter 6

EFFECTIVE WIDTH APPROACH

6.1 General

Since the more rigorous analytical approach for the prediction of the ultimate strength of columns subject to local and overall buckling is not satisfactory where large interaction ranges exist, an approach of a somewhat different nature has been developed. This approach is referred to as the effective width approach. It is not only simpler and easier to use for situations where an elaborate computer analysis is not practical, but it gives good results for a large variety of columns.

Rather than having a strictly theoretical basis, the effective width approach is based partially on empirical results This has the advantage that certain variables are taken from test data and can thus be relied on to give a good representation of the actual behavior. The disadvantage is, of course, that one has to limit the resulting analytical approach to the area in which test data have been collected.

Uribe[2,26] has developed semi-empirical approaches for treating columns with stiffened elements and columns with unstiffened elements. His work, primarily intended for studying cold-forming effects on column behavior, includes columns subject to local buckling, though only with local buckling stresses relatively close to the material yield strength and thus with limited postbuckling strength. He treated columns which

are made of unstiffened elements with width-thickness ratios of about 17 in the same number that the AISI Specification[1] treats columns made of stiffened elements. These columns had AISI Q-values from 0.82 to 0.84. For the tested columns composed of unstiffened elements with little postbuckling strength he obtained good results.

For columns composed of stiffened elements with width-thickness ratios of approximately 60 and AISI Q-values of 0.81 to 0.83, he assumed that failure occurred at the tangent-modulus stress given by Eq. 4-2. To account for the effect of local buckling, he based the area used in finding the radius of gyration on the effective area, determined from the effective width formula of the AISI Specification and the moment of inertia on the full area. Thus the radius of gyration $r = \sqrt{I_{full}/A_{eff}}$. While he reduced the area in the tangent-modulus formula to account for the effects of local buckling, he did not reduce the moment of inertia and thus the stiffness of the column. For the columns considered, he obtained good results using this procedure.

For the columns tested in this investigation, with a much broader range of loads at which local buckling occurs and thus with greater ranges of postbuckling strengths, the above procedures are not always satisfactory. For column sections with large postbuckling strengths and slenderness ratios in the range of interaction, the above procedures produce loads that are on the unconservative side, as will be shown. This is based on the stiffened sections studied in this investigation.

The discrepancy between the analytical procedures and the tests can be quite large, with the analytical value as much as twice the test value. The reason is that Uribe has not considered the decrease in the stiffness of the column due to local buckling to calculate the load at which overall buckling occurs.

The following semi-empirical analytical approach has an added advantage over that of Uribe and the AISI Specification. It is applicable to columns composed only of stiffened elements, those composed only of unstiffened elements and those composed of both stiffened and unstiffened elements. It is therefore not necessary to have two different approaches depending on the type of column.

Since Uribe has studied the effects of cold-forming on steel columns, his work is used to include the effects of cold-forming in the following analytical approach.

6.2 Basis of Effective Width Approach

6.2.1 Load at which Overall Buckling Occurs

As is discussed in Chapter 2, the tangent-modulus stress is considered the best representation of the stress at which overall, or flexural, buckling occurs. The tangent-modulus stress is given as:

$$\sigma = \frac{\pi^2 E_t}{(\frac{KL}{r})^2} \qquad 6\text{-}1$$

where E_t is the tangent-modulus for the material. This equation as it is shown here is based on a column which has uniform material properties and which is not subject to local buckling.

The tangent-modulus formula is used as the basis to deter-

mine the stress at which overall buckling and thus column failure occurs in the approach presented in this chapter. It includes both the elastic and inelastic ranges of column behavior. In the following section, the tangent-modulus formula is expanded to consider non-uniform material properties, that is, the cold-forming effects for the types of sections under study. Then in Section 6.2.3, the effect local buckling has on the overall buckling of the column is considered.

6.2.2 Effect of Cold-Forming

Karren at Cornell[27] has shown that cold-forming subjects the material to strain-hardening in the bend areas, increasing the yield strength in these areas. As also is shown, cold-forming increases the strength of the column, and can be used to achieve some economy in designing cold-formed columns. Uribe, in the above column and in Ref. 26, has presented a procedure, discussed below, for the inclusion of the cold-forming effects on the column strength into the effective width approach.

The tangent-modulus formula given in Eq. 6-1 can be written as:

$$\sigma = \frac{\pi^2 E_t I}{K^2 L^2 A} \qquad 6\text{-}2$$

If the cross-section is broken up into separate elements, one element for each flat portion and one element for each corner, Eq. 6-2 becomes:

$$\sigma = \frac{\pi^2 \sum_{i=1}^{j} E_{ti} I_i}{K^2 L^2 A} \qquad 6\text{-}3$$

where σ is the average stress on the column cross-section, j is the total number of elements the cross-section is divided into, E_{ti} is the tangent modulus of the i^{th} element, and I_i is the moment of inertia of the i^{th} element about the axis about which overall buckling occurs.

Eq. 6-3 thus allows for the inclusion of cold-forming effects in the calculation of the stress at which overall, or flexural, buckling occurs by considering the material stress-strain properties of each element as shown. This procedure is expanded in the following section to include the effect local buckling has on the overall column strength.

6.2.3 Effect of Local Buckling

6.2.3.1 General

Providing that local buckling does not occur, the full column cross-section resists overall, or flexural buckling. However, if local buckling occurs within any of the plate elements, the longitudinal stiffness of those elements is reduced. This effect may be expressed by reducing the full column cross-section to a smaller effective cross-section. This effective cross-section is made of the full areas of those elements, corners and flats, that have not buckled locally and the effective areas of those flats that have buckled locally.

The following section includes the basis for determining the effective portion of a flat plate element which has buckled locally, and the subsequent section includes the basis for determining the effective portion of the entire cross-section and its use with the tangent-modulus formula to determine when

failure of a locally buckled column occurs.

6.2.3.2 Effective Width

The effective portion of a flat plate element which has buckled locally is equal to the effective width of the plate element times the thickness. This is discussed in Chapter 5, and a diagram showing the effective width for a stiffened plate element that has buckled locally is given in Fig. 5.1 (b). An unstiffened plate element has its maximum stress at the supported edge and a minimum at the unsupported edge, and thus the effective portion for such an element is assumed located adjacent to the supported side of the plate.

For the effective width approach, the effective widths are based on the effective width expression developed by Winter in the 1940's on the basis of extensive tests on stiffened plate elements[34] and recently revised by Winter[35] for the present AISI Specification. This expression is the basis then for treating stiffened elements in the Specification.

Winter's original expression for stiffened elements is:

$$\frac{b}{w} = \sqrt{\frac{\sigma_{cr}}{\sigma_{max}}} \left(1 - 0.25 \sqrt{\frac{\sigma_{cr}}{\sigma_{max}}} \right) \qquad 6\text{-}4$$

where b is the effective width, t is the plate thickness, w is the plate width, σ_{cr} is the classical critical stress, and σ_{max} is the maximum stress in the plate, the stress at the edge. The revision consists of replacing the coefficient of 0.25 with 0.22. Thus:

$$\frac{b}{w} = \sqrt{\frac{\sigma_{cr}}{\sigma_{max}}} \left(1.0 - 0.22 \sqrt{\frac{\sigma_{cr}}{\sigma_{max}}} \right) \qquad 6\text{-}5$$

The classical critical stress, the stress at which local buckling occurs, is given by Bryan's equation:

$$\sigma_{cr} = k \frac{\pi^2 E}{12(1-\nu^2)(\frac{w}{t})^2} \qquad 6\text{-}6$$

where k is the factor which is dependent chiefly on the manner in which the plate is supported along the edges in the direction of the compressive stress. This equation is based on local buckling occurring elastically.

For steel, with E equal to 29,500 ksi and ν equal to 0.3, substituting the value of σ_{cr} from Eq. 6-6 into Eq. 6-5, the effective width becomes:

$$b = 0.95t \sqrt{\frac{kE}{\sigma_{max}}} \left[1.0 - 0.209 \frac{t}{w} \sqrt{\frac{kE}{\sigma_{max}}} \right] \qquad 6\text{-}7$$

For stiffened elements with simply supported edges, the case for which Eq. 6-5 was developed, k is equal to 4.0. Using this value of k, the equation given in the AISI Specification is obtained.

The limiting width-thickness ratio, above which the plate is not fully effective and Eq. 6-7 governs, is found by replacing b with w in Eq. 6-7 and solving for w. Thus:

$$w_{lim} = 0.64t \sqrt{\frac{kE}{\sigma_{max}}} \qquad 6\text{-}8$$

As pointed out, Eq. 6-4 was derived for stiffened elements, based on using k equal to 4.00. With the above derivation, leaving k in the equation, one could suspect it to be applicable to both stiffened and unstiffened elements. However, it is necessary through testing to show that Eq. 6-7 is in fact

applicable to unstiffened elements. Also whereas k used in the Specification is equal to 4.00, this investigation will consider varying degrees of edge fixidity, not just simply supported edges. For stiffened elements, k varies from 4.00 to 6.97, the latter applying to fully fixed edge conditions, and for unstiffened elements, k varies from 0.425 to 1.277. For the practical situation, the value falls somewhere between these extremes, with the lower value usually used to give safe, or conservative, results.

Some precedent exists for applying the effective width expression of Winter given in Eq. 6-5 to unstiffened sections as well as stiffened sections. Winter[34] proposed the following for unstiffened elements, based on tests of unstiffened elements:

$$b = 0.8t \sqrt{\frac{E}{\sigma_{max}}} \left(1.0 - 0.202 \frac{t}{w} \sqrt{\frac{E}{\sigma_{max}}}\right) \qquad 6\text{-}9$$

Based on the tests, he concluded that this expression is valid to about $t/w\sqrt{E/\sigma_{max}} = 1.75$. According to Wang[4], the above equation reduces to Eq. 6-4 with a coefficient of 0.252 instead of 0.250 if the actual boundary conditions are considered.

Wang, in his study of stainless steel, has proposed using Winter's effective width expression, Eq. 6-4, for unstiffened elements and Eq. 6-5 for stiffened elements. This was based on test results, and further shows that Winter's effective width expression might be applicable to unstiffened steel elements. The only difference proposed for unstiffened elements, other than using different k values to account for the different

boundary conditions, is that Wang did not use the recent modification of the effective width expression given in Eq. 6-5.

Uribe[2], as already discussed, proposed using the modified effective width expression, Eq. 6-5, for both unstiffened and stiffened elements, and though his tests were limited in terms of width-thickness ratio, he obtained good results.

In the work that follows, the effective width expression Eq. 6-7, which is based on Eq. 6-5, is used for both stiffened and unstiffened elements. The recent modification as proposed by Winter changing the coefficient from 0.25 to 0.22 is thus used for both types of elements. As is shown, this yields results that are slightly conservative when compared with the tests in this investigation. Though Winter has proposed a method to determine the value of the coefficient based on test data in his earlier paper, it is not possible to apply it to the data in this investigation since only two of the four unstiffened columns were significantly subject to local buckling.

6.2.3.3 Use of Effective Width to Account for Local Buckling

The effective areas of the separate plate elements as determined with Eq. 6-7 are used to obtain an effective section. The effective section represents that portion of the section that resists overall buckling, and is used in conjunction with the tangent-modulus formula, Eq. 6-2, to determine when overall buckling occurs. The effective sections are discussed in the following, first for the stiffened sections and then for the unstiffened sections, which are not as simple and straight-

forward as the stiffened sections.

For the stiffened section, once local buckling has occurred in the two flanges, i.e., the elements with the largest width-thickness ratios, the section is no longer fully effective and is as shown in Fig. 6.1. The cross-hatched area represents the effective section. The webs were designed so that local buckling does not occur before yielding, and thus they are fully effective at all load levels.

The effective area is then the sum of the effective areas of the elements, and the effective moment of inertia is the sum of the moments of inertia for the effective portions of the elements about the axis of buckling. These two properties are needed in the tangent-modulus formula. The effective area is merely a computational device in that it concentrates the effective portions of the element at the locations of the maximum stress and strain, i.e., the edges rather than distributing it in a manner similar to the actual stress distribution. However, the resulting values of the effective area and the effective moment of inertia realistically evaluate the actual conditions. This is so because the plate is parallel to the axis about which overall buckling occurs, so that it does not matter where the effective portion of the area is located to calculate the effective moment of inertia.

For the unstiffened section, the determination of the effective section for use in calculating the effective area and the effective moment of inertia is not as straightforward as for the stiffened section. Fig. 6-2 (a) shows the effective

section based on locating the effective area of the flanges, the only elements that are subject to local buckling, adjacent to the supported edges. For determining the effective area, this causes no error. However, if this representation of the effective section is used to determine the effective moment of inertia about the axis through the web of the section, the value obtained is not realistic. In actuality, the effective portions of the flanges should be distributed along the total flange in a manner similar to the distribution of stress. This would result in a moment of inertia that is between the value based on the full section and that based on the distribution shown in Fig. 6.2 (a).

An approximate solution is to distribute the effective flange areas as shown in Fig. 6.2 (b), which is more like the actual stress distribution. In this distribution, the effective area, as determined from the effective width expression given in Eq. 6-7, is distributed linearly between the edge of the flange connected to the web and the free edge. Fig. 6.2 (b) shows an example where the effective area of the flange is over half of the full flange area. If the effective area is less than half of the full flange area, it is suggested that the effective area be distributed linearly between the web and the free end, with the thickness of the effective area at the web edge less than the plate width and decreasing to zero at the free edge.

These areas and moments of inertia which are based on the effective section are then used in Eq. 6-3 to account for the

effect of local buckling in the determination of the ultimate column strength. Eq. 6-3, written in terms of the effective section properties, then gives the stress at which overall buckling, and thus column failure, occurs. Thus:

$$\sigma = \frac{\pi^2 \sum_{i=1}^{j} E_{ti} I_{i,eff}}{K^2 L^2 A_{eff}} \qquad 6\text{-}10$$

where E_{ti}, j, K, and L are as defined for Eq. 6-3, $I_{i,eff}$ is the moment of inertia of the effective portion of the i^{th} element about the axis about which overall buckling occurs, and A_{eff} is the sum of the effective areas of the elements which are partially effective and the full areas of all other elements. σ is the average stress on the effective section. If the material stress-strain properties are uniform throughout the section, that is if cold-forming effects are negligible, the assumed stress distribution on the effective section is uniform and equal to the edge stress for the flat plate elements. Otherwise, the stress for each element is obtained from the material stress-strain curve for that element using the strain obtained from the composite stress-strain curve for the value of σ.

The total column load is then given by:

$$P = \sigma A_{eff} \qquad 6\text{-}11$$

This procedure gives the maximum strength of a column subject to combined overall and local buckling, considering non-uniform material properties such as those produced by cold-forming. It also can be used where local buckling has not occurred with

the effective section replaced by the full section; in this case Eq. 6-10 reduces to Eq. 6-3.

6.2.3.4 Method of Solution

The solution of Eq. 6-10 when the cross-section is not entirely elastic or not fully effective is by iteration since the tangent modulus and the effective areas are dependent on the stress, which is in turn dependent on the tangent modulus and the effective areas.

To facilitate the solution of Eq. 6-10, it is written in terms of the length rather than the stress, i.e.:

$$L = \sqrt{\frac{\pi^2 \sum_{i=1}^{j} E_{ti} I_{i,eff}}{\sigma K^2 A_{eff}}} \qquad 6\text{-}12$$

The solution of Eq. 6-12 to obtain a column curve of average stress versus slenderness ratio involves the following steps: (1) select a uniform longitudinal compressive strain ε; (2) from the stress-strain relationships of the material, find for each flat plate element and corner sub-area its tangent modulus E_{ti} and its stress σ_i corresponding to the selected strain ε; (3) compute the effective width of each flat plate element at the stress σ_i and the effective area using Eq. 6-7; (4) compute the moment of inertia $I_{i,eff}$ of each sub-area about the buckling axis of the total column cross-section; (5) compute the total effective area $A_{eff} = \sum A_{i,eff}$ for the column cross-section; (6) compute the total force $P = \sum \sigma_i A_{i,eff}$ and from it the average stress $\sigma = P/A_{eff}$ on the effective section; (7) from Eq. 6-12, find the length of the column on the verge

of buckling for the particular average stress σ acting on the effective section; (8) from Eq. 6-11, obtain the column load; (9) if desired, the average stress on the total cross-section is then $\sigma_{av} = P/A_{full}$. A column curve of average stress versus slenderness ratio is calculated by repeating this process for different strains. A computer program based on the method is given in Appendix C.

It is important to note that while the equations in this chapter are based on the average stress on the effective section, for convenience, the curves given in the figures in all cases are plotted in terms of the average stress on the total cross-section. Similarly, the radii of gyration for plotting the slenderness ratios for the curves are based on the total cross-section. This is done to facilitate proper comparisons with the test results, for which the effective areas and the effective radii of gyration are unknown.

6.3 Comparison of Test Results to Effective Width Approach

6.3.1 Cold-Forming Effects

The effect of cold-forming on the strength of press-braked sections depends on the area of the corners, as a fraction of the total area[36]. For all of the test sections in this investigation, the corner areas are less than one percent of the total area. Therefore the effects of cold-forming are here assumed to be negligible and the material in the column is assumed as uniform, with the stress-strain curve as determined from a standard tension test on a flat specimen.

6.3.2 Stress-Strain Curve

The Ramberg-Osgood Equation[37,10] has been used to model the stress-strain curve for use in a computer analysis. The equation is:

$$\varepsilon = \frac{\sigma}{E} + K\left(\frac{\sigma}{E}\right)^n \qquad 6\text{-}13$$

where n is chosen to fit the particular steel under study, and K, as defined by Ramberg-Osgood, is:

$$K = \frac{3}{7}\left(\frac{\sigma_1}{E}\right)^{1-n} \qquad 6\text{-}14$$

σ_1 being the stress at the intercept of the material stress-strain curve and a line through the origin with a slope of 0.7 times the modulus of elasticity.

Since the material in this investigation has a fairly high proportional limit, a choice of n equal to 75 seems to fit the material stress-strain curve. The Ramberg-Osgood stress-strain curve and that for the material in this investigation are shown in Fig. 6-3. The Ramberg-Osgood curve does not give a definite yield plateau, unless an exponent of infinity is used, but this region is not important for the column behavior under study.

6.3.3 Effective Width

In Eq. 6-7, it is necessary to find the value of k, the plate buckling factor which depends on the manner in which the plate element is supported along the edges in the direction of the compressive stress. Though ways have been presented to calculate for structural shapes the value of k on a theoretical basis, such as in papers by Stowell and Lundquist[38,39], it is

not possible to do so for the sections in this investigation. The factor depends on the support available at the edges and this is related to the stiffness of the adjoining elements. In this study, those elements that undergo local buckling in the column sections frame into elements which are made of two plates joined with epoxy plus screws or rivets. Epoxy is a substance that is visco-elastic. Thus, the edge conditions are not strictly definable because it is not certain that the epoxy connects rigidly the two plates at the edges. Further, in the case of the stiffened sections, it is not certain how the epoxy at the corner connections on the inside of the section affects the restraint of the single thickness elements.

It is therefore necessary to resort to empirical means to obtain the values of k for the sections tested. The stress at which elastic local buckling occurs under ideal conditions is given by Eq. 6-6. This is used to obtain the value of k using σ_{cr} as determined from the stub column tests.

A number of methods are available for determining from tests the value of the critical strain, or strain at which local buckling occurs, and for it the value of σ_{cr}. Three methods discussed by Johnson[3] follow; a load-strain diagram is given with each showing the critical strain.

(1) Strain Reversal Method: The critical strain is the strain at which the strain increment for one of a pair of gages placed opposite to each other on the plate element begins to decrease. At this point the stress is beginning to change from uniform compression to combined bending and compression. This

method gives the lowest critical strain of the three methods.

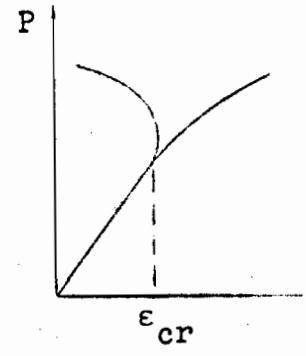

(2) Modified Strain Reversal Method: The critical strain is the maximum compressive strain in the gage on the convex side of the wave in the buckled plate. At this point, bending is pronounced and the tensile bending strains are about to become larger than the axial compressive strains. This method gives critical strains slightly larger than the last method.

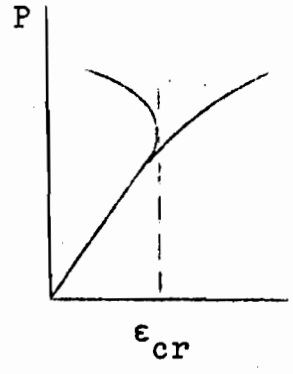

(3) Maximum Midthickness Strain Method: The critical strain is the maximum average for the paired gages. The bending strains have become large enough at this point so that the average compressive strain at the gage location is decreasing. This method gives the largest critical strain of the three methods.

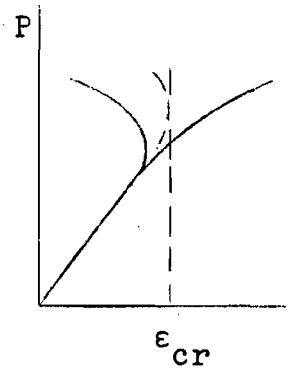

The second method, the modified strain reversal method, is thought to be the best of the three. It is not always possible to apply the first method since it is not always possible to ascertain when the strain increment begins to decrease. The third method results in critical strains that are obviously greater than the actual critical strain since the criterion is not met until considerable bending has occurred. The second method is simple to apply, and since it gives strains only slightly in excess of the first method, it is the one used in this investigation.

For the stiffened sections, the critical strains measured in the two flanges were averaged to obtain the critical strains for the sections, and for the unstiffened sections, the critical strains for the four flanges were averaged. The critical stresses so found from the stub column stress-strain curves, and the corresponding values of k determined from Eq. 6-6 are given in Table 6.1.

For unstiffened section U-1, it was not possible to determine when local buckling occurred using the modified strain reversal method. The strain readings were not spaced at small

enough intervals in the vicinity of failure, and it was therefore not possible to ascertain exactly what happened. It seems that local buckling did not occur before failure by yielding, the yield point of the steel being in the range of 40.1 to 42.5 ksi and the stub column failure stress being 43.8 ksi, and that the stub column section was fully effective for all load levels, with the failure stress $\sigma = \sigma_{yield}$. If the actual flange width and σ = 43.8 ksi are substituted into Eq. 6-8, k = 0.91 is obtained. Such a large value of k is not consistent with the k values for the other three unstiffened sections. Section U-1 should have the lowest k value since its ratio of the flange stiffness to the web stiffness is lowest. Thus for purposes of comparing the effective width approach with the test results, based on using a k value that is reasonable in comparison with the other values for unstiffened elements, k is assumed equal to 0.5. This gives a local buckling stress of 50.6 ksi using Eq. 6-6. The test results were also compared with Eq. 6-1, assuming the section to be fully effective.

For unstiffened section U-2, it is not possible to determine exactly when local buckling occurred using the modified strain reversal method, though it was clear from the load versus strain curves that local buckling did occur prior to failure. Local buckling occurred at some stage during the last two load increments, that is between 24.0 kips and failure at 26.1 kips. A value of 25.1 kips is assumed as the load at which local buckling occurred, and thus the value of k is based

on a local buckling stress of 40.3 ksi, the average stress P/A_{full} at this load.

The k value determined for stiffened section S-3, based on the stub column, is 4.71. This is considerably below the value for section S-2, and therefore, it is not consistent with the other k values or the increased degree of fixity along the edges of S-3 over that of S-2. The amount of fixity along the edges is directly related to the ratios of the stiffnesses of the two plate elements framing into the edge. Though the ultimate load for stub column S-3 is consistent with the ultimate loads for stub columns S-2 and S-4, it is felt that imperfections in the vicinity of the strain gages on S-3 caused the plate elements to wave earlier than they should have. If the column section S-3 with length equal to 22.0 in. is used for the determination of the critical strain instead of the stub column with a length of 18.1 in., the critical strain is 0.0004 in/in, and the resulting k value is 6.11. This is in line with the average of the k values for column sections S-2 and S-4, equal to 6.14. Thus, the value of 6.11 is used for S-3.

6.3.4 Comparison of Tests and Effective Width Approach for Stiffened Sections

6.3.4.1 General

Once the effective width expression is established, the primary factors of interest in the effective width approach are the moment of inertia and the k factor used to represent the plate element edge conditions. These factors are varied and

used in the effective width approach for comparison with the test results in the following sections.

The effective widths for different k values and for increasing strains are given in Tables 6.3 through 6.6 for the four stiffened sections. In addition, Tables 6.7 and 6.8 contain the comparisons between the test ultimate stresses and the effective width approach ultimate stresses for the different cases considered in the following sections.

6.3.4.2 Stub Column Curves

Stub column curves, compressive strain versus column load, are given for the stiffened sections in Figs. 6.4 through 6.7. Two curves are given for each section, one based on the effective width approach and one based on the stub column test. The strain is the longitudinal compressive strain applied to the column.

The strains for the curve based on the stub column tests represent an average of the four strain gages at the corners of the section; see Fig. 3.2 (a) for the location of the strain gages. Since readings of the gages were not possible at failure, the curves terminate below failure. However, the failure loads are indicated by the dashed horizontal lines. For S-3, two curves are given. One is for the stub column and one is for the column of length 22.0 in. since the latter is used as a basis for determining k. Very little difference exists between the two.

The curve reflecting the effective width approach utilizes Eq. 6-7 with the k value computed from the stub column tests as

given in Table 6.1. The calculated column load is equal to the uniform stress on the effective section times the effective area. The effective width at ultimate load, the ultimate load, and Q, the ratio of the effective area to the full area at failure, are given in Table 6.2 (a) for the stiffened stub columns.

The comparison indicates that the test curves are never more than about 10 percent above the calculated curve based on the calculated effective widths, and in all cases, the test ultimate load is either equal to or somewhat above that calculated from the effective widths. This indicates that the effective width approach is slightly conservative, which is expected since the effective width formula, Eq. 6-7, approximates the lower bound of a large number of test data.

6.3.4.3 Column Curves Using Different Moments of Inertia

Column curves comparing the tests with the effective width approach are given in Figs. 6.8 through 6.11. One is based on the moment of inertia of the full section and another on that of the effective section shown in Fig. 6.1. The k factor used is that computed from the stub column tests.

For the range of low slenderness ratios, the two curves are nearly identical, which is expected. In this range the column is not subject to overall buckling, so that its ultimate load is simply the sum of the component plate strengths. Also in the range of high slenderness ratios, the curves are identical. In this region, the strength is governed by the Euler buckling load based on the full section since the component

plates have not buckled.

In the range of moderate slenderness ratios, the strength is governed by the interaction between local and overall buckling, and the difference between using the full moment of inertia and the effective moment of inertia is significant. As expected the difference between the two is greater, the greater the effect that local buckling has on the column, with the calculated column strength based on the full moment of inertia as much as 1.5 times the value based on the effective moment of inertia. It is seen that using the effective moment of inertia is in better agreement with the tests, that is reduction in the stiffness due to local buckling must be considered in computing the load at which overall, or flexural, buckling occurs.

The following section contains a discussion on the variation of the k factor in order to obtain an even better approximation of the test data.

6.3.4.4 Comparison Using Different k Values

Since it has been shown that the effective moment of inertia is the correct basis for analyzing the stiffened sections by means of the effective width approach, the only other possible variable is k. Theoretically, k can vary from 4.00 to 6.97. Column curves based on the effective width approach using these two extreme k values and the k values determined from the stub column tests are given in Figs. 6.12 through 6.15 for the stiffened sections. For section S-4, the curve for $k = 6.97$ is not shown since the $k = 6.90$ determined from the stub column test is very close to 6.97. These figures also

contain the test results.

The variation between the column curves based on the two extremes of k is not very large, not more than about 10 percent of the values for the curve with k equal to 4.00. The value of k equal to 4.00 seems to be in better agreement with the tests in the range of interaction, which is the range of moderate slenderness ratios. In the range of low slenderness ratios, the higher k value seems to give better results. It is seen that the curve for k = 4.00 is in nearly all cases somewhat on the conservative side of the test data, and where it is on the unconservative side, the test value is not more than eight and a half percent below the curve.

It thus appears that using the effective width approach with the moment of inertia based on the effective section and conservatively with the k value equal to 4.00, as originally proposed by Winter, yields a very good prediction of the stiffened column strengths.

6.3.5 Comparison of Tests and Effective Width Approach for Unstiffened Sections

6.3.5.1 General

The same approach as for stiffened sections is used for the unstiffened sections, and only additions and modifications are mentioned in this section.

The effective widths for different k values and for increasing strains are given in Tables 6.9 through 6.12 for the four unstiffened sections. Tables 6.13 and 6.14 contain the comparisons between the test ultimate stresses and the effec-

tive width approach ultimate stresses for the different cases considered in the following sections.

6.3.5.2 Stub Column Curves

Stub column curves comparing the tests with the effective width approach for the unstiffened sections are given in Figs. 6.16 through 6.19. The test curves are based on the average of the four strain gages at the flange corners; see Fig. 3.2 (b) for the location of the gages. For section U-1, in addition to the curve from the effective width approach with k assumed equal to 0.5, the curve based on the section remaining fully effective for all loads is also given. For section U-3, one of the first tests conducted, strain gages were not placed at the corners, and thus the test curve is based on the shortest hinge-ended column with the length L=23.0 in. closest to that of the stub column (9.0 in). The effective width at ultimate load, the ultimate load, and Q, the ratio of the effective area to full area at failure, for the unstiffened stub columns are given in Table 6.2 (b).

Using the k values determined from the stub column tests in the effective width approach is seen to yield effective width curves somewhat on the conservative side of the test curve. The degree of conservatism is never more than approximately 10 percent. This is the same as the situation for the stiffened sections, and seems to indicate that the effective width expression of Eq. 6-7, which was originally developed for stiffened elements, is also applicable to unstiffened elements.

For U-1, the stub column curve based on Eq. 6-1, assuming

that local buckling does not occur, is in very good agreement with the test curve, with the calculated ultimate load 5 percent below the test value. This along with the fact that the ultimate load for the test was slightly above yield strength (probably due to a combination of cold-forming effects and the attainment of strain hardening during the test) is a further indication that local buckling did not occur prior to failure.

6.3.5.3 Comparison Using Different Moments of Inertia

Column curves comparing the tests with the effective width approach using different moments of inertia are given in Figs. 6.20 through 6.23. The three different moments of inertia are based, respectively, on the full cross-section, and on the two different effective sections shown in Figs. 6.2 (a) and (b). As discussed in Section 6.2.3.3, the effective section shown in Fig. 6.2 (b) is the more realistic one, though it is only an approximation.

The results are similar to the results for the stiffened sections. The choice of what section to base the moment of inertia on makes little, if any, difference in the regions of low slenderness where the component plate strengths govern the maximum strength of the column. Also, in the region of Euler buckling, the region of high slenderness ratios, the section is fully effective at failure.

In the range of moderate slenderness ratios, where the strength is governed by the interaction between local and overall buckling, a large difference exists between using these different moments of inertia. Basing the moment of inertia on

the full section is unconservative for all columns except U-1. Using the effective section shown in Fig. 6.2 (a) leads to results that are on the conservative side, quite significantly so in some cases. With the effective section shown in Fig. 6.2 (b), the best results of the three methods are obtained. The results are usually on the conservative side, and where they are unconservative, the maximum difference is 4.1 percent of the test value.

It is interesting to note that while it has been shown that local buckling did not occur in section U-1, the curve based on assuming that the section was fully effective at all loads, is about 6 percent on the unconservative side with a slenderness ratio of 55.7. The curve for k = 0.5 and the section shown in Fig. 6.2 (b) is about 13 percent on the conservative side with a slenderness ratio of 89.1. Thus, the effective width approach based on Eq. 6-7, which accounts for some imperfections, appears to be a better design approach than Eq. 6-1, even though the latter correctly models the theoretical behavior of this column.

It is concluded that the reduction in stiffness due to local buckling must be considered in computing the overall buckling load, as was done for the stiffened sections. The simplified approach, using a linear distribution of the effective area as a better approximation of the actual stress distribution in the flanges is reasonable for the sections considered here. The results are also dependent on the choice of k values, which is discussed in the following section.

6.3.5.4 Comparison Using Different k Values

For unstiffened sections, the k factor can vary theoretically between 0.425 and 1.277. Results using these extreme k values and the k value calculated from the stub column test results, with the moment of inertia based on the effective section of Fig. 6.2 (b) are given in Figs. 6.24 through 6.27. The range of values for k is much greater for the unstiffened sections than for the stiffened sections. For the unstiffened sections, k for fixed edge conditions is nearly three times that for simple edge conditions, while for stiffened sections the ratio is only 1.75. Thus, the variation in the column curves is much greater for the unstiffened sections than for the stiffened sections, and it is therefore more important to determine realistic k values for the unstiffened sections.

Using the minimum k value of 0.425 leads generally to quite conservative results, as much as 39.3 percent below the test values, while the maximum value of 1.277 leads to results that are in most cases unconservative, as much as 14.9 percent above the test values. The effective width approach based on the k values from the stub column tests gives the best results. The curves based on these k values are in most cases on the conservative side, and when on the unconservative side, the test value is no more than 4.1 percent below the curve. For U-1, it was shown in the previous section, that the effective width approach with k = 0.5 gives better results than assuming that the section is fully effective at all load levels (cf. Figs. 6.20 and 6.24).

Thus, while for the stiffened sections the lowest k value led to reasonable results, the choice of the k value is more important for the unstiffened sections. It is necessary to have some method for finding k values that model the actual edge conditions, such as the method used in this investigation by means of stub column tests. For sections that can be modeled correctly on a theoretical basis, the theoretical approaches referred to in Section 6.3.3 should give good results.

6.4 Comparison of Effective Width Approach to Other Test Results

6.4.1 General

Further verification of the effective width approach might result from comparison with experimental results of other researchers. Three such sets of results from tests on steel columns which were referred to in Chapter 2 are used for comparison here. In addition, one other set of data on stub columns is presented and compared with the effective width expression.

It is not always easy to use test results from other investigations, particularly when the data presented is not sufficient for use in a specific analytical method. With this in mind, it has been necessary to make certain assumptions which can result in some error, though hopefully not very much. The assumptions are discussed where pertinent.

6.4.2 Comparison with Test Results of Skaloud and Zörnerová

Skaloud and Zörnerová[28] conducted an experimental investigation on tubular columns made of two hat sections connected

as shown in Fig. 6.28 (a). The cross-hatched portion represents the effective section. They conducted tests with five series of columns, each with different dimensions. The results for three of the series are used here for comparison with the effective width approach. The remaining two series were not satisfactory because the stiffeners, i.e., the lips forming the connections for the two hat sections, were not adequate by the AISI Specification to assure that the adjoining sub-elements behave as fully stiffened elements. The cross-section dimensions for the three series used for comparison are given in Table 6.15.

The material yield stress for the three series was 35.8 ksi. A material stress-strain curve is not presented in the paper, and thus one has been assumed using the Ramberg-Osgood equation, Eq. 6-13. σ_1 was set equal to the yield stress and the value of n was set to 24, an arbitrary value that gives a curve with a lower proportional limit and with a more gradually yielding nature than the material used in this investigation. In the effective width approach, this results in slightly smaller loads in the range of moderate slenderness ratios, between that of very short columns not subject to flexural buckling and that of longer columns that fail by Euler buckling. The resulting stress-strain curve is shown in Fig. 6.28 (b).

For determining the cross-section properties for use in the effective width approach, it was assumed that the inside radius of the corners was 0.0 since no value was given in the

paper. Also, as for the stiffened sections in this investigation, the value of k was taken as 4.00. Neither of these assumptions should cause much error. Since no information was given on cold-working effects, these were assumed negligible, which can lead to some inaccuracy, possibly quite considerable. One other assumption was made in the case of series B. Since the width-thickness ratio of the vertical elements in Fig. 6.28 (a), disregarding the stiffeners, was 38.0, while the limiting width-thickness ratios was 36.8, it was assumed that the element with stiffener would be fully effective at all load levels.

The results of comparing the effective width approach and the experimental results of Skaloud and Zörnerová are shown in Figs. 6.29 through 6.31 for Series A, B, and C, respectively, and are tabulated in Table 6.16. Series C was fully effective at all loads, since the maximum width-thickness ratio was below the limiting value. Also it should be noted that the lengths, and thus the slenderness ratios, for the columns in Series A and C were based on the distance between the points of contraflexure in the actual deflection curves from the tests. This is because the experimental hinges did not ensure free rotation of the ends of the columns, the columns being more or less restrained at their boundaries. Overall deflection curves were carefully measured with a great number of dial gauges placed along the column, allowing the determination of the points of contraflexure.

Some considerable discrepancies exist between the tests

and the effective width approach. The stub columns, i.e., the shortest columns, for series B and C attained loads significantly above the yield stress, as much as 30 percent. This is most likely attributable to strain hardening, which, in the European steels, often occurs at relatively low strains, and to possible cold-working in the corners. The longer columns for series A and C, i.e., those with slenderness ratios above 100, which should fail by Euler buckling, were overestimated by from 23.3 to 70 percent of the test value. Local buckling could not have occurred in these columns since the shorter columns had failure loads close to yield. Initial crookedness or a wrong estimate of the effective length may be the reason for these discrepancies.

In the regions of moderate slenderness ratios, from 25 to approximately 100, the effective width approach with the above assumptions produced good results. The maximum variations from the tests are 10.6 percent below to 5.4 percent above.

It is difficult to come to any definite conclusions from this evaluation because of the assumptions necessary in applying the approach, because local buckling was not a very significant factor for any of the columns, and because of the discrepancies shown for the shorter and longer columns. However, in the region of moderate slenderness ratios, the region in which the interaction of local and overall buckling occurs, the test results are fairly close to the effective width approach results.

6.4.3 Comparison with Test Results of Deliege, Baar and Hick

Deliege, Baar, and Hick[31] present the results of an extensive number of tests using the shape shown in Fig. 6.32. The cross-hatched portions represent the effective section. The dimensions were the same for all columns with the exception of the thickness. Also some columns were galvanized and some were not. The four series of columns tested are listed in Table 6.17.

The stress-strain curves for the materials are not given, and as for the test data of Skaloud and Zörnerová, the curves have been assumed based on the Ramberg-Osgood Eq. 6-13. As for Skaloud and Zornerova, σ_1 was set equal to the yield stress and n equal to 24. The resulting stress-strain curves are given in Fig. 6.33.

The inside radii of the corners have been assumed equal to 0.0 and the value of k as 4.00. It has also been assumed that the cold-working effects on the section were negligible.

Since the elements with the largest width-thickness ratios join at an angle of 120 degrees rather than 90 degrees, some question arises whether to treat the elements separately as stiffened elements or to treat the two with the stiffener in between as a multiple-stiffened element as defined in the AISI Specification. If treated as a multiple-stiffened element, the Specification requires that the effective width be reduced further and that the stiffener area be reduced if the width-thickness ratio of the sub-elements is greater than 60. Sections A and B have ratios greater than 60, and it is felt that

the behavior of the sections will be somewhere between the two extremes, that is with the two sub-elements joined at 90 degrees or at 180 degrees. Thus, the effective width approach is applied for both of these cases, using the AISI Specification Section 2.3.1.2 on multiple-stiffened elements for the latter.

For multiple-stiffened elements with sub-element width-thickness ratios greater than 60, Section 2.3.1.2 specifies that the effective design width b_e be figured according to:

$$\frac{b_e}{t} = \frac{b}{t} - 0.10 \left(\frac{w}{t} - 60\right) \qquad 6\text{-}16$$

where b is the width figured from the effective width expression (Eq. 6-7 is used here and corresponds to the expression in the Specification if k is equal to 4.00), w the width of the sub-element, and t the thickness. The stiffener area A_{st} is reduced by multiplying it by α, which for sub-element width-thickness ratios between 60 and 90 is given by:

$$\alpha = \left(3 - \frac{2b_e}{w}\right) - \frac{1}{30}\left(1 - \frac{b_e}{w}\right)\left(\frac{w}{t}\right) \qquad 6\text{-}17$$

and for width-thickness ratios greater than 90 is given by:

$$\alpha = \frac{b_e}{w} \qquad 6\text{-}18$$

The effective section is based on the cross-hatched area shown in Fig. 6.32. This is not really correct since the effective sub-areas should be distributed in proportion to the stresses on the section as discussed previously. However, this is felt as a reasonable representation and not thought to

result in much error. The calculated moment of inertia with the effective areas located adjacent to the edges rather than distributed throughout the section is not as significantly influenced as was the case for the unstiffened elements used in this investigation.

The results for the comparisons are given in Figs. 6.34 through 6.37 for series A through C, respectively. They are also tabulated in Table 6.18. Since for series A and C as many as 13 tests were conducted for the same slenderness ratio, only the extreme values and the mean values have been presented in the figures.

For series A, the section with the largest width-thickness ratio, the curve based on considering the section with multiple-stiffened elements gives very good results. The effective width approach is within 12 percent of the mean test results, and always on the conservative side. The approach not considering the reductions for multiple-stiffened elements is 30.8 percent higher than the mean test result for the shortest column and a maximum of 19.1 percent higher for the other columns. However, there is evidently something wrong with the shortest column test results which fall sizeably below those for much longer columns.

For series B, also with sub-element width-thickness ratios greater than 60, the approach with consideration for the multiple-stiffened elements gives results within 9.3 percent of the tests, though on the unconservative side. This is not thought too unreasonable in view of the assumptions that have

been made. The curve which does not consider the reductions for multiple-stiffened elements is always on the unconservative side of the tests, as much as 24.1 percent. The results of the shortest columns are dubious for similar reasons as series A. For both series A and B it is safe and reasonably accurate to assume that the two elements with the largest width-thickness ratios behave as a multiple-stiffened element.

For series C and D, the effective width approach gives good predictions of the failure loads. For series C, the results range from 4.9 percent below to 15.1 percent above the mean test results (in this case, the mean is above the Euler load, which makes the test result, or at least the slenderness ratio for it, somewhat doubtful). For series D, the calculated results range from 9.4 percent below to 2.2 percent above the test results.

6.4.4 Comparison with Test Results of Uribe

Uribe[2,26] conducted tests on four series of columns in order to study the effects of cold-forming on column behavior. The four sections, with dimensions, are shown in Figs. 6.38 and 6.39. The cross-hatched portions represent the effective sections used in the effective width approach. The maximum width-thickness ratios and the tensile yield stresses for the corners and flats are given in Table 6.19.

Uribe has presented the stress-strain curves for his sections, for both the corners and the flats, and these are given as the solid lines in Figs. 6.40 through 6.42. The Ramberg-Osgood equation, Eq. 6-13, has been used to model the stress-

strain curves, and are given as the dashed lines in these figures.

The effective section for column section UC-1, which is like the unstiffened section in this investigation, was assumed distributed in the same manner. For UC-2, with the axis about which buckling occurs parallel to the unstiffened, partially effective elements, the effective area was located near the webs since the distribution is irrelevant in calculating the effective moment of inertia. For both UC-1 and UC-2, with section dimensions and material stress-strain curves very close to those for unstiffened section U-1 in this investigation, k was assumed as equal to 0.50 as was used for U-1.

For the other two sections, SC-1 and SC-2, both with stiffened elements, the effective sections are based on locating the effective portions of the elements near the edges as shown. For SC-1, this results in no error in calculating the effective moment of inertia, and for SC-2, the error is not very large as discussed in relation to the sections of Deliege, Baar, and Hick. For these sections, k was assumed as 4.00.

The results of the effective width approach, including the effects of cold-forming on the corners as discussed in Section 6.2.2, are compared with the test results in Figs. 6-43 through 6-46. Numerical results are given in Table 6.20.

For sections UC-1 and UC-2, the ultimate loads as predicted by the effective width approach in the range of slenderness ratios below 50 are almost identical to the test loads. For slenderness ratios above 50, the effective width approach

gave results from 16 to 17 percent higher than the test results. If k were less than 0.50, some improvement would result, though not very much. It seems that Uribe's tests on sections with unstiffened elements are not as well modeled with the effective width approach as U-1, the section tested in this investigation which had similar dimensions and material properties, with the exception of the cold-working in the corners. According to Uribe, the section UC-1 should not have been significantly influenced by cold-working in the corners in the range of slenderness ratios where failure occurred by flexural buckling since the corners in the section are close to the axis about which buckling occurs. Therefore, it is not clear why the two comparisons, between the effective width approach and U-1 on the one hand and UC-1 on the other, are so different, i.e., the first shows conservative analytical results and the second unconservative.

For Uribe's sections composed of stiffened elements, SC-1 and SC-2, the effective width approach underestimates the ultimate strength by as much as 12.2 percent. In all cases the discrepancy was on the conservative side, and thus the approach is thought reasonable and safe as a means of predicting the strength of these sections.

6.4.5 Comparison with Test Results of Dhalla

Dhalla in an investigation on the influence of ductility on the behavior of cold-formed members[40], conducted tests on four stub columns with unstiffened elements identical to the section shown in Fig. 3.2 (b). The dimensions are given in

Table 6.21 (a). The material was high strength steel, with a tensile yield stress of 88.8 ksi, and a compressive yield stress of 78.6 ksi. This is in contrast to moderate strength steels, such as those already discussed, which exhibit compressive yield stresses much closer to the tensile yield stresses.

Since only stub columns were tested, it is only possible to test the part of the effective width approach that treats local buckling, i.e., the ultimate strength of a stub column being equal to the effective area times the yield stress. Since the compressive yield stress is considerably below the tensile value, both will be used to determine the ultimate strength of the stub column and the results compared. k is assumed equal to 0.5, a value that is conservative. The first three columns did not exhibit local buckling prior to failure according to the modified strain reversal method; the fourth exhibited local buckling at 87.5 percent of the failure load.

The results from the tests and the effective width approach are given in Table 6.21 (b). For UFC-1, the section is calculated to be fully effective for either the tensile or compressive yield stress. Using the tensile yield stress in the analysis, the tests are overestimated by from 0.8 to 7.1 percent, while using the compressive yield stress, they are underestimated by from 0.6 to 9.7 percent, with all results on the conservative side.

Thus using the effective width approach and the tensile yield stress resulted in unconservative ultimate loads, even though conservative values of k were used for the columns. As

is to be expected for steels such as this, with a large difference between the compressive and tensile yield stresses, it is more accurate to base the effective width approach on the compressive than on the tensile yield stress.

6.5 Conclusions

(1) The effective width approach, utilizing Winter's effective width expression, has been developed to include the effects of local buckling, inelastic column behavior, and strain hardening in the corners due to cold working. It is applicable to both the stiffened and unstiffened columns in this investigation, and it has been shown to yield good predictions of the ultimate strength of these columns.

(2) The effective width expression developed by Winter for stiffened elements is shown also applicable to the unstiffened elements in this investigation. For the strengths of the stub columns containing unstiffened elements, the expression is shown to give results on the conservative side, with a maximum of 10.7 percent below the test strength. This compares with the columns with stiffened elements which were also conservatively modeled with the effective width expression, with a maximum of 6.9 percent below the test strength.

(3) In calculating the column strength governed by overall buckling, the reduction in stiffness due to local buckling of the plate components must be considered. This is done by using an effective section to calculate the cross-section properties, as shown in Fig. 6.1 for the stiffened sections and Fig. 6.2 (b) for the unstiffened sections. It is shown that using a

stiffness based on the full section can result in failure loads as much as 50 percent higher than using that based on the effective section, which gives much better results.

(4) The effect that the k factor, which accounts for the plate edge conditions, has on the stiffened sections is not great. The range of possible k values for stiffened elements, from 4.00 to 6.97, is not large, and thus the variation in the calculated ultimate strengths due to varying k values is not large. If the low value of 4.00 is used, the results from the effective width approach are somewhat better in the range of moderate slenderness ratios, from approximately 50 to 125, than if a higher value computed from the behavior of the stub columns is used. In the range of low slenderness ratios, the value computed from the stub columns yields somewhat better results. The value of 4.00 is thought best for all columns in this investigation since it is in nearly all cases conservative, and where unconservative, the maximum difference is less than 9.2 percent.

(5) The effect that the k factor has on the unstiffened sections is much greater than for the stiffened sections since the range of possible k values is much greater, from 0.425 to 1.277. Taking the minimum value of k produces ultimate strengths that are often considerably on the conservative side, as much as 39.3 percent. It is thus better to use k values which better account for the actual plate edge conditions. For U-2, U-3, and U-4, the k values computed from the stub column tests, based on the stress at which local buckling was observed,

yield results which are in most cases conservative, and where unconservative, by no more than 4.1 percent; the maximum difference on the conservative side is 14.7 percent of the test value. For U-1, while local buckling was not observed prior to attainment of the yield stress, the effective width approach indicates that the section is not fully effective at all loads because the effective width expression, Eq. 6-7, approximates the lower values from tests and allows for some imperfections in the plate elements. For U-1, the approach is in all cases conservative, with the test values no more than 13.5 percent above the calculated value. The values, assuming that the section is not subject to local buckling and thus fully effective at all loads, is as much as 6 percent higher than the test values. Approximating U-1 with the effective width approach with the assumed k is conservative, but not excessively so, indicating that, as for U-2, U-3, and U-4, the approach is a good method for predicting the ultimate strength of the sections with unstiffened elements tested in this investigation.

(6) Comparisons to test results of four experimental investigations by others has generally shown that the effective width approach can be applied to a broader range of sections than those tested in this investigation. Assumptions were necessary in applying the effective width approach to other test data, some of which can be expected to result in errors, and in some cases it was not possible to account for some of the test results. Skaloud and Zörnerová's tests indicate that in the range of interaction, the effective width approach

yields good results with maximum variations of 5.4 percent above and 10.6 percent below. For their stub columns, the effective width approach was as much as 21.6 percent on the conservative side, which is probably due to strain hardening or cold-working effects or both. Their longer columns were considerably below the Euler buckling stress predicted by the effective width approach, as much as 41 percent. The effective width approach gave predictions that ranged from 15.1 percent below to 9.4 percent above the tests of Deliege, Baar, and Hick. Uribe's tests on sections with stiffened elements were predicted conservatively by the effective width approach by up to 12.2 percent. His sections with unstiffened elements were predicted up to 17 percent unconservatively. Since one of his sections was very much like U-1 of this investigation which was conservatively predicted by the effective width approach, it appears that more investigation into sections with unstiffened elements may be desirable. Dhalla's work, which involved stub columns only, has shown that with high strength steel, with significantly different compressive and tensile yield strengths, the compressive yield stress is the better choice for use in the effective width approach. The tensile yield stress gave results generally on the unconservative side, with a maximum of 7.1 percent, and the compressive yield stress gave results on the conservative side in all cases, with a maximum of 9.7 percent.

Chapter 7

DESIGN METHOD

7.1 Basis for the Design Method

A design method based on the effective width approach has been developed for routine design use. It is relatively simple, and follows the method in the present AISI Specification, with modifications which arise from the evidence in preceding chapters.

The main difficulty in applying the effective width approach to routine design is the necessity to determine the tangent-modulus. In the Specification this is taken care of by approximating the tangent-modulus formula in the inelastic range with the so-called CRC equation, which is given in Chapter 4 as Eq. 4-3. In the elastic range, the Euler formula, Eq. 4-2, applies. These same two formulas are used here as the basis of the present design method.

Essentially two differences exist between the Specification design method and the proposed method. The first treats unstiffened elements by limiting the stress to prevent excessive out-of-plane deformations. The design method proposed here utilizes the full postbuckling strength of unstiffened as well as stiffened elements by employing for both types of elements the effective width expression presently used only for stiffened elements. This is done by appropriate changes to account for the different edge conditions. The effective width expression for both stiffened and unstiffened elements is given

by Eq. 6-7, with the limiting width-thickness ratio, up to which the element is fully effective, given in Eq. 6-8. These two equations reduce to the equations in the Specification for stiffened elements by substitution of 4.00 for k and application of the safety factor of 1.67 to the stress. For stiffened elements, k can theoretically range from 4.00 to 6.97, with k equal to 4.00 a satisfactory and conservative value for design. For unstiffened elements, k varies over a wider range, from 0.425 to 1.277, and a value of k equal to 0.50 is generally conservative since the lower value which applies to simply supported sides is not really achievable in real structures. As shown in the effective width approach in the previous chapter, a substantial improvement is made with a more accurate determination of k for unstiffened elements. Thus, it is thought that though a minimum value of k = 0.5 should be specified, the option should be left to the designer to determine and use a more accurate value. This proposal for unstiffened elements is based on tests with width-thickness ratios from 16.2 to 29.1, and further tests should be conducted to check ratios higher than these.

The second difference between the Specification method and the proposed design approach is the consideration of the reduced stiffness due to local buckling in the latter. This is achieved by utilizing for both area and moment of inertia an effective section, based on the effective widths of the separate component elements, as was done in the effective width approach. This means that the effective portion of the various elements depends

on the buckling stress and also should be so located that they result in a stiffness that closely approximates the actual stiffness of the section with respect to flexural buckling. Thus, for elements perpendicular to the axis about which buckling occurs, the area should be distributed in some manner that reflects the actual non-uniform stress distribution, such as in the assumed linear distribution shown in Chapter 6 for the unstiffened elements. For elements parallel to the axis about which flexural buckling occurs, the manner of distributing the effective area is inconsequential, as shown in Chapter 6.

The next section contains the design approach followed by the comparison of the proposed design approach with the sections studied in this investigation. Design examples are given in Appendix B. A Computer program based on the method is given in Appendix D.

7.2 Proposed Design Method for Axially Loaded Compression Members

7.2.1 Effective Design Width

The effective width of an element, either stiffened or unstiffened, is given by:

$$\frac{b}{t} = 0.95\sqrt{\frac{kE}{f}}\left(1.0 - 0.209\,\frac{t}{w}\sqrt{\frac{kE}{f}}\right) \qquad 7\text{-}1$$

where b is the effective width in in, t the element thickness in in, w the actual element width in in, E the modulus of elasticity in ksi, equal to 29,500 ksi for steel, and f the maximum, or edge, stress in the element in ksi. k is a factor which accounts for the edge conditions, and unless determined by experimental or analytical means is taken as 4.00 for

stiffened elements and 0.50 for unstiffened elements. This equation is the same as Eq. 6-7.

The limiting value of w/t, up to which the element is fully effective, is given by:

$$\left(\frac{w}{t}\right)_{lim} = 0.64\sqrt{\frac{kE}{f}} \qquad 7\text{-}2$$

This is the same as Eq. 6-8.

For stiffened elements, with k = 4.00 and E = 29500 ksi, Eqs. 7-1 and 7-2 become:

$$\frac{b}{t} = \frac{326}{\sqrt{f}}\left[1.0 - \frac{71.3}{\left(\frac{w}{t}\right)\sqrt{f}}\right] \qquad 7\text{-}1\ a$$

$$\left(\frac{w}{t}\right)_{lim} = \frac{221}{\sqrt{f}} \qquad 7\text{-}2\ a$$

and for unstiffened elements, with k = 0.50:

$$\frac{b}{t} = \frac{115}{\sqrt{f}}\left[1.0 - \frac{25.2}{\left(\frac{w}{t}\right)\sqrt{f}}\right] \qquad 7\text{-}1\ b$$

$$\left(\frac{w}{t}\right)_{lim} = \frac{78}{\sqrt{f}} \qquad 7\text{-}2\ b$$

7.2.2 Effective Section Properties

The effective section properties are based on the effective areas of the individual elements as determined in Section 7.2.1.

The effective area is:

$$A_{eff} = \sum b_i t_i + \sum A_{cj} \qquad 7\text{-}3$$

where b_i is the effective width of the i^{th} flat determined from Eq. 7-1, t_i is the thickness of the i^{th} flat, and A_{cj} is the

area of the j^{th} corner.

The effective moment of inertia is:

$$I_{eff} = \sum I_{fi} + \sum I_{ci} \qquad 7\text{-}4$$

where I_{fi} is the moment of inertia of the effective portion of the i^{th} flat about the pertinent principal axis of the total cross section and I_{ci} is the moment of inertia of the j^{th} corner about the same axis. When the flat is not fully effective, the effective portion of the flat is to be distributed as follows:

(a) Stiffened element, either parallel or perpendicular to buckling axis: Half of effective area is to be located at each edge, as shown in Fig. 7.1 (a).

(b) Unstiffened element, parallel to buckling axis: All of effective area is to be located at edge connected to the adjoining element as shown in Fig. 7.1 (b).

(c) Unstiffened element, perpendicular to buckling axis: If the effective area is equal to or greater than half of the full area, the effective area is to be decreased linearly from thickness t_i at the edge with the adjoining element to the free edge, as shown in Fig. 7.1 (c). If the effective area is less than half of the full area, it is to be distributed linearly between the edge with the adjoining element and the free edge with thickness of the effective area at the stiffened edge less than the real thickness and decreasing to zero at the free edge, as shown in Fig. 7.1 (d).

The effective radius of gyration is:

$$r_{eff} = \sqrt{\frac{I_{eff}}{A_{eff}}} \qquad 7\text{-}5$$

7.2.3 Stress on an Axially Loaded Compression Member Not Subject to Torsional-Flexural Buckling

The ultimate axial stress F_{ae} on the effective area of a compression member which is not subject to torsional-flexural buckling shall not exceed the following values:

If $F_{ae} = P/A_{eff}$ is less than $F_y/2$:

$$F_{ae} = \frac{\pi^2 E}{\left(\frac{KL}{r_{eff}}\right)^2} \qquad 7\text{-}6$$

If $F_{ae} = P/A_{eff}$ is greater than $F_y/2$:

$$F_{ae} = F_y - \frac{(F_y)^2}{4\pi^2 E}\left(\frac{KL}{r_{eff}}\right)^2 \qquad 7\text{-}7$$

If $F_{ae} = P/A_{eff}$ is less than the minimum value of F_{eff} computed for each element as follows:

$$F_{eff} = \frac{0.41\ kE}{\left(\frac{w}{t}\right)^2} \qquad 7\text{-}8$$

the section is fully effective and $A_{eff} = A$ and $r_{eff} = r$.

The average stress on the full, unreduced cross-section is then:

$$F_a = F_{ae}\frac{A_{eff}}{A} \qquad 7\text{-}9$$

This is then divided by the safety factor to obtain the allowable stress.

In the above equations, P is the column load in kips, F_y the material yield stress in ksi, A the full area of the cross-section in in^2, K the effective length factor, L the unbraced

length of the column in in, and F_{eff} is the maximum stress at which the element is fully effective. Appendix A contains the background for Eqs. 7-6 through 7-9.

7.2.4 Method of Solution

To find the average compressive stress F_a, given the column length and cross-section dimensions, the procedure is as follows:

Compute the minimum value of F_{eff} from Eq. 7-8.

If the minimum F_{eff} is equal or greater than F_y, the section is fully effective at all loads and $r_{eff} = r$. The procedure is then: (1) Compute the slenderness ratio KL/r; (2) If KL/r is equal or greater than $\sqrt{2\pi^2E/F_y}$, the slenderness ratio at which the Euler stress is equal to $F_y/2$, Eq. 7-6 gives the stress F_{ae}; (3) If KL/r is less than $\sqrt{2\pi^2E/F_y}$, Eq. 7-7 gives the stress F_{ae}.

If the minimum F_{eff} is less than F_y, the procedure is: (1) Assume a reasonable value for $F_{ae} = P/A_{eff}$, the stress on the effective section; (2) If the assumed F_{ae} is less than the minimum F_{eff}, compute F_{ae} from either Eq. 7-6 or 7-7 using $r_{eff} = r$, depending on which governs, if the assumed F_{ae} is greater than the minimum F_{eff}, compute r_{eff} as outlined in Sections 7.2.1 and 7.2.2 with $f = P/A_{eff}$ and then calculate F_{ae} from either Eq. 7-6 or 7-7, depending on which governs; (3) If F_{ae} is not equal to the assumed $F_{ae} = P/A_{eff}$, repeat steps (1) through (3).

The average ultimate stress is then computed from Eq. 7-9, and the ultimate column load is:

$$P = F_a A \qquad 7\text{-}10$$

7.3 Comparison of Design Method with Tests

The data from the tests of this investigation is compared with the design approach in Figs. 7-2 through 7-5 for the stiffened sections and in Figs. 7-6 through 7-9 for the unstiffened sections. Numerical values are given in Tables 7-1 and 7-2. For convenience of presentation, these figures show the average stress on the full unreduced column cross-section at failure versus the slenderness ratio based on the full radius of gyration and for a factor of safety of 1.00. Both the minimum recommended k values and those computed from the stub column tests, based on the stress at which local buckling occurred, are used.

For the stiffened sections, with k equal to 4.00, the predicted loads are in all but one case conservative, with a maximum difference between the design approach and the tests of 13.3 percent of the test value. In the unconservative case, the variation is only 0.7 percent. Using the values of k determined from the stub columns, the design approach is not always conservative, and the variation ranges from 12.5 percent below to 9.5 percent above. Thus as was determined for the effective width approach as applied to stiffened elements, using k equal to 4.00 is simpler and safer, though not quite as economical as using more realistic k values.

For the unstiffened sections, with k equal either to 0.50 or to the value determined from the stub column tests, the design approach is conservative in all cases. With k equal to 0.50, the variation ranges from 1.4 to 33.8 percent of the test

value. With the k values determined from the stub column tests, the variation ranges from 2.2 to 25.1 percent. This variation is large, but not entirely unreasonable when it is remembered that the design method (Eq. 7-7) implies fairly gradual yielding steels, while the steel for the test columns was of a rather sharp-yielding nature. Thus, the test columns remained elastic, and maintained a larger stiffness, EI, to a higher load level than if the steel were of a more gradual yielding nature.

7.4 Conclusions

(1) A simple, straightforward design method is presented which is modeled after the effective width approach.

(2) Comparison with the test data from this investigation shows that with the minimum k values of 4.00 for stiffened sections and 0.50 for unstiffened sections, the method is in all but one case conservative; where unconservative, the difference between the test and predicted value is less than one percent. The maximum variations range from 2.4 to 13.3 percent of the test values for the stiffened sections and from 1.4 to 33.8 percent for the unstiffened sections.

(3) Better agreement is obtained when using more realistic k values determined from the stub column tests. In this case for the stiffened sections, the variations range from 12.5 percent on the unconservative side to 9.5 percent on the conservative side. For the unstiffened sections, the design method is always conservative, with a variation of from 2.2 to 25.1 percent.

(4) The best results are obtained with k equal to 4.00 for

the stiffened sections and a value determined to model more closely the actual edge conditions for the unstiffened sections. With these k values, the design method eliminates the large degree of unconservatism in the present AISI Specification approach for stiffened sections with relatively low Q values as shown in Chapter 4; for these the Specification now gives values as much as 52.2 percent of the test value on the unconservative side. The design method proposed here also significantly decreases the excessive conservatism for the unstiffened sections, from a present maximum of 47.9 percent of the test value to a maximum of 25.1 percent.

(5) As shown, the design approach applied to the unstiffened sections is not as accurate as applied to the stiffened sections. This is felt to be a consequence of using the CRC column formula and is not caused by the use of effective widths. This is so because when the effective width approach was utilized with the tangent-modulus formula (Chapter 6), it yielded comparably accurate results for the unstiffened and stiffened sections.

(6) The simplified design method of this chapter, while less laborious and better suited for use in connection with existing design specifications, can be significantly less accurate, though conservative, than the explicit tangent modulus analysis of Chapter 6.

Chapter 8

SUMMARY AND CONCLUSIONS

The purpose of this investigation has been to study both experimentally and analytically the behavior of cold-formed steel compression members subject to local and overall buckling. The impetus for the study was to check the approach for the design of these sections in the present American Iron and Steel Institute "Specification for the Design of Cold-Formed Steel Structural Members," and if necessary to propose a revised or entirely new approach for design.

A review of the literature on the interaction of local and overall buckling has shown that the work done has been quite limited both in the application of rigorous analysis to the subject and in the types of sections considered. In fact, from the theoretical point of view, even the behavior of isolated compressed plates in the latter stages of postbuckling is not fully understood.

An extensive series of tests on full scale cold-formed steel columns, including both stiffened and unstiffened elements, has been carried out. These, when compared with the design approach in the 1968 AISI Specification, demonstrate clearly the shortcomings of the Specification approach. For stiffened sections, the approach yields good results for columns in which local buckling occurs at a stress that is close to the yield stress. However, as the stress at which local buckling occurs becomes lower, due primarily to greater

width-thickness ratios, and thus as the postbuckling range becomes larger, the approach in the Specification becomes unconservative. The degree of unconservatism can be quite large, with the Specification value as much as 1.5 times the test value, indicating that refinement is both desirable and necessary.

For the unstiffened sections tested, the approach in the Specification is quite conservative, with calculated values as small as one-half of the test values. This is primarily due to the limit that the Specification places on the stress on unstiffened elements in order to limit out-of-plane distortions. For the sections tested, the out-of-plane distortions were found negligible until failure occurred. Thus the treatment of unstiffened elements in the present Specification needs improvement, which will result in substantial design economies.

The attempt of applying a "rigorous" analytical approach to the sections composed of stiffened elements, which had large postbuckling ranges, was not successful. This was primarily attributable to shortcomings in the analytical treatment of the advanced postbuckling behavior of plates.

Since the "rigorous" analytical approach was not successful, a semi-empirical approach was developed. This method, called the effective width approach, has proved successful. Using minimum values of k, which account for the edge conditions of the plate elements, the results for the stiffened sections were in nearly all cases conservative, by no more than 12.6 percent, and where unconservative, by no more than 9.2

percent. For the unstiffened sections, the results are always conservative, with a maximum difference of 39.3 percent of one test value. Using more realistic k values determined from the stub column tests, the results for the stiffened sections ranged from 17.9 percent on the unconservative side to 6.9 percent on the conservative side. For the unstiffened sections, the results were almost always conservative, by no more than 14.7 percent, and where unconservative, by no more than 4.1 percent. The effective width approach has also been compared with test results from other investigations, and has produced results generally within the above percentages. One exception was with sections with unstiffened elements in Uribe's work; for these using the minimum k value, the results were up to 17 percent on the unconservative side, which does not seem consistent with the other results in this investigation. Other exceptions were noted, but were not thought valid due to the assumptions necessary in applying the effective width approach to test results of other investigations.

Pertaining to the AISI Specification, this investigation has shown that two changes should be made. First, for sections which are significantly affected by local buckling, the stiffness, EI, which resists overall, or flexural, buckling must be reduced in the range in which local buckling interacts with overall buckling. This means using effective values for I, A, and r rather than the full values now used in connection with the Q-method. Secondly, for sections with unstiffened elements which have width-thickness ratios up to approximately 30, the

present Specification approach of limiting the stress in order to prevent excessive out-of-plane distortions is unrealistic. For width-thickness ratios in this range, the out-of-plane distortions have been shown to be negligible until failure, and thus the full postbuckling range can be utilized for substantial economies. The effective width approach originally developed for sections composed of stiffened elements is directly applicable to sections composed of unstiffened elements. However, more care in choosing k values to represent the plate element edge conditions is necessary for sections composed of unstiffened elements than for those composed of stiffened elements.

The proposed design method is similar to the present approach in the Specification, with the exception that it takes into consideration the two changes recommended above. Using minimum k values, the results when compared to the sections tested in this investigation are in all but one case conservative; where unconservative, the difference between the test and predicted value is less than one percent. The maximum discrepancies are 13.3 and 33.8 percent of the test values for the stiffened and unstiffened sections, respectively. Using k values determined from the stub column tests, the variation of the design approach values from the test values ranges from 12.5 percent above to 9.5 percent below for the stiffened sections. For the unstiffened sections, the design approach is always conservative, with a maximum variation of 25.1 percent.

No research investigation is complete and all encompassing. In fact, any investigation ought to turn up further avenues of interest and raise new questions. This investigation, while answering some questions, has certainly not covered the entire field concerning cold-formed compression members subject to local and overall buckling. The following contains a few of the more important areas that are thought to need further research.

As has been pointed out by many different researchers dealing with numerous topics in thin-walled behavior, further work is needed to develop a theory that adequately treats the postbuckling behavior of plates with large width-thickness ratios in the later stages of postbuckling. If a theory were available to cover the complete range of postbuckling of such plates, approaches such as the rigorous analytical approach attempted in this investigation and discussed in Chapter 5 might prove more successful for the studied stiffened sections.

One shortcoming of the present investigation, which has already been mentioned, is that the range of width-thickness ratios for the unstiffened elements studied is not as great as the range likely to be encountered in thin-walled construction. The present AISI Specification allows unstiffened elements with width-thickness ratios as high as 60, while the maximum width-thickness ratio in this investigation was only 29. Thus, it is thought necessary, particularly from the point of view of studying the magnitude of the out-of-plane distortions that can occur, to study unstiffened sections with width-thickness

ratios at least as high as 60.

Another area of future study involves sections composed of elements with stiffeners, either stiffened elements with intermediate stiffeners or elements with edge stiffeners. The effect that stiffeners have on element behavior is not always clearly understood, though the present AISI Specification includes some guidelines. It would be worthwhile to check these guidelines with the effective width approach in order to see if modification is necessary.

The design method proposed in this investigation, as well as that in the present AISI Specification, is based on the CRC column formula, which was developed for hot-rolled structural steel members. Though the results from the formula are not bad, further improvement would be desirable. It appears from the test data in this investigation that the shape of the column curve from the CRC formula is not of the same shape as that of the curve through the test points. That is, the CRC formula curve is more rounded while the test data seem to level more closely to a plateau in the range of low slenderness ratios. It is felt, therefore, that the general form of the CRC column formula should be studied to see more exactly where it applies and to see whether another formula might not be better suited to cold-formed structural members.

REFERENCES

1. Specification for the Design of Cold-Formed Steel Structural Members, American Iron and Steel Institute, New York, N.Y., 1968.

2. Uribe, J., and Winter, G., "Cold-Forming Effects in Thin-Walled Steel Members," Effects of Cold Work in Cold-Formed Steel Structural Members, Cornell Engineering Research Bulletin, No. 70-1, Ithaca, New York, 1970.

3. Johnson, A. L., "The Structural Performance of Austenitic Stainless Steel Members," Dept. of Structural Engineering, Report No. 327, Cornell University, November 1966.

4. Wang, S. T., "Tempered Austenitic Stainless Steel: Materials Properties and Structural Performance," Dept. of Structural Engineering, Report No. 334, Cornell University, July 1969.

5. Graves Smith, T. R., "The Ultimate Strength of Locally Buckled Columns of Arbitrary Length," Ph.D. Thesis, Cambridge University, Cambridge, England, 1966.

6. Klöppel, K., and Schubert, J., "Die Berechnung der Traglast mittig und aussermittig gedrückter, dünnwandiger Stützen mit kastenförmigem Querschnitt in überkritischen Bereich," Veröffentlichung des Institutes für Statik und Stahlbau der Technischen Hochschule Darmstadt, Darmstadt, 1971.

7. Johnston, B. G., ed., Design Criteria for Metal Compression Members, John Wiley & Sons, New York, N.Y., 2nd Edition, 1966.

8. Timoshenko, S. P., and Gere, J. M., Theory of Elastic Stability, McGraw-Hill, New York, N.Y., 1961.

9. Shanley, F. R., "Inelastic Column Theory," The Journal of the Aeronautical Sciences, Vol. 14, May 1947, pp. 261-267.

10. Duberg, J. E., and Wilder, T. W., "Inelastic Column Behavior," NACA Report 1072, 1952.

11. Batterman, R. H., and Johnston, B. G., "Behavior and Maximum Strength of Metal Columns," J. of the Structural Div., ASCE, Vol. 93, April 1967, pp. 205-230.

12. Koiter, W. T., "Introduction to the Postbuckling Behavior of Flat Plates," Colloquium on the Postbuckling Behavior of Plates used in Metal Structures, Univ. of Liege, Belgium, 1963, pp. 17-35.

13. Bulson, P. S., The Stability of Flat Plates, American Elsevier, 1969.

14. Stowell, E. Z., "Compressive Strength of Flanges," NACA Report 1029, 1951.

15. Mayers, J., and Budiansky, B., "Analysis of Behavior of Simply Supported Flat Plates Compressed Beyond the Buckling Load into the Plastic Range," NACA Tech. Note 3368, 1955.

16. Qureshi, I. H., "Strength of Thin Flat Plates under Lengthwise Compression," Pakistan Engineer, Vol. 8, Oct. 1968, pp. 739-776.

17. Jombock, J. R., and Clark, J. W., "Postbuckling Behavior of Flat Plates," J. of the Structural Div., ASCE, Vol. 87, June 1961, pp. 17-33.

18. Winter, G., "Commentary on the 1968 Edition of the Specification for the Design of Cold-Formed Steel Structural Members," American Iron and Steel Institute, New York, N.Y., 1970.

19. Bijlaard, P. P., and Fisher, G. P., "Interaction of Column and Local Buckling in Compression Members," NACA Tech. Note 2640, 1952.

20. Bijlaard, P. P., and Fisher, G. P., "Column Strength of H-Sections and Square Tubes in Postbuckling Range of Component Plates," NACA Tech. Note 2994, 1953.

21. Scidenfaden, J., "Interaction in the Post-Buckled Range for the Channel Section," Z. f. Flugwiss, Vol. 2, 1954, p. 169.

22. Pfluger, A., "Thin-Walled Compression Members," Part III, Technische Hochschule, Hannover, March 1961.

23. Graves Smith, T. R., "The Post-Buckled Strength of Thin-Walled Columns," Int. Assoc. Bridge and Structural Engineering, Eighth Congress, Final Report, 1968, pp. 311-320.

24. Graves Smith, T. R., "The Ultimate Strength of Locally Buckled Columns of Arbitrary Length," Thin Walled Steel Structures, Their Design and Use in Building, Crosby Lockwood and Son, London, 1968.

25. Bulson, P. S., "Local Stability and Strength of Structural Sections," Thin Walled Steel Structures, Their Design and Use in Building, Crosby Lockwood and Son, London, 1969.

26. Uribe, J., "Aspects of the Effects of Cold-Forming on the Properties and Performance of Light-Gage Structural Members," Dept. of Structural Engineering, Report No. 333, Cornell University, May 1969.

27. Karren, K. W., "Corner Properties of Cold-Formed Steel Shapes," J. of the Structural Div., ASCE, Vol. 93, Feb. 1967, pp. 401-432.

28. Skaloud, M., and Zörnerová, M., "Experimental Investigation into the Interaction of Buckling of Compressed Thin-Walled Columns with Buckling of their Plate Elements," ACTA Technica CSAV, No. 4, 1970, pp. 389-424.

29. Klöppel, K., Schmied, R., and Schubert, J., "Die Traglast mittig und aussermittig gedrückter dünnwandiger Kastenträger unter Verwendung der nichtlinearen Beultheorie. Teil I. Analytische Behandlung," Der Stahlbau, Vol. 35, 1966, p. 321.

30. Klöppel, K., Schmied, R., and Schubert, J., "Die Traglast mittig und aussermittig gedrückter Stützen mit kastenförmigem Querschnitt im überkritischen Bereich unter Verwendung der nichtlinearen Beultheorie. Teil II. Experimentelle Untersuchungen, Vergleich der experimentellen und theoretischen Ergebnisse," Der Stahlbau, Vol. 38, 1969, p. 9.

31. Deliege, J., Baar, S., and Hick, F., "Flambement des Colonnes en Profiles Minces Compte Tenu du Veilement Local des Parois," Station d'Essais et de Recherches de la Construction Métallique, Liege, March 1969.

32. Hick, F., "Flambement des Colonnes en Profiles Minces Compte Tenu du Voilement Local des Parois," Station d'Essais et de Recherches de la Construction Métallique, Liege, August 1969.

33. Pekoz, T. B., "Torsional-Flexural Buckling of Thin-Walled Sections Under Eccentric Load," Dept. of Structural Engineering, Report No. 329, Cornell University, April 1967.

34. Winter, G., "Strength of Thin Steel Compression Flanges," Trans. ASCE, Vol. 112, 1947. Also in Cornell University Engineering Experimental Station, Reprint No. 32, October 1947.

35. Winter, G., "Thin-Walled Structures - Theoretical Solutions and Test Results," Int. Assoc. Bridge and Structural Engineering, Eighth Congress, Prel. Publ., pp. 1001-112, 1968.

36. Karren, K. W., and Winter, G., "Effects of Cold-Forming on Light-Gage Steel Members," J. of the Structural Div., ASCE, Vol. 93, Feb. 1967, pp. 433-469.

37. Ramberg, W., and Osgood, W. R., "Description of Stress-Strain Curves by Three Parameters," NACA Tech. Note 902, 1943.

38. Stowell, E. Z., and Lundquist, E. E., "Local Instability of Columns with I-, Z-, Channel, and Rectangular Sections," NACA Tech. Note 743, 1939.

39. Stowell, E. Z., Heimerl, G. J., Libove, C., and Lundquist, E. E., "Buckling Stresses for Flat Plates and Sections," Proc. ASCE, Vol. 77, July 1951, pp. 1-31.

40. Dhalla, A. K., "Influence of Ductility on the Structural Behavior of Cold-Formed Steel Members," Dept. of Structural Engineering, Report No. 336, Cornell University, June 1971.

Appendix A

BASIS OF DESIGN METHOD

In the region of small and moderate slenderness, i.e., the region of inelastic flexural buckling and the interaction of local and overall buckling, the AISI Specification utilizes the so-called CRC column formula, Eq. 4-3. This is used for the present design method, with the exception that it is written in terms of the effective section properties given in Section 7.2.2. Thus:

$$F_{ae} = F_y - \frac{(F_y)^2}{4\pi^2 E}\left(\frac{KL}{r_{eff}}\right)^2 \qquad \text{A-1}$$

This equation is the same as Eq. 7-7 and does not include any safety factor.

In the region of large slenderness, where the buckling is elastic, the Euler stress, Eq. 4-2, governs and is used for the present design method, with the exception that it is written in terms of the effective section properties:

$$F_{ae} = \frac{\pi^2 E}{\left(\frac{KL}{r_{eff}}\right)^2} \qquad \text{A-2}$$

This is the same as Eq. 7-6.

The slenderness ratio at the intersection of these two equations is obtained by equating their right-hand sides and solving:

$$\left(\frac{KL}{r_{eff}}\right)_{lim} = \sqrt{\frac{2\pi^2 E}{F_y}} \qquad \text{A-3}$$

The corresponding stress at the intersection is found by substituting the value of the slenderness ratio in Eq. A-3 into either Eq. A-1 or A-2 and solving:

$$\sigma_{lim} = \frac{F_y}{2} \qquad \text{A-4}$$

This limiting stress applies whether the section is fully effective or partially effective, though in the latter it corresponds to the stress on the effective section.

Whether or not a section is fully effective depends on the limit to the effective width expression given in Eq. 7-2 and as follows:

$$\left(\frac{w}{t}\right)_{lim} = 0.64\sqrt{\frac{kE}{\sigma_{max}}} \qquad \text{A-5}$$

This may be solved for the value of stress at which an element of given width-thickness ceases to be fully effective:

$$(\sigma_{max})_{lim} = \frac{0.41kE}{\left(\frac{w}{t}\right)^2} \qquad \text{A-6}$$

By checking all elements with this equation, the maximum stress at which the section is fully effective is found. Eq. A-6 corresponds to Eq. 7-8.

The design method is like that in the present Specification of the American Iron and Steel Institute with the exception that the governing equations are based on the effective section and the unstiffened elements are treated in the same manner as stiffened elements.

Appendix B

DESIGN METHOD EXAMPLES

B.1 Section with Stiffened Elements Subject to Local Buckling

For the column cross-section shown, made of two channels connected together to assure a complete bond between surfaces, with a length of 120. in, K equal to 1.00, and F_y equal to 42.0 ksi, the allowable load is desired based on a safety factor equal to 1.92.

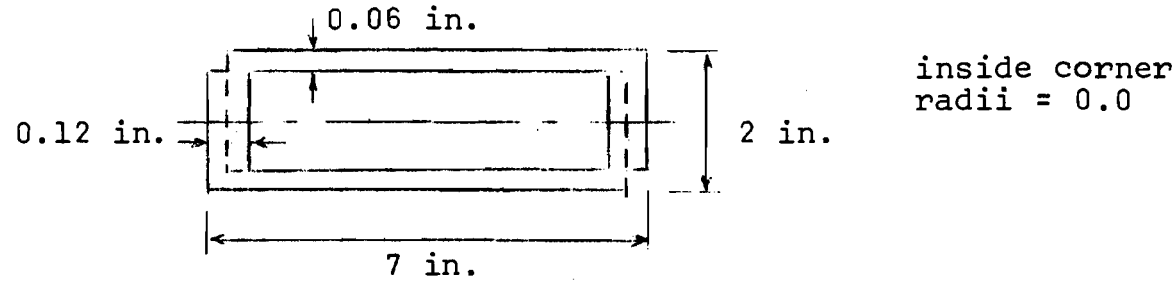

The section properties based on the full section are:

$$A = 1.29 \text{ in}^2$$

$$I = 0.924 \text{ in}^4$$

$$r = 0.845 \text{ in}$$

$$\frac{KL}{r} = \frac{120.0}{0.845} = 142$$

Since the section is made of stiffened elements, k is assumed equal to 4.00. The minimum value of F_{eff} is:

$$F_{eff} = \frac{0.41 \times 4.00 \times 29500.}{(\frac{6.76}{0.06})^2} = 3.8 \text{ ksi}$$

Therefore, the section is not fully effective at all loads.

The vertical elements have a width-thickness ratio below the limiting value at all stresses up to yield, while the hori-

zontal elements do not. The assumed effective section used to calculate A_{eff} and r_{eff} is then:

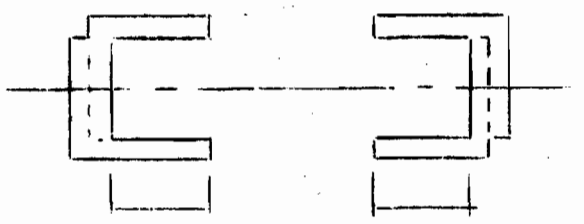

Assume that P/A_{eff} is equal to 5.0 ksi. This is the edge stress in the horizontal elements and also is equivalent to the stress on the effective section.

The effective width is calculated with Eq. 7-1:

$$\frac{b}{t} = 0.95\sqrt{\frac{4.00\times29500}{5.0}}\left[1.0-0.209\,\frac{.06}{(7.00-.24)}\sqrt{\frac{4.00\times29500}{5.0}}\right] = 105$$

Then the effective width is:

$$b = 105 \times 0.06 = 6.3 \text{ in.}$$

The effective section properties are:

$$A_{eff} = 4 \times 0.12 + 2 \times 6.3 \times 0.06 = 1.235 \text{ in}^2$$

$$I_{eff} = 2 \times \frac{1}{12} \times 0.12 \times (2.0)^3 + 2 \times 6.3 \times 0.06 \times (1.00-.03)^2$$

$$= 0.871 \text{ in}^4$$

$$r_{eff} = \sqrt{\frac{0.871}{1.235}} = 0.840 \text{ in}$$

The stress on the effective cross-section is then calculated with Eq. 7-6:

$$F_{ae} = \frac{\pi^2 \times 29500}{\left(\frac{1.0 \times 120.}{0.84}\right)^2} = 14.3 \text{ ksi}$$

For a second try, assume that P/A_{eff} is equal to 13.0 ksi. Then b/t = 75, A_{eff} = 1.02 in^2, I_{eff} = 0.665 in^4, and r_{eff} = 0.81 in. Using Eq. 7-6, the average stress on the effective cross-section is 13.2 ksi. This is close enough. The average stress on the full section is then computed from Eq. 7-9:

$$F_a = 13.2 \frac{1.02}{1.29} = 10.45 \text{ ksi}$$

The allowable stress on the full cross-section is 10.45/1.92 = 5.43 ksi, and the allowable load is:

$$P = 5.43 \times 1.29 = 7.0 \text{ kips}$$

B.2 Section with Unstiffened Elements Subject to Local Buckling

For the column cross-section shown, with complete bonding at the connected surface, a length of 70.0 in, K equal to 1.00, F_y equal to 42.0 ksi, and safety factor of 1.00, the column load is desired.

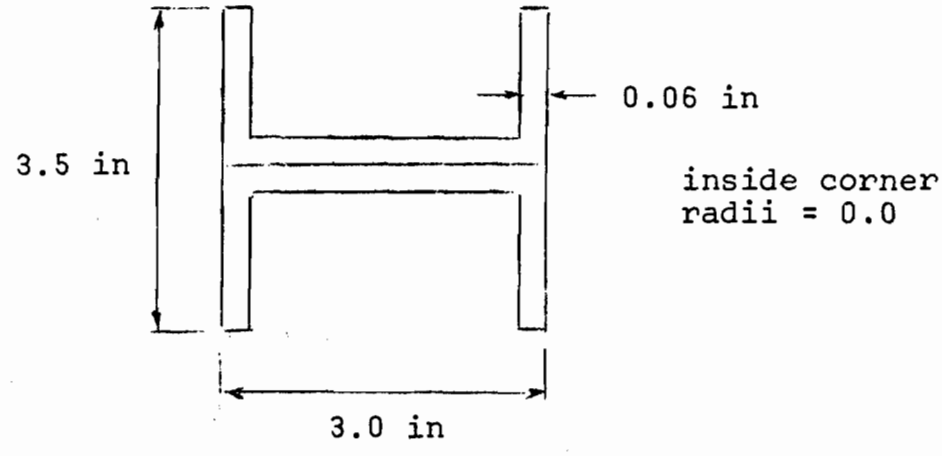

The section properties based on the full section are:

$$A = 0.766 \text{ in}^2$$

$$I = 0.429 \text{ in}^4$$

$$r = 0.748 \text{ in}$$

$$\frac{KL}{r} = 94$$

For the stiffened elements, k is assumed equal to 4.00, and for the unstiffened elements, k is assumed equal to 0.50.

The minimum value of F_{eff} is:

$$F_{eff} = \frac{0.41 \times 0.5 \times 29500}{(\frac{1.69}{0.06})^2} = 7.62 \text{ ksi}$$

Therefore, the section is not fully effective at all loads.

The horizontal element is fully effective at all stresses to yield, and the assumed effective section is:

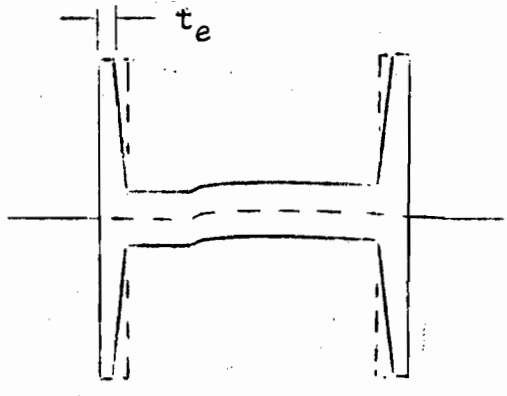

Assume that $P/A_{eff} = 25$ ksi. The effective width, Eq. 7-1, is:

$$\frac{b}{t} = 0.95\sqrt{\frac{0.5\times29500}{25.0}}\left(1.0 - 0.209\,\frac{0.06}{1.69}\sqrt{\frac{0.5\times29500}{25.0}}\right) = 19.0$$

$$b = 19.0 \times 0.06 = 1.14 \text{ in}$$

The effective area of the unstiffened elements is:

$$4 \times 1.14 \times 0.06 = 0.274 \text{ in}^2$$

The width of the effective area for the unstiffened element at the free end, t_e, is determined as follows:

$$\frac{.274}{4} = 1.69t_e + (0.06 - t_e)\frac{1.69}{2}$$

$$t_e = 0.021 \text{ in}$$

The effective properties are then:

$$A_{eff} = 0.274 + 0.12 \times 3.0 = 0.634 \text{ in}^2$$

$$I_{eff} = \frac{2}{12} \times 0.021 \times 3.5^3 + \frac{4}{12}(0.06 - 0.021) \times 1.69^3 = 0.213 \text{ in}^4$$

$$r_{eff} = \frac{0.213}{0.634} = 0.580 \text{ in}$$

The stress on the effective cross-section is then calculated with Eq. 7-7:

$$F_{ae} = 42.0 - \frac{(42.0)^2}{4\pi^2 \times 29500}\left(\frac{70}{.580}\right)^2 = 20.0 \text{ ksi}$$

For a second iteration, assume $P/A_{eff} = 22.0$ ksi. Then b = 1.19 in, $t_e = 0.025$ in, $A_{eff} = 0.646 \text{ in}^2$, $I_{eff} = 0.235 \text{ in}^4$, and $r_{eff} = 0.604$ in. Using Eq. 7-7, $F_{ae} = 21.6$ ksi. This is sufficiently close to the assumed f. The stress on the full section, from Eq. 7-9, is:

$$F_a = 21.6 \frac{0.646}{0.766} = 18.2 \text{ ksi}$$

The column load is:

$$P = 18.2 \times .766 = 13.95 \text{ kips}$$

B.3 Section with Both Stiffened and Unstiffened Elements Subject to Local Buckling

For the column cross-section shown, with length of 90 in, K equal to 1.00, F_y equal to 42.0 ksi, and a safety factor of 1.00, the column load is desired.

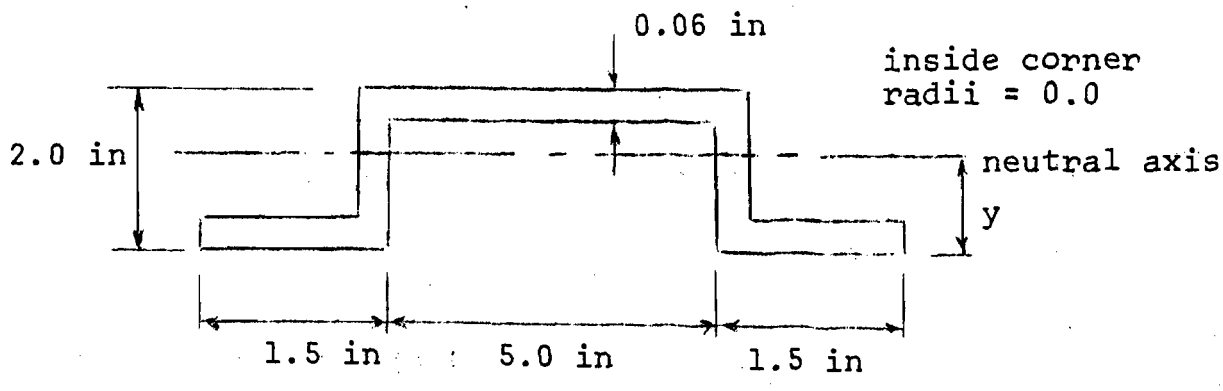

The section properties based on the full section are

$$A = 0.712 \text{ in}^2$$

$$y = 1.165 \text{ in}$$

$$I = 0.502 \text{ in}^4$$

$$r = 0.840 \text{ in}$$

$$\frac{KL}{r} = 107$$

For the stiffened elements, k is assumed as 4.00, and for the unstiffened elements, k is assumed as 0.50.

The value of F_{eff} for the horizontal element is:

$$(F_{eff})_s = \frac{0.41 \times 4.0 \times 29500}{(\frac{5.00}{0.06})^2} = 6.97 \text{ ksi}$$

Therefore, the section is not fully effective at all loads.

The vertical elements are fully effective at all stresses to yield, and the assumed effective section is:

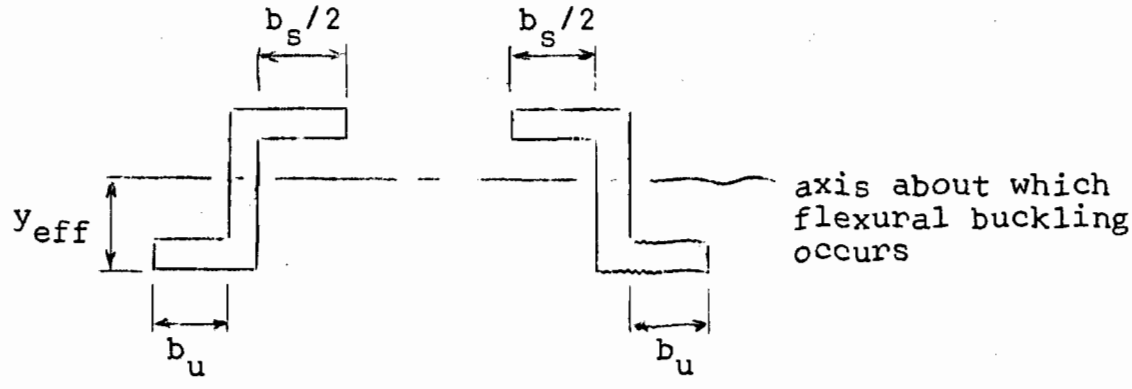

Assume that P/A_{eff} = 24 ksi. The effective widths, using Eq. 7-1 and using subscripts s and u for the stiffened and unstiffened elements, respectively, are:

$$\left(\frac{b}{t}\right)_s = 0.95\sqrt{\frac{4.0\times29500}{24.0}}\left[1.0 - 0.209\,\frac{.06}{5.0}\sqrt{\frac{4.0\times29500}{24.0}}\right] = 54.9$$

$$b_s = 54.9 \times 0.06 = 3.29 \text{ in}$$

$$\left(\frac{b}{t}\right)_u = 0.95\sqrt{\frac{0.5\times29500}{24.0}}\left[1.0 - 0.209\,\frac{.06}{1.44}\sqrt{\frac{0.5\times29500}{24.0}}\right] = 18.5$$

$$b_u = 18.5 \times 0.06 = 1.11 \text{ in}$$

The effective section properties are:

$$A_{eff} = 0.60(2 \times 1.11 + 3.29 + 4.00) = 0.571 \text{ in}^2$$

$$y_{eff} = \frac{0.06(1.97 \times 3.29 + 4.00)}{0.571} = 1.10 \text{ in}$$

$$I_{eff} = \frac{1}{12}\times.12\times2^3 + .12\times2(0.1)^2 + 3.29\times.06(0.87)^2 + 1.11\times0.12(1.07)^2$$

$$= 0.384 \text{ in}^4$$

$$r_{eff} = \sqrt{\frac{.384}{.571}} = 0.821 \text{ in}$$

The stress on the effective cross-section is then calculated from Eq. 7-7:

$$F_{ae} = 42 - \frac{(42)^2}{4\pi^2\times29500}\left(\frac{90}{.821}\right)^2 = 23.8 \text{ ksi}$$

This is nearly identical with the assumed f, and therefore, it is not necessary to repeat the process. The stress on the full section, Eq. 7-9, is:

$$F_a = 23.8 \frac{0.571}{0.712} = 19.1 \text{ ksi}$$

The column load is then:

$$P = 19.1 \times 0.712 = 13.6 \text{ kips}$$

Appendix C

PROGRAM FOR EFFECTIVE WIDTH APPROACH

This appendix contains the following:

(1) Program for the effective width approach based on Chapter 6. The program is limited to the two types of sections investigated in this project, i.e., the stiffened and unstiffened sections.

(2) Sample input for two column curves. The first is for section S-1 with k determined from the stub column test and I for the full section. The second is for section U-2 with k determined from the stub column test and I for the effective section.

(3) Sample output for the two column sections in (2). These are shown in Figs. 6.8 and 6.21.

(4) Flow charts for the major portions of the program. Flow charts are not given for the subroutines EFFW and EMOI since the procedure is straightforward and for RTMI since the routine is from the IBM System/360 Scientific Subroutine Package.

```
C
C
C                PROGRAM FOR EFFECTIVE WIDTH APPROACH
C
C
C
C        THIS PROGRAM DETERMINES THE COLUMN CURVE, ULTIMATE
C   STRESS ON FULL SECTION VERSUS SLENDERNESS RATIO BASED ON
C   FULL SECTION, FOR COLD-FORMED STEEL COLUMNS BASED ON THE
C   EFFECTIVE WIDTH APPROACH IN CHAPTER 6.  THE COLUMN MAY
C   OR MAY NOT BE SUBJECT TO LOCAL BUCKLING.  THE INPUT CON-
C   SISTS OF THE CHANNEL DIMENSIONS, MATERIAL PROPERTIES, AND
C   PARAMETERS NECESSARY FOR DEFINING THE EXTENT OF THE COL-
C   UMN CURVE DESIRED.
C
C        THE PROGRAM IS WRITTEN IN BASIC FORTRAN IV LANGUAGE.
C   THE ROUTINE FOR THE SOLUTION OF THE NONLINEAR EQUATION
C   IS FROM THE IBM SYSTEM/360 SCIENTIFIC SUBROUTINE PACKAGE.
C
C        THE PROGRAM AS IT IS PRESENTED HERE APPLIES TO ONLY
C   TWO COLUMN SECTIONS.  THE FIRST IS MADE OF TWO CHANNELS
C   CONNECTED AT THE FLANGES TO FORM A TUBULAR SECTION AND
C   CORRESPONDS TO THE STIFFEND SECTION IN THIS INVESTIGA-
C   TION.  THE SECOND IS MADE OF TWO CHANNELS CONNECTED
C   BACK-TO-BACK TO FORM AN H-SHAPED SECTION AND CORRESPONDS
C   TO THE UNSTIFFENED SECTION IN THIS INVESTIGATION.  THE
C   FIRST BUCKLES ABOUT THE AXIS PARALLEL TO THE SINGLE
C   THICKNESS ELEMENTS AND THE SECOND BUCKLES ABOUT THE AXIS
C   THROUGH THE DOUBLE THICKNESS ELEMENT.  IN THE FIRST, ONLY
C   THE SINGLE THICKNESS ELEMENT IS SUBJECT TO LOCAL BUCKLING
C   AND IN THE SECOND, ONLY THE CHANNEL FLANGES ARE SUBJECT
C   TO LOCAL BUCKLING.
C
C        THE PROGRAM FIGURES THE EFFECTS OF THE ROUNDED COR-
C   NERS IN DETERMINING THE SECTION PROPERTIES AND USES THE
C   FLAT WIDTHS EXCLUSSIVE OF FILLETS IN FIGURING THE EFFEC-
C   TIVE WIDTHS.
C
C        THE PROGRAM CONSIDERS THE STRAIN-HARDENING IN THE
C   CORNERS DUE TO COLD-WORKING BY ALLOWING FOR DIFFERENT
C   STRESS-STRAIN CURVES IN THE FLANGE, WEB, AND CORNERS.
C   THE STRESS-STRAIN CURVES ARE MODELED USING THE RAMBERG-
C   OSGOOD EQUATION, AND THE NECESSARY VARIABLES ARE DIS-
C   CUSSED IN CHAPTER 6.
C
C
C
C                          INPUT
C
C
C        ALL INPUT DATA AND OUTPUT DATA ARE IN KIPS AND
C   INCHES.  THERE ARE SIX TYPES OF INPUT CARDS, WHICH ARE
C   DEFINED AS FOLLOWS.  THE FORMAT IS GIVEN FOR EACH CARD,
C   AND THE INPUT VARIABLES ARE IN THE CORRECT ORDER.
```

```
C
C  FIRST INPUT CARD (I5) -
C         N        = NUMBER OF COLUMN SECTIONS TO BE ANALYZED
C
C     REPEAT THE FOLLOWING FOR EACH COLUMN SECTION TO BE
C     ANALYZED.
C
C  SECOND INPUT CARD (2F10.6,I5) -
C         SN       = SMALLEST STRAIN FOR ESTABLISHING THE
C                    COLUMN CURVE AS EXPLAINED IN SECTION
C                    6.2.3.4
C         SNI      = INCREMENT IN STRAIN TO BE ADDED TO THE
C                    PREVIOUS STRAIN
C         LI       = NUMBER OF INCREMENTS IN STRAIN
C
C  THIRD INPUT CARD (5F10.4,2I5) -
C         D        = TOTAL DEPTH OF CHANNEL SECTION
C         B        = TOTAL WIDTH OF CHANNEL SECTION
C         T        = THICKNESS OF CHANNEL
C         R        = INSIDE RADIUS OF CORNERS OF CHANNEL
C         CK       = EDGE FACTOR FOR ELEMENT SUBJECT TO LOCAL
C                    BUCKLING (FROM 4.00 TO 6.97 FOR STIF-
C                    FENED ELEMENTS AND FROM 0.425 TO 1.277
C                    FOR UNSTIFFENED ELEMENTS); FOR THE STIF-
C                    FENED SECTION THIS IS FOR THE SINGLE
C                    THICKNESS ELEMENT AND FOR THE UNSTIF-
C                    FENED SECTION IT IS FOR THE CHANNEL
C                    FLANGES
C         IEF      = EQUALS 1 IF THE FULL MOMENT OF INERTIA
C                    IS DESIRED IN CONJUNCTION WITH THE TAN-
C                    GENT MODULUS FORMULA AND 2 IF THE EFFEC-
C                    TIVE MOMENT OF INERTIA IS DESIRED (FOR
C                    UNSTIFFENED SECTIONS, THE EFFECTIVE
C                    MOMENT OF INERTIA IS BASED ON THE VARI-
C                    ABLE THICKNESS FLANGE ELEMENT)
C         IC         EQUALS 1 FOR STIFFENED SECTIONS AND 2
C                    FOR UNSTIFFENED SECTIONS
C
C  FOURTH INPUT CARD (3F10.4) -
C         F(1)     = YIELD STRESS FOR CHANNEL FLANGE
C         CN(1)    = EXPONENT FOR USE IN THE RAMBERG-OSGOOD
C                    EQUATION AS EXPLAINED IN SECTION 6.3.2
C                    FOR CHANNEL FLANGE
C         S1(1)    = STRESS AT INTERCEPT BETWEEN MATERIAL
C                    STRESS-STRAIN CURVE AND A LINE THROUGH
C                    THE ORIGIN WITH A SLOPE OF 0.7 TIMES THE
C                    INITIAL MODULUS OF ELASTICITY FOR THE
C                    CHANNEL FLANGE
C
C  FIFTH INPUT CARD (3F10.4) -
C         F(2)     = YIELD STRESS FOR CHANNEL WEB
C         CN(2)    = EXPONENT FOR USE IN THE RAMBERG-OSGOOD
C                    EQUATION AS EXPLAINED IN SECTION 6.3.2
C                    FOR CHANNEL WEB
```

```
C          S1(2)    = STRESS AT INTERCEPT BETWEEN MATERIAL
C                     STRESS-STRAIN CURVE AND A LINE THROUGH
C                     THE ORIGIN WITH A SLOPE OF 0.7 TIMES THE
C                     INITIAL MODULUS OF ELASTICITY FOR THE
C                     CHANNEL WEB
C
C   SIXTH INPUT CARD (3F10.4) -
C          F(3)     = YIELD STRESS FOR CHANNEL CORNERS
C          CN(3)    = EXPONENT FOR USE IN THE RAMBERG-OSGOOD
C                     EQUATION AS EXPLAINED IN SECTION 6.3.2
C                     FOR CHANNEL CORNERS
C          S1(3)    = STRESS AT INTERCEPT BETWEEN MATERIAL
C                     STRESS-STRAIN CURVE AND A LINE THROUGH
C                     THE ORIGIN WITH A SLOPE OF 0.7 TIMES THE
C                     INITIAL MODULUS OF ELASTICITY FOR THE
C                     CHANNEL CORNERS
C
C
C
C                          PROGRAM VARIABLES
C
C
C          THE FOLLOWING IS A LIST OF THE IMPORTANT VARIABLES
C   USED IN THE PROGRAM.  THE ARE BROKEN UP INTO THE PORTIONS
C   OF THE PROGRAM THEY OCCUR IN.  MANY VARIABLES ARE USED
C   THROUGHOUT THE PROGRAM.  THE VARIABLES FOR SUBROUTINE
C   RTMI ARE NOT DEFINED SINCE THE ROUTINE IS FROM THE IBM
C   SCIENTIFIC SUBROUTINE PACKAGE.
C
C   VARIABLES IN COLS
C          AEF      = AREA OF EFFECTIVE CROSS-SECTION
C          CL       = LENGTH AT WHICH A SECTION WITH A GIVEN
C                     STRESS DISTRIBUTION BUCKLES, BASED ON
C                     THE TANGENT-MODULUS FORMULA; THE EFFEC-
C                     TIVE LENGTH FACTOR IS ASSUMED AS 1.0
C          CLR      = SLENDERNESS RATIO CORRESPONDING TO CL
C                     AND RG
C          EI       = TANGENT-MODULUS TIMES EFFECTIVE MOMENT
C                     OF INERTIA FOR SECTION
C          EW       = EFFECTIVE WIDTH OF ELEMENT SUBJECT TO
C                     LOCAL BUCKLING
C          RG       = RADIUS OF GYRATION OF FULL CROSS-SECTION
C                     ABOUT WEAK AXIS
C          SA       = STRESS TIMES EFFECTIVE PORTION OF AREA
C          ST       = AVERAGE STRESS ON THE FULL CROSS-SECTION
C          TMI      = MOMENT OF INERTIA OF FULL CROSS-SECTION
C                     ABOUT WEAK AXIS
C          TOA      = AREA OF FULL CROSS-SECTION
C          W        = WIDTH EXCLUSSIVE OF FILLETS OF ELEMENT
C                     SUBJECT TO LOCAL BUCKLING
C
C   VARIABLES IN ROSSC AND EQVAL
C          A1,A2,A3= COEFFICIENTS OF RAMBERG-OSGOOD EQUATION
C                     WITH EVERYTHING SET TO ONE SIDE OF THE
```

```
C                     EQUAL SIGN
C          EQ       = VALUE OF RAMBERG-OSGOOD EQUATION
C          EQP      = VALUE OF RAMBERG-OSGOOD EQUATION FROM
C                     PREVIOUS TRIAL
C          ET       = TANGENT-MODULUS
C          SR       = STRESS
C          SR1      = LOWER BOUND STRESS FOR USE IN RTMI
C          SR2      = UPPER BOUND STRESS FOR USE IN RTMI
C
C   VARIABLES IN EFFW
C          EW       = EFFECTIVE WIDTH
C          WLI      = WIDTH UP TO WHICH THE ELEMENT IS FULLY
C                     EFFECTIVE
C
C   VARIABLES IN EMOI
C          A        = AREA OF ELEMENTS OF PARTICULAR TYPE
C          DC       = DISTANCE TO CENTROID OF CORNER AREA FROM
C                     EDGE OF CORNER ELEMENT
C          SM       = MOMENT OF INERTIA ABOUT WEAK AXIS OF
C                     ELEMENTS OF PARTICULAR TYPE
C          TT       = THICKNESS AT FREE END IF EFFECTIVE AREA
C                     GREATER THAN HALF OF FULL AREA AND AT
C                     FIXED END IF EFFECTIVE AREA LESS THAN
C                     HALF OF FULL AREA FOR UNSTIFFENED ELE-
C                     MENTS
C                          MAIN PROGRAM
C
C
C     THE MAIN PROGRAM READS AND PRINTS THE DATA.  IT CALLS
C     SUBROUTINE COLS TO CALCULATE THE COLUMN CURVE.
C
C
      DIMENSION F(3),CN(3),S1(3)
C
C     IR AND IW ARE THE LOGICAL RECORD UNITS FOR THE READ
C     AND WRITE STATEMENTS, RESPECTIVELY
C
      IR=5
      IW=6
C
C     READS IN THE NUMBER OF COLUMNS TO BE ANALYZED AND SETS
C     THE LOOP TO DO SO
C
      READ(IR,10)N
   10 FORMAT(I5)
      DO 50 NS=1,N
      WRITE(IW,11)NS
   11 FORMAT(1X,15HCOLUMN NUMBER =,I4/)
C
C     READS AND PRINTS THE INPUT DATA
C
      READ(IR,12)SN,SNI,LI
   12 FORMAT(2F10.6,I5)
      READ(IR,13)D,B,T,R,CK,IEF,IC
```

```
   13 FORMAT(5F10.4,2I5)
      IF(IC-1)14,14,16
   14 WRITE(IW,15)
   15 FORMAT(3X,16HSTIFFENED COLUMN/)
      GO TO 19
   16 WRITE(IW,17)
   17 FORMAT(3X,18HUNSTIFFENED COLUMN/)
   19 WRITE(IW,20)
   20 FORMAT(3X,18HCHANNEL DIMENSIONS/)
      WRITE(IW,21)D,B,T,R,CK
   21 FORMAT(5X,14HFLANGE WIDTH =,F6.2,5X,11HWEB DEPTH =,
     +F6.2/5X,11HTHICKNESS =,F6.4,5X,
     +22HINSIDE CORNER RADIUS =,F6.4/5X,
     +45HPLATE EDGE FACTOR, SINGLE THICKNESS ELEMENT =,F6.3)
      DO 22 J=1,3
   22 READ(IR,23)F(J),CN(J),S1(J)
   23 FORMAT(3F10.4)
      WRITE(IW,24)
   24 FORMAT(/3X,19HMATERIAL PROPERTIES/)
      WRITE(IW,25)
   25 FORMAT(8X,8HSUB-AREA,7X,8HMATERIAL,7X,
     +21HRAMBERG-OSGOOD VALUES)
      WRITE(IW,26)
   26 FORMAT(21X,12HYIELD STRESS,7X,6HSTRESS,4X,8HEXPONENT/)
      WRITE(IW,27)F(1),S1(1),CN(1)
   27 FORMAT(5X,14HCHANNEL FLANGE,4X,F7.2,9X,F7.2,4X,F7.2)
      WRITE(IW,28)F(2),S1(2),CN(2)
   28 FORMAT(5X,11HCHANNEL WEB,7X,F7.2,9X,F7.2,4X,F7.2)
      WRITE(IW,29)F(3),S1(3),CN(3)
   29 FORMAT(5X,15HCHANNEL CORNERS,3X,F7.2,9X,F7.2,4X,F7.2/)
C
C     CALLS COLS TO CALCULATE THE COLUMN CURVE
C
      CALL COLS(SN,LI,SNI,T,B,D,R,F,CN,S1,CK,IC,IR,IW,IEF)
   50 WRITE(IW,52)
   52 FORMAT(1H1)
      STOP
      END
      SUBROUTINE COLS(SN,LI,SNI,T,B,D,R,F,CN,S1,CK,IC,IR,IW,
     +IEF)
C
C     THE SUBROUTINE COLS CALLS THE SUBROUTINE FOR DETERMI-
C     NING THE EFFECTIVE WIDTH, THE FULL AND EFFECTIVE SEC-
C     TION PROPERTIES, AND THE MATERIAL PROPERTIES FOR THE
C     RAMBERG-OSGOOD EQUATION, AND IT CALCULATES THE COLUMN
C     CURVE USING THE TANGENT-MODULUS EQUATION.
C
C
      DIMENSION F(3),SR(3),ET(3),SM(3),A(3),CN(3),S1(3)
C
C     SETS THE EFFECTIVE WIDTH TO THE FULL WIDTH FOR THE
C     ELEMENT SUBJECT TO LOCAL BUCKLING IN ORDER TO OBTAIN
C     THE FULL SECTION PROPERTIES
C
```

```
      IF(IC-1)6,6,8
    6 EW=D-2.*(R+T)
      GO TO 9
    8 EW=B-R-T
C
C     CALLS EMOI TO DETERMINE THE SECTION PROPERTIES OF EACH
C     OF THE TYPES OF ELEMENTS
C
    9 DO 10 J=1,3
   10 CALL EMOI(T,B,D,R,EW,J,SM(J),A(J),IC,IEF)
C
C     DETERMINES THE SECTION PROPERTIES FOR THE FULL SECTION
C     AND PRINTS THE RESULTS
C
      TOA=0.
      TMI=0.
      DO 11 J=1,3
      TOA=TOA+A(J)
   11 TMI=TMI+SM(J)
      RG=SQRT(TMI/TOA)
      WRITE(IW,12)
   12 FORMAT(3X,18HSECTION PROPERTIES/)
      WRITE(IW,13)TOA,TMI,RG
   13 FORMAT(5X,12HAREA, FULL =,F6.4,5X,
     +25HMOMENT OF INERTIA, FULL =,F7.4/5X,
     +26HRADIUS OF GYRATION, FULL =,F7.4/)
C
C     PRINTS OUT WHETHER EFFECTIVE WIDTH APPROACH BASED ON
C     FULL OR EFFECTIVE MOMENT OF INERTIA AND THE NECESSARY
C     HEADINGS FOR THE COLUM CURVE RESULTS
C
      IF(IEF-1)14,14,16
   14 WRITE(IW,15)
   15 FORMAT(3X,34HEFFECTIVE WIDTH APPROACH WITH FULL,
     +18H MOMENT OF INERTIA/)
      GO TO 18
   16 WRITE(IW,17)
   17 FORMAT(3X,39HEFFECTIVE WIDTH APPROACH WITH EFFECTIVE,
     +18H MOMENT OF INERTIA/)
   18 WRITE(IW,19)
   19 FORMAT(6X,6HSTRAIN,3X,7HAVERAGE,3X,6HLENGTH,4X,
     +7HLENGTH/,4X,4HEFF.,5X,4HEFF.)
      WRITE(IW,20)
   20 FORMAT(14X,9HSTRESS ON,12X,7HRAD. OF,3X,5HWIDTH,5X,
     +4HAREA)
      WRITE(IW,21)
   21 FORMAT(14X,9HFULL AREA,11X,8HGYRATION/)
C
C     LOOP TO OBTAIN COLUMN CURVE
C
      DO 100 I=1,LI
C
C     FOR THE PARTICULAR STRAIN, THE STRESS AND THE TANGENT-
C     MODULUS ARE OBTAINED BY CALLING SUBROUTINE ROSSC FOR
```

```
C       EACH TYPE OF ELEMENT
C
        DO 30 J=1,3
   30 CALL ROSSC(CN(J),S1(J),ET(J),SN,SR(J),IW)
C
C       FIGURES THE EFFECTIVE WIDTH AND THE EFFECTIVE SECTION
C       PROPERTIES FOR THE ELEMENTS SUBJECT TO LOCAL BUCKLING
C
        IF(IC-1)35,35,40
   35 W=D-2.*(R+T)
        J=2
        GO TO 45
   40 W=B-R-T
        J=1
   45 CALL EFFW(T,ET(J),SR(J),W,EW,CK)
        CALL EMOI(T,B,D,R,EW,J,SM(J),A(J),IC,IEF)
C
C       COMPUTES THE LENGTH AND AVERAGE STRESS ON THE TOTAL
C       SECTION FROM THE TANGENT-MODULUS FORMULA AND PRINTS
C       THE RESULTS
C
        EI=0.
        SA=0.
        AEF=0.
        DO 50 J=1,3
        EI=EI+ET(J)*SM(J)
        SA=SA+SR(J)*A(J)
   50 AEF=AEF+A(J)
        CL=SQRT((3.1416**2)*EI/SA)
        CLR=CL/RG
        ST=SA/TOA
        WRITE(IW,60)SN,ST,CL,CLR,EW,AEF
   60 FORMAT(5X,F8.5,2X,F6.2,4X,F6.2,3X,F7.2,3X,F6.2,3X,
      +F6.2)
        IF(CLR-5.)110,110,100
  100 SN=SN+SNI
  110 RETURN
        END
        SUBROUTINE ROSSC(CN,S1,ET,SN,SR,IW)
C
C
C       THE SUBROUTINE ROSSC CALCULATES THE STRESS AND THE
C       TANGENT-MODULUS GIVEN THE STRAIN BY USING THE RAMBERG-
C       OSGOOD EQUATION.
C
C
        A1=-SN
        A2=1./29500.
        A3=(3./(7.*29500.))*S1
C
C       CALCULATES THE TWO BOUNDS ON THE ASSUMED STRESS FOR
C       USE IN SUBROUTINE RTMI WHICH CALCULATES THE CORRECT
C       STRESS; SUBROUTINE EQVAL CALCULATES THE VALUE OF THE
C       RAMBERG-OSGOOD EQUATION
```

```
C
      SR=1.0
      CALL EQVAL(A1,A2,A3,CN,SR,EQ,S1)
   20 EQP=EQ
      SR=SR+1.0
      CALL EQVAL(A1,A2,A3,CN,SR,EQ,S1)
      IF(EQ/EQP)30,20,20
C
C     USING THE BOUNDS ON THE STRESS, RTMI IS CALLED TO
C     CALCULATE THE STRESS GIVEN THE STRAIN
C
   30 SR1=SR-1.
      SR2=SR
      EPS=.0001
      IEND=100
      CALL RTMI(SR,EQ,SR1,SR2,EPS,IEND,IER,A1,A2,A3,CN,S1)
      IF(IER)50,50,40
   40 WRITE(IW,45)IER
   45 FORMAT(//10X,15HERROR IN STRESS,5X,5HIER =,I3//)
C
C     CALCULATES THE STRESSES FOR STRAINS SLIGHTLY SMALLER
C     AND SLIGHTLY LARGER AND FROM THESE THE TANGENT-MODULUS
C     WHICH IS THE CHANGE IN STRESS OVER THE CHANGE IN
C     STRAIN
C
   50 A1=A1-.000001
      CALL RTMI(SB,EQ,SR1,SR2,EPS,IEND,IER,A1,A2,A3,CN,S1)
      A1=A1+.000002
      CALL RTMI(SA,EQ,SR1,SR2,EPS,IEND,IER,A1,A2,A3,CN,S1)
      ET=(SB-SA)/(.000002)
C
C     CHECK IN CASE THE NUMERICAL ACCURACY OF THE SYSTEM
C     RESULTS IN A TANGENT-MODULUS THAT IS NEGATIVE
C
      IF(ET)55,60,60
   55 WRITE(IW,56)ET
   56 FORMAT(10X,4HET =,F15.5/)
      ET=0.0000001
   60 CONTINUE
      RETURN
      END
      SUBROUTINE EQVAL(A1,A2,A3,CN,SR,EQ,S1)
C
C
C     THE SUBROUTINE EQVAL CALCULATES THE VALUE OF THE
C     RAMBERG-OSGOOD EQUATION.
C
C
      IF(CN*ALOG10(SR/S1)+70.)10,10,20
C
C     IF THE STRAIN IS SMALL, THE THIRD TERM IN THE RAMBERG-
C     OSGOOD EQUATION GOES TO ZERO, AND THUS IT IS NOT NE-
C     CESSARY AND NOT DESIRABLE FOR REASONS OF EXCEEDING
C     THE NUMERICAL POTENTIAL OF THE SYSTEM TO CALCULATE THE
```

```
C      VALUE OF THIS TERM
C
   10 EQ=A1+A2*SR
      GO TO 30
C
C      FULL RAMBERG-OSGOOD EQUATION
C
   20 EQ=A1+A2*SR+A3*(SR/S1)**CN
   30 CONTINUE
      RETURN
      END
      SUBROUTINE RTMI(X,F,XLI,XRI,EPS,IEND,IER,A1,A2,A3,CN,
     +S1)
C
C
C     ..................................................
C
C        THIS SUBROUTINE IS FROM THE IBM SYSTEM/360 SCIENTI-
C        FITIC SUBROUTINE PACKAGE, (360A-CM-03X) VERSION
C        III, PROGRAMMER'S MANUAL.
C
C     ..................................................
C
C
C        PURPOSE
C            TO SOLVE GENERAL NONLINERAR EQUATIONS OF THE
C            FORM FCT(X)=0 BY MEANS OF MUELLER-S ITERATION
C            METHOD.
C
C         USUAGE
C            CALL RTMI (X,F,FCT,XLI,XRI,EPS,IEND,IER)
C            PARAMETER FCT REQUIRES AN EXTERNAL STATEMENT.
C
C         DESCRITION OF PARAMETERS
C            X       - RESULTANT ROOT OF EQUATION FCT(X)=0.
C            F       - RESULTANT FUNCTION VALUE AT ROOT X.
C            FCT     - NAME OF THE EXTERNAL FUNCTION SUBPRO-
C                      GRAM USED.
C            XLI     - INPUT VALUE WHICH SPECIFIES THE INI-
C                      TIAL LEFT BOUND OF THE ROOT X.
C            XRI     - INPUT VALUE WHICH SPECIFIES THE INI-
C                      TIAL RIGHT BOUND OF THE ROOT X.
C            EPS     - INPUT VALUE WHICH SPECIFIES THE UPPER
C                      BOUND OF THE ERROR OF RESULT X.
C            IEND    - MAXIMUM NUMBER OF INTERATION STEPS
C                      SPECIFIED.
C            IER     - RESULTANT ERROR PARAMETER CODED AS
C                      FOLLOWS
C                        IER=0 - NO ERROR.
C                        IER=1 - NO CONVERGENCE AFTER IEND
C                                ITERATION STEPS FOLLOWED BY
C                                IEND SUCCESSIVE STEPS OF
C                                BISECTION.
C                        IER=2 - BASIC ASSUMPTION FCT(XLI)*
```

```
C                                FCT(XRI) LESS THAN OR EQUAL
C                                TO ZERO IS NOT SATISFIED.
C
C          REMARKS
C             THE PROCEDURE ASSUMES THAT FUNCTION VALUES AT
C             INITIAL BOUNDS XLI AND XRI HAVE NOT THE SAME
C             SIGN.  IF THIS BASIC ASSUMPTION IS NOT SATIS-
C             FIED BY INPUT VALUES XLI AND XRI, THE PROCEDURE
C             IS BYPASSED AND GIVES THE ERROR MESSAGE IER=2.
C
C          SUBROUTINES AND FUNCTION SUBPROTRAMS REQUIRED
C             THE EXTERNAL FUNCTION SUBPROGRAM FCT(X) MUST BE
C             FURNISHED BY THE USER.
C
C          METHOD
C             SOLUTION OF EQUATION FCT(X)=0 IS DONE BY MEANS
C             OF MUELLER-S ITERATION METHOD OF SUCCESSIVE BI-
C             SECTIONS AND INVERSE PARABOLIC INTERPOLATION,
C             WHICH STARTS AT THE INITIAL BOUNDS XLI AND XRI.
C             CONVERGENCE IS QUADRATIC IF THE DERIVATIVE OF
C             FCT(X) AT ROOT X IS NOT EQUAL TO ZERO.  ONE
C             ITERATION STEP REQUIRES TWO EVALUATIONS OF
C             FCT(X).  FOR TEST ON SATISFACTORY ACCURACY SEE
C             FORMULAE (3,4) OF MATHEMATICAL DESCRITION.  FOR
C             REFERENCE, SEE G. K. KRISTIANSEN, ZERO OF ARBI-
C             TRARY FUNCTION, BIT, VOL. 3 (1963), PP. 205-
C             206.
C
C     ..................................................
C
C
C
C       PREPARE ITERATION
        IER=0
        XL=XLI
        XR=XRI
        X=XL
        CALL EQVAL(A1,A2,A3,CN,X,F,S1)
        IF(F)1,16,1
      1 FL=F
        X=XR
        CALL EQVAL(A1,A2,A3,CN,X,F,S1)
        IF(F)2,16,2
      2 FR=F
        IF(SIGN(1.,FL)+SIGN(1.,FR))25,3,25
C
C       BASIC ASSUMPTION FL*FR LESS THAN 0 IS SATISFIED.
C       GENERATE TOLERANCE FOR FUNCTION VALUES
      3 I=0
        TOLF=100.D0*EPS
C
C
C       START ITERATION LOOP
      4 I=I+1
```

```
C
C       START BISECTION LOOP
        DO 13 K=1,IEND
        X=.5*(XL+XR)
        CALL EQVAL(A1,A2,A3,CN,X,F,S1)
        IF(F)5,16,5
    5   IF(SIGN(1.,F)+SIGN(1.,FR))7,6,7
C
C       INTERCHANGE XL AND XR IN ORDER TO GET THE SAME SIGN IN
C       F AND FR
    6   TOL=XL
        XL=XR
        XR=TOL
        TOL=FL
        FL=FR
        FR=TOL
    7   TOL=F-FL
        A=F*TOL
        A=A+A
        IF(A-FR*(FR-FL))8,9,9
    8   IF(I-IEND)17,17,9
    9   XR=X
        FR=F
C
C       TEST ON SATISFACTORY ACCURACY IN BISECTION LOOP
        TOL=EPS
        A=ABS(XR)
        IF(A-1.D0)11,11,10
   10   TOL=TOL*A
   11   IF(ABS(XR-XL)-TOL)12,12,13
   12   IF(ABS(FR-FL)-TOLF)14,14,13
   13   CONTINUE
C       END OF BISECTION LOOP
C
C       NO CONVERGENCE AFTER IEND ITERATION STEPS FOLLOWED BY
C       IEND SUCCESSIVE STEPS OF BISECTION OR STEADILY IN-
C       CREASING FUNCTION VALUES AT RIGHT BOUNDS.  ERROR RE-
C       TURN.
        IER=1
   14   IF(ABS(FR)-ABS(FL))16,16,15
   15   X=XL
        F=FL
   16   RETURN
C
C       COMPUTATION OF ITERATED X-VALUE BY INVERSE PARABOLIC
C       INTERPOLATION
   17   A=FR-F
        DX=(X-XL)*FL*(1.+F*(A-TOL)/(A*(FR-FL)))/TOL
        XM=X
        FM=F
        X=XL-DX
        CALL EQVAL(A1,A2,A3,CN,X,F,S1)
        IF(F)18,16,18
C
```

```
C       TEST ON SATISFACTORY ACCURACY IN ITERATION LOOP
   18 TOL=EPS
      A=ABS(X)
      IF(A-1.)20,20,19
   19 TOL=TOL*A
   20 IF(ABS(DX)-TOL)21,21,22
   21 IF(ABS(F)-TOLF)16,16,22
C
C       PREPARATION OF NEXT BISECTION LOOP
   22 IF(SIGN(1.,F)+SIGN(1.,FL))24,23,24
   23 XR=X
      FR=F
      GO TO 4
   24 XL=X
      FL=F
      XR=XM
      FR=FM
      GO TO 4
C       END OF ITERATION LOOP
C
C
C       ERROR RETURN IN CASE OF WRONG INPUT DATA
   25 IER=2
      RETURN
      END
      SUBROUTINE EFFW(T,E,S,W,EW,CK)
C
C
C       THE SUBROUTINE EFFW COMPUTES THE EFFECTIVE WIDTH
C       BASED ON THE STRESS WITHOUT ANY SAFETY FACTOR.
C
C
      SQ=SQRT(29500.*CK/S)
      WLI=.639*T*SQ
      IF(W-WLI)20,20,10
   10 EW=.950*T*SQ*(1.-0.209*SQ*T/W)
      GO TO 30
   20 EW=W
   30 RETURN
      END
      SUBROUTINE EMOI(T,B,D,R,EW,J,SM,A,IC,IEF)
C
C
C       THE SUBROUTINE EMOI COMPUTES THE AREAS AND THE MOMENTS
C       OF INERTIA ABOUT THE WEAK AXIS OF THE SEPARATE SUB-
C       AREAS FOR EITHER THE STIFFENED OR UNSTIFFENED SEC-
C       TIONS.
C
C
      IF(IC-1)10,10,100
C
C       FOR STIFFENED SECTION
C
   10 GO TO (20,40,60),J
```

```
C
C       DOUBLE THICKNESS ELEMENTS
C
   20 A=4.*T*(B-T-R)
      SM=T*(B-T-R)**3/3.
      RETURN
C
C       SINGLE THICKNESS ELEMENTS
C
   40 A=EW*T*2.
      IF(IEF-2)42,44,44
   42 SM=2.*T*(D-2.*(R+T))*((B+R)/2.)**2
      RETURN
   44 SM=A*((B+R)/2.)**2
      RETURN
C
C       CORNERS
C
   60 A=(3.1416)*((R+T)**2-R**2)
      DC=(4./(3.*3.1416))*(((R+T)**3-R**3)/((R+T)**2-R**2))
      SM=1.*A*(((B-T-R)/2.)+DC)**2
      RETURN
C
C       FOR UNSTIFFENED SECTION
C
  100 GO TO (120,140,160),J
C
C       SINGLE THICKNESS ELEMENTS
C
  120 A=EW*T*4.
      BF=B-T-R
      IF(IEF-2)125,128,128
  125 SM=(1./3.)*T*BF**3+4.*T*BF*((B+R+T)/2.)**2
      RETURN
  128 AL=BF*T-EW*T
      AT=T*BF
      IF(AL-(AT/2.))130,135,135
  130 TT=2.*AL/BF
      SM=4.*((TT*BF**3)/12.+(TT*BF/2.)*(R+T)**2+((T-TT)*
     +BF**3)/12.+(T-TT)*BF*((B+T+R)/2.)**2)
      RETURN
  135 TT=(EW*T*2.)/BF
      SM=4.*((TT*BF**3)/12.+((TT*BF)/2.)*(T+R)**2)
      RETURN
C
C       DOUBLE THICKNESS ELEMENTS
C
  140 A=2.*T*(D-2.*(R+T))
      SM=(2./3.)*(D-2.*(R+T))*T**3
      RETURN
C
C       CORNERS
C
  160 A=(3.1416)*((R+T)**2-R**2)
```

```
DC=(4./(3.*3.1416))*(((R+T)**3-R**3)/((R+T)**2-R**2))
SM=A*(R+T-DC)**2
RETURN
END
```

```
 2
.0001        .0001        20
 3.5          2.             .0581                4.85        1      1
41.9         75.          41.9
41.9         75.          41.9
41.9         75.          41.9
.0001        .0001        20
 3.           1.25            .0581                .64         2      2
41.9         75.          41.9
41.9         75.          41.9
41.9         75.          41.9
```

SAMPLE INPUT FOR SECTIONS S-1 AND U-2, RESPECTIVELY

COLUMN NUMBER = 1

STIFFENED COLUMN

CHANNEL DIMENSIONS

FLANGE WIDTH = 3.50 WEB DEPTH = 2.00
THICKNESS =0.0581 INSIDE CORNER RADIUS =0.0000
PLATE EDGE FACTOR, SINGLE THICKNESS ELEMENT = 4.850

MATERIAL PROPERTIES

SUB-AREA	MATERIAL YIELD STRESS	RAMBERG-OSGOOD VALUES STRESS	EXPONENT
CHANNEL FLANGE	41.90	41.90	75.00
CHANNEL WEB	41.90	41.90	75.00
CHANNEL CORNERS	41.90	41.90	75.00

SECTION PROPERTIES

AREA, FULL =0.8551 MOMENT OF INERTIA, FULL = 0.5455
RADIUS OF GYRATION, FULL = 0.7987

EFFECTIVE WIDTH APPROACH WITH FULL MOMENT OF INERTIA

STRAIN	AVERAGE STRESS ON FULL AREA	LENGTH	LENGTH/ RAD. OF GYRATION	EFF. WIDTH	EFF. AREA
0.00010	2.95	250.93	314.16	3.38	0.86
0.00020	5.90	177.43	222.14	3.38	0.86
0.00030	8.85	144.88	181.38	3.38	0.86
0.00040	11.80	125.46	157.08	3.38	0.86
0.00050	14.75	112.22	140.50	3.38	0.86
0.00060	17.65	102.60	128.46	3.36	0.85
0.00070	20.20	95.91	120.07	3.22	0.84
0.00080	22.68	90.50	113.31	3.10	0.82
0.00090	25.11	86.01	107.69	2.98	0.81
0.00100	27.49	82.20	102.91	2.88	0.80
0.00110	29.84	78.90	98.78	2.79	0.79
0.00120	32.15	76.00	95.15	2.71	0.78
0.00130	34.42	71.90	90.02	2.63	0.77
0.00140	35.94	42.65	53.40	2.59	0.76
0.00150	36.43	26.95	33.75	2.57	0.76
0.00160	36.68	20.76	25.99	2.56	0.76
0.00170	36.84	17.39	21.78	2.56	0.76
0.00180	36.96	15.25	19.10	2.55	0.76
0.00190	37.05	13.71	17.17	2.55	0.76
0.00200	37.13	12.56	15.73	2.55	0.76

SAMPLE OUTPUT FOR SECTION S-1

COLUMN NUMBER = 2

UNSTIFFENED COLUMN

CHANNEL DIMENSIONS

FLANGE WIDTH = 3.00 WEB DEPTH = 1.25
THICKNESS =0.0581 INSIDE CORNER RADIUS =0.0000
PLATE EDGE FACTOR, SINGLE THICKNESS ELEMENT = 0.640

MATERIAL PROPERTIES

SUB-AREA	MATERIAL YIELD STRESS	RAMBERG-OSGOOD VALUES STRESS	EXPONENT
CHANNEL FLANGE	41.90	41.90	75.00
CHANNEL WEB	41.90	41.90	75.00
CHANNEL CORNERS	41.90	41.90	75.00

SECTION PROPERTIES

AREA, FULL =0.6227 MOMENT OF INERTIA, FULL = 0.1517
RADIUS OF GYRATION, FULL = 0.4935

EFFECTIVE WIDTH APPROACH WITH EFFECTIVE MOMENT OF INERTIA

STRAIN	AVERAGE STRESS ON FULL AREA	LENGTH	LENGTH/ RAD. OF GYRATION	EFF. WIDTH	EFF. AREA
0.00010	2.95	155.05	314.16	1.19	0.62
0.00020	5.90	109.64	222.14	1.19	0.62
0.00030	8.85	89.52	181.38	1.19	0.62
0.00040	11.80	77.52	157.08	1.19	0.62
0.00050	14.75	69.34	140.50	1.19	0.62
0.00060	17.70	63.30	128.26	1.19	0.62
0.00070	20.36	57.57	116.65	1.15	0.61
0.00080	22.89	52.65	106.69	1.11	0.60
0.00090	25.36	48.57	98.41	1.07	0.59
0.00100	27.79	45.10	91.39	1.04	0.59
0.00110	30.18	42.12	85.35	1.00	0.58
0.00120	32.53	39.52	80.07	0.97	0.57
0.00130	34.84	36.46	73.87	0.95	0.57
0.00140	36.39	21.27	43.10	0.93	0.56
0.00150	36.89	13.37	27.09	0.93	0.56
0.00160	37.14	10.27	20.81	0.92	0.56
0.00170	37.31	8.59	17.40	0.92	0.56
0.00180	37.43	7.52	15.24	0.92	0.56
0.00190	37.52	6.76	13.69	0.92	0.56
0.00200	37.60	6.19	12.53	0.92	0.56

SAMPLE OUTPUT FOR SECTION U-2

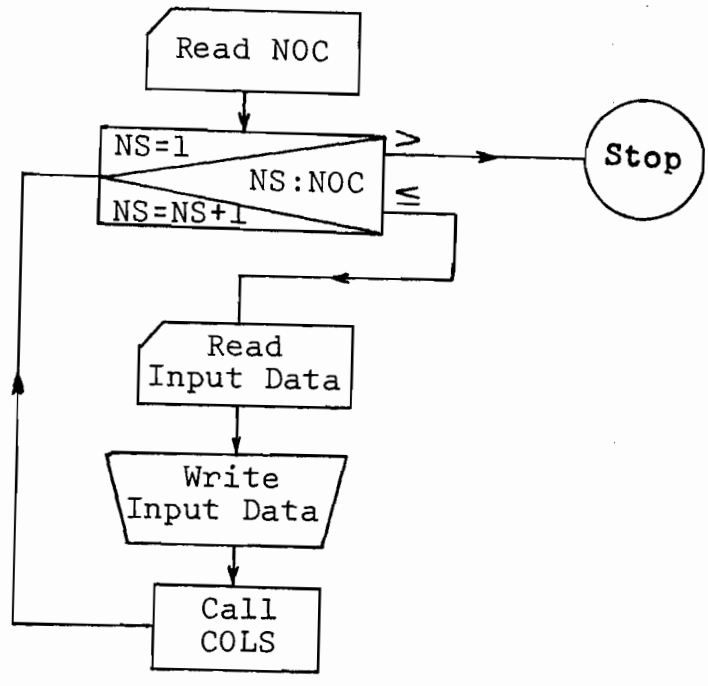

FLOW CHART FOR MAIN PROGRAM, EFFECTIVE WIDTH APPROACH

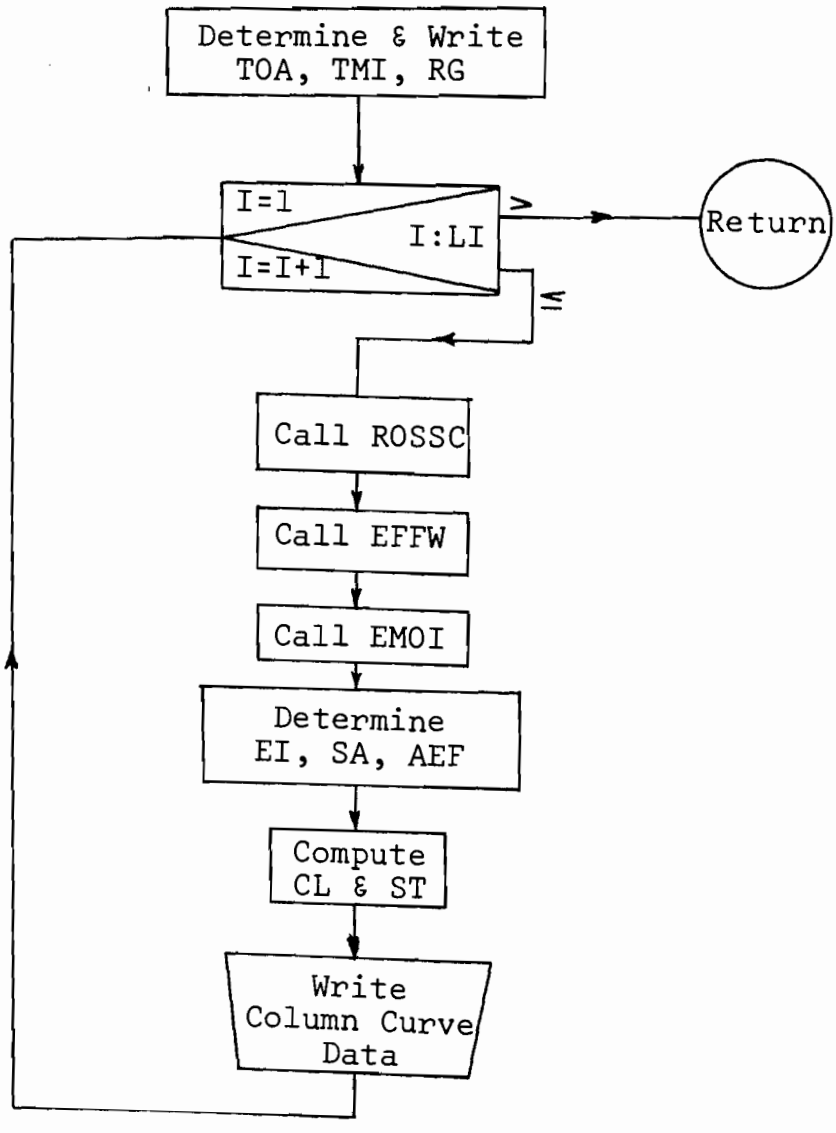

FLOW CHART FOR SUBROUTINE COLS, EFFECTIVE WIDTH APPROACH

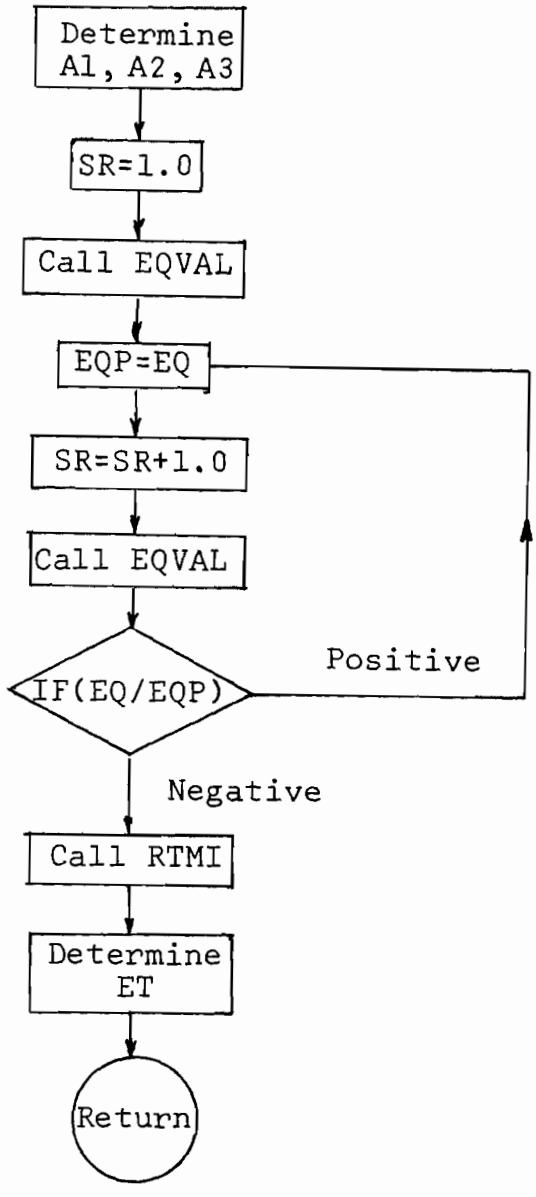

FLOW CHART FOR SUBROUTINE ROSSC, EFFECTIVE WIDTH APPROACH

Appendix D

PROGRAM FOR DESIGN METHOD

This appendix contains the following:

(1) Program for the design method based on Chapter 7. The program will consider any type of section made of the five types of elements shown in Fig. D.1.

(2) Sample input for the three design examples given in Appendix B.

(3) Sample output for the three design examples given in Appendix B.

(4) Flow chart for the program.

```
C
C
C                    PROGRAM FOR DESIGN METHOD
C
C
C
C         THIS PROGRAM ANALYZES COLD-FORMED STEEL COLUMNS
C   BASED ON THE DESIGN METHOD DISCUSSED IN CHAPTER 7.  THE
C   COLUMNS MAY OR MAY NOT BE SUBJECT TO LOCAL BUCKLING.  THE
C   INPUT CONSISTS OF THE CROSS-SECTION DIMENSIONS, PLATE
C   EDGE FACTORS, YIELD STRESS, LENGTH, EFFECTIVE LENGTH
C   FACTOR, AND SAFETY FACTOR, AND THE PROGRAM THEN FIGURES
C   THE ALLOWABLE LOAD FOR THE COLUMN.  THE PROGRAM IS WRIT-
C   TEN IN BASIC FORTRAN IV LANGUAGE.
C
C         COLUMNS TREATED BY THE PROGRAM MAY BE MADE OF
C   STIFFENED ELEMENTS, UNSTIFFENED ELEMENTS, OR A COMBI-
C   NATION OF THE TWO.  COLUMNS WITH STIFFENERS MAY BE ANA-
C   LYZED PROVIDING THE STIFFENERS ARE ADEQUATE TO ASSURE
C   THAT THE ADJOINING ELEMENTS BEHAVE AS FULLY-STIFFENED
C   ELEMENTS.  THE ONLY LIMITATION IS THAT IN THE CALULATION
C   OF THE SECTION PROPERTIES, A AND I, THE PROGRAM ASSUMES
C   THAT THE CORNERS ARE PERFECTLY SQUARE.  THIS CORRESPONDS
C   TO NORMAL DESIGN PRACTICE AND IS ADEQUATE FOR MOST
C   DESIGN SITUATIONS.  WHERE IT IS NECESSARY TO CONSIDER
C   ROUNDED CORNERS, ELEMENTS MAY BE ADDED TO THE PRESENT
C   PROGRAM TO DO SO.  FOR FIGURING THE WIDTH-THICKNESS
C   RATIO FOR USE IN THE EFFECTIVE WIDTH-EXPRESSION, THE
C   FLAT WIDTH EXCLUSSIVE OF FILETS IS USED.
C
C         IN ADDITION, THE ALLOWABLE DESIGN STRESS USING THE
C   1968 EDITION OF THE SPECIFICATION FOR THE DESIGN OF COLD-
C   FORMED STEEL STRUCTURAL MEMBERS IS CALCULATED FOR COMPAR-
C   ISON PURPOSES.  THE STRESS IS BASED ON THE AISI SPECIFI-
C   CATION SAFETY FACTORS AND IT DOES NOT INCLUDE CONSIDERA-
C   TION OF SQUARE AND RECTANGULAR TUBES, ANGULAR STRUTS, AND
C   SECTIONS WITH UNSTIFFENED ELEMENTS WITH WIDTH-THICKNESS
C   RATIOS GREATER THAN 60.  USING A SAFETY FACTOR OF 1.92 IS
C   NEARLY EQUIVALENT TO THE AISI SPECIFICATION METHOD WITH
C   ITS SAFETY FACTORS.
C
C
C
C                          INPUT
C
C
C         ALL INPUT DATA AND OUTPUT DATA ARE IN KIPS AND
C   INCHES.  THERE ARE ONLY THREE TYPES OF INPUT CARDS, WHICH
C   ARE DEFINED AS FOLLOWS.  THE FORMAT IS GIVEN FOR EACH
C   CARD, AND THE INPUT VARIABLES ARE IN THE CORRECT ORDER.
C
C   FIRST INPUT CARD (I5) -
C          NOC     = NUMBER OF COLUMNS TO BE ANALYZED
C
```

```
C     REPEAT THE FOLLOWING FOR EACH COLUMN TO BE ANALYZED
C
C  SECOND INPUT CARD (2I5,4F10.4) -
C         NE       = NUMBER OF TYPES OF ELEMENTS IN COLUMN
C         LC       = 1 IF SECTION SYMMETRICAL ABOUT BUCKLING
C                    AXIS, 2 IF SECTION NOT SYMMETRICAL
C         FY       = MATERIAL YIELD STRESS
C         CL       = UNBRACED COLUMN LENGTH
C         CK       = COLUMN EFFECTIVE LENGTH FACTOR
C         FS       = FACTOR OF SAFETY
C
C     REPEAT THE FOLLOWING FOR EACH TYPE OF ELEMENT IN THE
C     CROSS-SECTION (NOTE THAT IF MORE THAN ONE ELEMENT OF A
C     PARTICULAR TYPE HAS THE SAME DIMENSION AND LOCATION
C     WITH RESPECT TO THE AXIS ON WHICH YE(L) IS FIGURED, IT
C     IS NECESSARY TO USE ONLY ONE CARD FOR ALL OF THE
C     IDENTICAL ELEMENTS).
C
C  THIRD INPUT CARD (2I5,5F10.4) -
C         NTE(L)   = NUMBER OF ELEMENTS OF PARTICULAR TYPE,
C                    PROPERTIES, AND LOCATION.
C         NT(L)    = ELEMENT TYPE, AS FOLLOWS -
C                         1 - STIFFENED ELEMENT PARALLEL TO
C                             BUCKLING AXIS
C                         2 - STIFFENED ELEMENT PERPENDICULAR
C                             TO BUCKLING AXIS
C                         3 - UNSTIFFENED ELEMENT PERPENDICU-
C                             LAR TO BUCKLING AXIS WITH FREE
C                             EDGE MOST DISTANT EDGE FROM AXIS
C                             YE(L) FIGURED WITH RESPECT TO
C                         4 - UNSTIFFENED ELEMENT PERPENDICU-
C                             LAR TO BUCKLING AXIS WITH FREE
C                             EDGE CLOSEST TO AXIS YE(L) FIG-
C                             URED WITH RESPECT TO
C                         5 - UNSTIFFENED ELEMENT PARALLEL TO
C                             BUCKLING AXIS
C         W(L)     = FLAT WIDTH, EXCLUSSIVE OF FILETS.
C         T(L)     = THICKNESS
C         FW(L)    = FULL WIDTH OF ELEMENT, EQUAL TO W(L) OR
C                    GREATER - CONSIDERS CORNER AREAS FOR
C                    CALCULATION OF SECTION PROPERTIES, AND
C                    THUS THE CORNER AREAS SHOULD BE ADDED
C                    INTO ONLY ONE OF THE ADJOINING ELEMENTS
C         PK(L)    = PLATE EDGE FACTOR (FROM 4.00 TO 6.97 FOR
C                    STIFFENED ELEMENTS AND FROM 0.425 TO
C                    1.277 FOR UNSTIFFENED ELEMENTS)
C         YE(L)    = DISTANCE TO CENTROID OF ELEMENT FROM
C                    CENTROID OF SECTION IF LC=1 AND FROM
C                    ARBITRARY AXIS PARALLEL TO THE BUCKLING
C                    AXIS WHICH DOES NOT INTERSECT THE SEC-
C                    TION IF LC=2
C
C
C                         PROGRAM VARIABLES
```

```
C
C
C       THE FOLLOWING IS A LIST OF THE IMPORTANT VARIABLES
C   USED IN THE PROGRAM.  THEY ARE BROKEN UP INTO THE POR-
C   TIONS OF THE PROGRAM THEY OCCUR IN.  MOST VARIABLES IN
C   THE SUBROUTINES ARE THE SAME AS IN THE MAIN PROGRAM AND
C   ARE THEREFORE DEFINED WITH THAT LIST.
C
C   VARIABLES IN MAIN PROGRAM
C          CAE      = TOTAL AREA OF SECTION BASED ON THE EF-
C                     FECTIVE CROSS-SECTION
C          CAF      = TOTAL AREA  OF SECTION BASED ON THE FULL
C                     CROSS-SECTION
C          CIE      = TOTAL MOMENT OF INERTIA OF SECTION BASED
C                     ON THE EFFECTIVE CROSS-SECTION
C          CIF      = TOTAL MOMENT OF INERTIA OF SECTION BASED
C                     ON FULL CROSS-SECTION
C          F        = EDGE STRESS IN ELEMENTS - THIS IS EQUI-
C                     VALENT TO THE STRESS ON THE EFFECTIVE
C                     SECTION
C          FA1      = STRESS ON FULL CROSS-SECTION - INCLUDES
C                     SAFETY FACTOR WHEN PRINTED (EQS. 7-6 OR
C                     7-7)
C          FC       = STRESS ON THE EFFECTIVE SECTION
C          P        = TOTAL COLUMN LOAD - ENCLUDES SAFETY
C                     FACTOR WHEN PRINTED OUT
C          RE       = RADIUS OF GYRATION OF SECTION BASED ON
C                     THE EFFECTIVE CROSS-SECTION
C          RT       = RADIUS OF GYRATION OF SECTION BASED ON
C                     FULL CROSS-SECTION
C          SR       = SLENDERNESS RATIO OF COLUMN
C          SRL1     = LIMITING SLENDERNESS RATIO BASED ON
C                     WHETHER OR NOT THE SECTION IS FULLY
C                     EFFECTIVE - IT IS DETERMINED FROM THE
C                     INTERSECTION OF THE EULER CURVE WITH THE
C                     MAXIMUM STRESS AT WHICH THE SECTION IS
C                     STILL FULLY EFFECTIVE
C          SRL2     = LIMITING SLENDERNESS RATIO BASED ON
C                     WHETHER OR NOT THE SECTION IS ELASTIC -
C                     IT IS DETERMINED FROM THE INTERSECTION
C                     OF THE EULER CURVE WITH THE CRC CURVE
C                     ASSUMING THAT THE SECTION IS FULLY EF-
C                     FECTIVE AT THIS POINT
C          Y        = DISTANCE FROM ARBITRARY AXIS TO CENTROID
C                     OF SECTION WHEN LC=2
C
C   VARIABLES IN SUBROUTINE PROP
C          A        = AREA OF SEPARATE ELEMENT
C          AT       = SUM OF AREAS OF SECTION FOR DETERMINING
C                     DISTANCE TO CENTROID OF TOTAL SECTION
C          AY       = AREA TIMES DISTANCE TO CENTRIOD OF SE-
C                     PARATE ELEMENTS
C          AYT      = SUM OF AREA TIMES DISTANCE TO CENTRIOD
C                     OF THE ELEMENTS
C
```

```
C          CA       = AREA OF SECTION
C          CI       = MOMENT OF INERTIA OF SECTION
C          TE       = THICKNESS OF EFFECTIVE PORTION OF AREA
C                     AT EDGE WITH ADJOINING ELEMENT IF THE
C                     EFFECTIVE AREA IS LESS THAN HALF OF THE
C                     FULL AREA
C          TT       = THICKNESS OF EFFECTIVE PORTION OF AREA
C                     AT FREE EDGE IF THE EFFECTIVE AREA IS
C                     MORE THAN HALF OF THE FULL AREA
C
C   VARIABLES IN SUBROUTINE EFFW
C          EW       = EFFECTIVE WIDTH OF ELEMENT (EQ. 7.1)
C          W        = ELEMENT FLAT WIDTH
C          WL1      = MAXIMUM WIDTH AT WHICH THE ELEMENT IS
C                     FULLY EFFECTIVE (EQ. 7.2)
C
C   VARIABLES IN SUBROUTINE AISI
C          AE       = EFFECTIVE DESIGN AREA OF COLUMN
C          AEE      = EFFECTIVE DESIGN AREA FOR A PARTICULAR
C                     ELEMENT
C          FA       = ALLOWABLE AVERAGE COMPRESSIVE STRESS ON
C                     COLUMN
C          FC       = MAXIMUM ALLOWABLE COMPRESSIVE STRESS ON
C                     UNSTIFFENED ELEMENTS
C          FCC      = ALLOWABLE STRESS FOR A PARTICULAR UN-
C                     STIFFENED ELEMENT
C          P        = ALLOWABLE LOAD ON COLUMN
C          Q        = FACTOR TO ACCOUNT FOR LOCAL BUCKLING
C          QA       = Q FOR SECTION COMPOSED OF STIFFENED
C                     ELEMENTS
C          QS       = Q FOR SECTION COMPOSED OF UNSTIFFENED
C                     ELEMENTS
C          WT(L)    = WIDTH-THICKNESS RATIO FOR ELEMENT
C
C
C        THE PROGRAM IS DIMENSIONED TO TREAT SECTIONS WITH AS
C   MANY AS 20 SEPARATE GROUPS OF ELEMENTS AND CONSIDERS 5
C   DIFFERENT TYPES OF POSSIBLE ELEMENTS.
```

```
C                          MAIN PROGRAM
C
C
C
C      THE MAIN PROGRAM READS IN THE DATA, FIGURES WHICH
C      EQUATION GOVERNS FOR DETERMINING THE STRESS ON THE
C      SECTION, FIGURES THE ALLOWABLE STRESS AND THE ALLOW-
C      ABLE LOAD ON THE COLUMN, AND PRINTS ALL THE DATA.
C
C
      DIMENSION NTE(20),NT(5),W(20),T(20),FW(20),PK(20),
     +EW(20),YE(20)
C
C      IR AND IW ARE THE LOGICAL RECORD UNITS FOR THE READ
C      AND WRITE STATEMENTS, RESPECTIVELY.
C
      IR=5
      IW=6
      WRITE(IW,101)
C
C      READS IN THE NUMBER OF COLUMNS TO BE ANALYZED AND
C      SETS THE LOOP FOR THE DESIGN.
C
      READ(IR,10)NOC
   10 FORMAT(I5)
      DO 100 I=1,NOC
      WRITE(IW,15)I
   15 FORMAT(2X,12HCOLUMN NO. =,I4//)
C
C      READS AND WRITES THE INPUT DATA FOR THE COLUMN.
C
      READ(IR,20)NE,LC,FY,CL,CK,FS
   20 FORMAT(2I5,4F10.4)
      WRITE(IW,21)FY,CL,CK,FS
   21 FORMAT(5X,4HFY =,F6.2,5X,11HCOL. LEN. =,F6.2/5X,
C
C      READS AND WRITES THE INPUT DATA FOR EACH ELEMENT IN
C      THE COLUMN.
C
     +8HCOL. K =,F5.2,5X,12HSAF. FACT. =,F5.2/)
      DO 25 L=1,NE
   22 READ(IR,23)NTE(L),NT(L),W(L),T(L),FW(L),PK(L),YE(L)
   23 FORMAT(2I5,5F10.4)
      EW(L)=FW(L)
      WRITE(IW,24)NT(L)
   24 FORMAT(5X,14HELEMENT TYPE =,I3)
   25 WRITE(IW,26)NTE(L),T(L),W(L),FW(L),PK(L),YE(L)
   26 FORMAT(10X,14HNO. ELEMENTS =,I4,5X,8HTHICK. =,F7.4/
     +10X,12HFLAT WIDTH =,F6.2,5X,12HFULL WIDTH =,F6.2/
     +10X,18HPLATE EDGE FACT. =,F6.3/10X,16HDIST. TO CENT. =
     +,F6.2/)
      IF(LC-1)27,27,29
   27 WRITE(IW,28)
   28 FORMAT(5X,32HSECTION SYM. ABOUT BUCKLING AXIS)
      GO TO 32
```

```
   29 WRITE(IW,30)
   30 FORMAT(5X,36HSECTION NOT SYM. ABOUT BUCKLING AXIS)
   32 CONTINUE
C
C     CALLS PROP TO DETERMINE THE FULL SECTION PROPERTIES.
C     EW(L) IS SET TO THE FULL WIDTH ABOVE FOR THIS REASON.
C
      CALL PROP(W,T,FW,EW,PK,NT,NTE,NE,FY,LC,Y,CAF,CIF,YE)
      RT=SQRT(CIF/CAF)
C
C     WRITES THE FULL SECTION PROPERTIES.
C
      WRITE(IW,40)
   40 FORMAT(/5X,23HFULL SECTION PROPERTIES)
      WRITE(IW,42)CAF,CIF,RT
   42 FORMAT(10X,6HAREA =,F7.3,5X,15HMOM. OF INER. =,F7.3,/
     +10X,14HRAD. OF GYR. =,F7.3)
      IF(LC-1)45,45,43
   43 WRITE(IW,44)Y
   44 FORMAT(10X,3HY =,F6.2)
C
C     FIGURES AND WRITES THE COLUMN SLENDERNESS RATIO.
C
   45 SR=CK*CL/RT
      WRITE(IW,46)SR
   46 FORMAT(/5X,13HSLEND. RAT. =,F7.3)
C
C     FIGURES AND WRITES THE LIMITING SLENDERNESS RATIOS.
C
      SRL1=0.0
      DO 50 K=1,NE
      SRL=(W(K)/T(K))*SQRT(24.1/PK(K))
      IF(SRL-SRL1)50,50,48
   48 SRL1=SRL
   50 CONTINUE
      SRL2=SQRT(2.*3.1416**2*29500./FY)
      WRITE(IW,54)SRL1,SRL2
   54 FORMAT(10X,25HLIM. - SECT. FULLY EFF. =,F8.2/
     +10X,22HLIM. - SECT. ELASTIC =,F8.2)
      WRITE(IW,55)
   55 FORMAT(10X,38HTHESE LIMITS REFER TO THE EULER STRESS/
     +10X,29HONLY THE LARGER RATIO APPLIES)
C
C     DETERMINES WHICH LIMITING SLENDERNESS RATIO GOVERNS
C     AND DIRECTS THE SEQUENCE OF OPERATIONS TO THE CORRECT
C     DESIGN EQUATION FOR DETERMINING THE ALLOWABLE STRESS.
C
      IF(SRL1-SR)56,56,70
   56 IF(SRL2-SR)66,66,70
C
C     FIGURES THE ALLOWABE STRESS AND THE COLUMN LOAD IF THE
C     EULER STRESS WITH FULL SECTION PROPERTIES GOVERNS.
C
   66 WRITE(IW,68)
```

```
   68 FORMAT(/5X,35HEULER STRESS GOVERNS, SECTION FULLY,
     +10H EFFECTIVE)
      FA1=(1./FS)*(3.1416**2*29500./(SR**2))
      P=FA1*CAF
      GO TO 97
C
C     FIGURES THE ALLOWABLE STRESS AND THE COLUMN LOAD IF
C     THE EULER STRESS WITH FULL SECTION PROPERTIES DOES NOT
C     GOVERN.
C
   70 IF(SRL1-SRL2)71,71,72
   71 F=FY/2.
      FF=F
      GO TO 73
   72 F=3.1416**2*29500./(SRL1**2)
      FF=F
C
C     CALLS EFFW TO DETERMINE THE EFFECTIVE WIDTHS FOR EACH
C     OF THE ELEMENTS.
C
   73 DO 74 K=1,NE
      CALL EFFW(T(K),W(K),F,PK(K),EW(K))
   74 EW(K)=EW(K)+(FW(K)-W(K))
C
C     CALLS PROP TO DETERMINE THE SECTION PROPERTIES FOR
C     THE EFFECTIVE SECTION.
C
      CALL PROP(W,T,FW,EW,PK,NT,NTE,NE,FY,LC,Y,CAE,CIE,YE)
      RE=SQRT(CIE/CAE)
C
C     FIGURES THE AVERAGE STRESS ON THE SECTION AND FROM
C     THIS THE EDGE STRESS.  THE NEW EDGE STRESS IS THEN
C     COMPARED TO THE ASSUMED STRESS AND IF THEY ARE NOT
C     WITHIN 0.1 KSI OF EACH OTHER, THE NEW EDGE STRESS IS
C     USED FOR ANOTHER ITERATION.
C
      IF((CK*CL/RE)-SQRT(2.*3.1416**2*29500./FY))76,75,75
C
C     THE EULER STRESS WITH THE EFFECTIVE RADIUS OF GYRATION
C     GOVERNS.
C
   75 FA1=(CAE/CAF)*(3.1416**2*29500./((CK*CL/RE)**2))
      KK=1
      GO TO 77
C
C     THE CRC EQUATION GOVERNS.
C
   76 FA1=(CAE/CAF)*(FY-((FY**2)/(4.*3.1416**2*29500.))*
     +(CK*CL/RE)**2)
      KK=2
   77 FC=FA1*CAF/CAE
      SRS=CL*CK/RE
      IF(ABS(FC-F)-.1)79,79,78
   78 F=FC
```

```
      GO TO 73
C
C     DETERMINES THE ALLOWABLE AVERAGE STRESS ON THE SEC-
C     TION AND THE ALLOWABLE LOAD AND WRITES THE DESIGN
C     DATA.
C
   79 IF(KK-1)80,80,82
   80 WRITE(IW,81)
   81 FORMAT(/5X,39HEULER STRESS GOVERNS, SECTION NOT FULLY,
     +10H EFFECTIVE/)
      GO TO 88
   82 IF(CAE-CAF)85,83,83
   83 WRITE(IW,84)
   84 FORMAT(/5X,35HCRC EQUATION GOVERNS, SECTION FULLY,
     +10H EFFECTIVE)
      GO TO 88
   85 WRITE(IW,86)
   86 FORMAT(/5X,39HCRC EQUATION GOVERNS, SECTION NOT FULLY,
     +10H EFFECTIVE/)
   88 FA1=FA1/FS
      P=FA1*CAF
      IF(CAE-CAF)89,97,97
   89 WRITE(IW,91)
   91 FORMAT(5X,33HEFF. WIDTHS (BASED ON FULL WIDTH))
      WRITE(IW,92)
   92 FORMAT(11X,9HELE. TYPE,5X,2HFW,8X,2HEW)
      DO 93 K=1,NE
   93 WRITE(IW,94)NT(K),FW(K),EW(K)
   94 FORMAT(13X,I3,6X,F6.2,4X,F6.2)
      WRITE(IW,95)
   95 FORMAT(/5X,28HEFFECTIVE SECTION PROPERTIES)
      WRITE(IW,42)CAE,CIE,RE
      IF(LC-1)97,97,96
   96 WRITE(IW,44)Y
   97 WRITE(IW,98)FA1,P
   98 FORMAT(/5X,13HALL. STRESS =,F6.2,5X,11HALL. LOAD =,
     +F6.2)
      WRITE(IW,99)FS
   99 FORMAT(10X,22H(BASED ON SAF. FACT. =,F5.2,1H))
C
C     CALLS AISI TO DETERMINE ALLOWABLE STRESS USING THE
C     PRESENT AISI SPECIFICATION.
C
C
      CALL AISI(NTE,NT,W,T,FW,EW,FY,CAF,SR,IW,NE,FS)
  100 WRITE(IW,101)
  101 FORMAT(1H1)
      STOP
      END
```

```
      SUBROUTINE PROP(W,T,FW,EW,PK,NT,NTE,NE,FY,LC,Y,CA,CI,
     +YE)
C
C
C     THE SUBROUTINE PROP FIGURES THE CENTRIOD OF THE SEC-
C     TION IF THE SECTION IS NOT SYMMETRICAL AND FIGURES
C     THE AREA AND MOMENT OF INERTIA.  THESE VALUES ARE
C     FIGURED FOR EITHER THE FULL OR THE EFFECTIVE SECTION
C     DEPENDING ON WHETHER EW(L) IS EQUAL TO FW(L) OR WHE-
C     THER EW(L) IS SET TO THE EFFECTIVE WIDTHS.
C
C
      DIMENSION NTE(20),NT(5),W(20),T(20),FW(20),PK(20),
     +EW(20),YE(20)
      Y=0.0
      CA=0.0
      CI=0.0
      IF(LC-1)100,100,10
C
C     FIGURES THE AREA AND THE AREA TIMES THE DISTANCE TO
C     THE CENTROID OF EACH ELEMENT IF THE SECTION IS NOT
C     SYMMETRICAL ABOUT THE BUCKLING AXIS.
C
   10 AT=0.0
      AYT=0.0
      DO 80 L=1,NE
      NN=NT(L)
C
C     DIRECTS SEQUENCE OF OPERATIONS TO APPROPRIATE SECTION
C     FOR PARTICULAR ELEMENT.
C
      GO TO (20,30,40,50,60),NN
C
C     ELEMENT TYPE 1
C
   20 A=EW(L)*T(L)*NTE(L)
      AY=A*YE(L)
      GO TO 70
C
C     ELEMENT TYPE 2
C
   30 A=EW(L)*T(L)*NTE(L)
      AY=A*YE(L)
      GO TO 70
C
C     ELEMENT TYPE 3
C
   40 A=EW(L)*T(L)*NTE(L)
      IF(EW(L)-.5*FW(L))42,42,44
   42 TE=2.*EW(L)*T(L)/FW(L)
      AY=A*(YE(L)-(1./6.)*FW(L))
      GO TO 70
   44 TT=T(L)*(EW(L)-(FW(L)/2.))/(FW(L)/2.)
      AY=(FW(L)*TT*YE(L)+(FW(L)*(T(L)-TT)/2.)*(YE(L)-FW(L)/
```

```
     +6.))*NTE(L)
      GO TO 70
C
C     ELEMENT TYPE 4
C
   50 A=EW(L)*T(L)*NTE(L)
      IF(EW(L)-.5*FW(L))52,52,54
   52 TE=2.*EW(L)*T(L)/FW(L)
      AY=A*(YE(L)+(1./6.)*FW(L))
      GO TO 70
   54 TT=T(L)*(EW(L)-(FW(L)/2.))/(FW(L)/2.)
      AY=(FW(L)*TT*YE(L)+(FW(L)*(T(L)-TT)/2.)*(YE(L)+FW(L)/
     +6.))*NTE(L)
      GO TO 70
C
C     ELEMENT TYPE 5
C
   60 A=EW(L)*T(L)*NTE(L)
      AY=A*YE(L)
C
C     SUMS THE AREAS AND THE AREAS TIMES THE DISTANCES TO
C     THE CENTRIOD OF THE ELEMENT AND FIGURES THE DISTANCE
C     TO THE CENTROID OF THE WHOLE SECTION.
C
   70 AT=AT+A
      AYT=AYT+AY
   80 CONTINUE
      Y=AYT/AT
C
C     FIGURES THE AREA AND THE MOMENT OF INERTIA ABOUT THE
C     CENTROID OF THE SECTION FOR THE SEPARATE ELEMENTS.
C
  100 DO 200 L=1,NE
      NN=NT(L)
      YE(L)=YE(L)-Y
C
C     DIRECTS SEQUENCE OF OPERATIONS TO APPROPRIATE SECTION
C     FOR PARTICULAR ELEMENT.
C
      GO TO (130,140,150,160,170),NN
C
C     ELEMENT TYPE 1
C
  130 A=EW(L)*T(L)*NTE(L)
      RI=A*YE(L)**2
      GO TO 180
C
C     ELEMENT TYPE 2
C
  140 A=EW(L)*T(L)*NTE(L)
      RI=NTE(L)*((1./6.)*T(L)*(EW(L)/2.)**3+(EW(L)*T(L)/2.)*
     +((YE(L)+(FW(L)/2.)-(EW(L)/4.))**2+(YE(L)-(FW(L)/2.)+
     +(EW(L)/4.))**2))
      GO TO 180
```

```
C
C      ELEMENT TYPE 3
C
  150 A=EW(L)*T(L)*NTE(L)
      IF(EW(L)-.5*FW(L))152,152,154
  152 TE=2.*EW(L)*T(L)/FW(L)
      RI=NTE(L)*((1./36.)*TE*FW(L)**3+(TE*FW(L)/2.)*(YE(L)-
     +(FW(L)/6.))**2)
      GO TO 180
  154 TT=T(L)*(EW(L)-(FW(L)/2.))/(FW(L)/2.)
      RI=NTE(L)*((1./12.)*TT*FW(L)**3+TT*FW(L)*YE(L)**2+
     +(1./36.)*(T(L)-TT)*FW(L)**3+((T(L)-TT)*FW(L)/2.)*
     +(YE(L)-(FW(L)/6.))**2)
      GO TO 180
C
C      ELEMENT TYPE 4
C
  160 A=EW(L)*T(L)*NTE(L)
      IF(EW(L)-.5*FW(L))162,162,164
  162 TE=2.*EW(L)*T(L)/FW(L)
      RI=NTE(L)*((1./36.)*TE*FW(L)**3+(TE*FW(L)/2.)*(YE(L)+
     +(FW(L)/6.))**2)
      GO TO 180
  164 TT=T(L)*(EW(L)-(FW(L)/2.))/(FW(L)/2.)
      RI=NTE(L)*((1./12.)*TT*FW(L)**3+TT*FW(L)*YE(L)**2+
     +(1./36.)*(T(L)-TT)*FW(L)**3+((T(L)-TT)*FW(L)/2.)*
     +(YE(L)+(FW(L)/6.))**2)
      GO TO 180
C
C      ELEMENT TYPE 5
C
  170 A=NTE(L)*EW(L)*T(L)
      RI=A*YE(L)**2
C
C      SUMS THE AREAS AND THE MOMENTS OF INERTIA ABOUT THE
C      CENTROID OF THE SECTION FOR THE TOTAL SECTION.
C
  180 CA=CA+A
      CI=CI+RI
      YE(L)=YE(L)+Y
  200 CONTINUE
      RETURN
      END
```

```
      SUBROUTINE EFFW(T,W,F,PK,EW)
C
C
C     THE SUBROUTINE EFFW FIGURES THE EFFECTIVE WIDTH OF AN
C     ELEMENT (EQ. 7-1).
C
C
      SQ=SQRT(29500.*PK/F)
      WLI=.639*T*SQ
      IF(W-WLI)20,20,10
   10 EW=.950*T*SQ*(1.-0.209*SQ*T/W)
      GO TO 30
   20 EW=W
   30 RETURN
      END
```

```
      SUBROUTINE AISI(NTE,NT,W,T,FW,EW,FY,CAF,SR,IW,NE,FS)
C
C
C     THIS SUBROUTINE FIGURES THE ALLOWABLE STRESS USING THE
C     1968 EDITION OF THE SPECIFICATION FOR THE DESIGN OF
C     COLD-FORMED STEEL STRUCTURAL MEMBERS.  THE ROUTINE IS
C     BASED ON THE SAFETY FACTORS IN THE SPECIFICATION.  THE
C     ROUTINE DOES NOT CONSIDER CLOSED SQUARE AND RECTANGU-
C     LAR TUBES, ANGULAR STRUTS, OR SECTIONS WITH UNSTIF-
C     FENED ELEMENT THICKNESS RATIOS GREATER THAN 60.
C
C
      DIMENSION NTE(20),NT(5),W(20),T(20),FW(20),EW(20),
     +WT(20)
      WRITE(IW,10)
   10 FORMAT(/5X,26HPRESENT AISI SPECIFICATION)
C
C     FIGURES Q BASED ON THE UNSTIFFENED ELEMENTS USING
C     SECTIONS 3.6.1.1 (2) AND 3.2 IN THE SPECIFICATION.
C
      FC=0.6*FY
      DO 55 L=1,NE
      WT(L)=W(L)/T(L)
      IF(NT(L)-2)55,55,25
   25 IF(WT(L)-63.3/(SQRT(FY)))28,28,30
   28 FCC=0.6*FY
      GO TO 50
   30 IF(FY-33.)32,36,36
   32 IF(WT(L)-25.)34,45,45
   34 FCC=0.6*FY-(WT(L)-63.3/(SQRT(FY)))*(0.6*FY-12.8)/
     +(25.*(1.0-2.53/(SQRT(FY))))
      GO TO 50
   36 IF(WT(L)-144./(SQRT(FY)))38,38,40
   38 FCC=FY*(0.767-0.00264*WT(L)*SQRT(FY))
      GO TO 50
   40 IF(WT(L)-25.)42,45,45
   42 FCC=8000./(WT(L)**2)
      GO TO 50
   45 IF(WT(L)-60.)46,46,48
   46 FCC=19.8-0.28*WT(L)
      GO TO 50
   48 WRITE(IW,49)NT(L)
   49 FORMAT(10X,31HWIDTH/THICKNESS OF ELEMENT TYPE,I2/10X,
     +30HGREATER THAN 60, NO AISI VALUE)
      GO TO 100
   50 IF(FCC-FC)52,55,55
   52 FC=FCC
   55 CONTINUE
      QS=FC/(0.6*FY)
C
C     FIGURES Q BASED ON THE STIFFENED ELEMENTS USING
C     SECTIONS 3.6.1.1 (1) AND 2.3.1.1 IN THE SPECIFICA-
C     TION.  THE BASIC DESIGN STRESS IS BASED ON THAT USED
C     FOR THE CALCULATION OF Q FOR THE UNSTIFFENED ELE-
```

```
C      MENTS.
C
       AE=0.0
       DO 68 L=1,NE
       IF(NT(L)-2)60,60,65
   60  IF(WT(L)-171./SQRT(FC))62,62,63
   62  EW(L)=W(L)
       GO TO 64
   63  EW(L)=T(L)*(253./SQRT(FC))*(1.-55.3/(WT(L)*SQRT(FC)))
   64  AEE=T(L)*(EW(L)+FW(L)-W(L))*NTE(L)
       GO TO 68
   65  AEE=T(L)*FW(L)*NTE(L)
   68  AE=AE+AEE
   70  QA=AE/CAF
C
C      DETERMINES Q FOR THE SECTION BASED ON SECTION 3.6.1.1
C      (3) IN THE SPECIFICATION.
C
       Q=QS*QA
C
C      DETERMINES THE AVERAGE AXIAL STRESS ON THE COLUMN
C      BASED ON 3.6.1.1 IN THE SPECIFICATION AND PRINTS THE
C      DATA.
C
       CC=SQRT(2.*3.1416**2*29500./FY)
       IF(SR-(CC/SQRT(Q)))80,85,85
   80  FA=0.522*Q*FY-(Q*FY*SR/1494.)**2
       GO TO 90
   85  FA=151900./(SR**2)
   90  P=FA*CAF
       WRITE(IW,92)Q
   92  FORMAT(10X,3HQ =,F7.4)
       WRITE(IW,94)FA,P
   94  FORMAT(10X,18HAISI ALL. STRESS =,F6.2/10X,
      +16HAISI ALL. LOAD =,F6.2)
       WRITE(IW,95)
   95  FORMAT(10X,30H(BASED ON AISI SAFETY FACTORS))
  100  RETURN
       END
```

```
3
2    1    42.        120.          1.          1.92
2    1     6.76        .06        6.94        4.          .97
2    2     1.88        .12        1.88        4.
2    1    42.         70.          1.          1.
1    1     2.88        .12        2.88        4.
4    3     1.69        .06        1.75         .5         .875
3    2    42.         90.          1.          1.
1    1     5.          .06        5.          4.         1.97
2    2     1.88        .06        2.          4.         1.
2    5     1.44        .06        1.44         .5         .03
```

SAMPLE INPUT FOR EXAMPLES B.1, B.2, AND B.3, RESPECTIVELY

```
COLUMN NO. =   1


    FY = 42.00      COL. LEN. =120.00
    COL. K = 1.00      SAF. FACT. = 1.92

    ELEMENT TYPE =  1
         NO. ELEMENTS =   2      THICK. = 0.0600
         FLAT WIDTH =  6.76      FULL WIDTH =  6.94
         PLATE EDGE FACT. = 4.000
         DIST. TO CENT. =  0.97

    ELEMENT TYPE =  2
         NO. ELEMENTS =   2      THICK. = 0.1200
         FLAT WIDTH =  1.88      FULL WIDTH =  1.88
         PLATE EDGE FACT. = 4.000
         DIST. TO CENT. =  0.00

    SECTION SYM. ABOUT BUCKLING AXIS

    FULL SECTION PROPERTIES
         AREA =  1.284      MOM. OF INER. =  0.916
         RAD. OF GYR. =  0.845

    SLEND. RAT. =142.038
         LIM. - SECT. FULLY EFF. =  276.55
         LIM. - SECT. ELASTIC =  117.75
         THESE LIMITS REFER TO THE EULER STRESS
         ONLY THE LARGER RATIO APPLIES

    EULER STRESS GOVERNS, SECTION NOT FULLY EFFECTIVE

    EFF. WIDTHS (BASED ON FULL WIDTH)
          ELE. TYPE      FW         EW
              1         6.94       4.63
              2         1.88       1.88

    EFFECTIVE SECTION PROPERTIES
         AREA =  1.006      MOM. OF INER. =  0.655
         RAD. OF GYR. =  0.807

    ALL. STRESS =  5.37      ALL. LOAD =  6.90
         (BASED ON SAF. FACT. = 1.92)

    PRESENT AISI SPECIFICATION
         Q = 0.6232
         AISI ALL. STRESS =  7.47
         AISI ALL. LOAD =  9.59
         (BASED ON AISI SAFETY FACTORS)
```

SAMPLE OUTPUT FOR EXAMPLE B.1

```
COLUMN NO. =   2


   FY = 42.00      COL. LEN. = 70.00
   COL. K = 1.00      SAF. FACT. = 1.00

   ELEMENT TYPE =  1
        NO. ELEMENTS =    1       THICK. = 0.1200
        FLAT WIDTH =   2.88       FULL WIDTH =   2.88
        PLATE EDGE FACT. = 4.000
        DIST. TO CENT. =   0.00

   ELEMENT TYPE =  3
        NO. ELEMENTS =    4       THICK. = 0.0600
        FLAT WIDTH =   1.69       FULL WIDTH =   1.75
        PLATE EDGE FACT. = 0.500
        DIST. TO CENT. =   0.88

   SECTION SYM. ABOUT BUCKLING AXIS

   FULL SECTION PROPERTIES
        AREA =  0.766      MOM. OF INER. =  0.429
        RAD. OF GYR. =  0.748

   SLEND. RAT. = 93.540
        LIM. - SECT. FULLY EFF. =  195.55
        LIM. - SECT. ELASTIC =  117.75
        THESE LIMITS REFER TO THE EULER STRESS
        ONLY THE LARGER RATIO APPLIES

   CRC EQUATION GOVERNS, SECTION NOT FULLY EFFECTIVE

   EFF. WIDTHS (BASED ON FULL WIDTH)
         ELE. TYPE      FW          EW
             1         2.88        2.88
             3         1.75        1.24

   EFFECTIVE SECTION PROPERTIES
        AREA =  0.644      MOM. OF INER. =  0.243
        RAD. OF GYR. =  0.614

   ALL. STRESS = 18.78      ALL. LOAD = 14.38
        (BASED ON SAF. FACT. = 1.00)

   PRESENT AISI SPECIFICATION
        Q = 0.4728
        AISI ALL. STRESS =  8.82
        AISI ALL. LOAD =  6.75
        (BASED ON AISI SAFETY FACTORS)
```

SAMPLE OUTPUT FOR EXAMPLE B.2

```
COLUMN NO. =   3

   FY = 42.00      COL. LEN. = 90.00
   COL. K = 1.00      SAF. FACT. = 1.00

   ELEMENT TYPE =  1
        NO. ELEMENTS =    1      THICK. = 0.0600
        FLAT WIDTH =   5.00      FULL WIDTH =   5.00
        PLATE EDGE FACT. = 4.000
        DIST. TO CENT. =  1.97

   ELEMENT TYPE =  2
        NO. ELEMENTS =    2      THICK. = 0.0600
        FLAT WIDTH =   1.88      FULL WIDTH =   2.00
        PLATE EDGE FACT. = 4.000
        DIST. TO CENT. =  1.00

   ELEMENT TYPE =  5
        NO. ELEMENTS =    2      THICK. = 0.0600
        FLAT WIDTH =   1.44      FULL WIDTH =   1.44
        PLATE EDGE FACT. = 0.500
        DIST. TO CENT. =  0.03

   SECTION NOT SYM. ABOUT BUCKLING AXIS

   FULL SECTION PROPERTIES
        AREA =  0.713      MOM. OF INER. =  0.503
        RAD. OF GYR. =  0.840
        Y =  1.17

   SLEND. RAT. =107.085
        LIM. - SECT. FULLY EFF. =  204.55
        LIM. - SECT. ELASTIC =  117.75
        THESE LIMITS REFER TO THE EULER STRESS
        ONLY THE LARGER RATIO APPLIES

   CRC EQUATION GOVERNS, SECTION NOT FULLY EFFECTIVE

   EFF. WIDTHS (BASED ON FULL WIDTH)
         ELE. TYPE      FW         EW
             1         5.00       3.31
             2         2.00       2.00
             5         1.44       1.11

   EFFECTIVE SECTION PROPERTIES
        AREA =  0.572      MOM. OF INER. =  0.385
        RAD. OF GYR. =  0.821
        Y =  1.11

   ALL. STRESS = 19.09      ALL. LOAD = 13.61
        (BASED ON SAF. FACT. = 1.00)

   PRESENT AISI SPECIFICATION
        Q = 0.4745
        AISI ALL. STRESS =  8.36
        AISI ALL. LOAD =  5.96
        (BASED ON AISI SAFETY FACTORS)
```

SAMPLE OUTPUT FOR EXAMPLE B.3

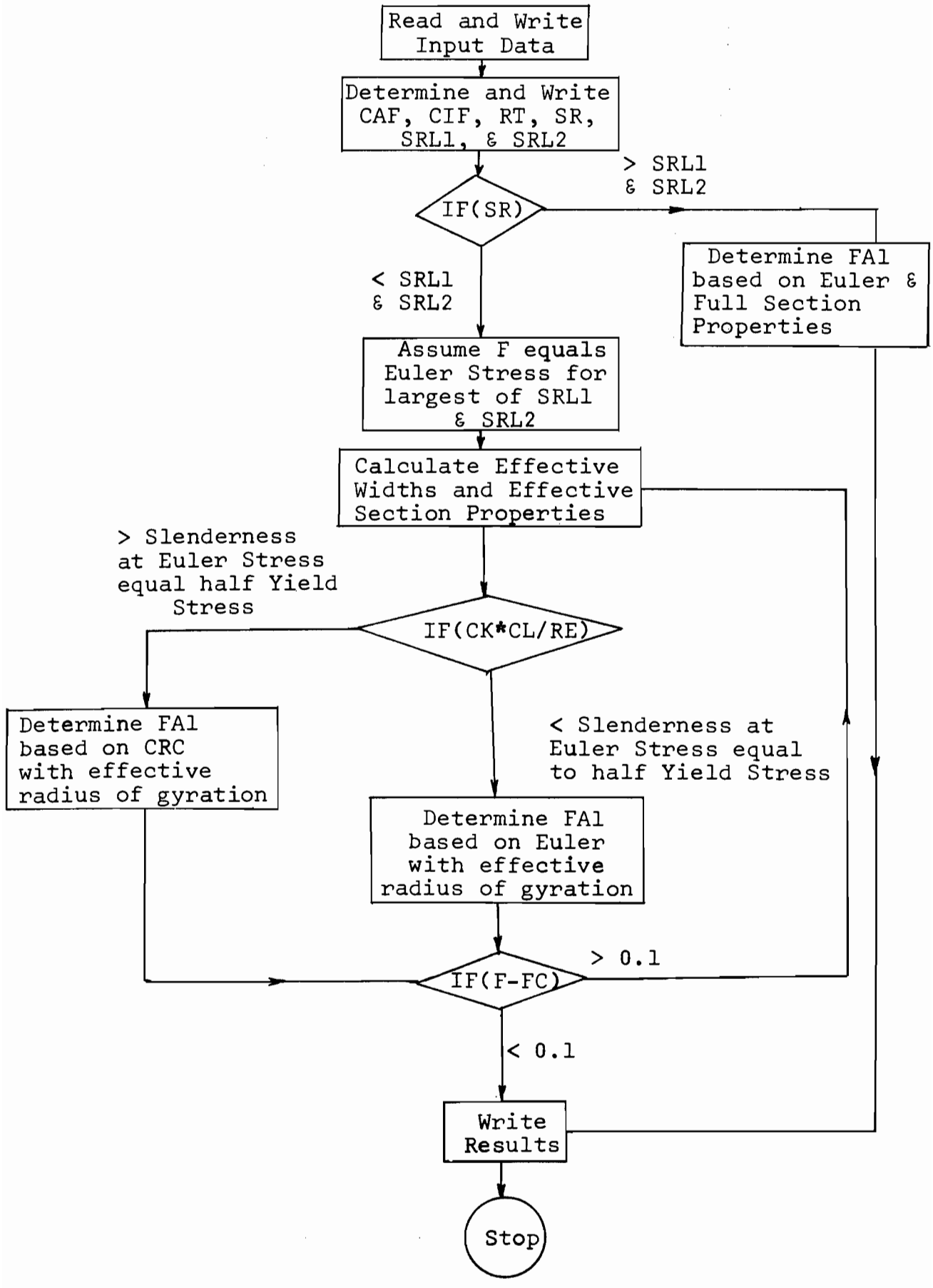

FLOW CHART FOR DESIGN METHOD PROGRAM

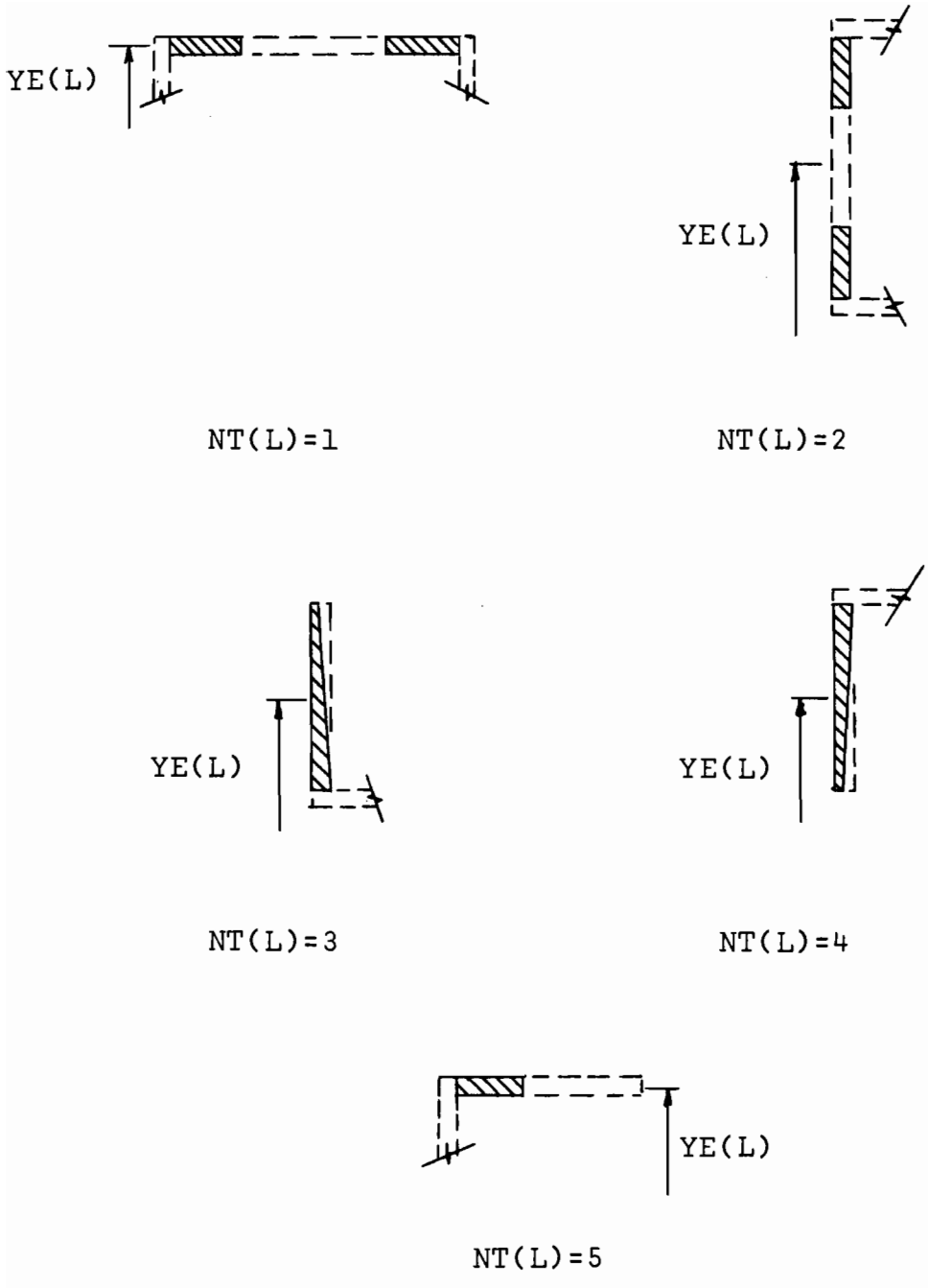

NT(L)=1

NT(L)=2

NT(L)=3

NT(L)=4

NT(L)=5

Note: Buckling axis is horizontal and effective portions are cross-hatched.

FIG. D.1 ELEMENT TYPES AND EFFECTIVE PORTIONS FOR DESIGN PROGRAM

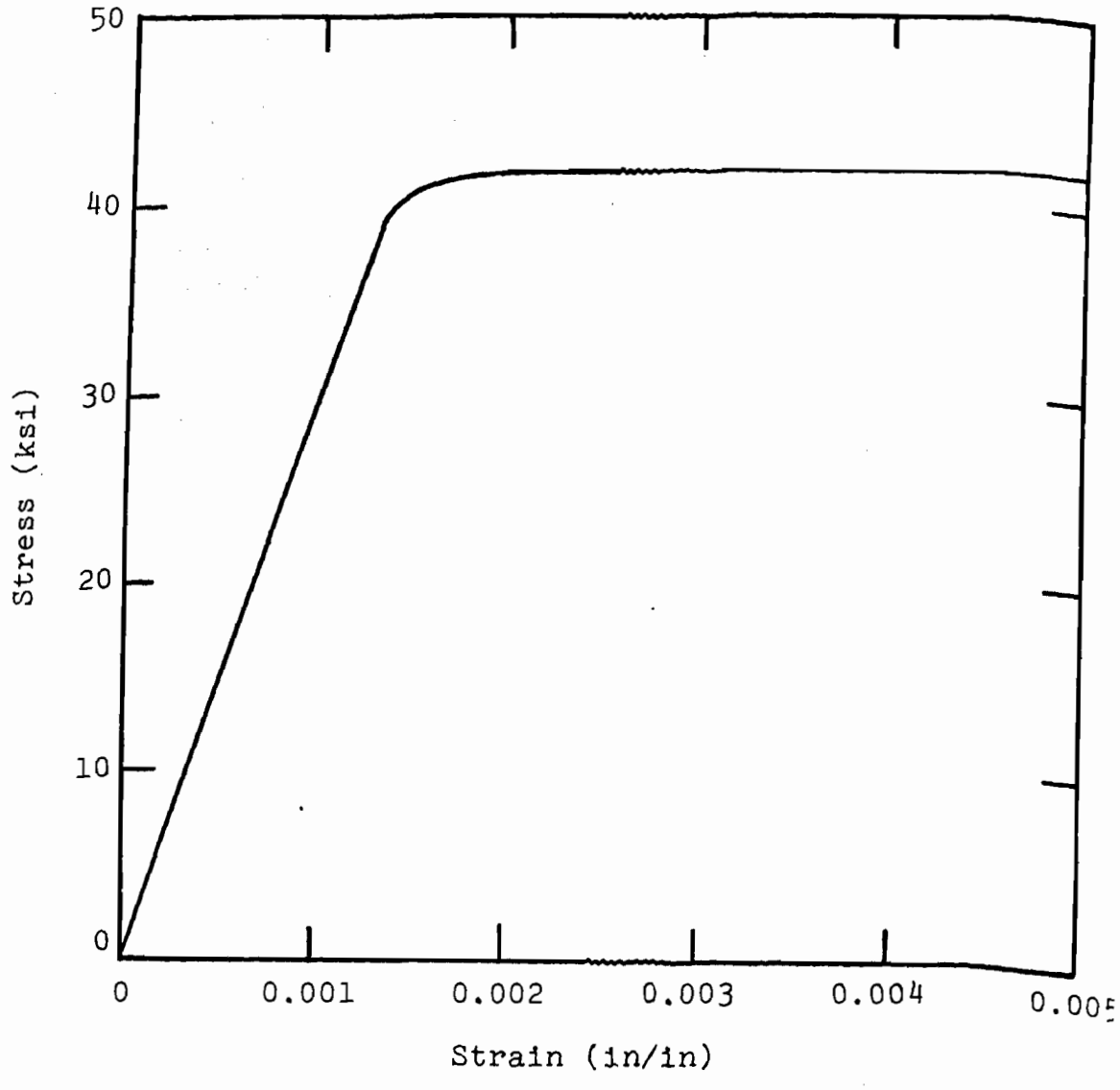

FIG. 3.1 MATERIAL STRESS-STRAIN CURVE

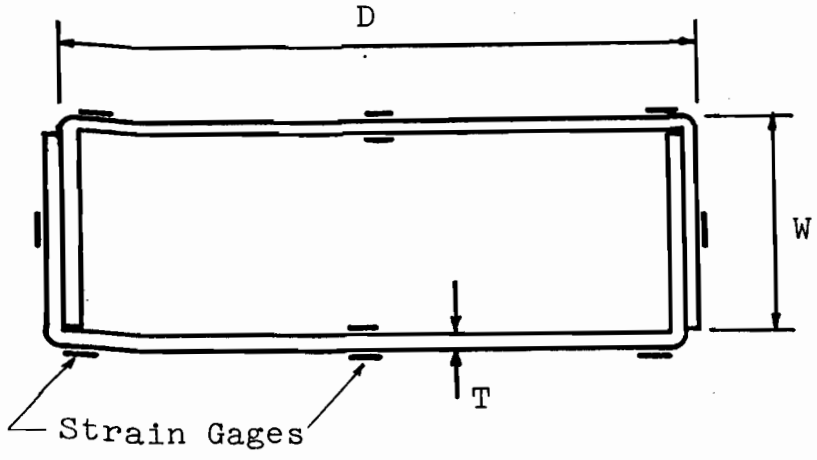

(a) Stiffened Section S

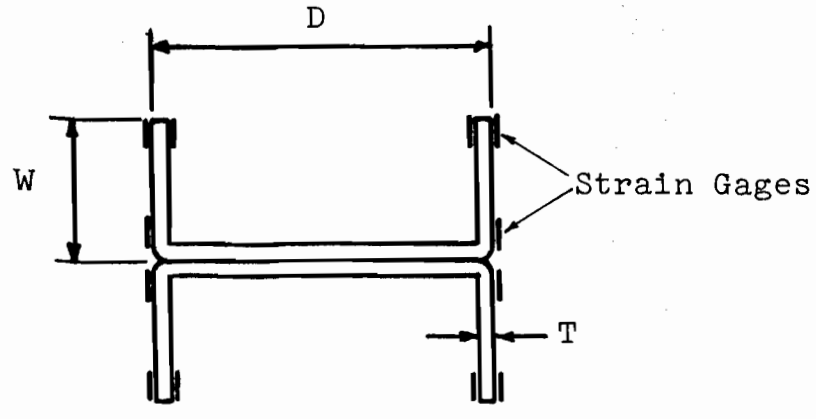

(b) Unstiffened Section U

Note: Dimensions referred to are given in Table 3.1.

FIG. 3.2 COLUMN SPECIMENS' CROSS-SECTIONS WITH STRAIN GAGES

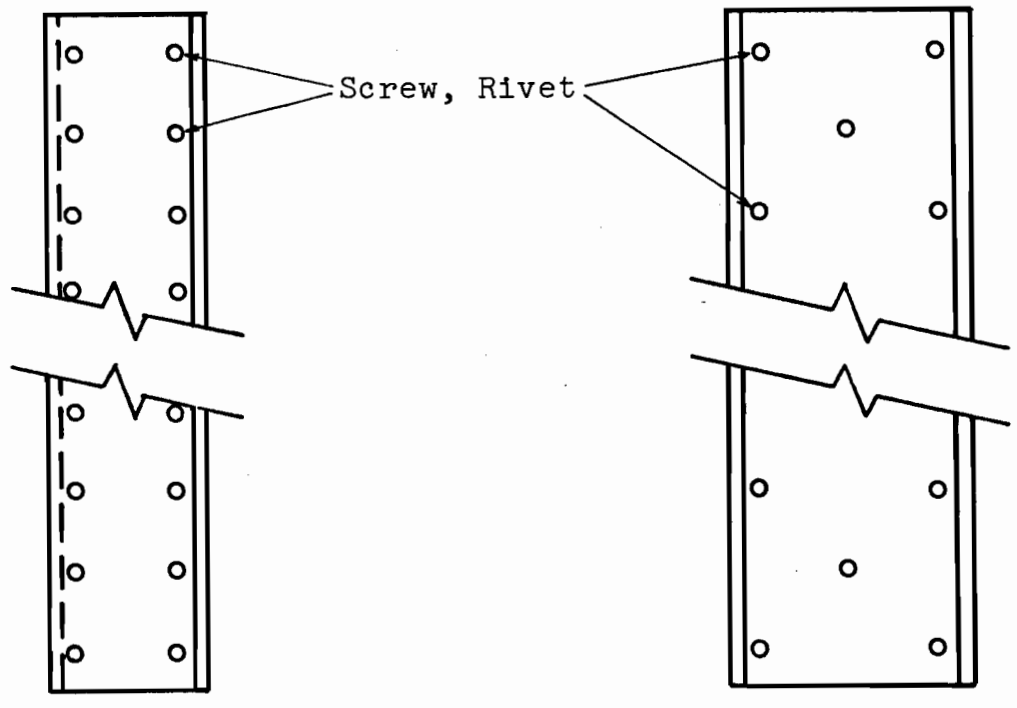

(a) Stiffened Section S

(b) Unstiffened Section U

FIG. 3.3 LOCATION OF SCREWS OR RIVETS FOR COLUMNS

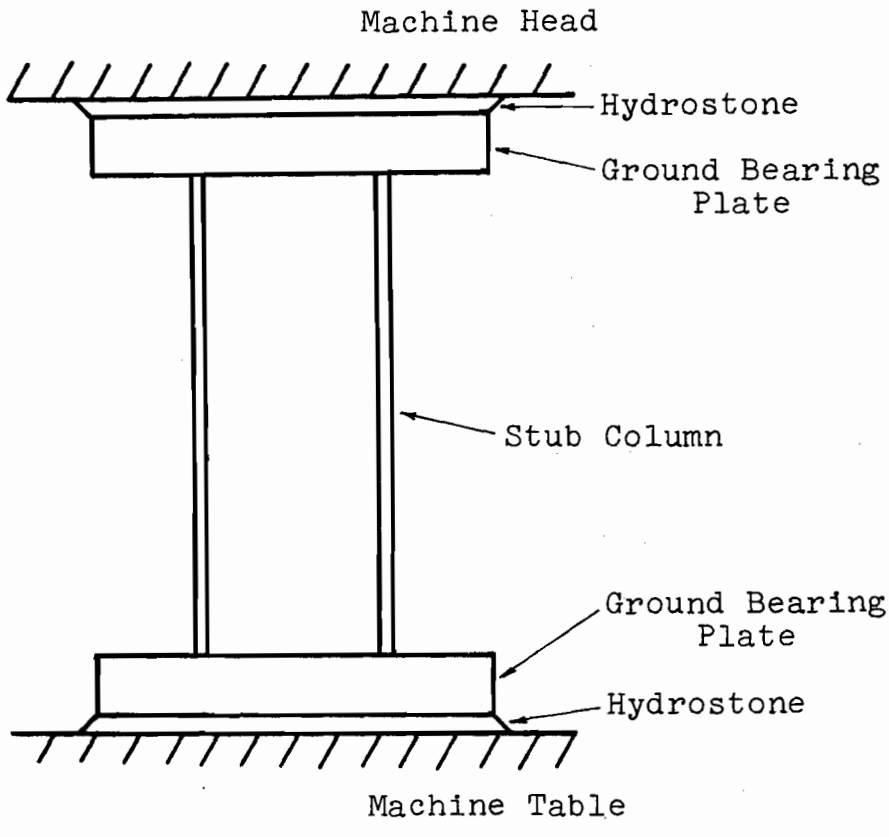

FIG. 3.4 STUB COLUMN TEST SET-UP

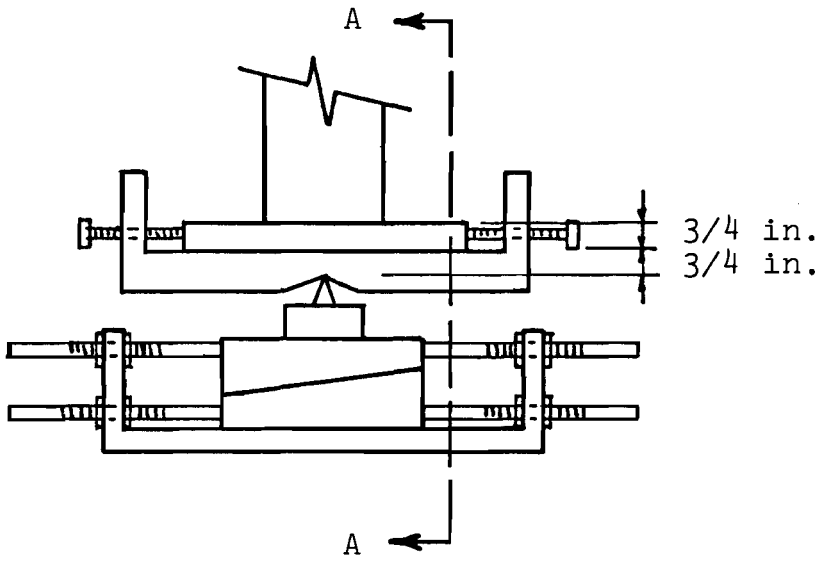

(a) Section through Support in Direction of Flexural Buckling

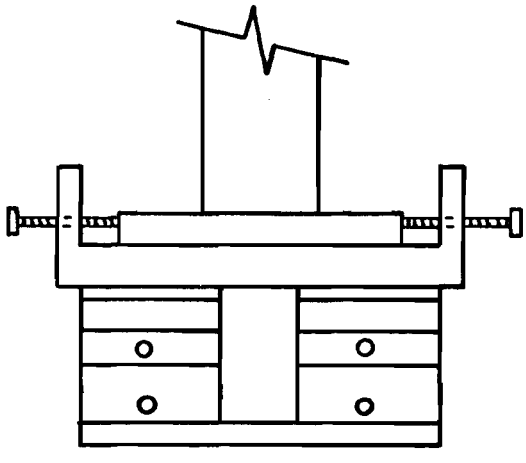

(b) Section A-A

FIG. 3.5 END FIXTURE FOR COLUMN TESTS

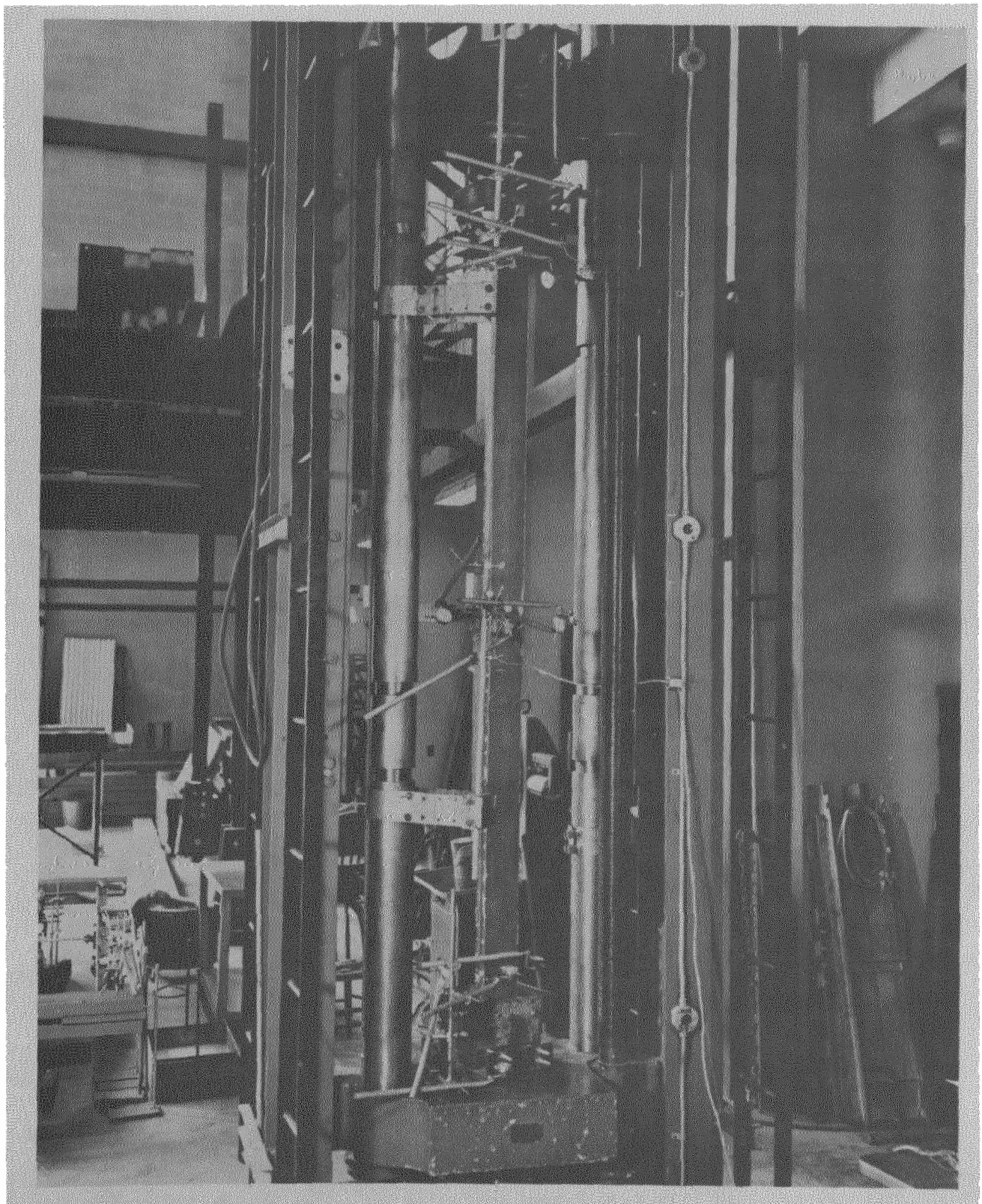

FIG. 3.6 COLUMN FOR PINNED-END TEST

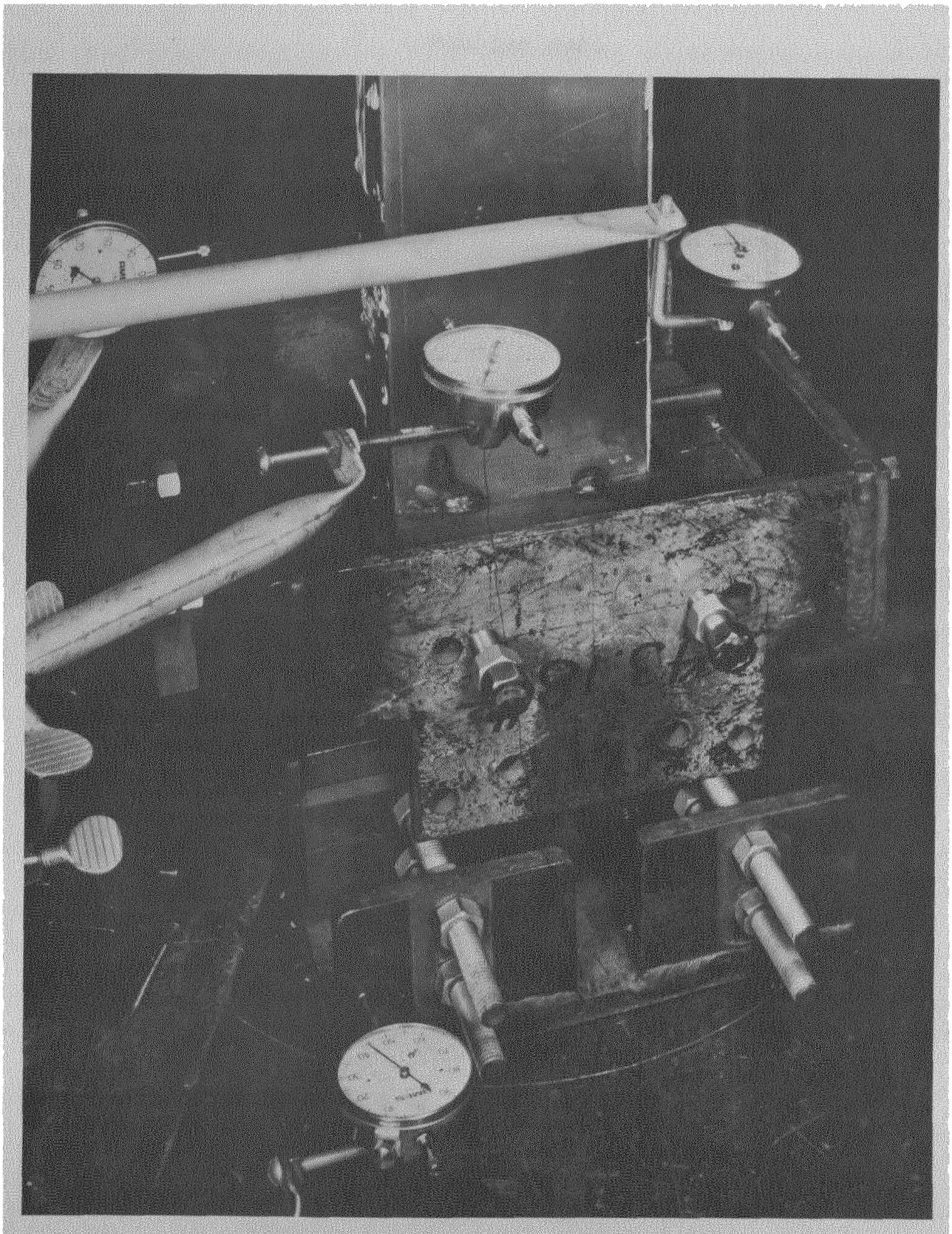

FIG. 3.7 CLOSEUP OF LOWER PINNED-END FIXTURE

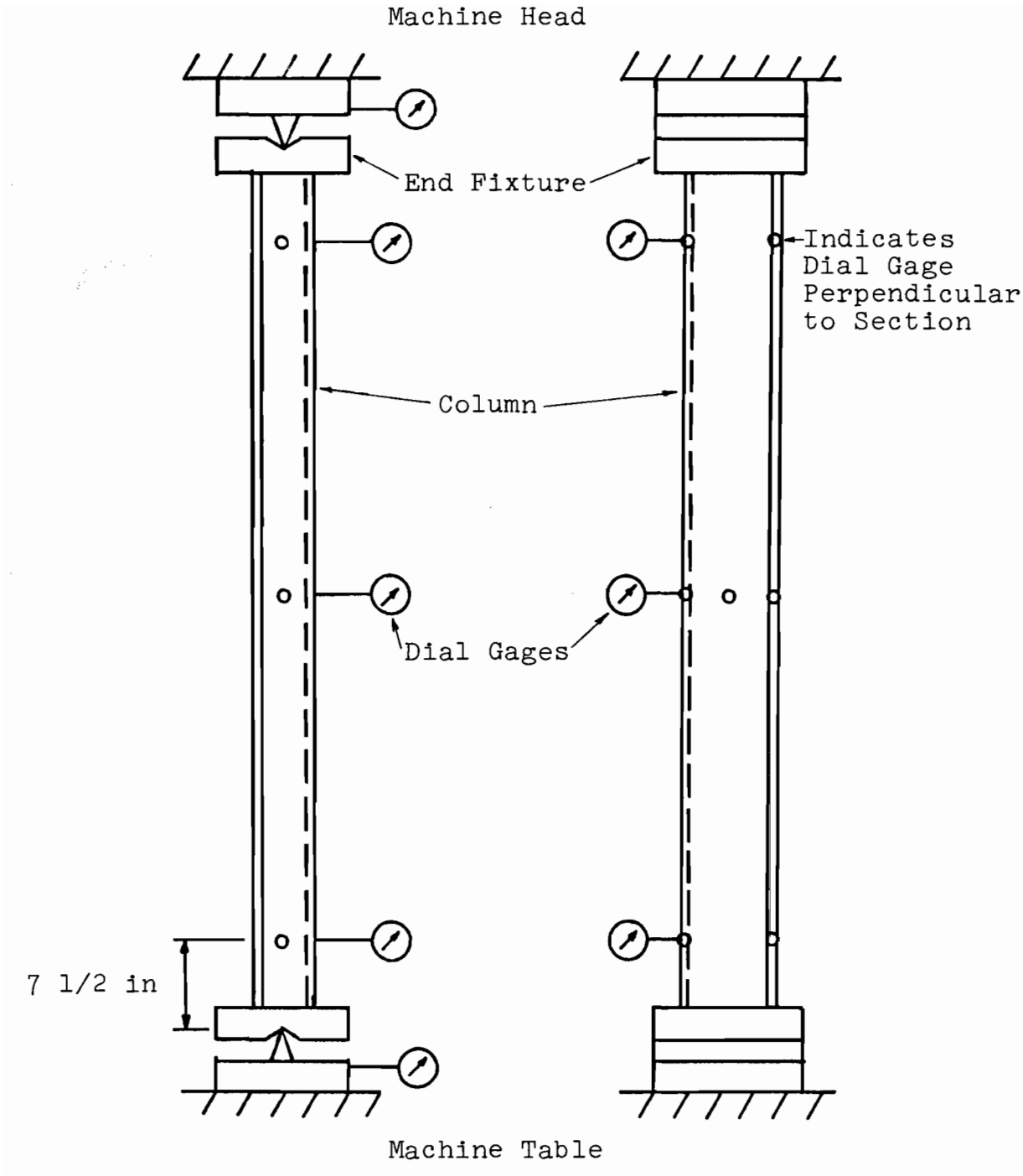

FIG. 3.8 LOCATION OF DIAL GAGES FOR THE STIFFENED SECTIONS S

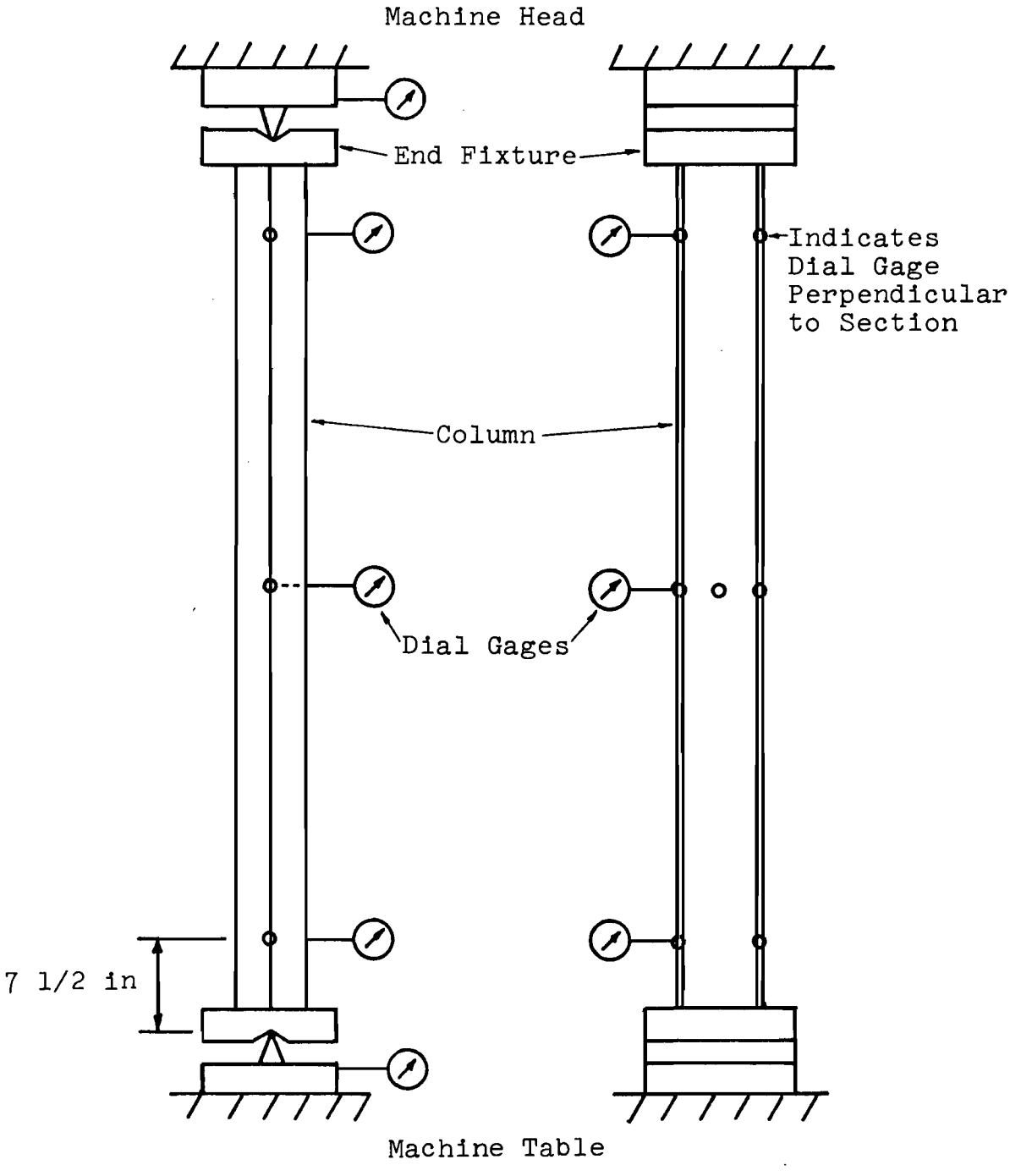

FIG. 3.9 LOCATION OF DIAL GAGES FOR THE UNSTIFFENED SECTIONS U

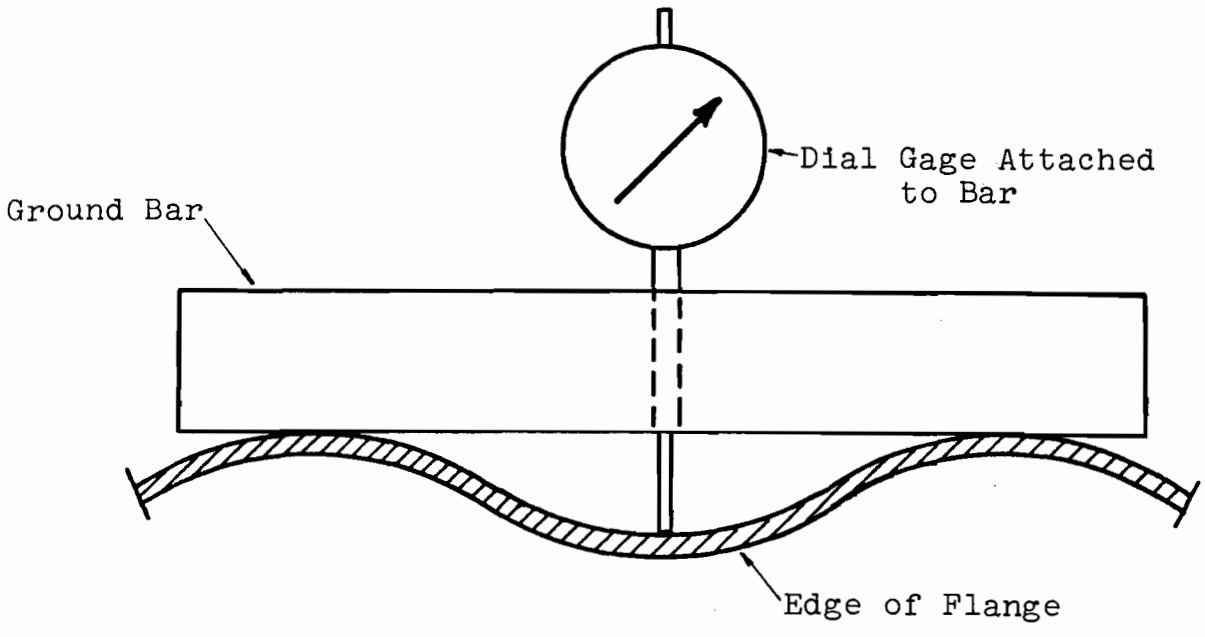

FIG. 3.10 DEVICE FOR MEASURING THE OUT-OF-PLANE DISTORTIONS OF UNSTIFFENED ELEMENTS

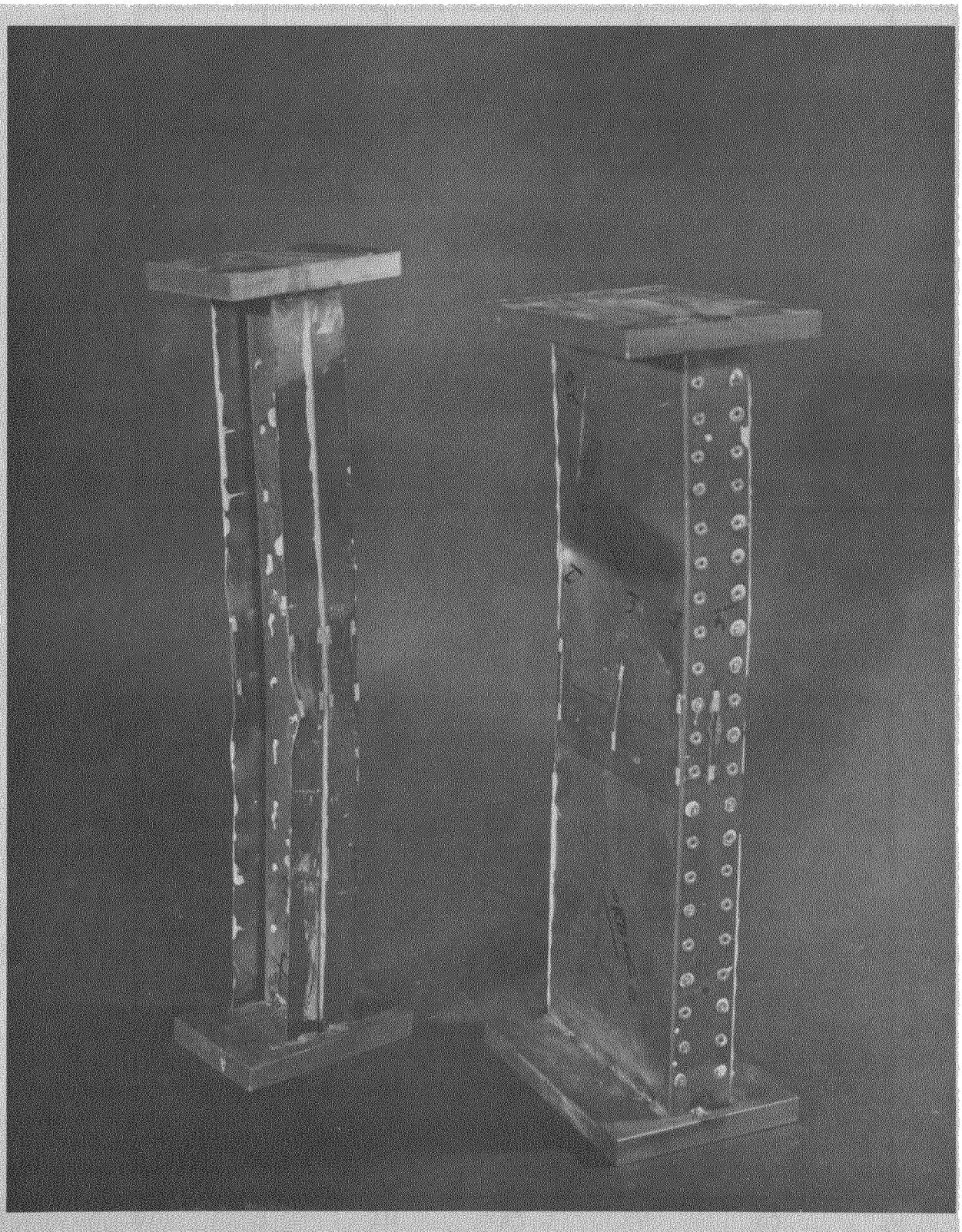

FIG. 3.11 UNSTIFFENED AND STIFFENED COLUMN AFTER FAILURE

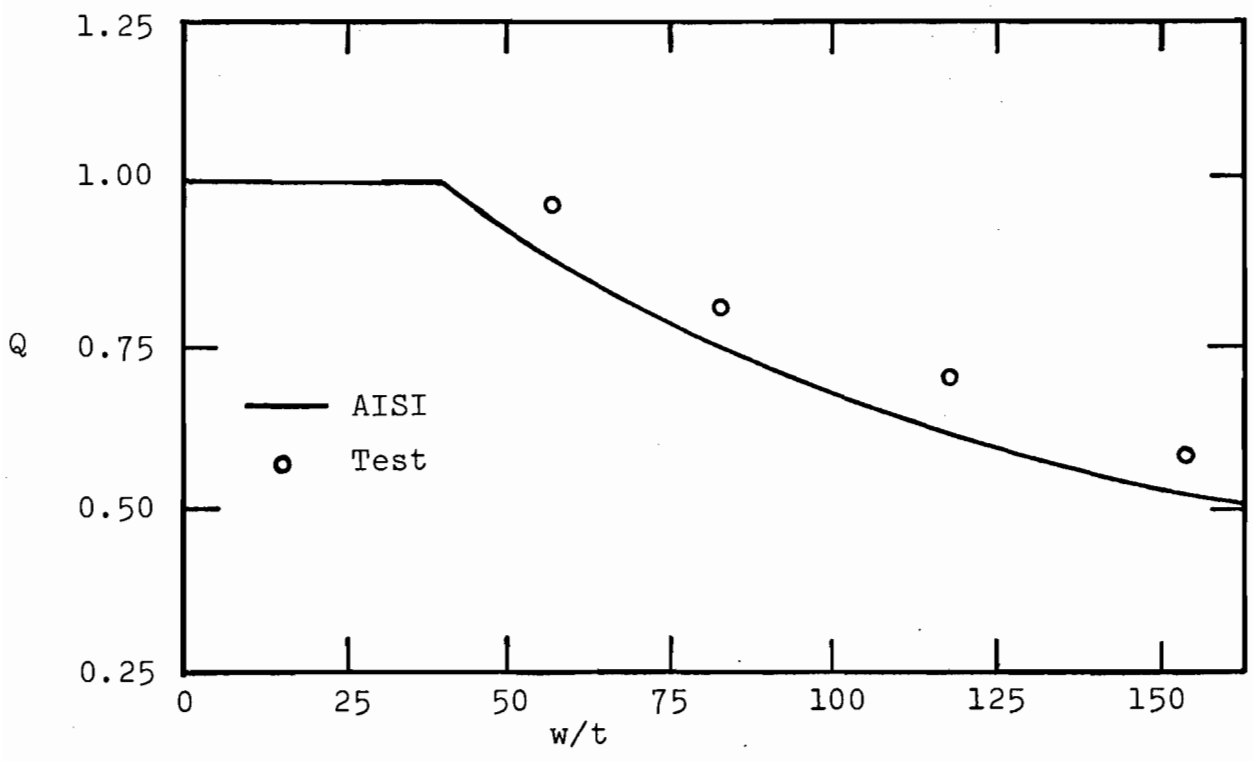

(a) Stiffened Sections S

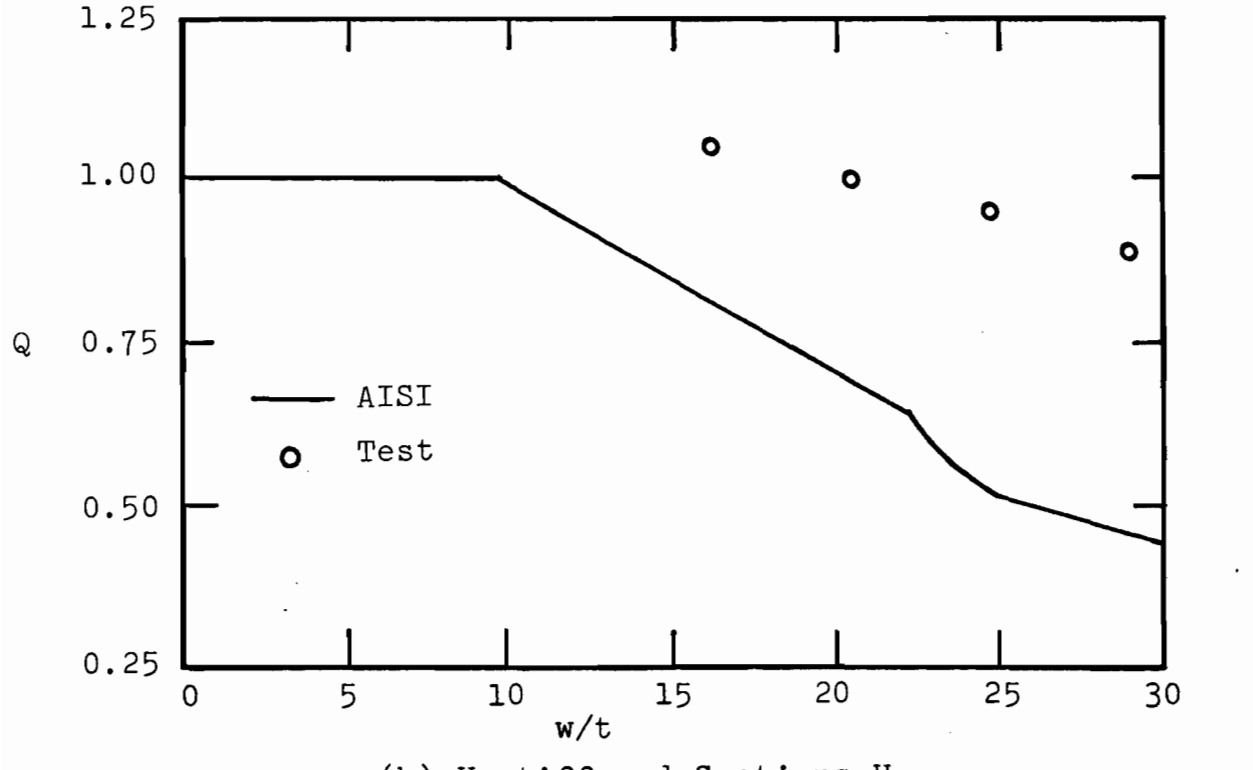

(b) Unstiffened Sections U

FIG. 4.1 COMPARISON OF Q VALUES AS DETERMINED FROM THE AISI SPECIFICATION AND FROM THE STUB COLUMN TESTS

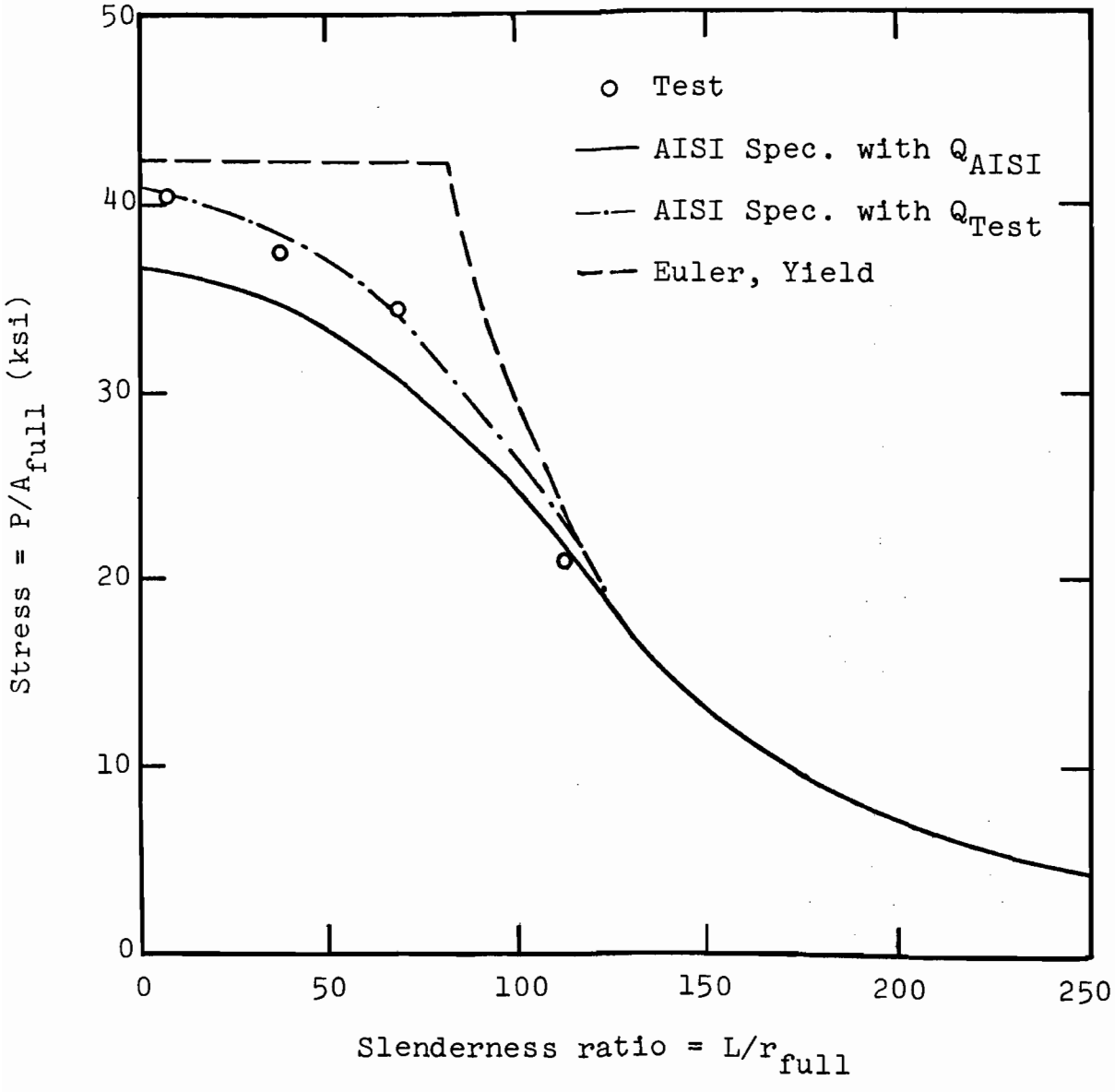

FIG. 4.2 COMPARISON OF TEST RESULTS AND AISI SPECIFICATION COLUMN CURVE FOR STIFFENED SECTION S-1

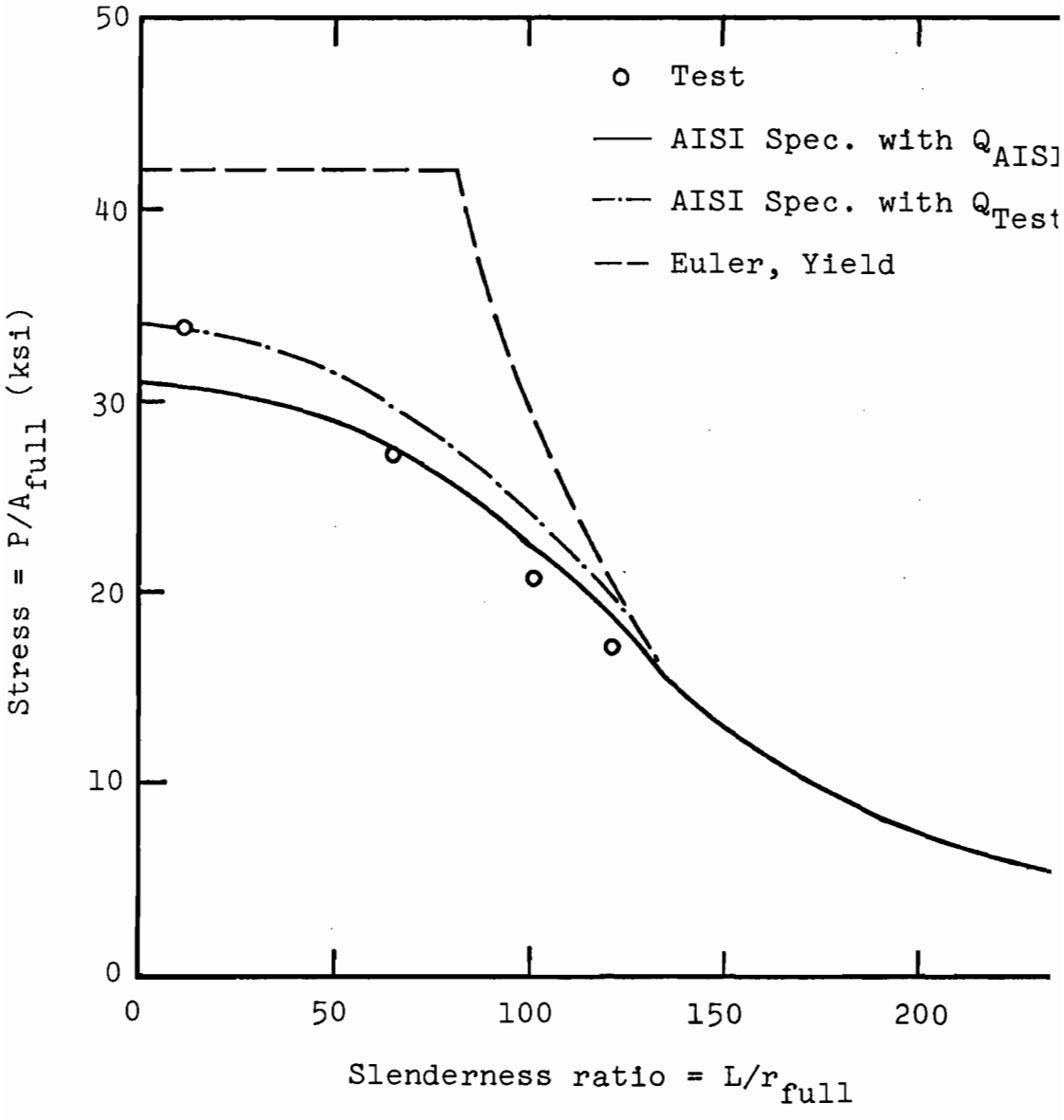

FIG. 3 COMPARISON OF TEST RESULTS AND AISI SPECIFICATION COLUMN CURVE FOR STIFFENED SECTION S-2

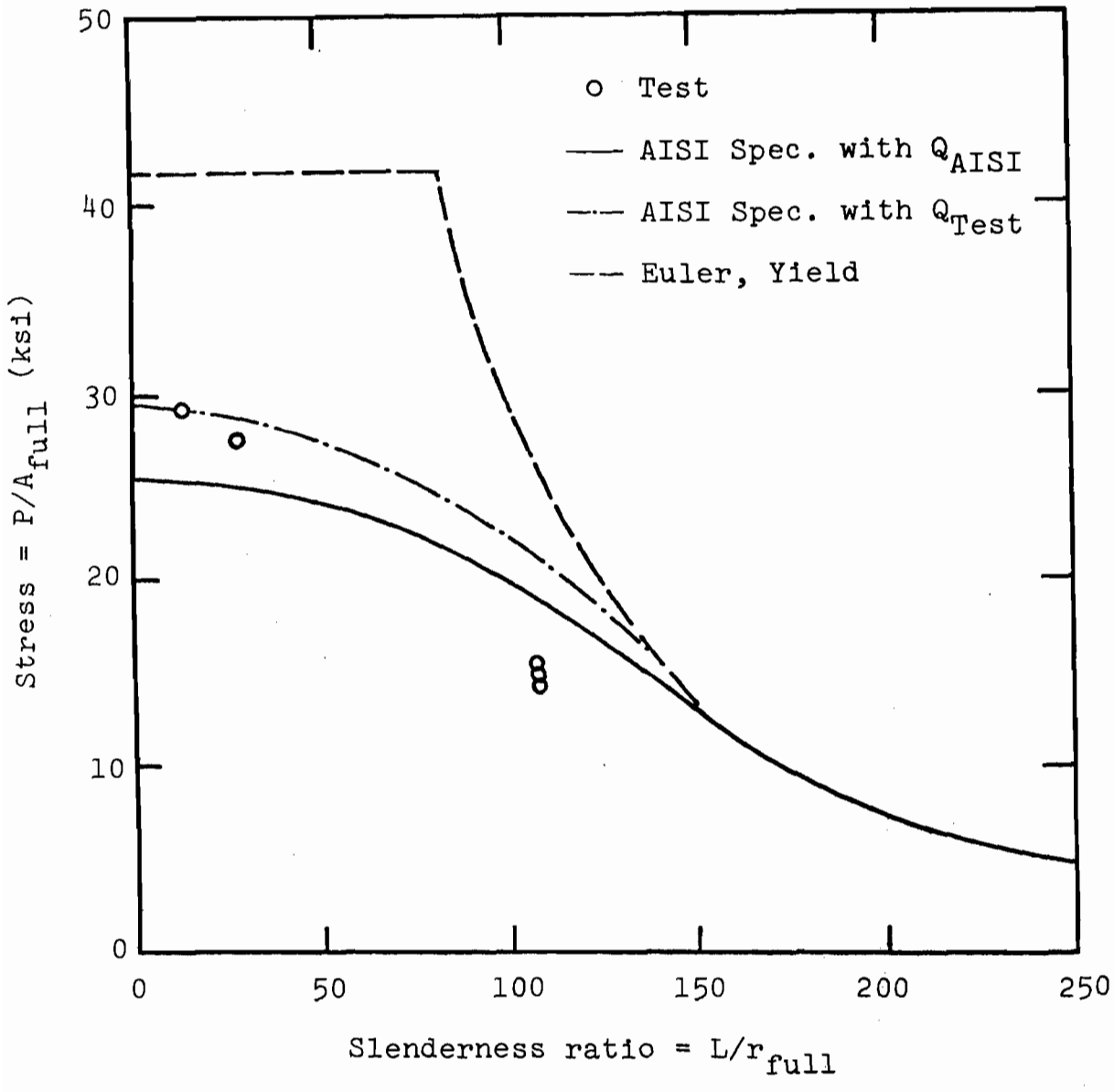

FIG. 4.4 COMPARISON OF TEST RESULTS AND AISI SPECIFICATION COLUMN CURVE FOR STIFFENED SECTION S-3

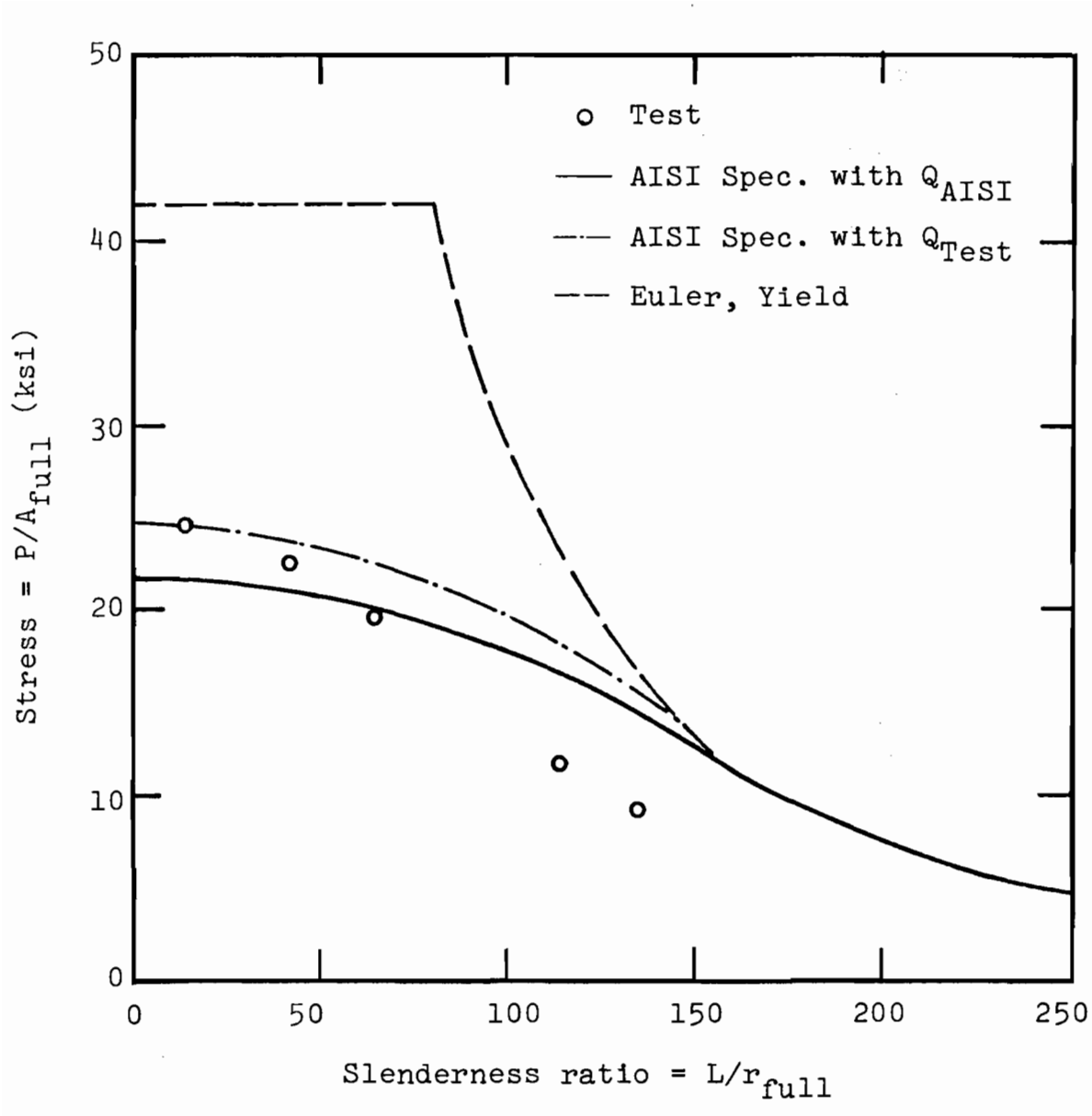

FIG. 4.5 COMPARISON OF TEST RESULTS AND AISI SPECIFICATION COLUMN CURVE FOR STIFFENED SECTION S-4

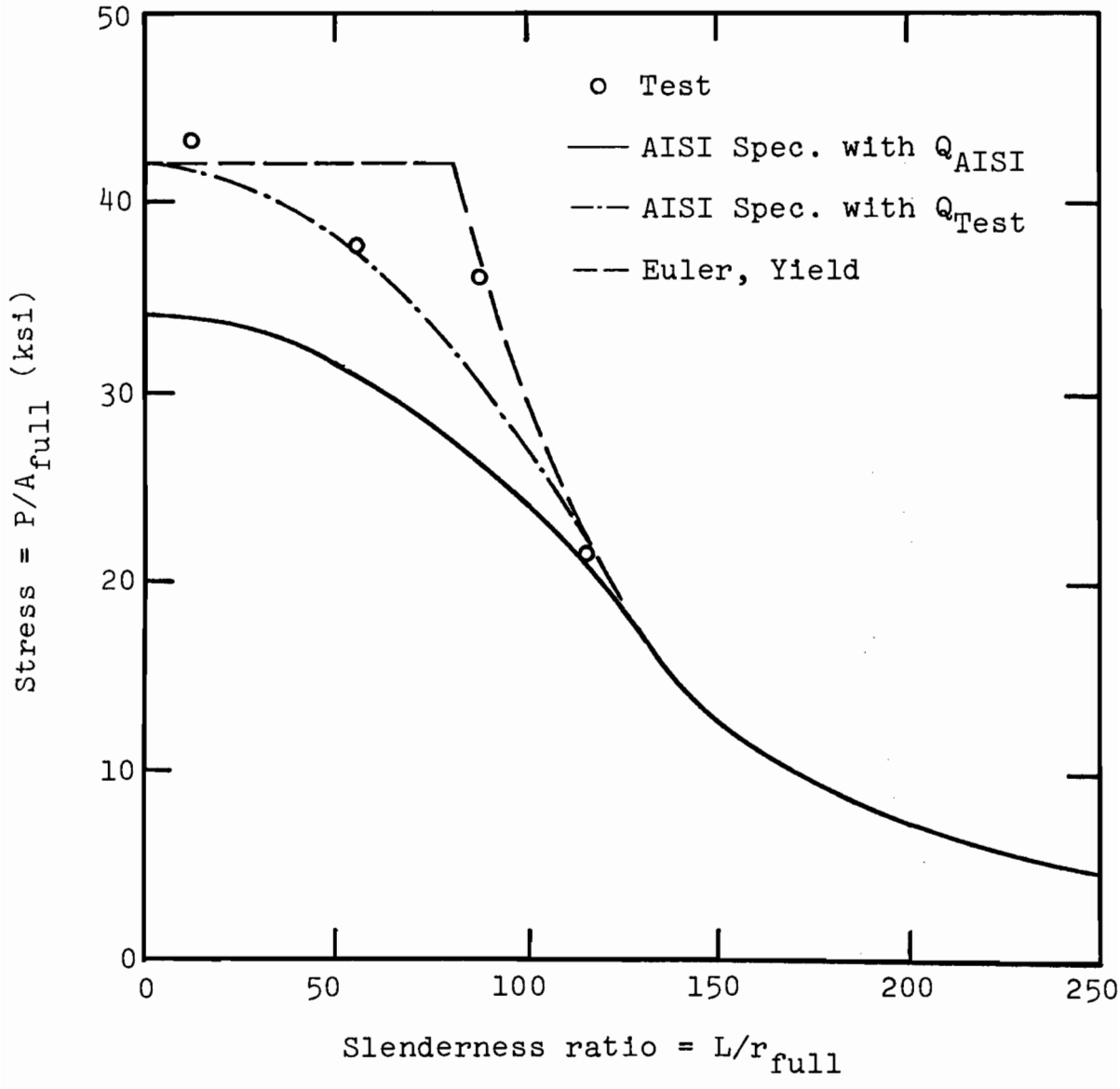

FIG. 4.6 COMPARISON OF TEST RESULTS AND AISI SPECIFICATION COLUMN CURVE FOR UNSTIFFENED SECTION U-1

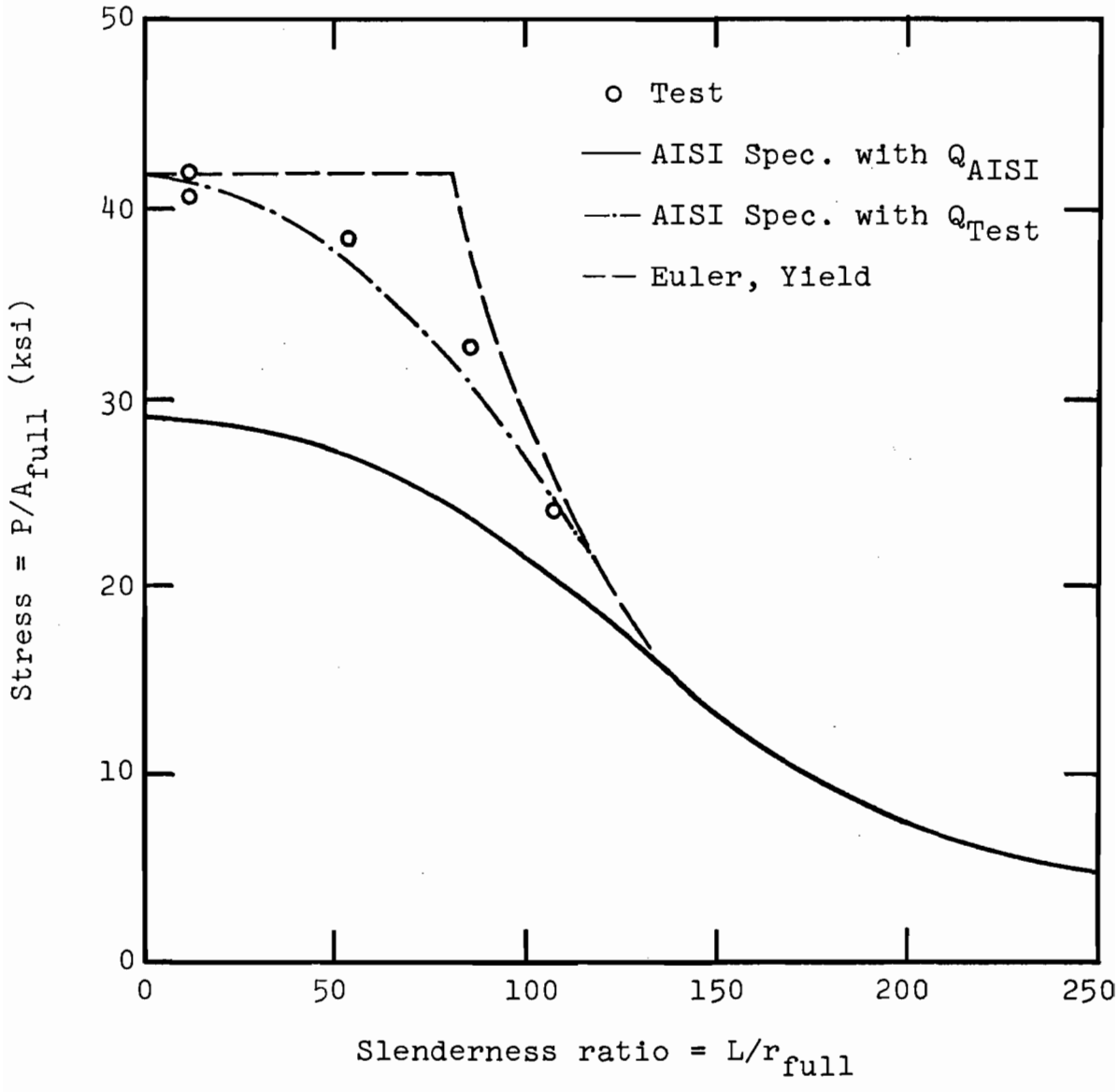

FIG. 4.7 COMPARISON OF TEST RESULTS AND AISI SPECIFICATION COLUMN CURVE FOR UNSTIFFENED SECTION U-2

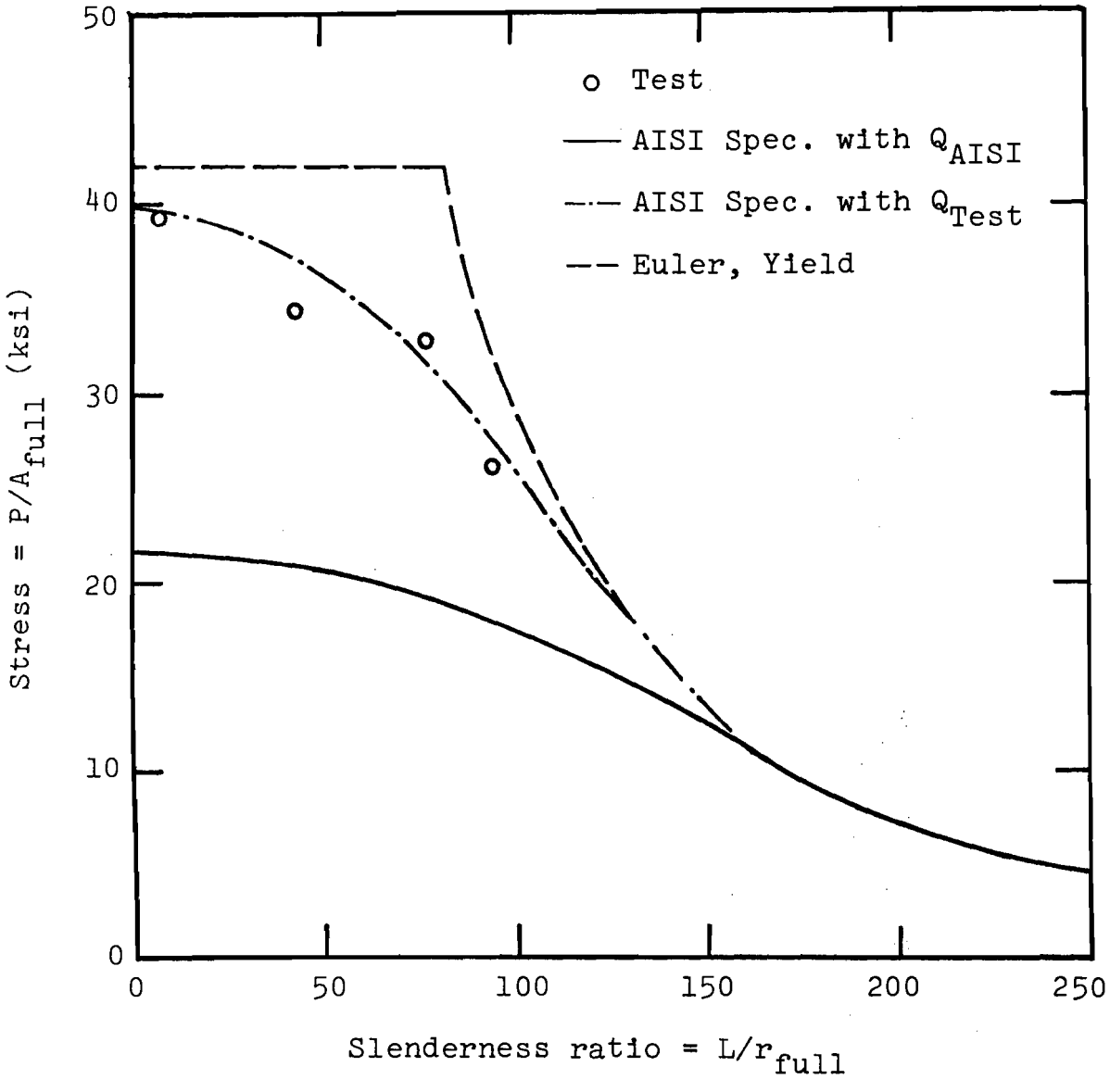

FIG. 4.8 COMPARISON OF TEST RESULTS AND AISI SPECIFICATION COLUMN CURVE FOR UNSTIFFENED SECTION U-3

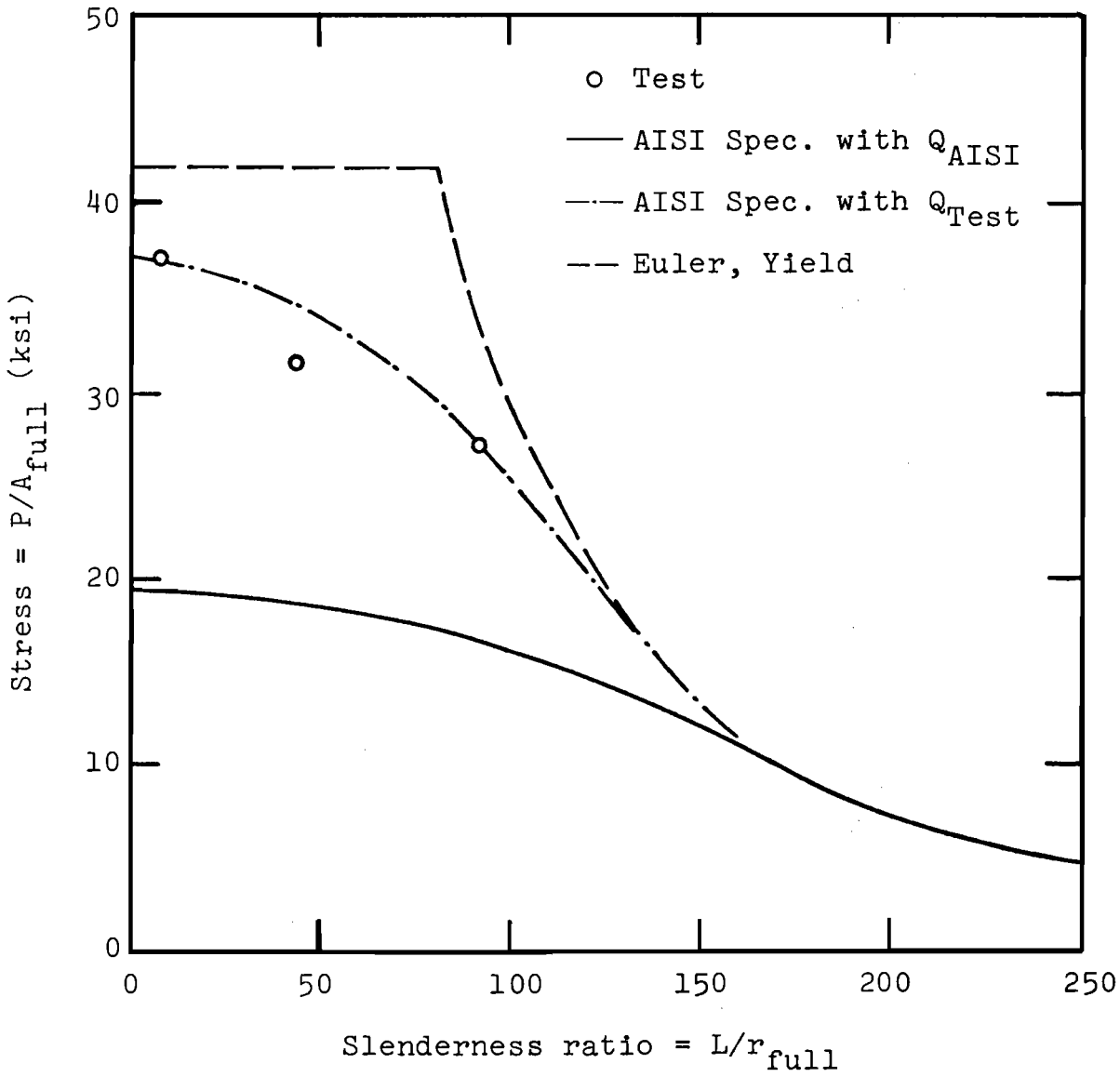

FIG. 4.9 COMPARISON OF TEST RESULTS AND AISI SPECIFICATION COLUMN CURVE FOR UNSTIFFENED SECTION U-4

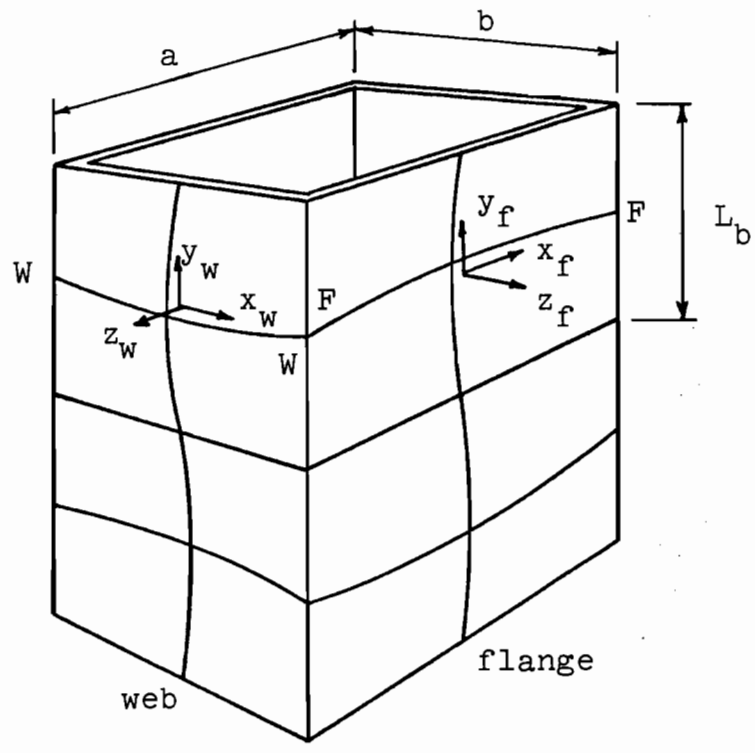

(a) Tubular Section with Local Buckles

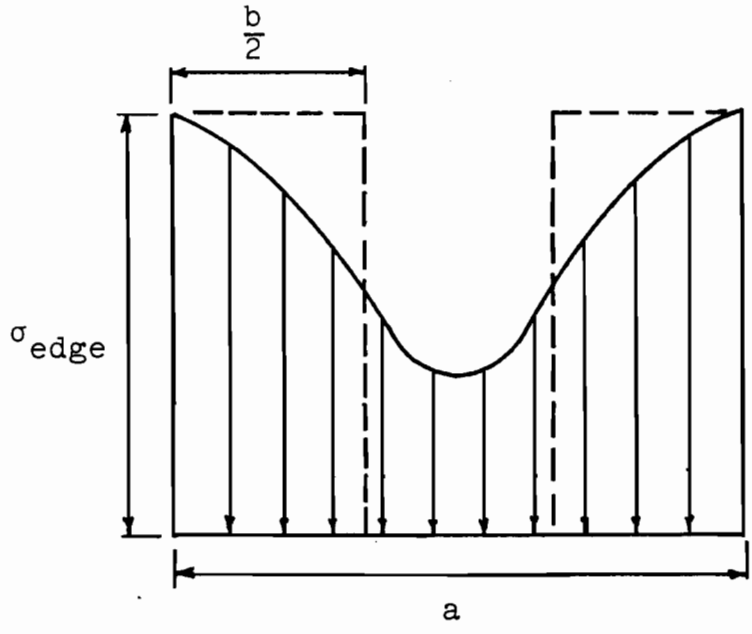

(b) Effective Width Representation through F-F

FIG. 5.1 REPRESENTATION OF COLUMN FOR RIGOROUS ANALYTICAL APPROACH

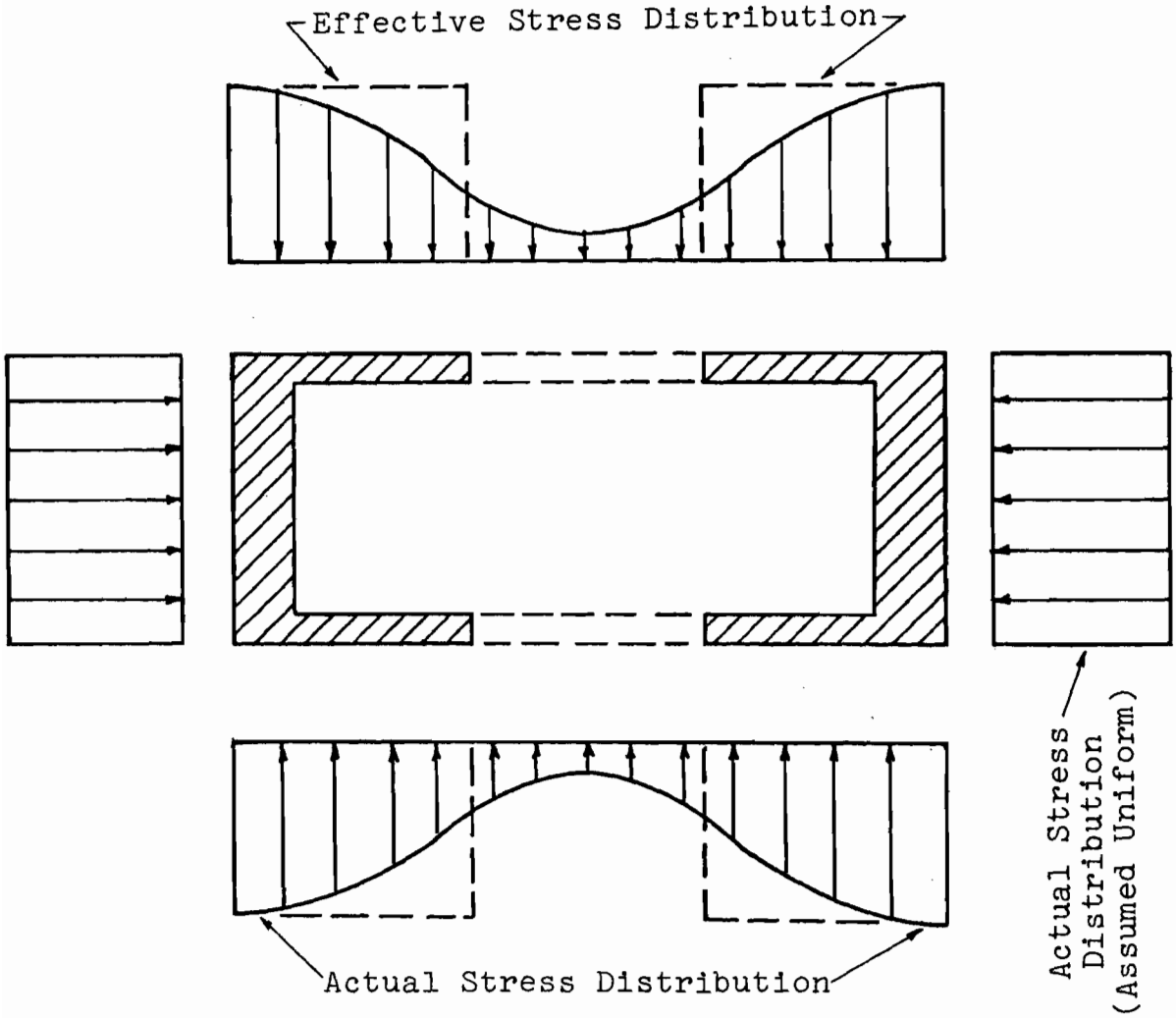

FIG. 5.2 EFFECTIVE STIFFENED SECTION WITH STRESS DISTRIBUTIONS FOR RIGOROUS ANALYTICAL APPROACH

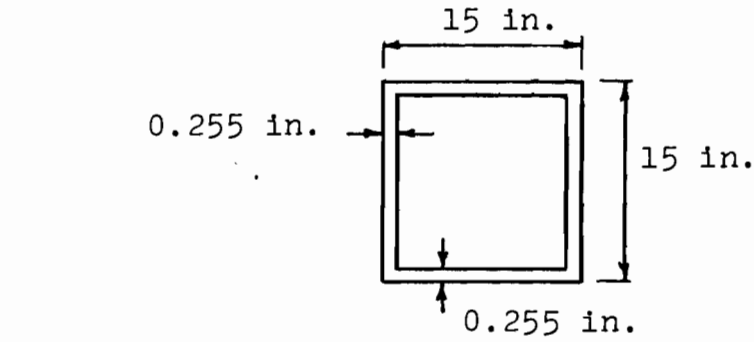

(a) Column Cross-Section

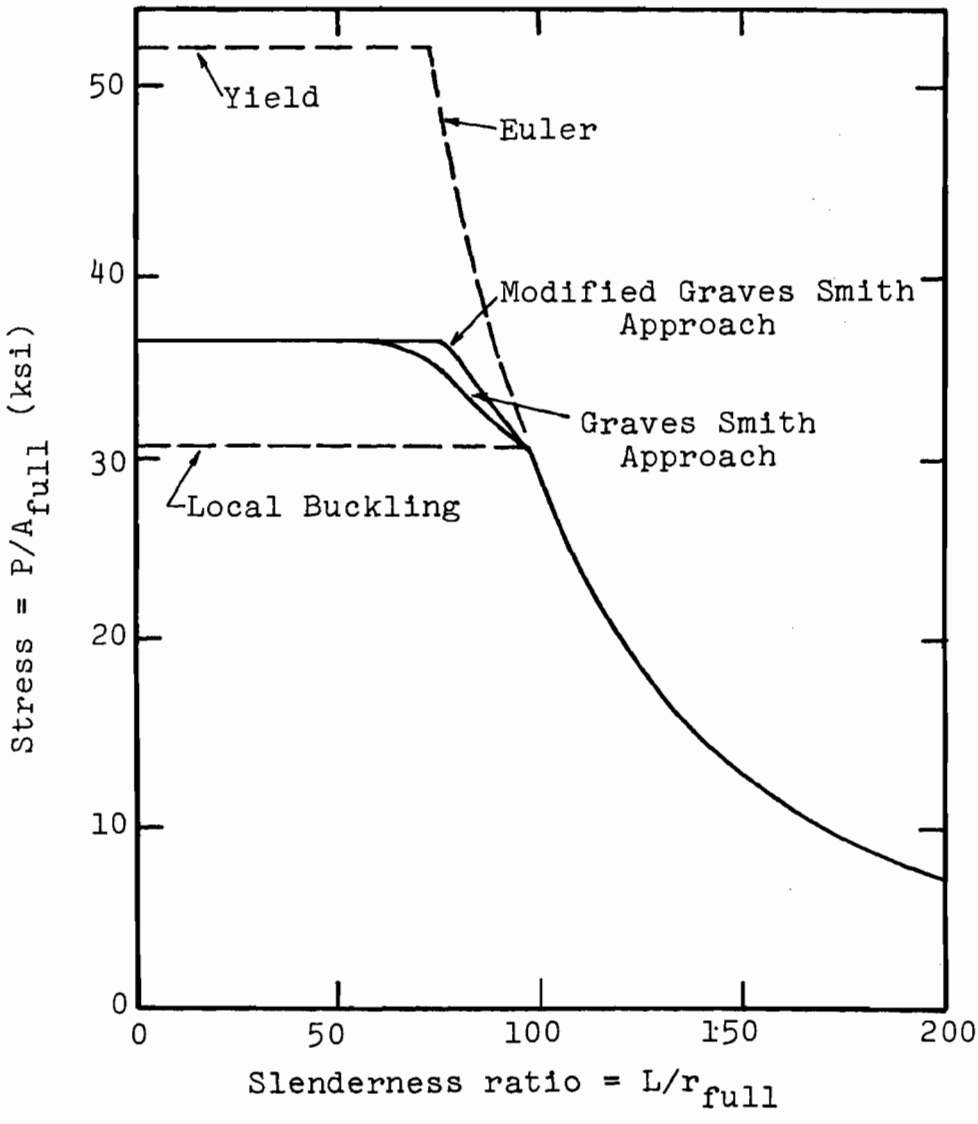

(b) Column Curves

FIG. 5.3 COMPARISON OF GRAVES SMITH APPROACH AND RIGOROUS ANALYTICAL APPROACH FOR SQUARE TUBE EXAMPLE

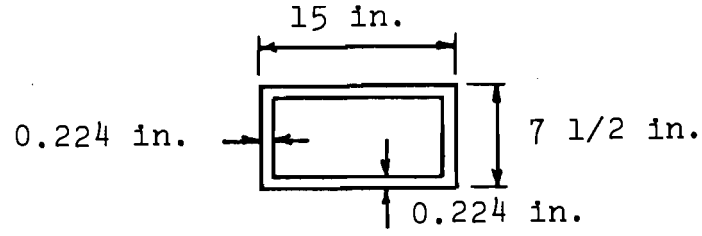

(a) Column Cross-Section

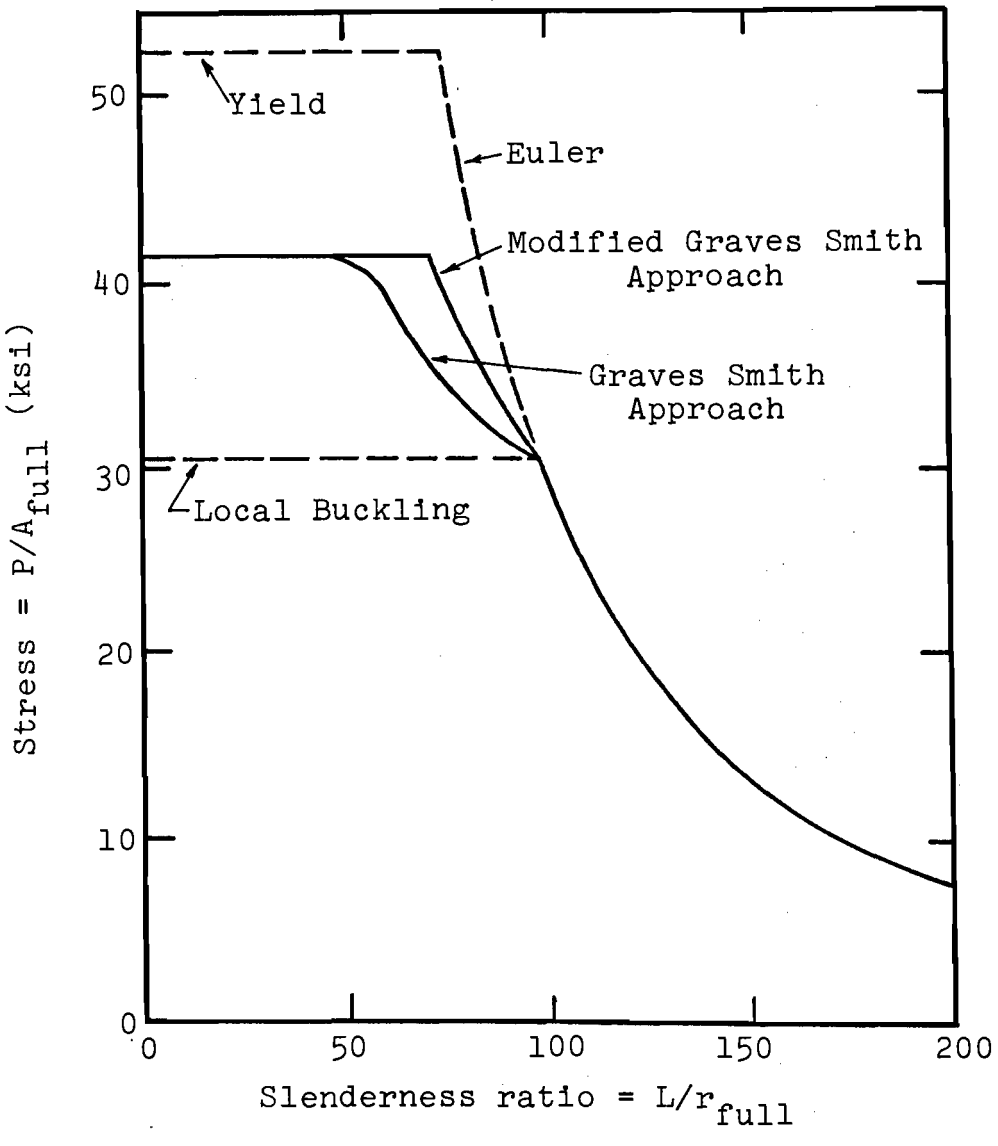

(b) Column Curves

FIG. 5.4 COMPARISON OF GRAVES SMITH APPROACH AND RIGOROUS ANALYTICAL APPROACH FOR RECTANGULAR TUBE EXAMPLE

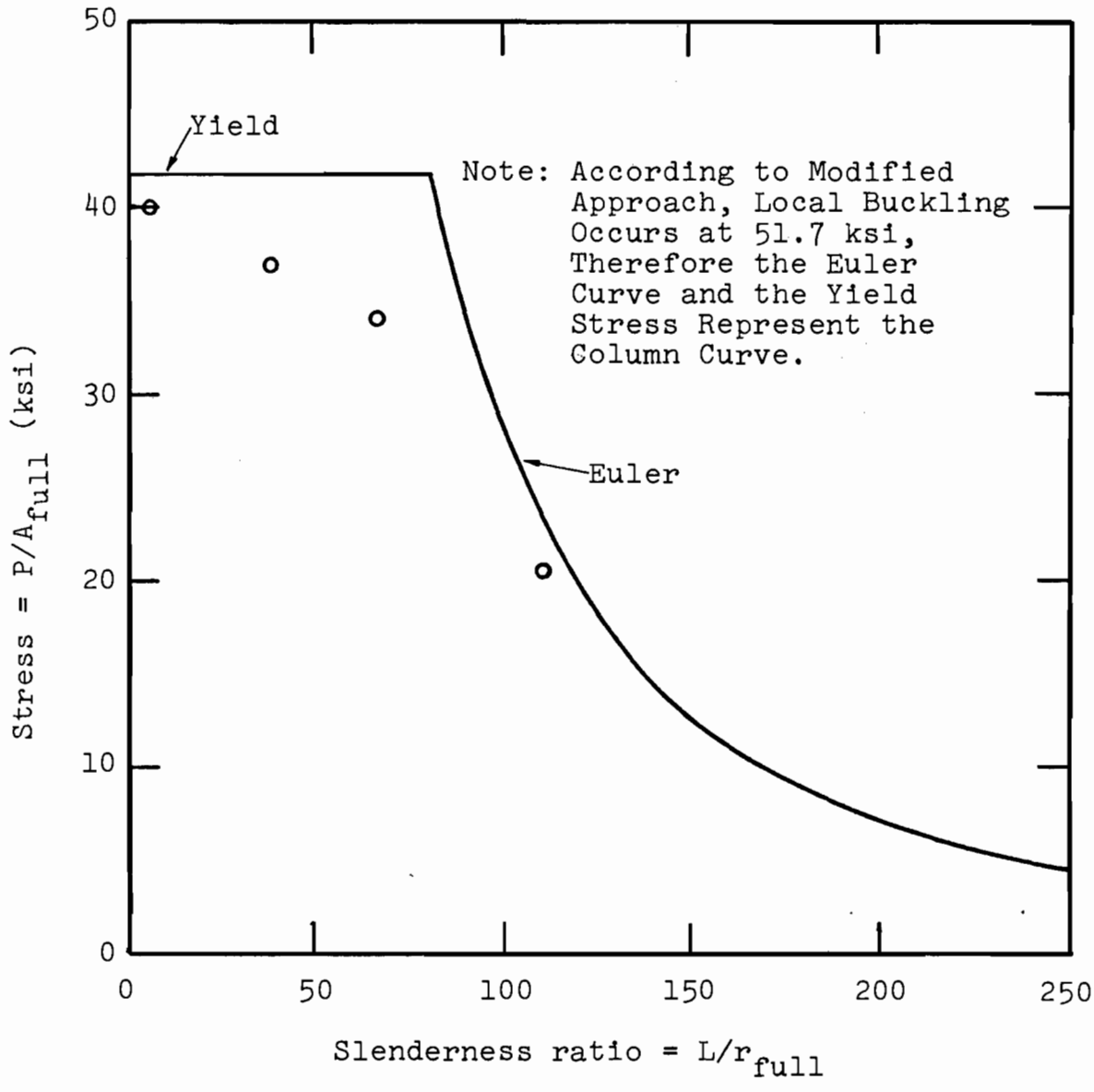

FIG. 5.5 COMPARISON OF TEST RESULTS AND RIGOROUS ANALYTICAL APPROACH FOR STIFFENED SECTION S-1

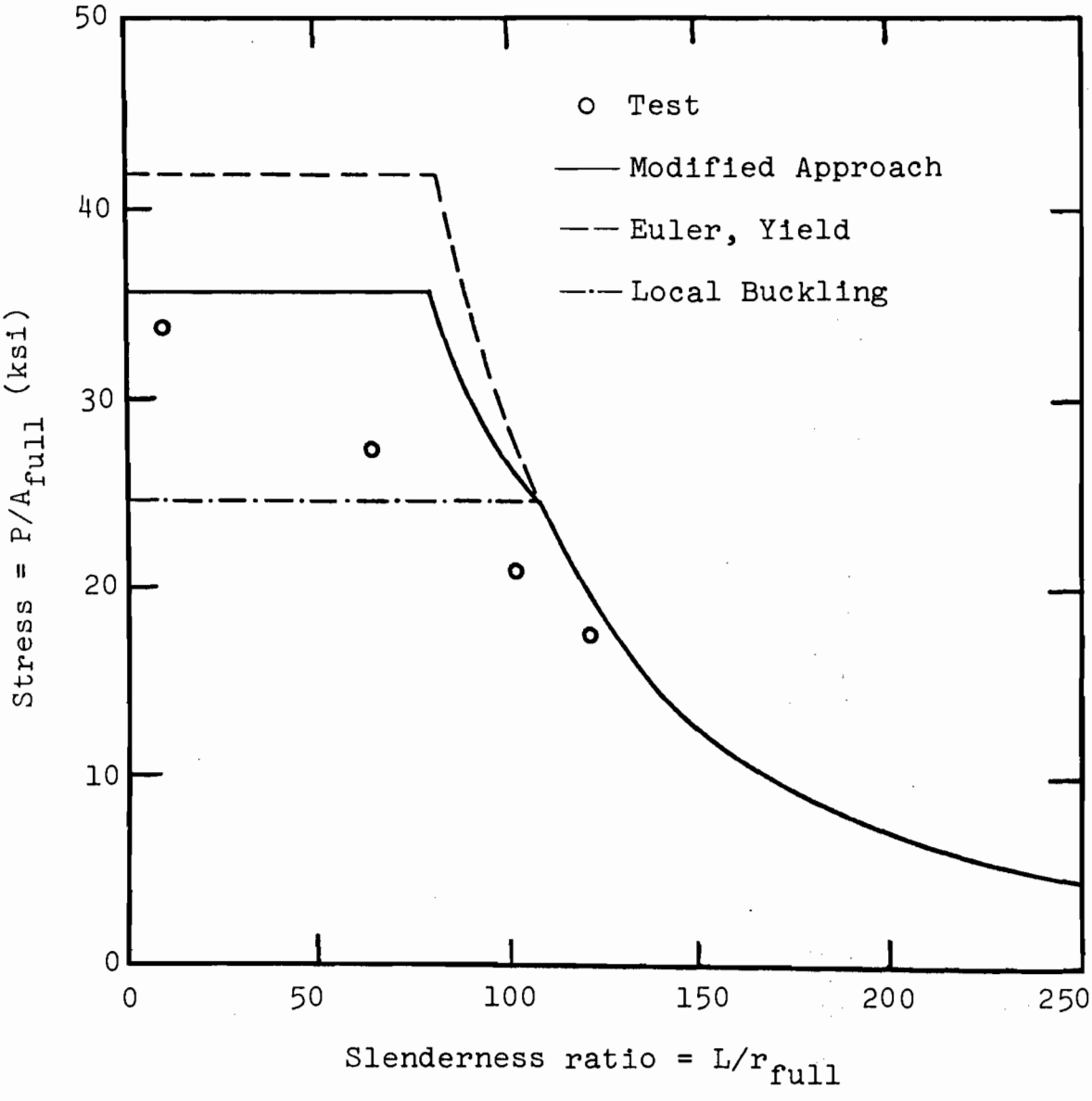

FIG. 5.6 COMPARISON OF TEST RESULTS AND RIGOROUS ANALYTICAL APPROACH FOR STIFFENED SECTION S-2

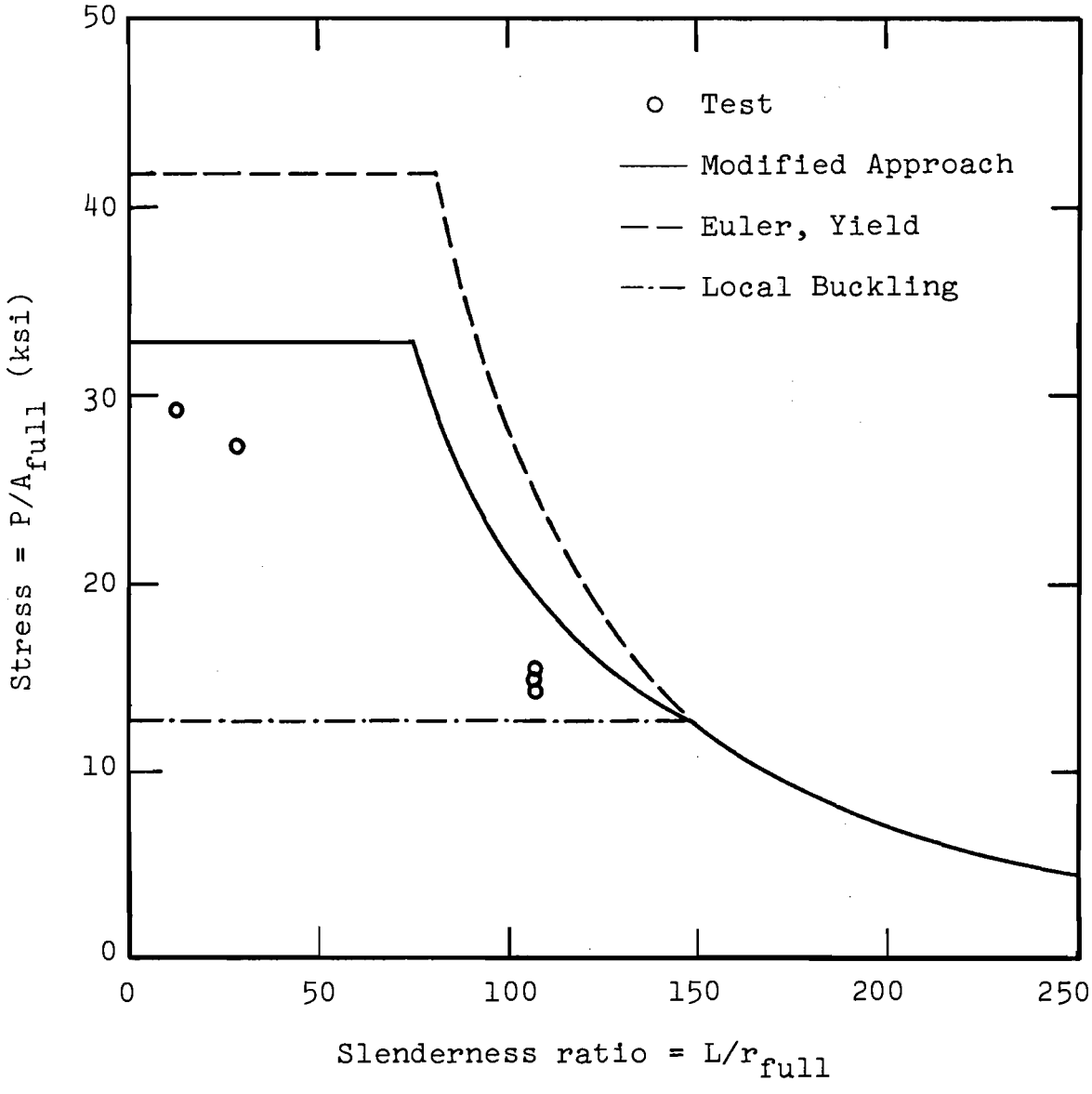

FIG. 5.7 COMPARISON OF TEST RESULTS AND RIGOROUS ANALYTICAL APPROACH FOR STIFFENED SECTION S-3

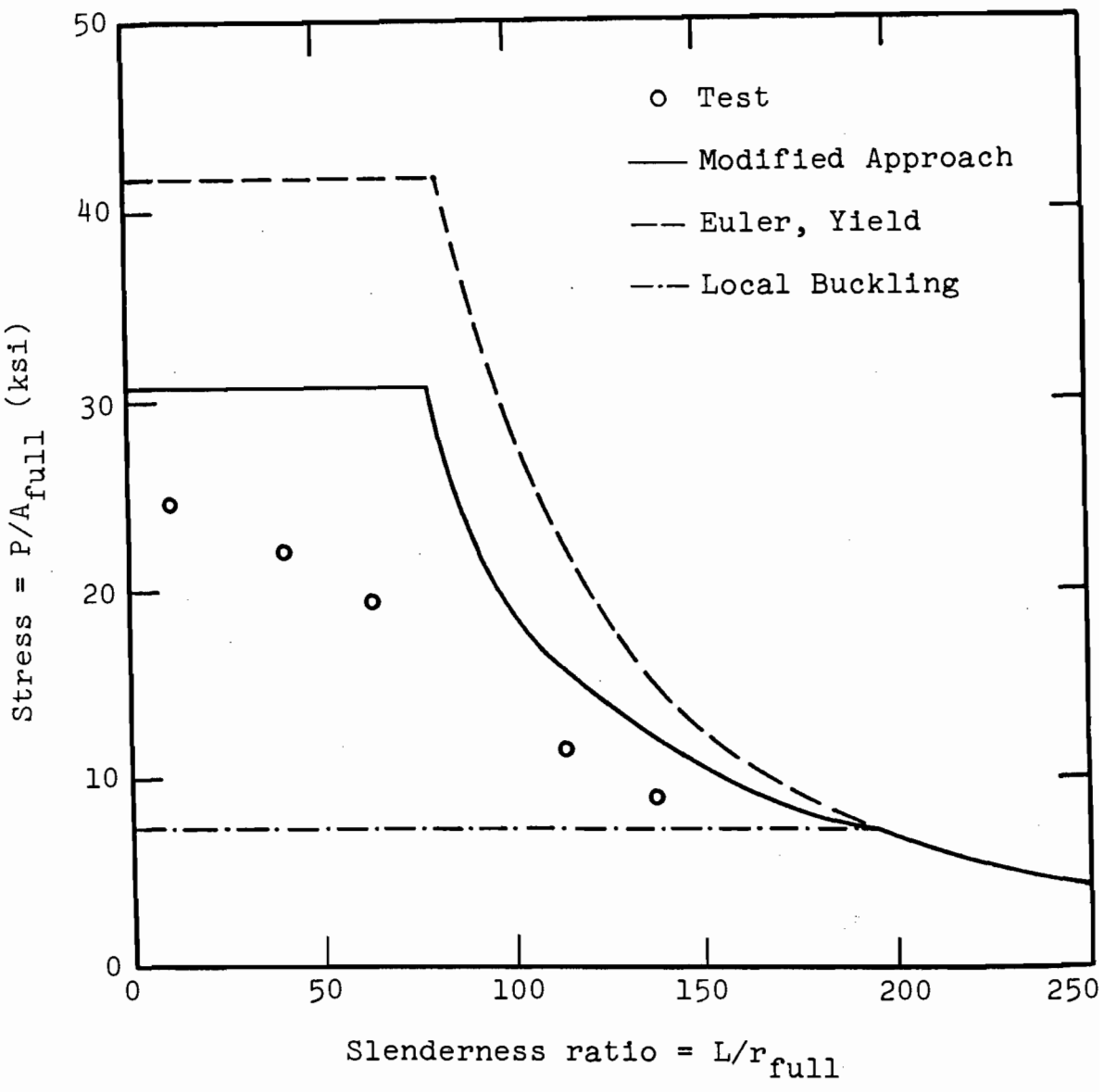

FIG. 5.8 COMPARISON OF TEST RESULTS AND RIGOROUS ANALYTICAL APPROACH FOR STIFFENED SECTION S-4

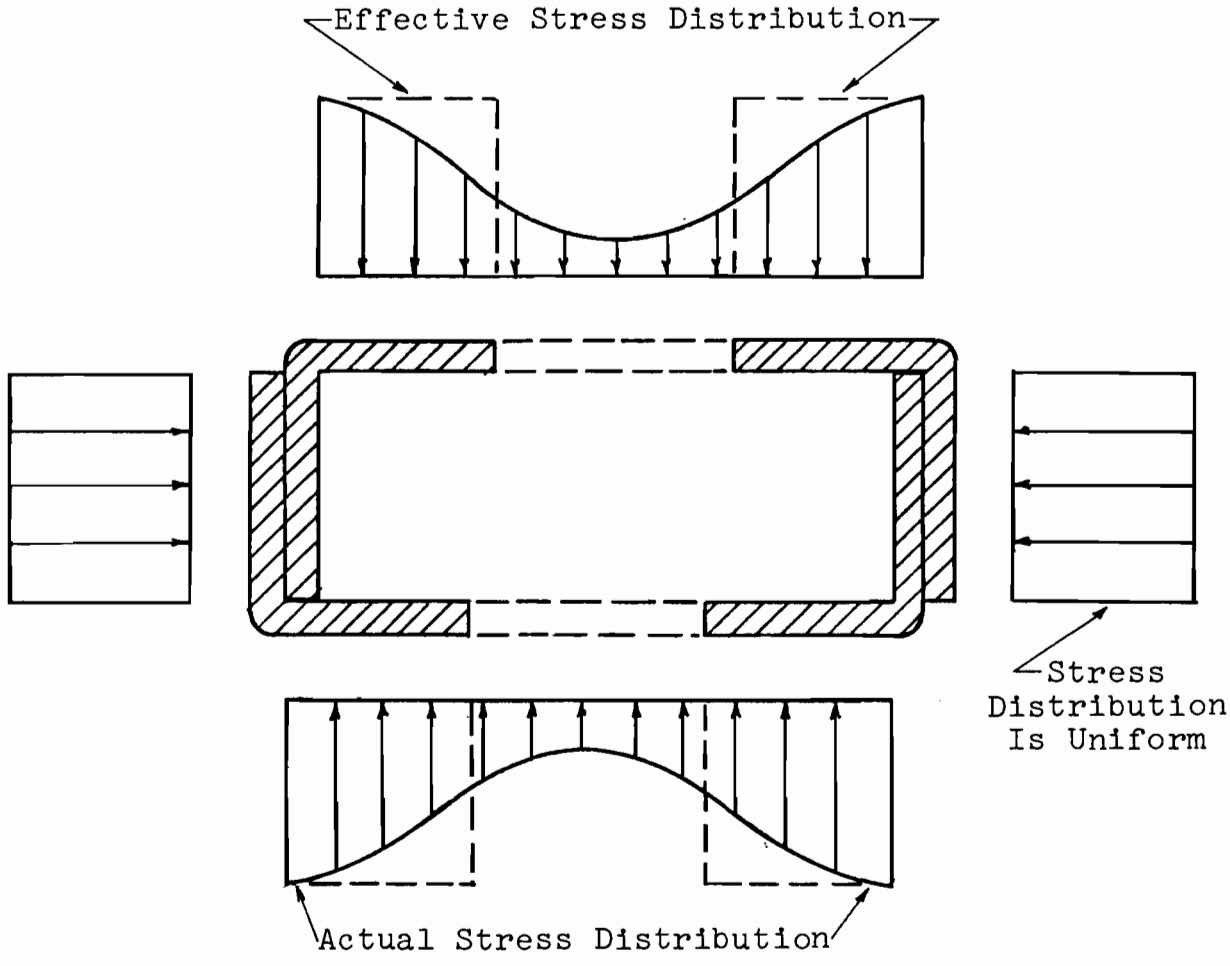

FIG. 6.1 EFFECTIVE SECTION AND STRESS DISTRIBUTIONS FOR STIFFENED SECTION

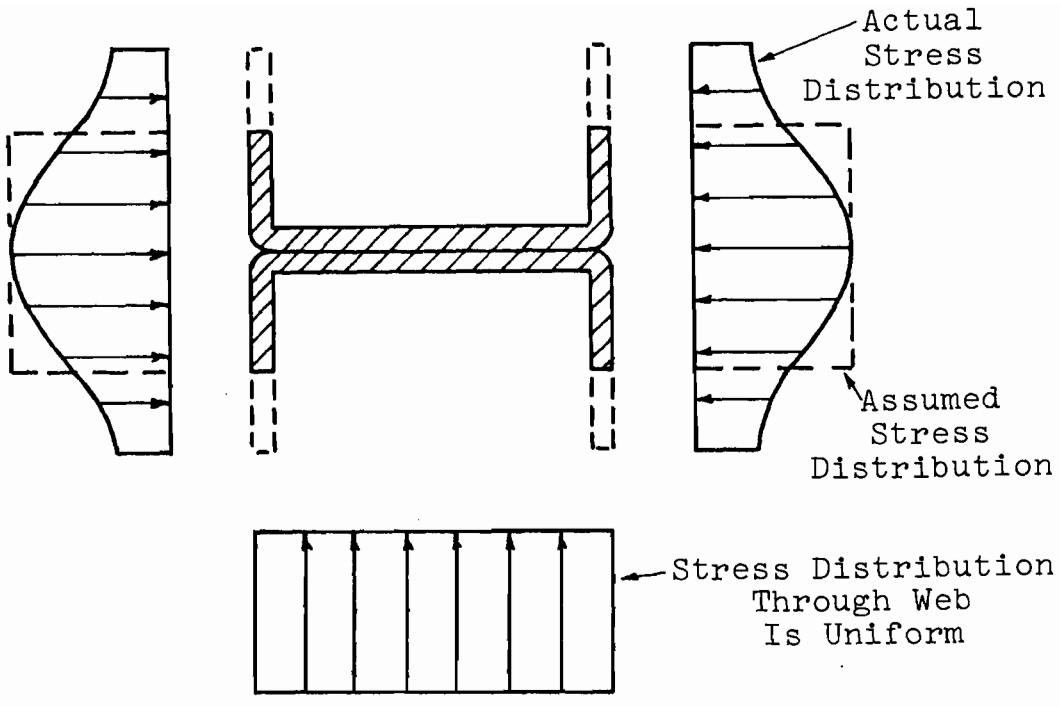

(a) Effective web areas located at web end of flange

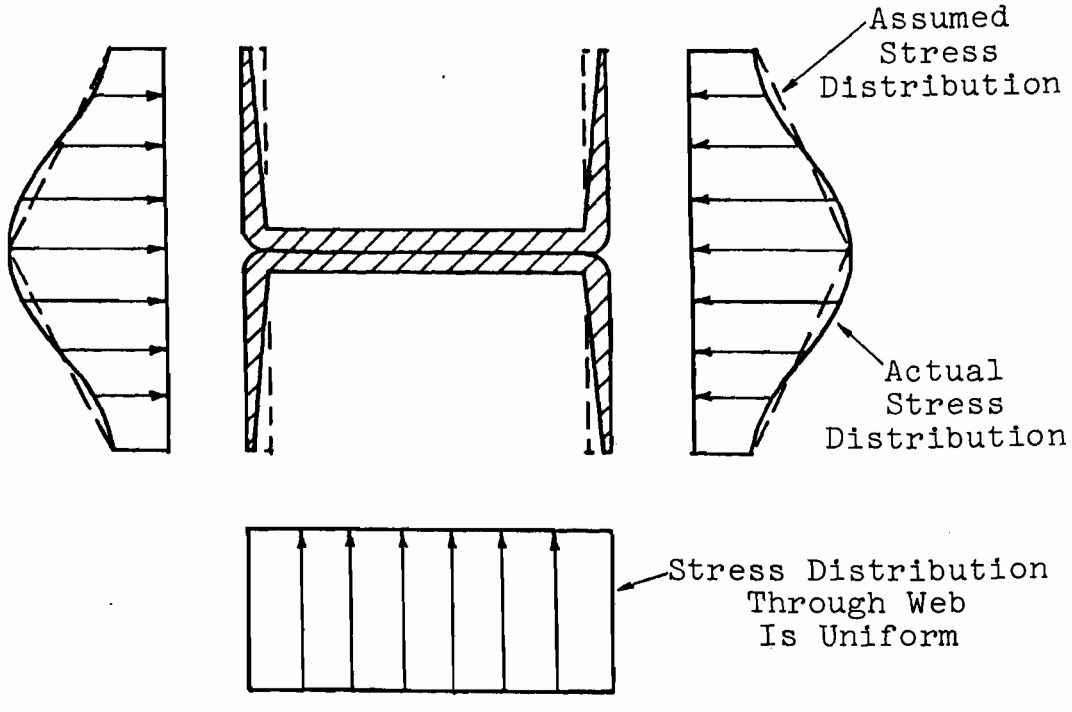

(b) Effective web areas distributed linearly through web

FIG. 6.2 EFFECTIVE SECTION AND STRESS DISTRIBUTIONS FOR UNSTIFFENED SECTION

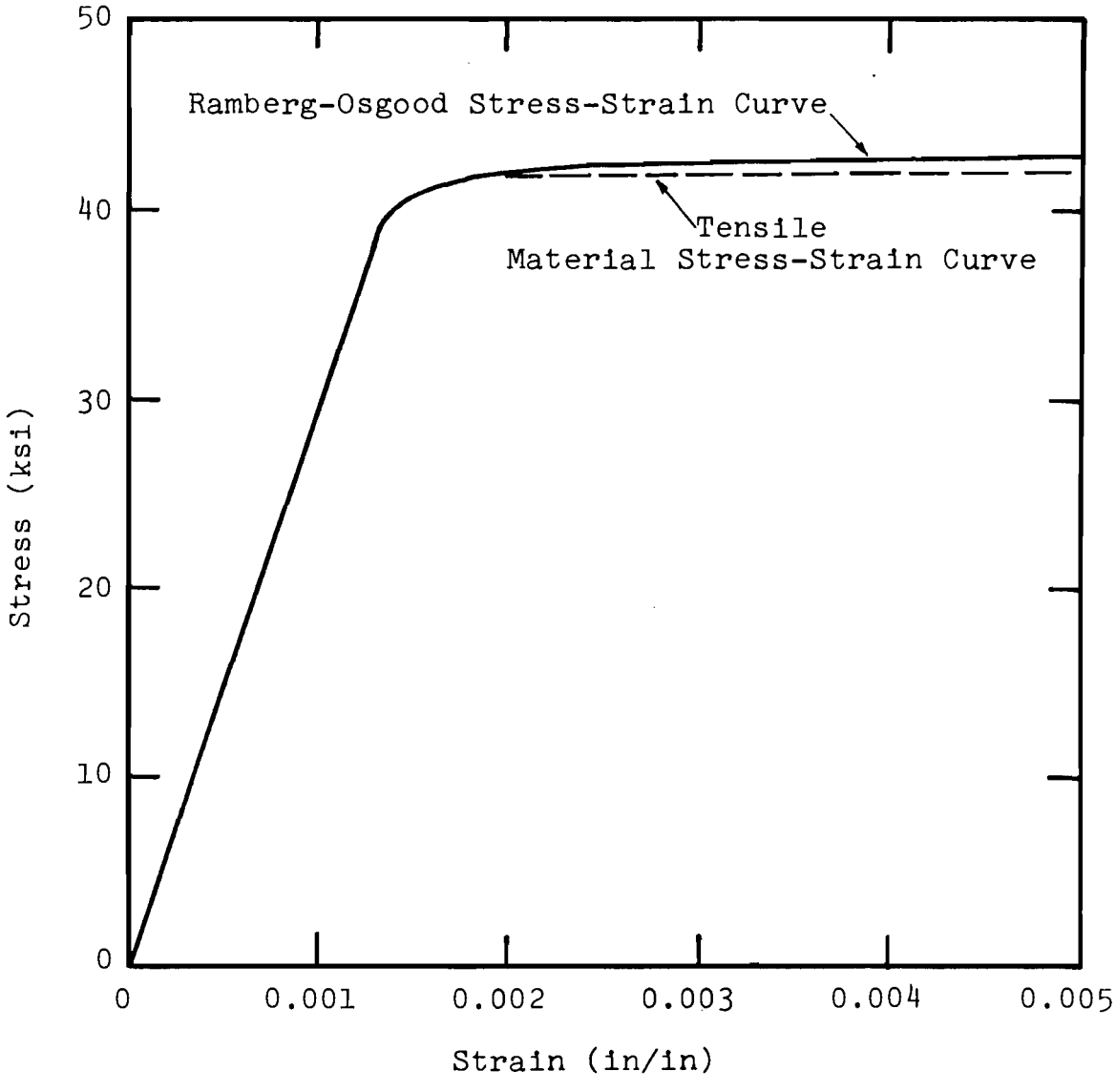

FIG. 6.3 MATERIAL STRESS-STRAIN CURVE USING THE RAMBERG-OSGOOD EQUATION

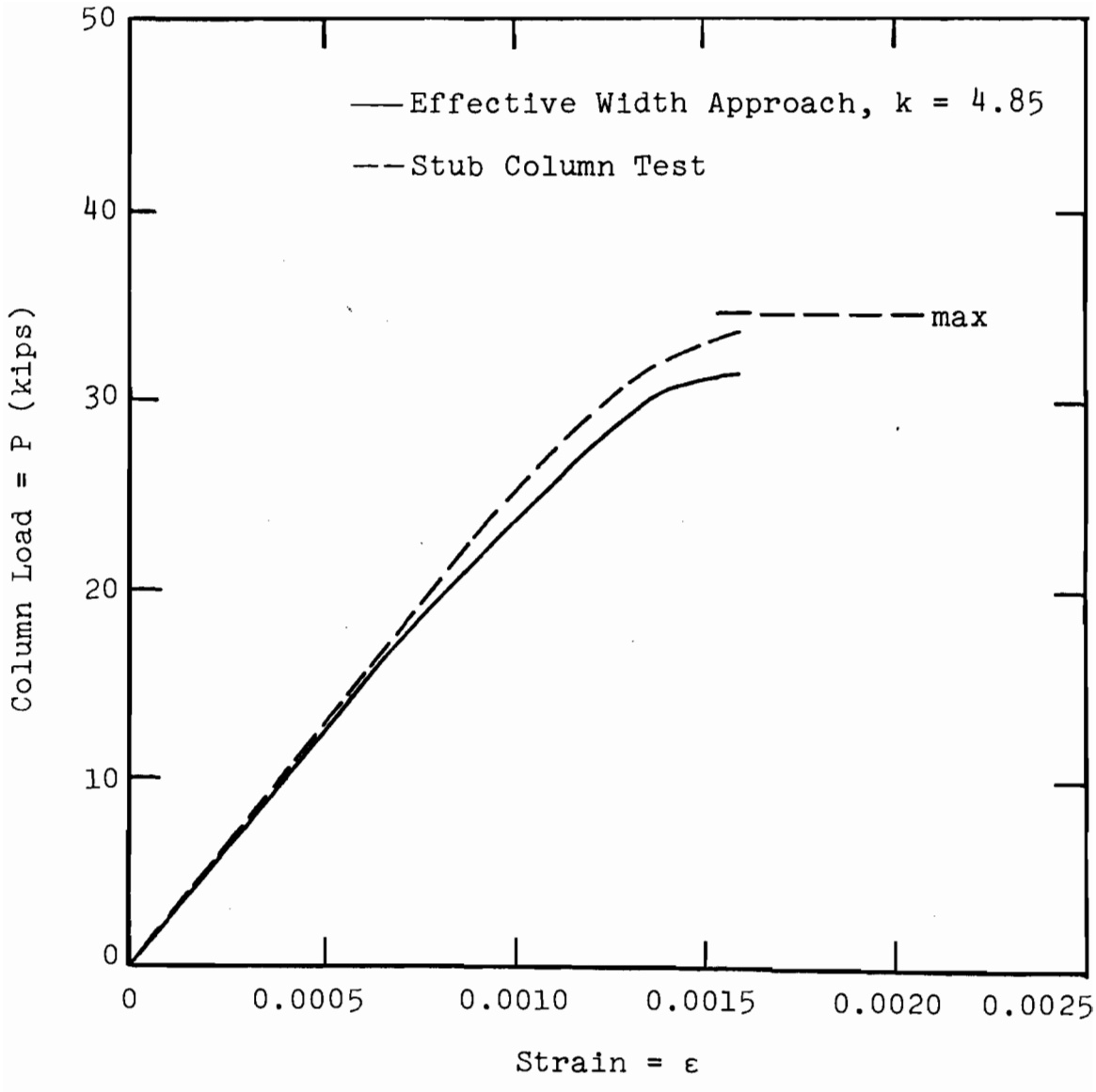

FIG. 6.4 COMPARISON OF STUB COLUMN CURVES BASED ON TESTS AND EFFECTIVE WIDTH APPROACH FOR STIFFENED SECTION S-1

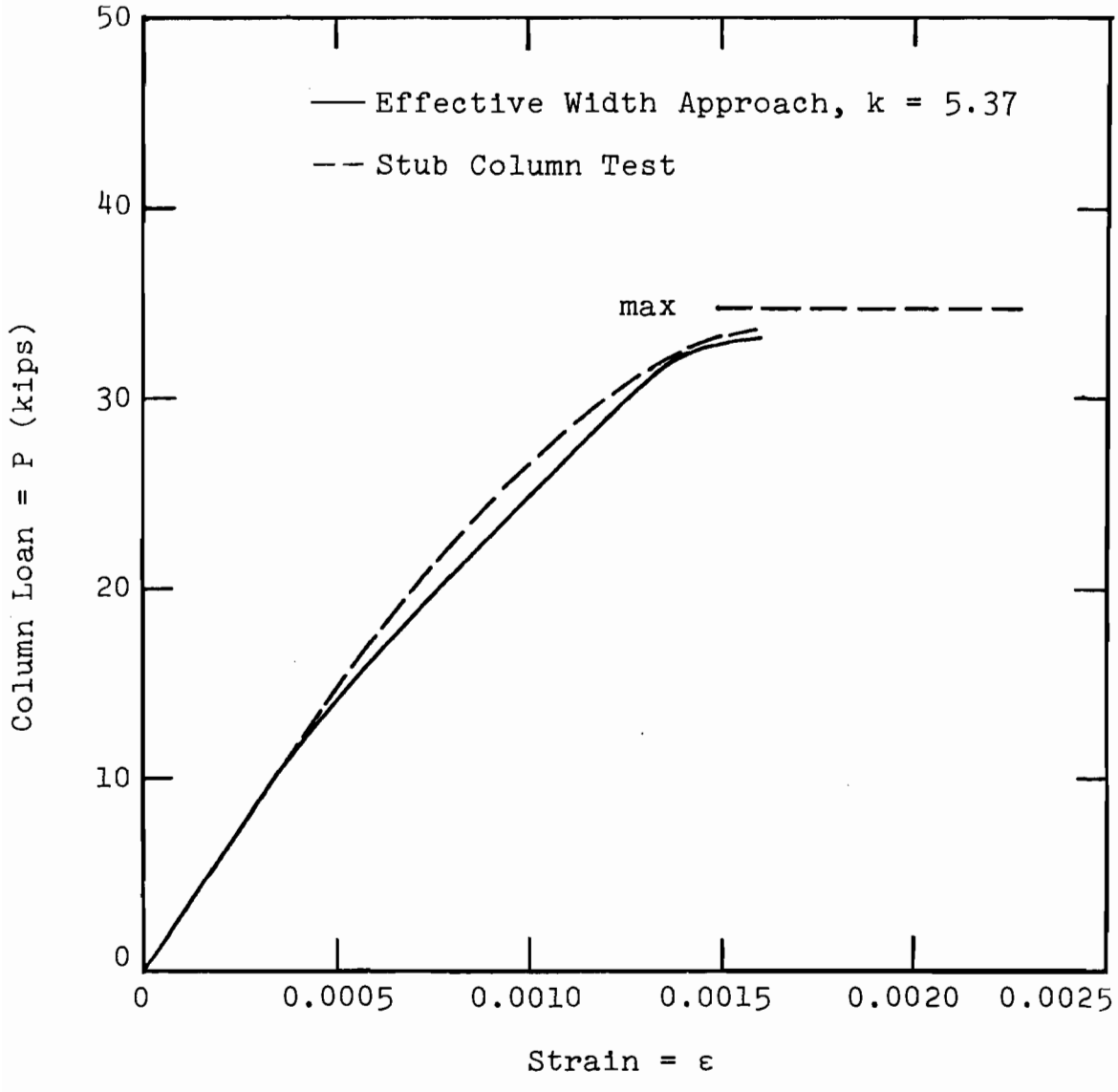

FIG. 6.5 COMPARISON OF STUB COLUMN CURVES BASED ON TESTS AND EFFECTIVE WIDTH APPROACH FOR STIFFENED SECTION S-2

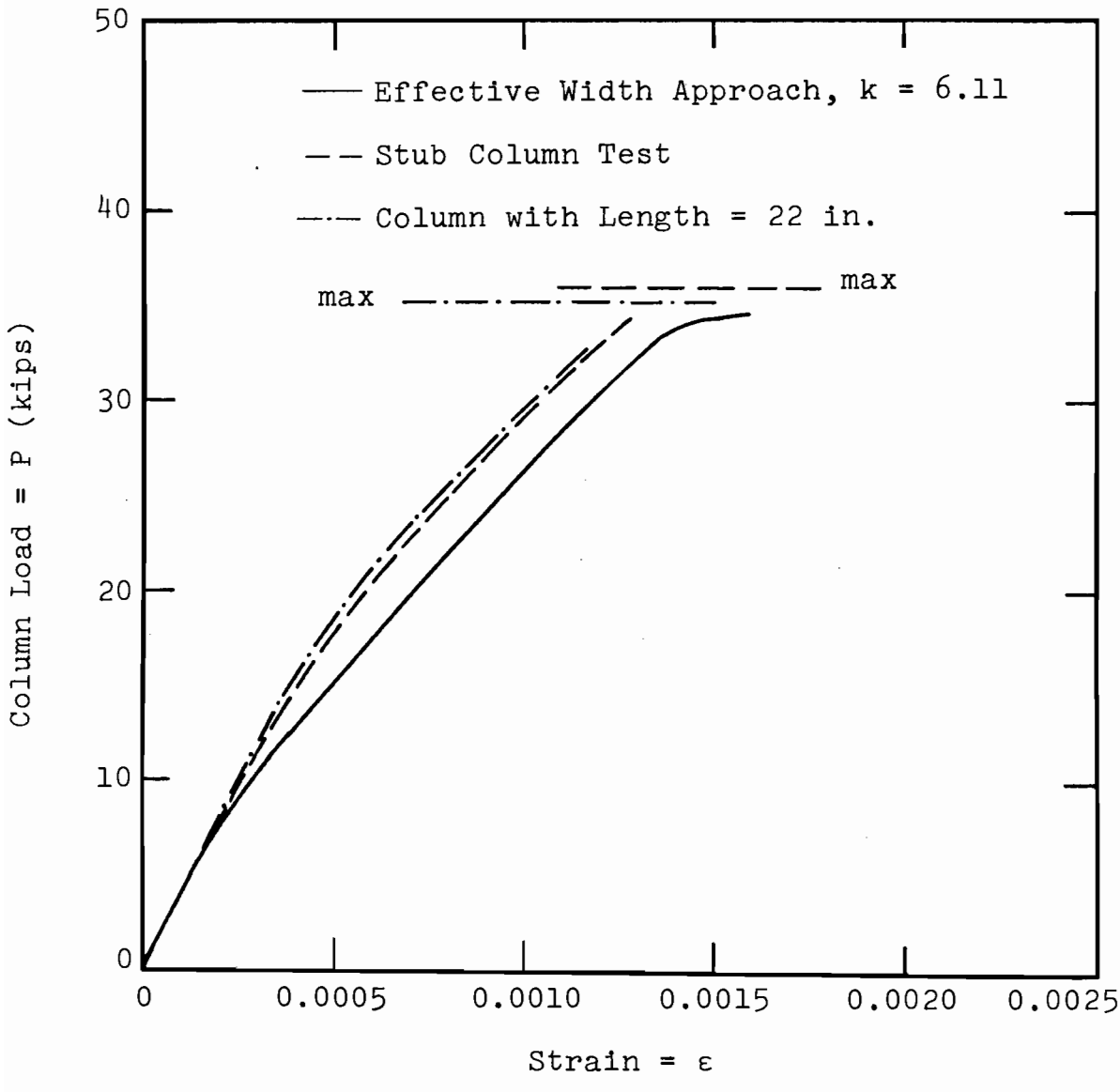

FIG. 6.6 COMPARISON OF STUB COLUMN CURVES BASED ON TESTS AND EFFECTIVE WIDTH APPROACH FOR STIFFENED SECTION S-3

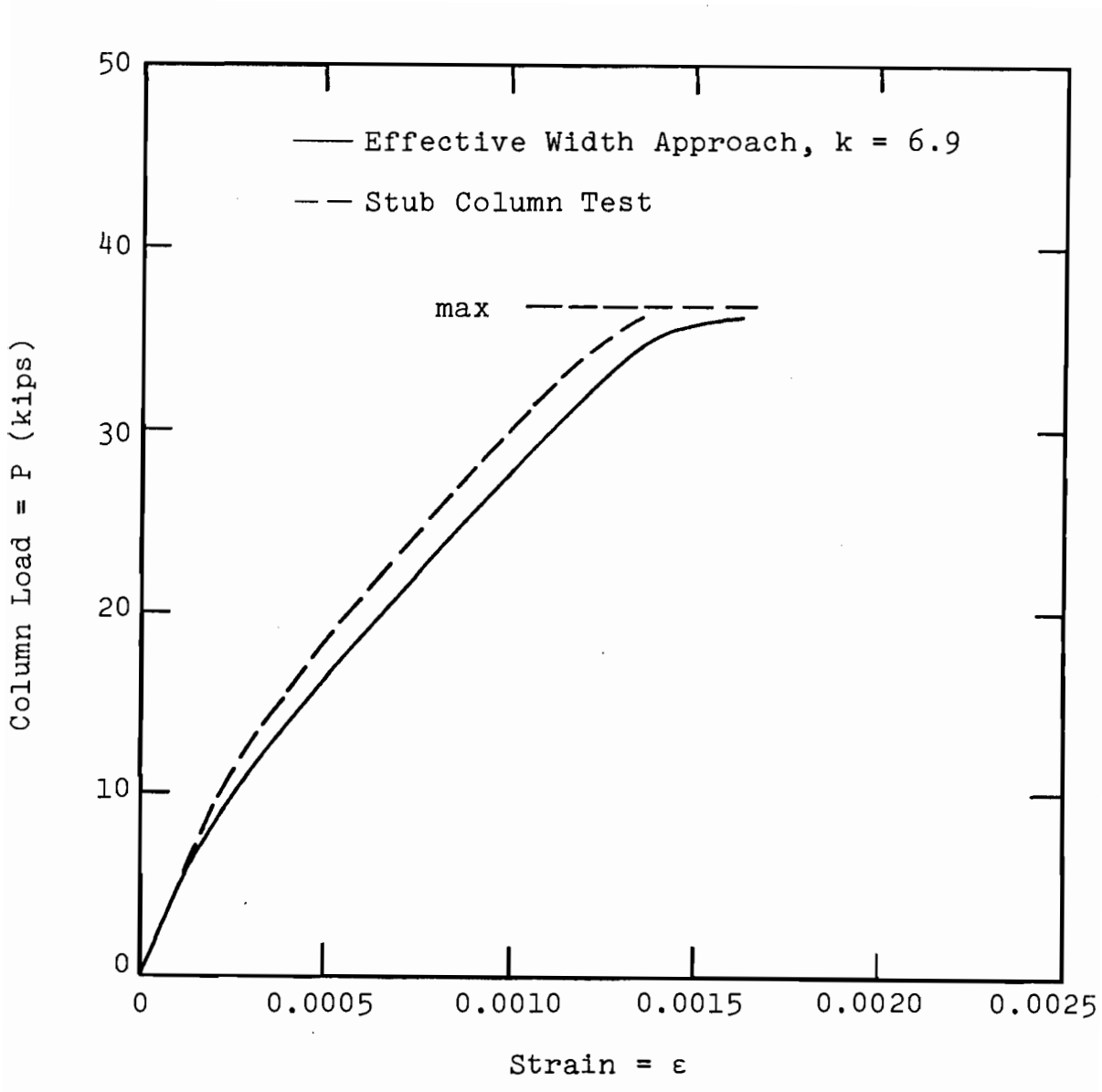

FIG. 6.7 COMPARISON OF STUB COLUMN CURVES BASED ON TESTS AND EFFECTIVE WIDTH APPROACH FOR STIFFENED SECTION S-4

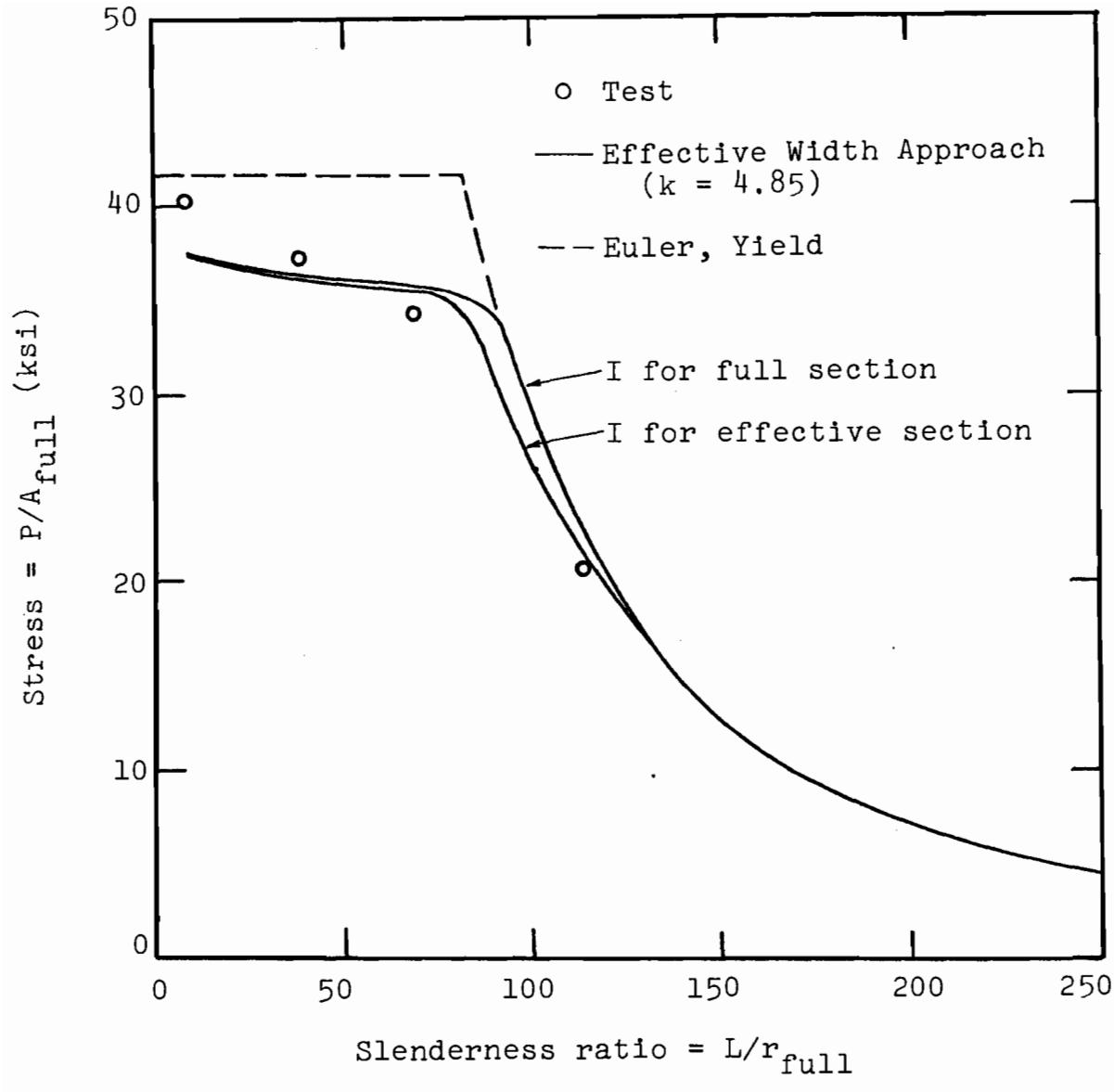

FIG. 6.8 COMPARISON OF TESTS AND EFFECTIVE WIDTH APPROACH USING DIFFERENT MOMENTS OF INERTIA FOR STIFFENED SECTION S-1

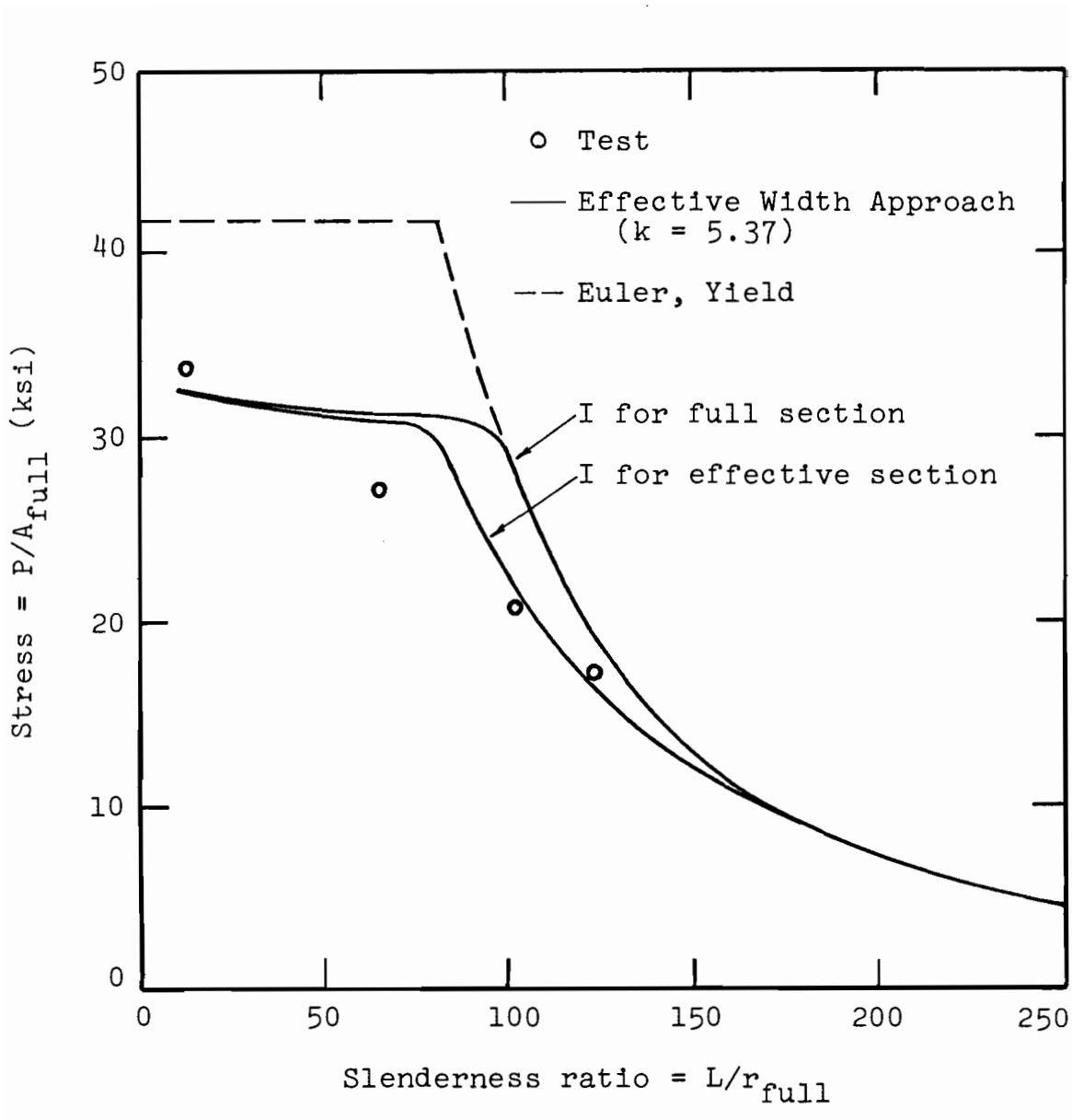

FIG. 6.9 COMPARISON OF TESTS AND EFFECTIVE WIDTH APPROACH USING DIFFERENT MOMENTS OF INERTIA FOR STIFFENED SECTION S-2

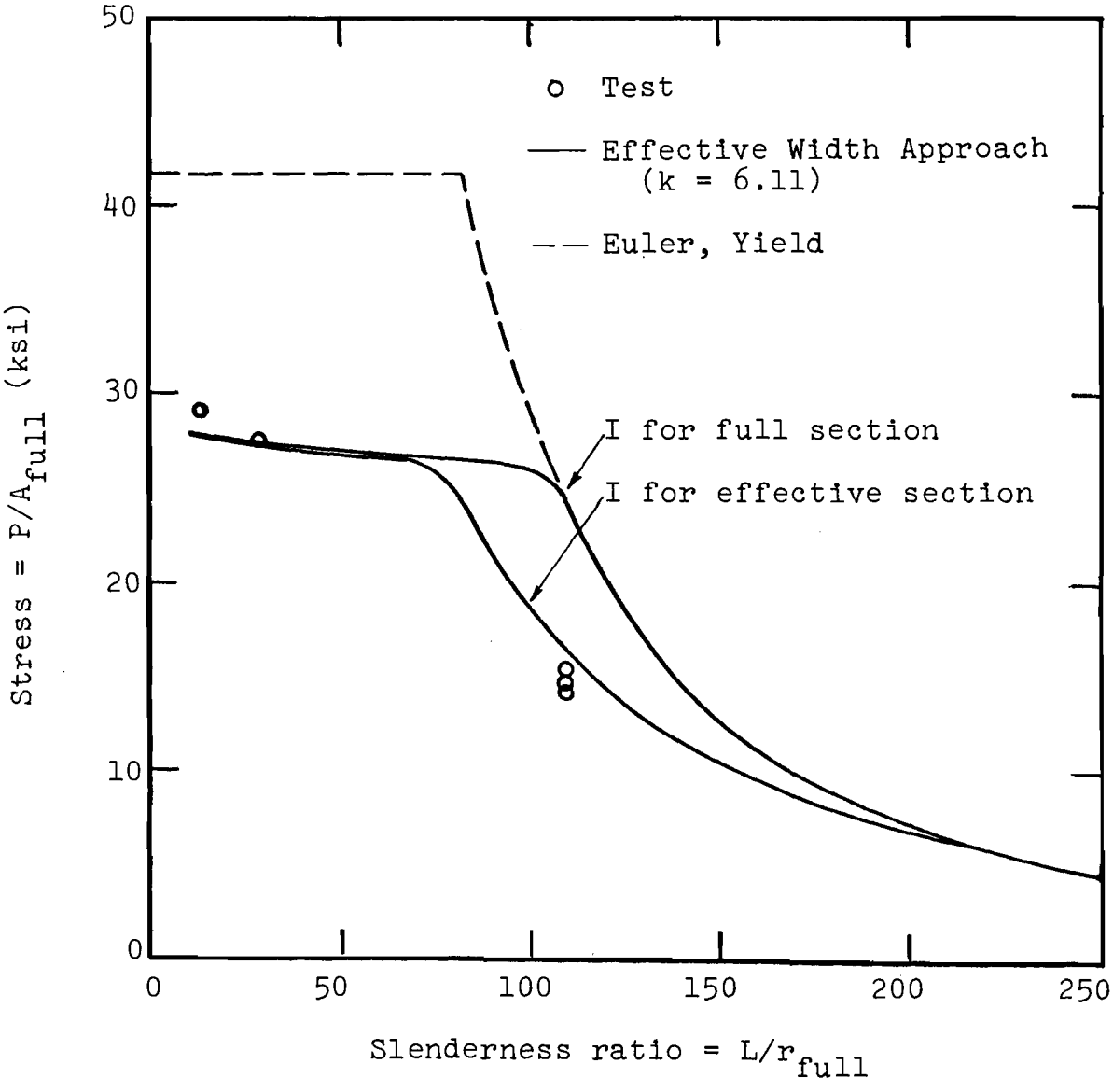

FIG. 6.10 COMPARISON OF TESTS AND EFFECTIVE WIDTH APPROACH USING DIFFERENT MOMENTS OF INERTIA FOR STIFFENED SECTION S-3

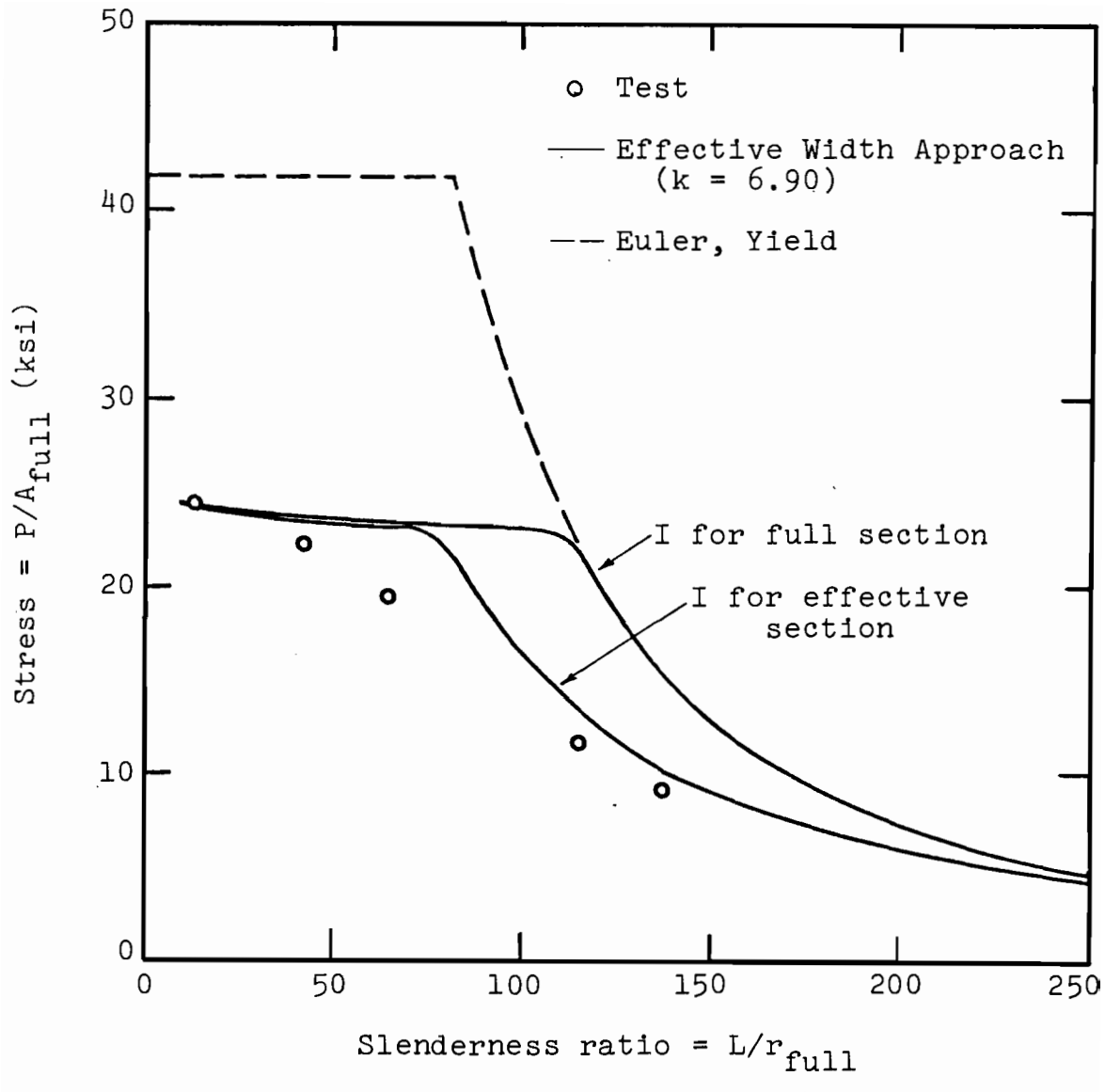

FIG. 6.11 COMPARISON OF TESTS AND EFFECTIVE WIDTH APPROACH USING DIFFERENT MOMENTS OF INERTIA FOR STIFFENED SECTION S-4

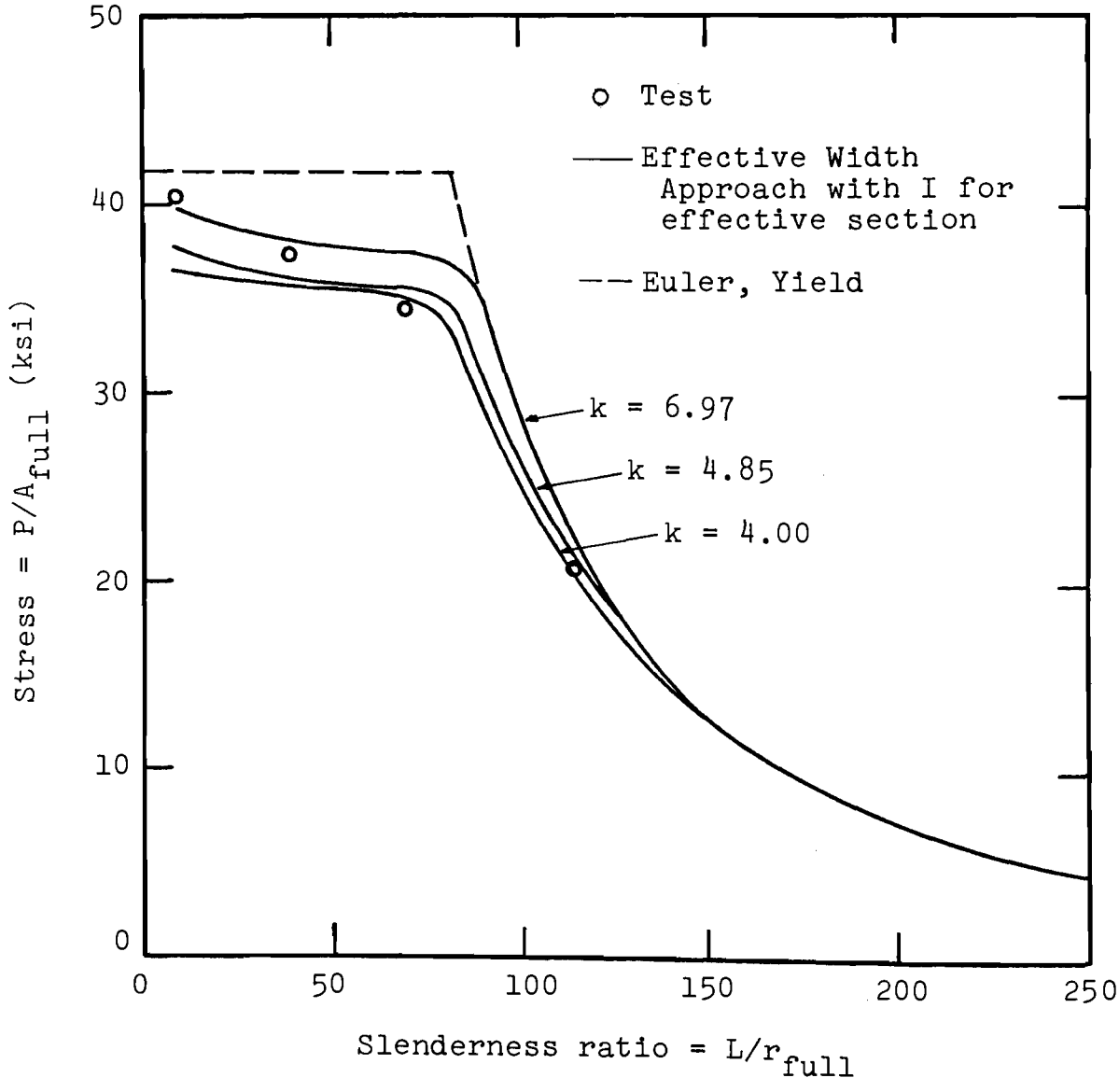

FIG. 6.12 COMPARISON OF TESTS AND EFFECTIVE WIDTH APPROACH BASED ON DIFFERENT EDGE SUPPORT CONDITIONS FOR STIFFENED SECTION S-1

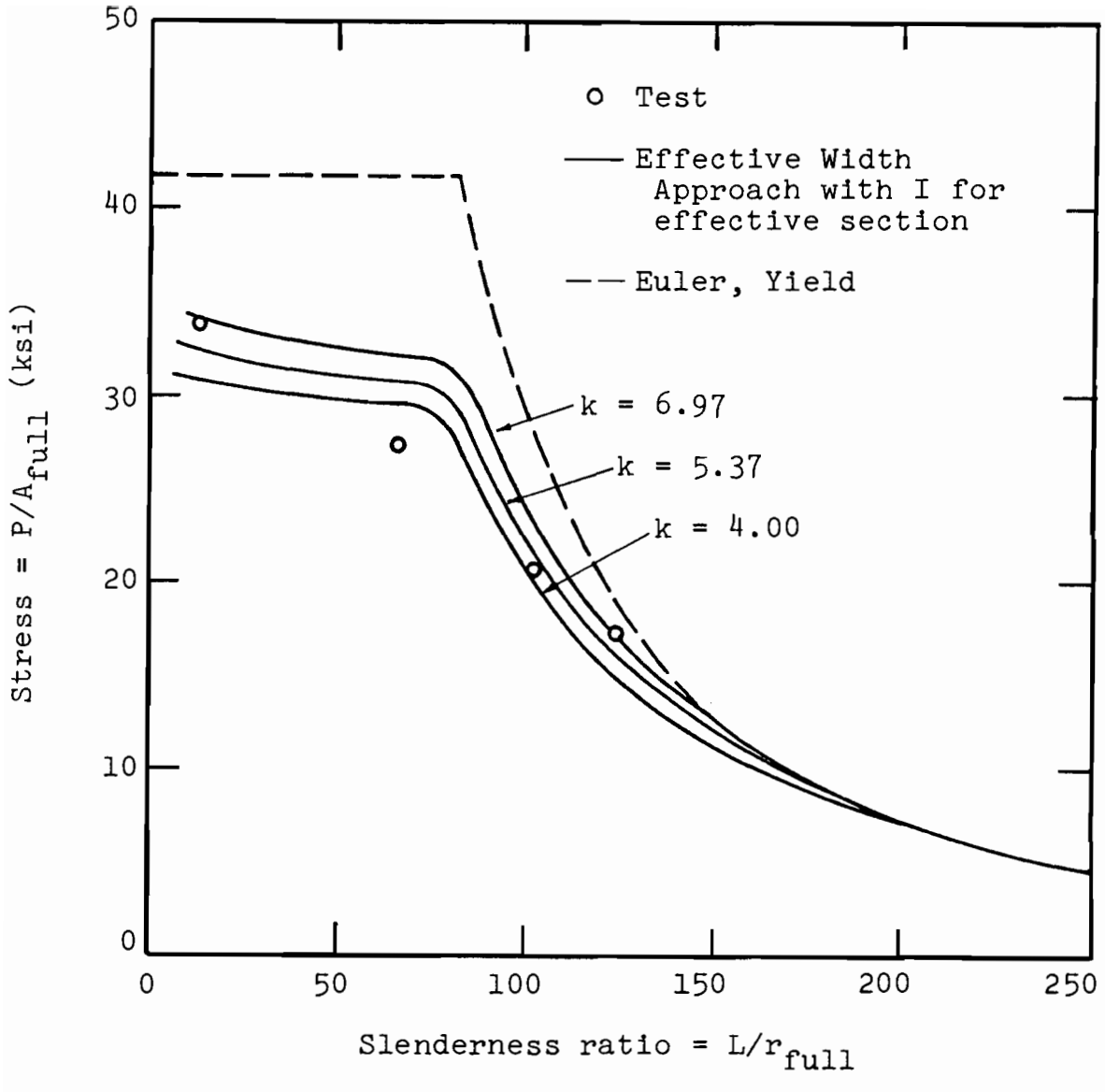

FIG. 6.13 COMPARISON OF TESTS AND EFFECTIVE WIDTH APPROACH BASED ON DIFFERENT EDGE SUPPORT CONDITIONS FOR STIFFENED SECTION S-2

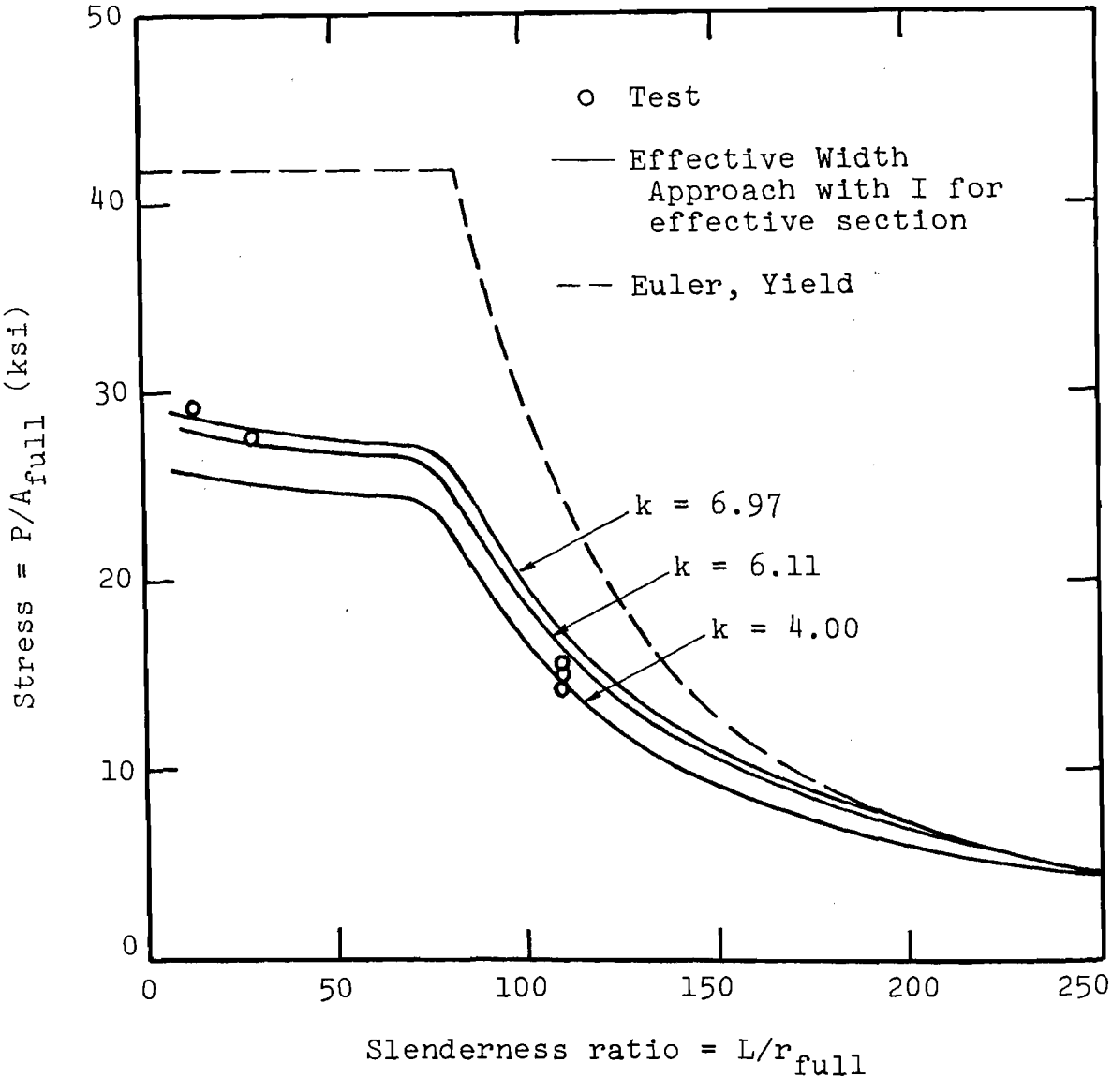

FIG. 6.14 COMPARISON OF TESTS AND EFFECTIVE WIDTH APPROACH BASED ON DIFFERENT EDGE SUPPORT CONDITIONS FOR STIFFENED SECTION S-3

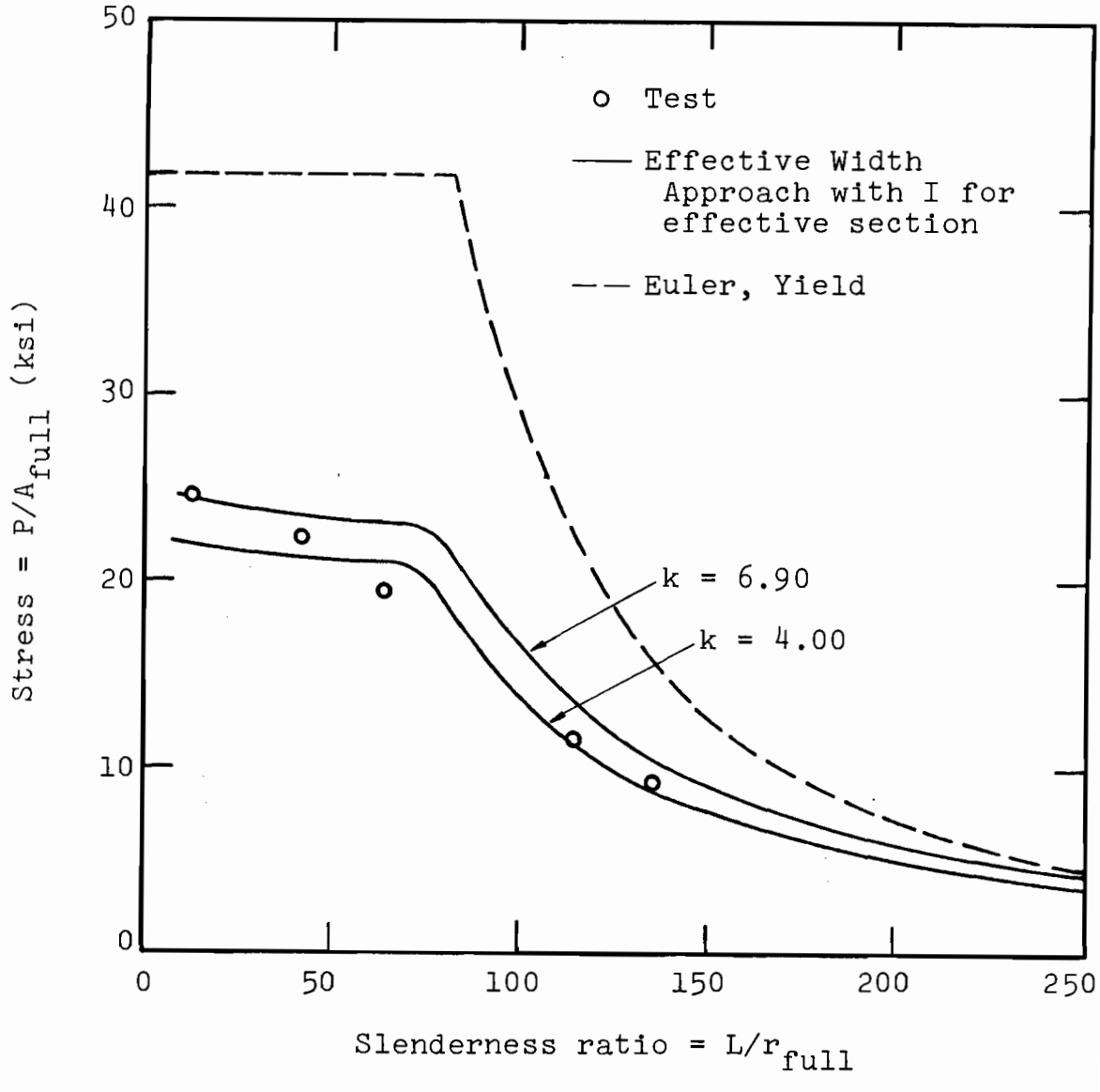

FIG. 6.15 COMPARISON OF TESTS AND EFFECTIVE WIDTH APPROACH BASED ON DIFFERENT EDGE SUPPORT CONDITIONS FOR STIFFENED SECTION S-4

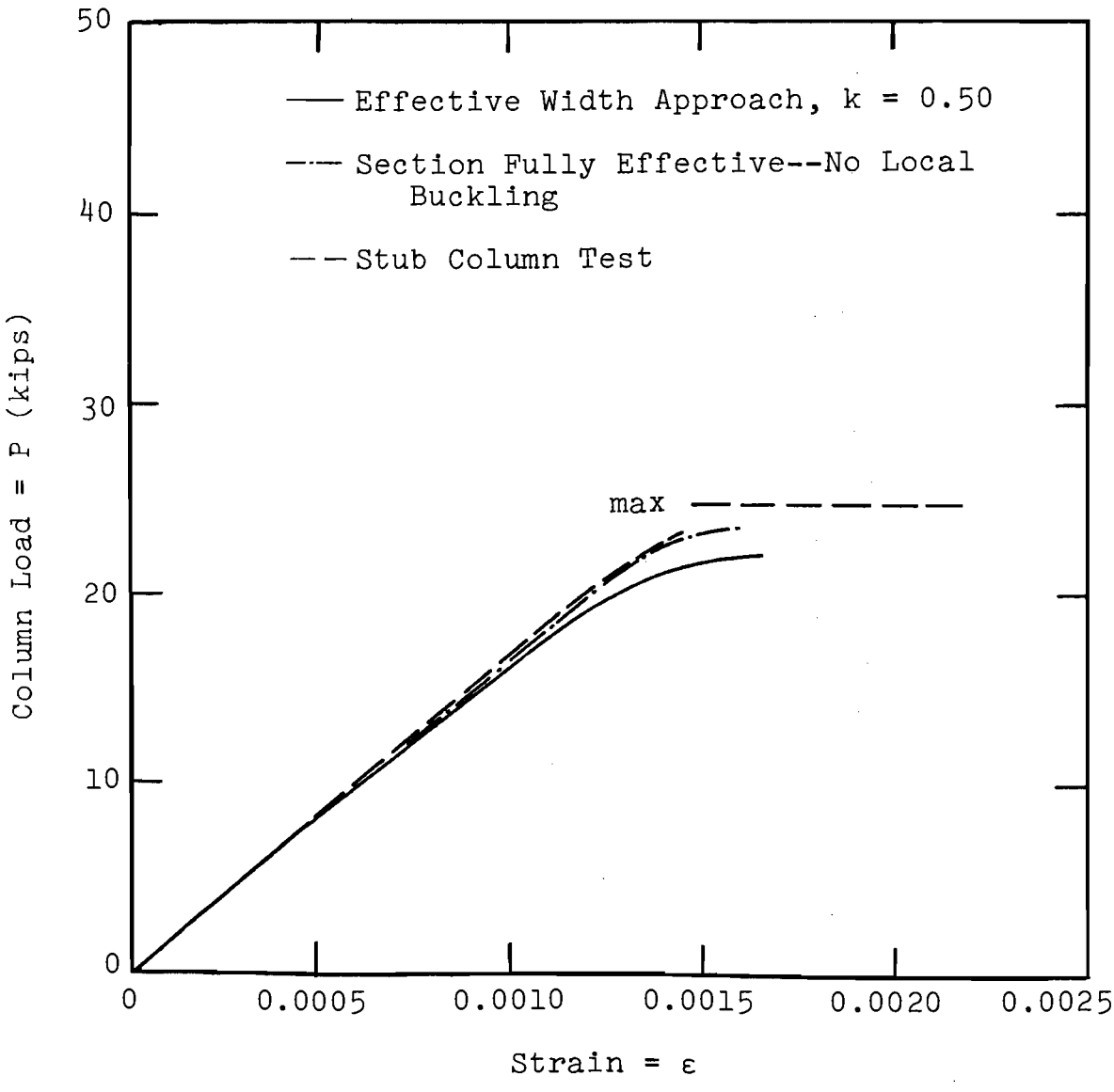

FIG. 6.16 COMPARISON OF STUB COLUMN CURVES BASED ON TESTS AND EFFECTIVE WIDTH APPROACH FOR UNSTIFFENED SECTION U-1

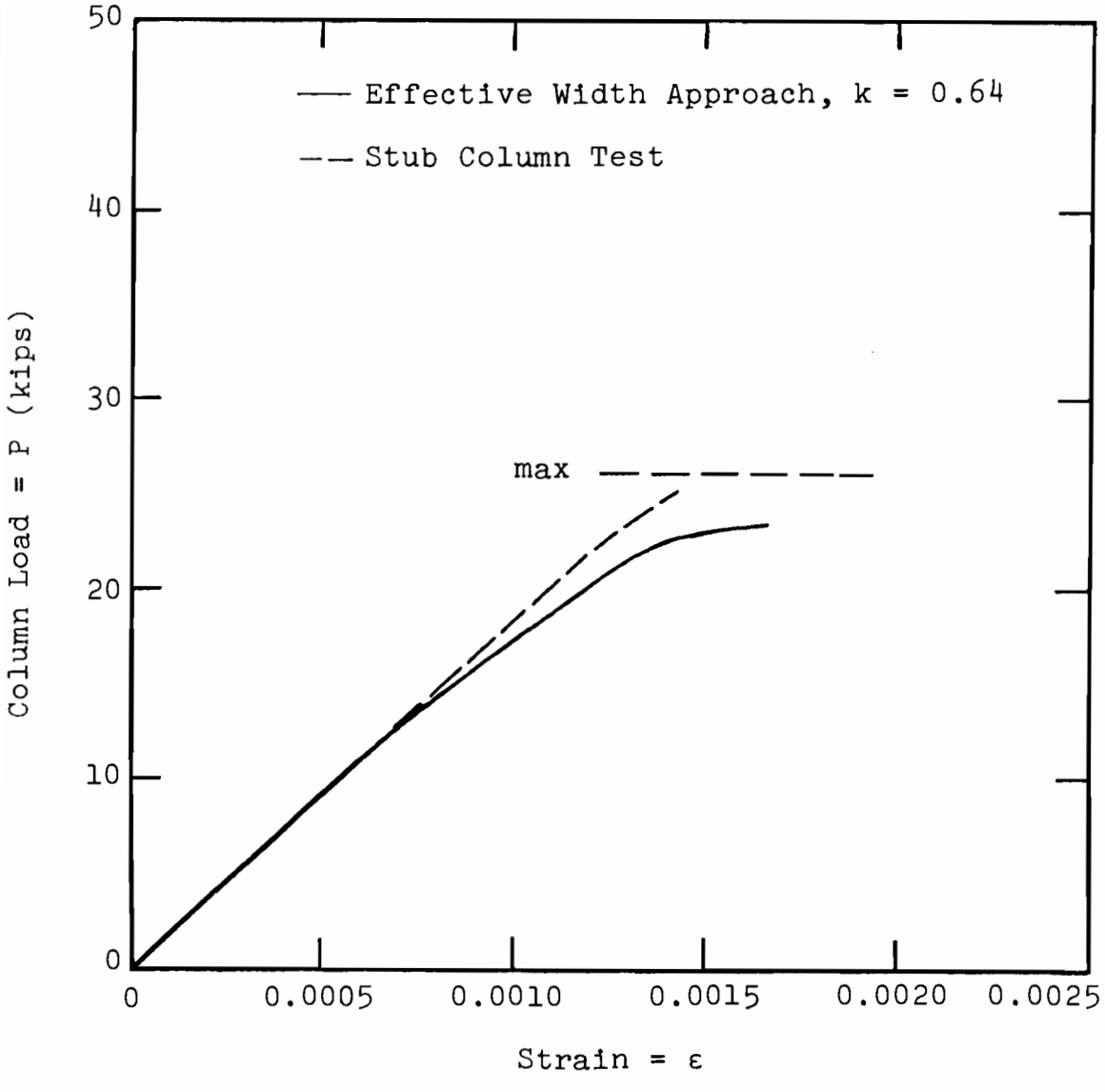

FIG. 6.17 COMPARISON OF STUB COLUMN CURVES BASED ON TESTS AND EFFECTIVE WIDTH APPROACH FOR UNSTIFFENED SECTION U-2

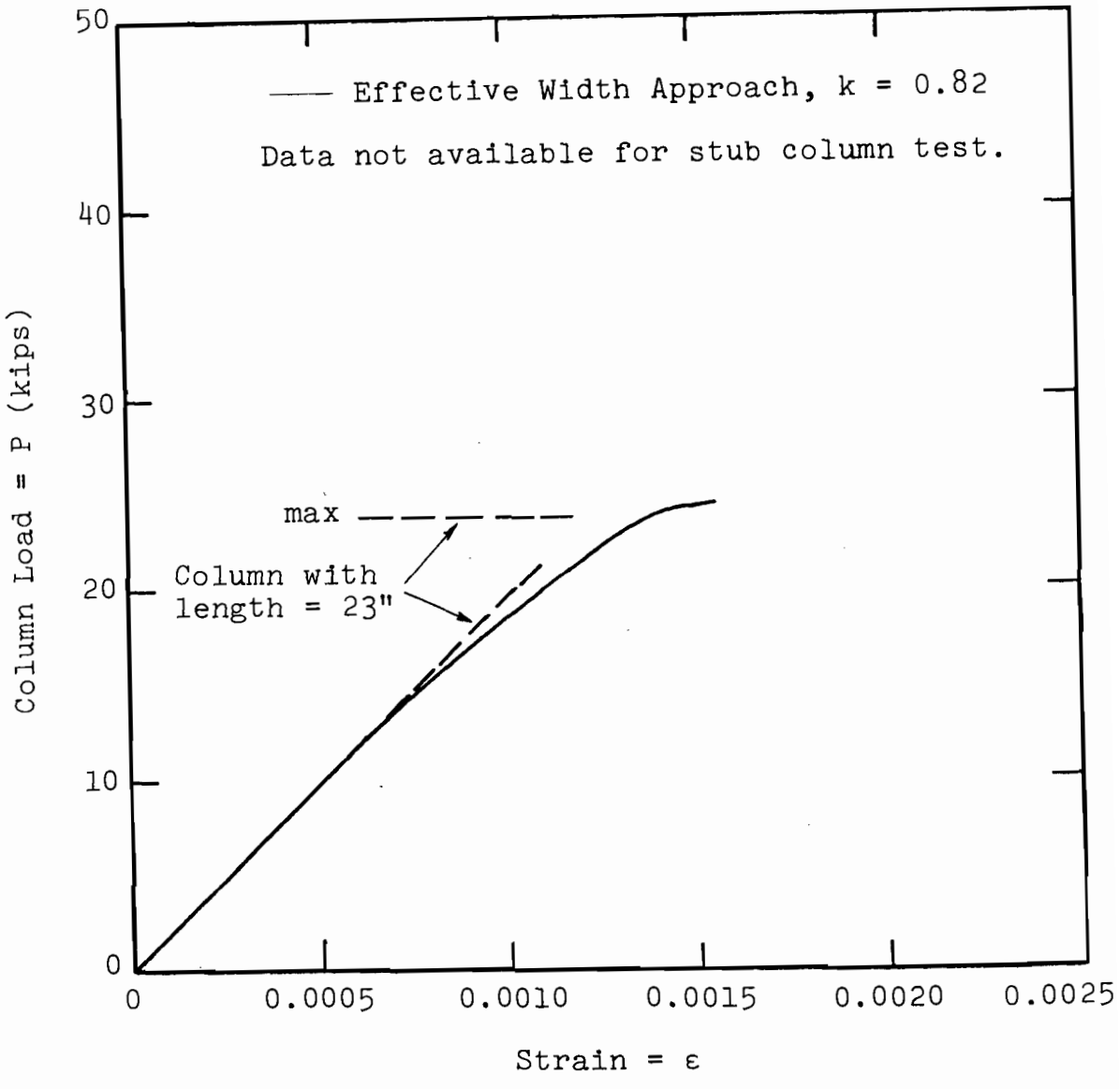

FIG. 6.18 COMPARISON OF STUB COLUMN CURVES BASED ON TESTS AND EFFECTIVE WIDTH APPROACH FOR UNSTIFFENED SECTION U-3

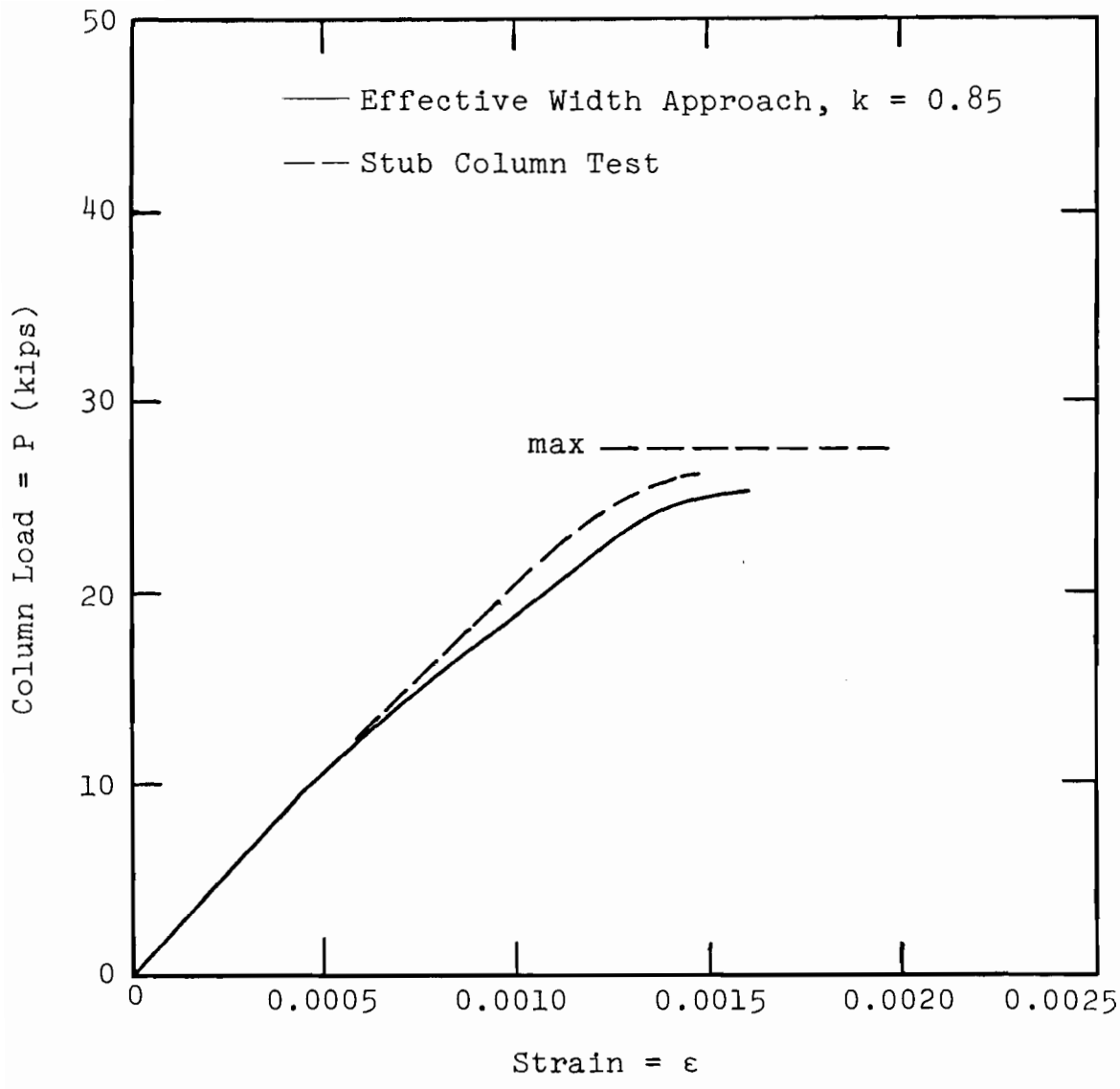

FIG. 6.19 COMPARISON OF STUB COLUMN CURVES BASED ON TESTS AND EFFECTIVE WIDTH APPROACH FOR UNSTIFFENED SECTION U-4

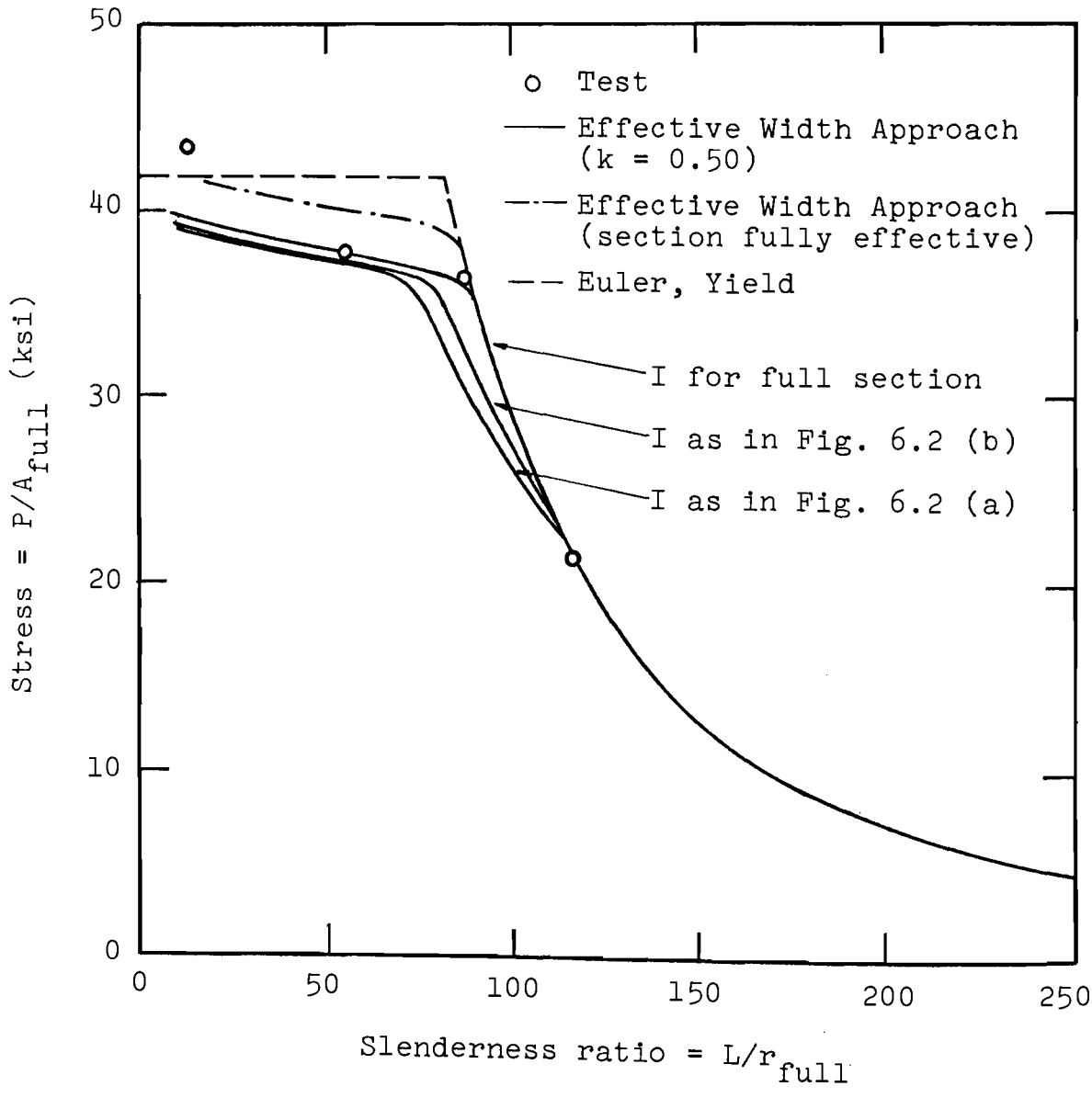

FIG. 6.20 COMPARISON OF TESTS AND EFFECTIVE WIDTH APPROACH USING DIFFERENT MOMENTS OF INERTIA FOR UNSTIFFENED SECTION U-1

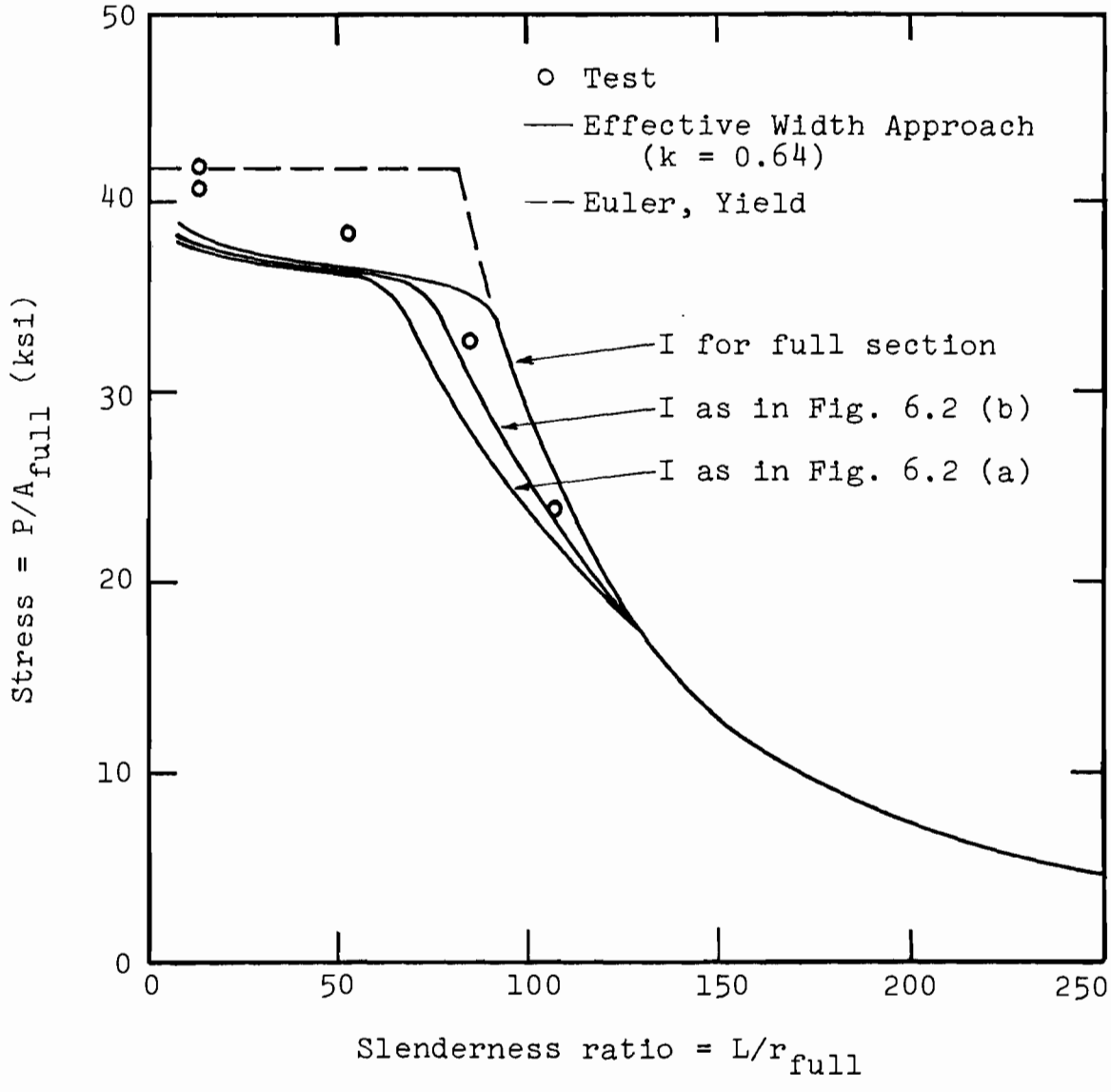

FIG. 6.21 COMPARISON OF TESTS AND EFFECTIVE WIDTH APPROACH USING DIFFERENT MOMENTS OF INERTIA FOR UNSTIFFENED SECTION U-2

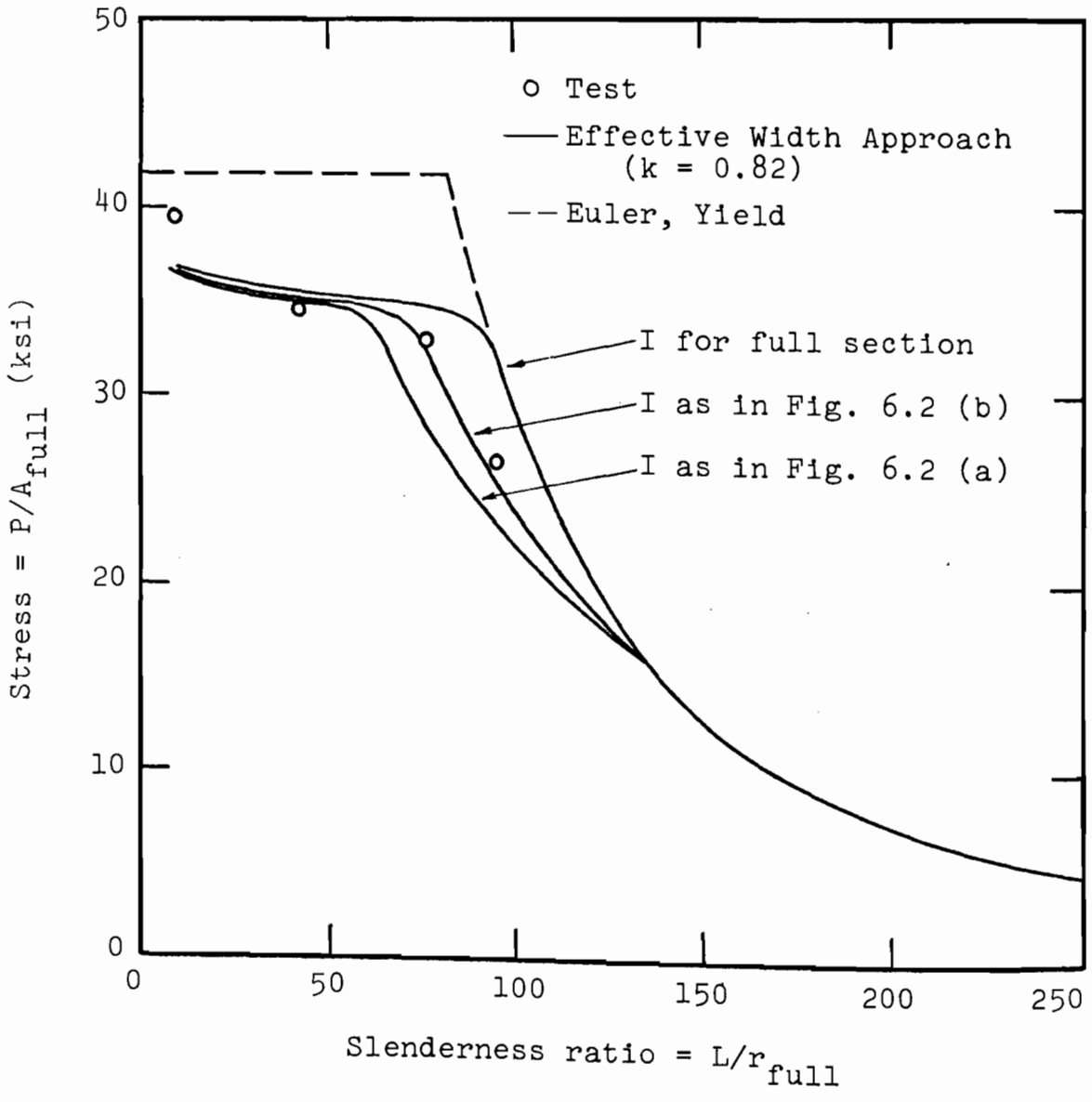

FIG. 6.22 COMPARISON OF TESTS AND EFFECTIVE WIDTH APPROACH USING DIFFERENT MOMENTS OF INERTIA FOR UNSTIFFENED SECTION U-3

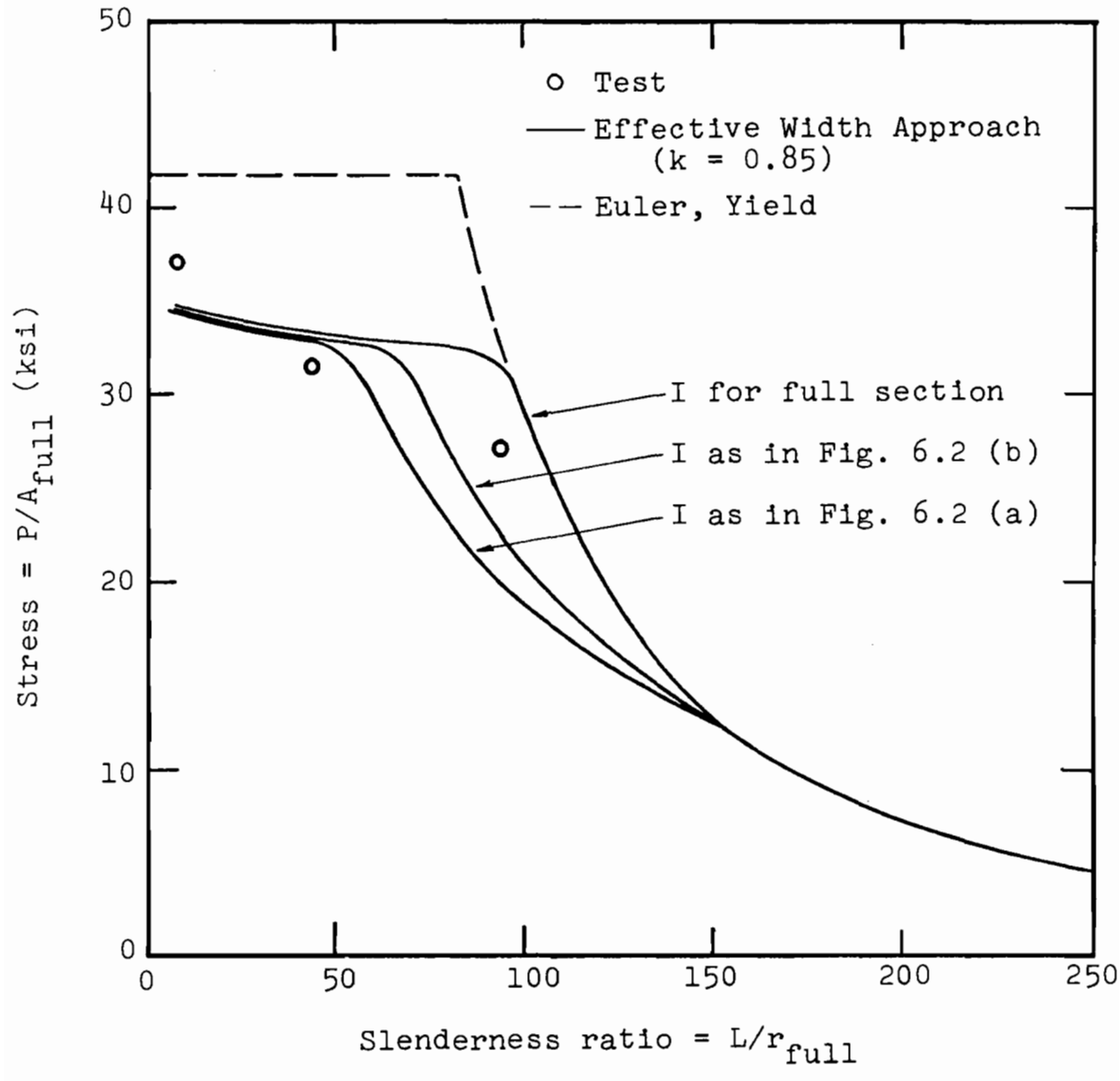

FIG. 6.23 COMPARISON OF TESTS AND EFFECTIVE WIDTH APPROACH USING DIFFERENT MOMENTS OF INERTIA FOR UNSTIFFENED SECTION U-4

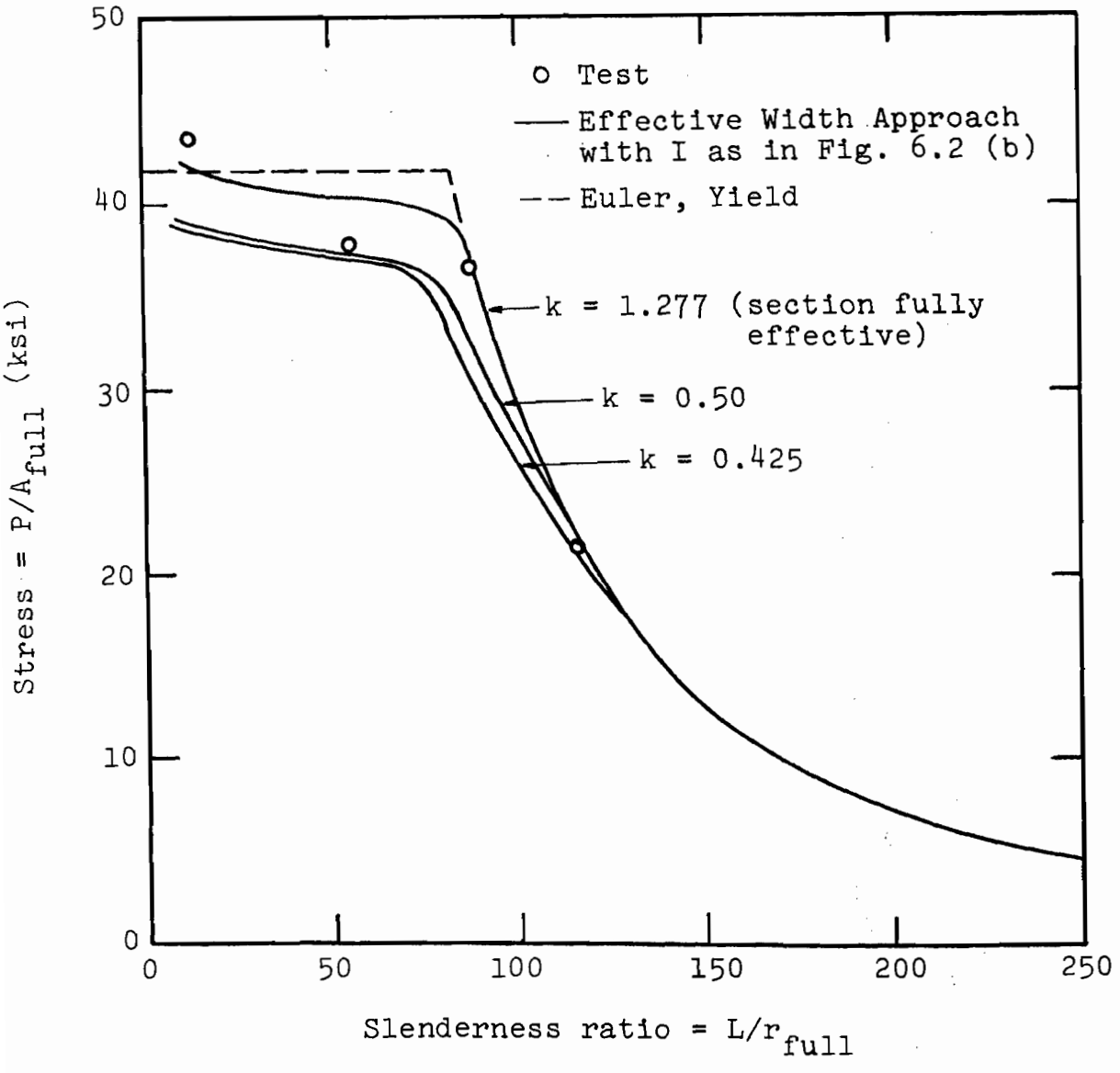

FIG. 6.24 COMPARISON OF TESTS AND EFFECTIVE WIDTH APPROACH BASED ON DIFFERENT EDGE SUPPORT CONDITIONS FOR UNSTIFFENED SECTION U-1

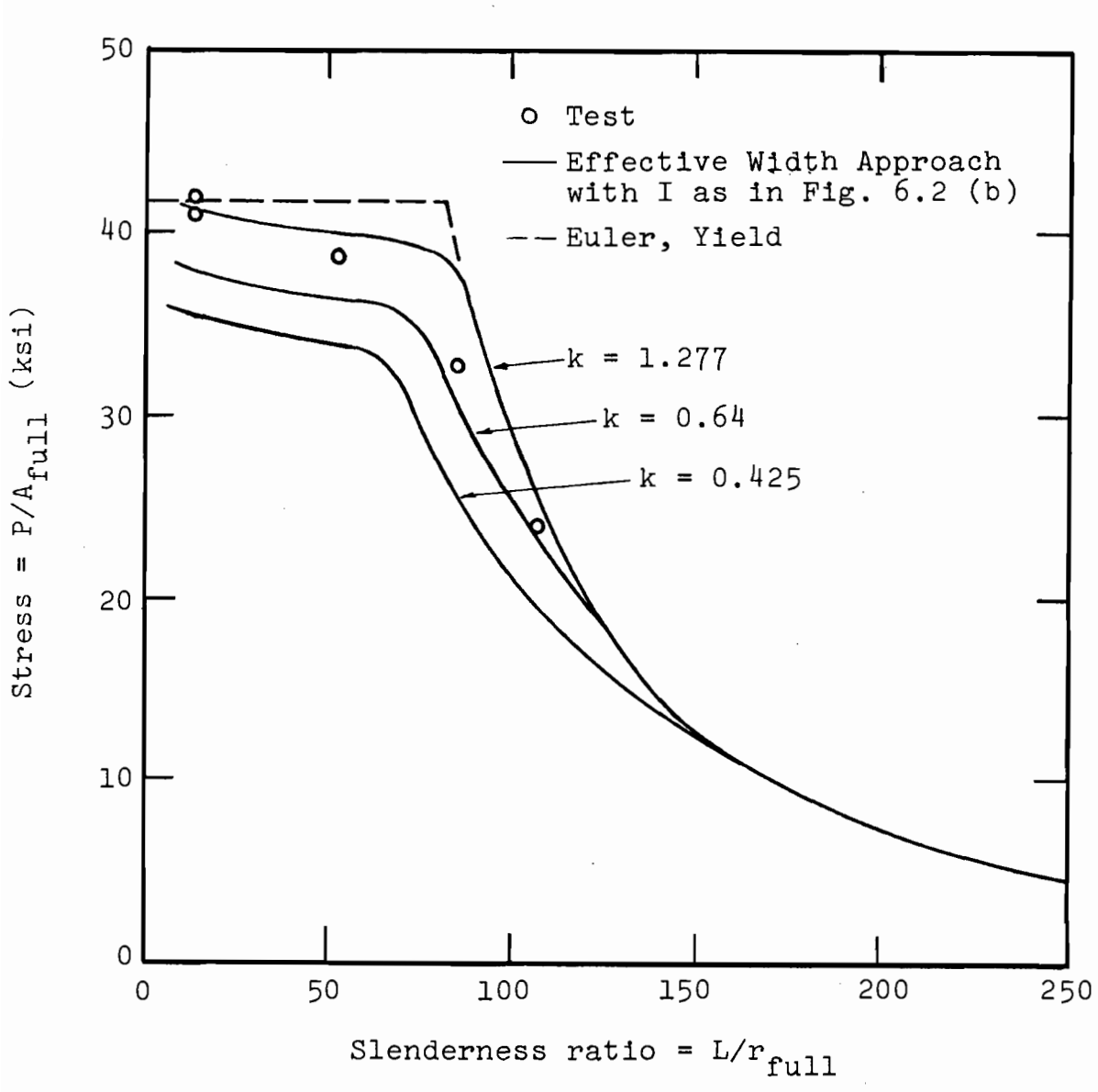

FIG. 6.25 COMPARISON OF TESTS AND EFFECTIVE WIDTH APPROACH BASED ON DIFFERENT EDGE SUPPORT CONDITIONS FOR UNSTIFFENED SECTION U-2

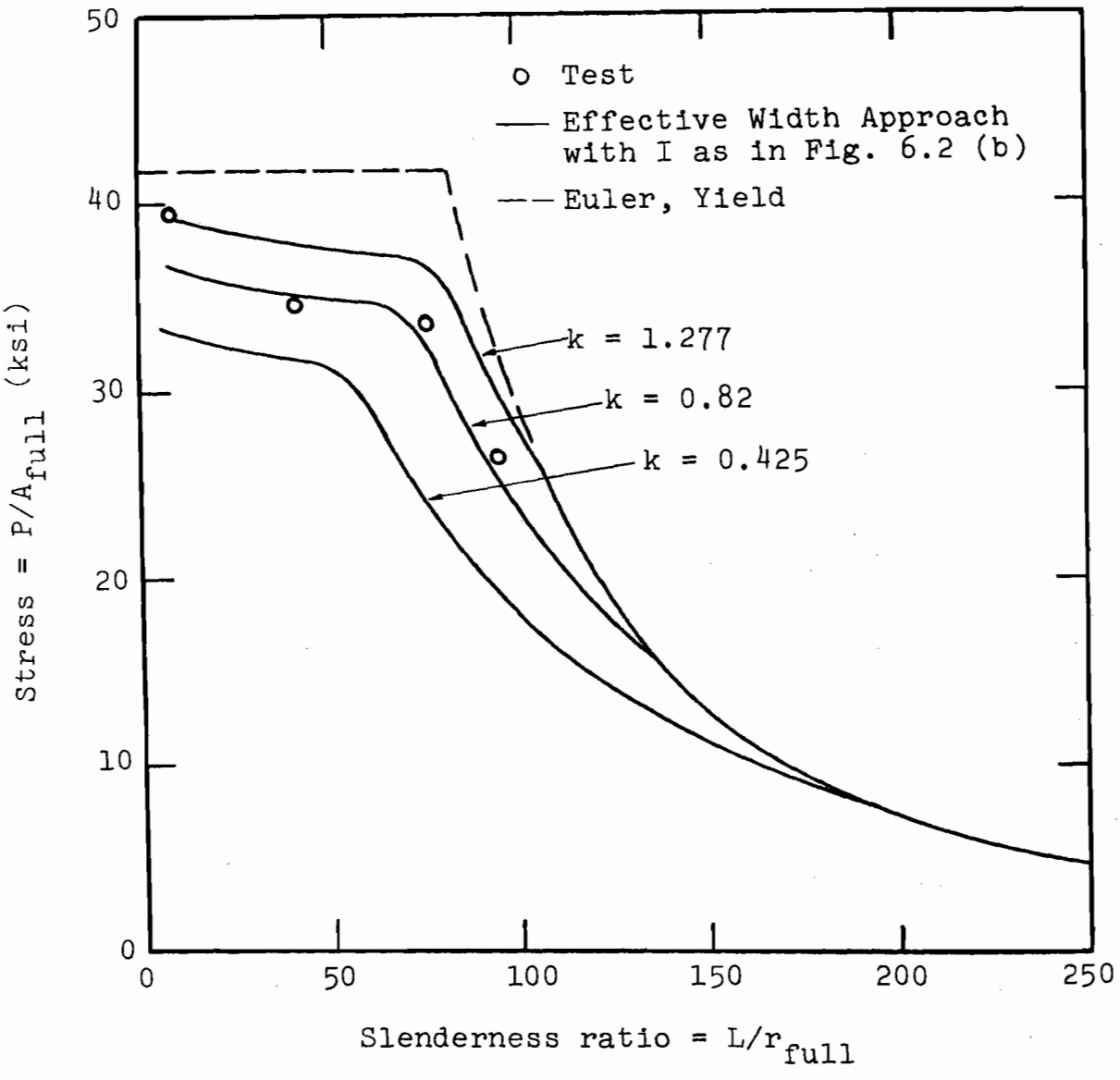

FIG. 6.26 COMPARISON OF TESTS AND EFFECTIVE WIDTH APPROACH BASED ON DIFFERENT EDGE SUPPORT CONDITIONS FOR UNSTIFFENED SECTION U-3

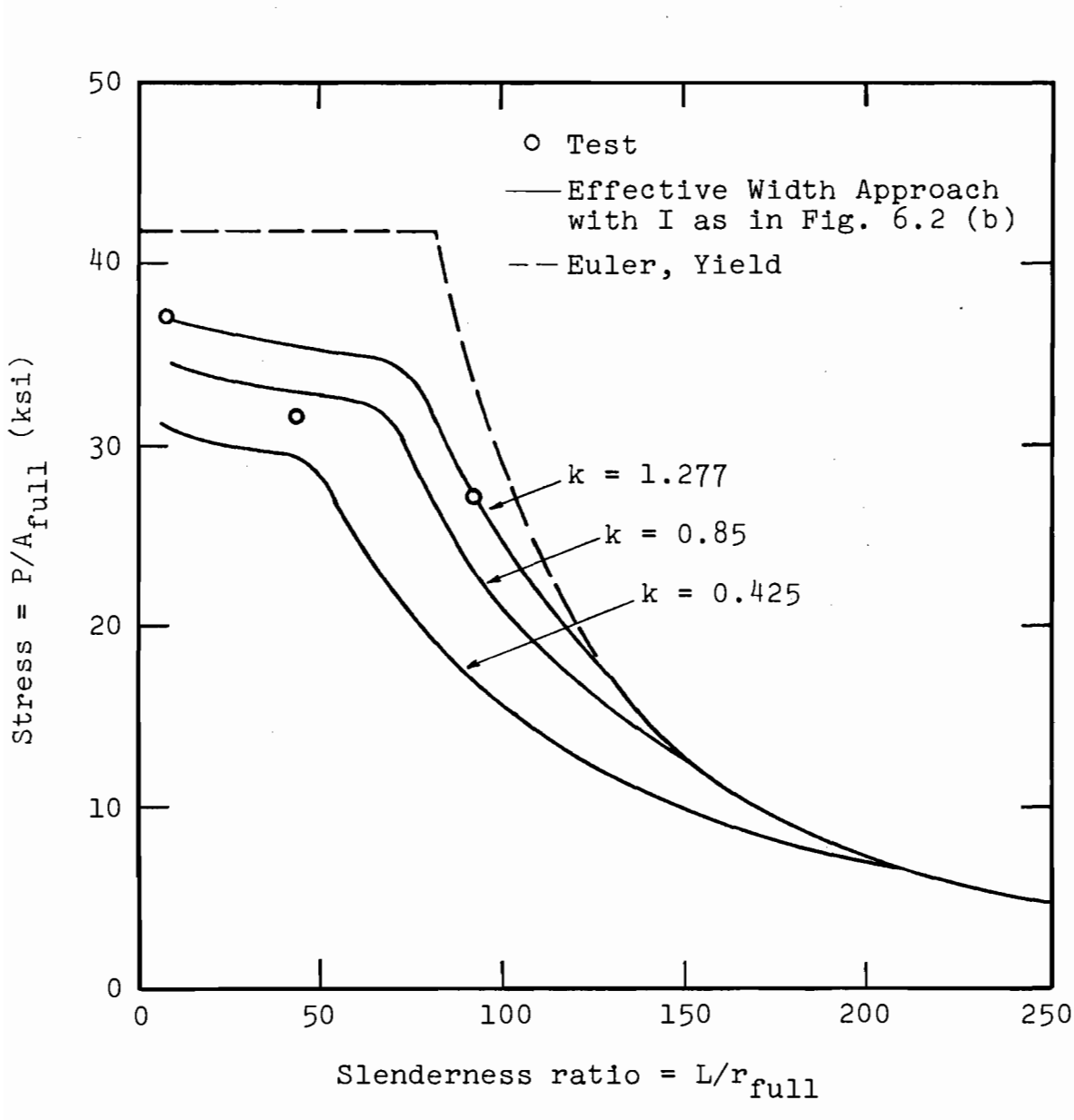

FIG. 6.27 COMPARISON OF TESTS AND EFFECTIVE WIDTH APPROACH BASED ON DIFFERENT EDGE SUPPORT CONDITIONS FOR UNSTIFFENED SECTION U-4

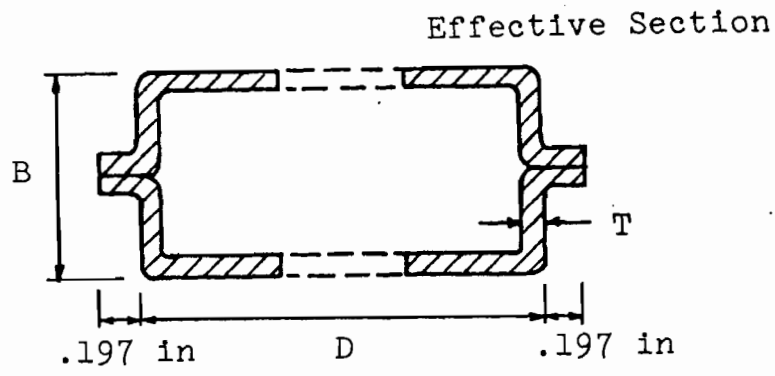

(a) Column Cross-Section

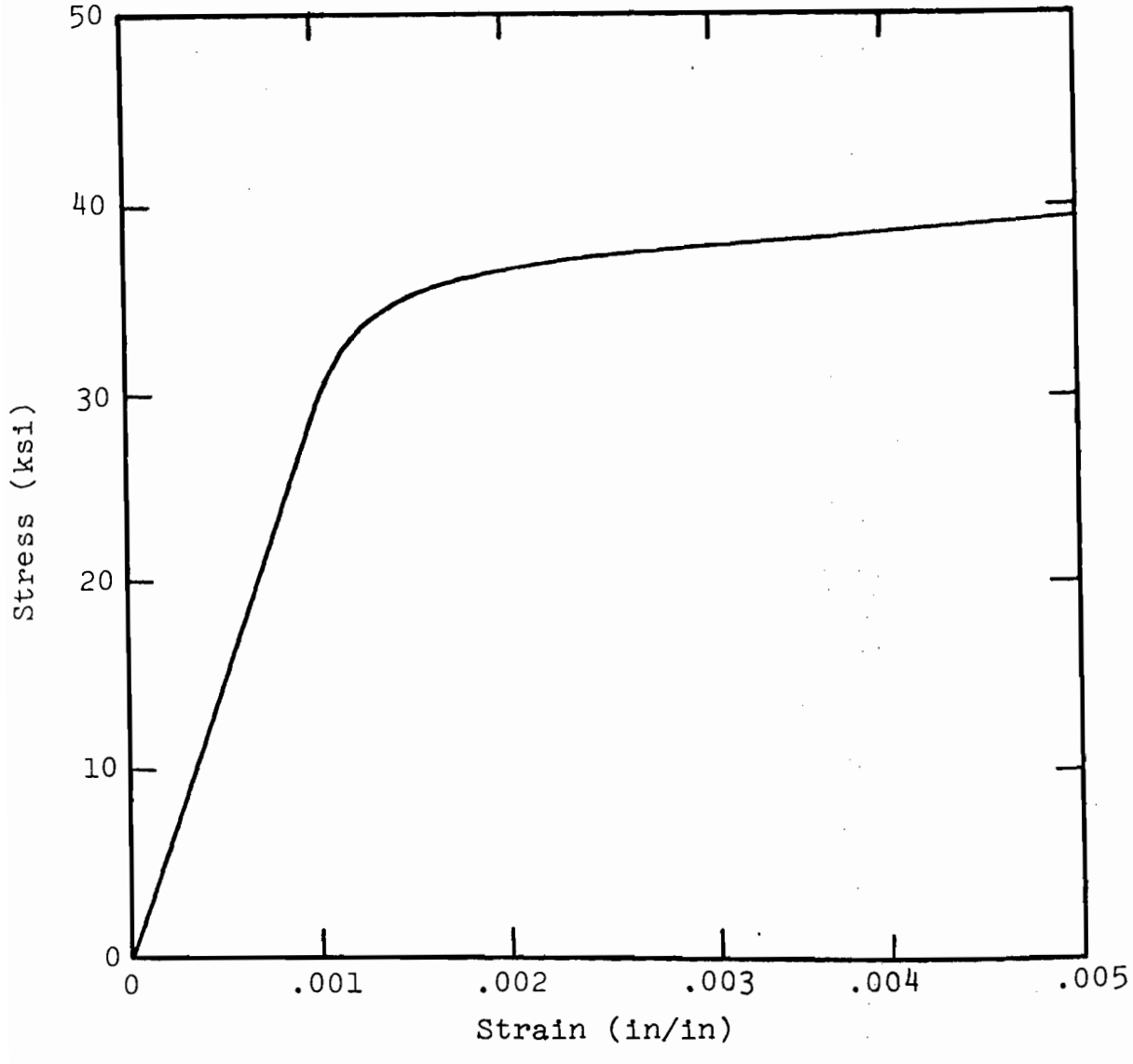

(b) Assumed Material Stress-Strain Curve

FIG. 6.28 SKALOUD'S AND ZORNEROVA'S EXPERIMENTAL COLUMNS

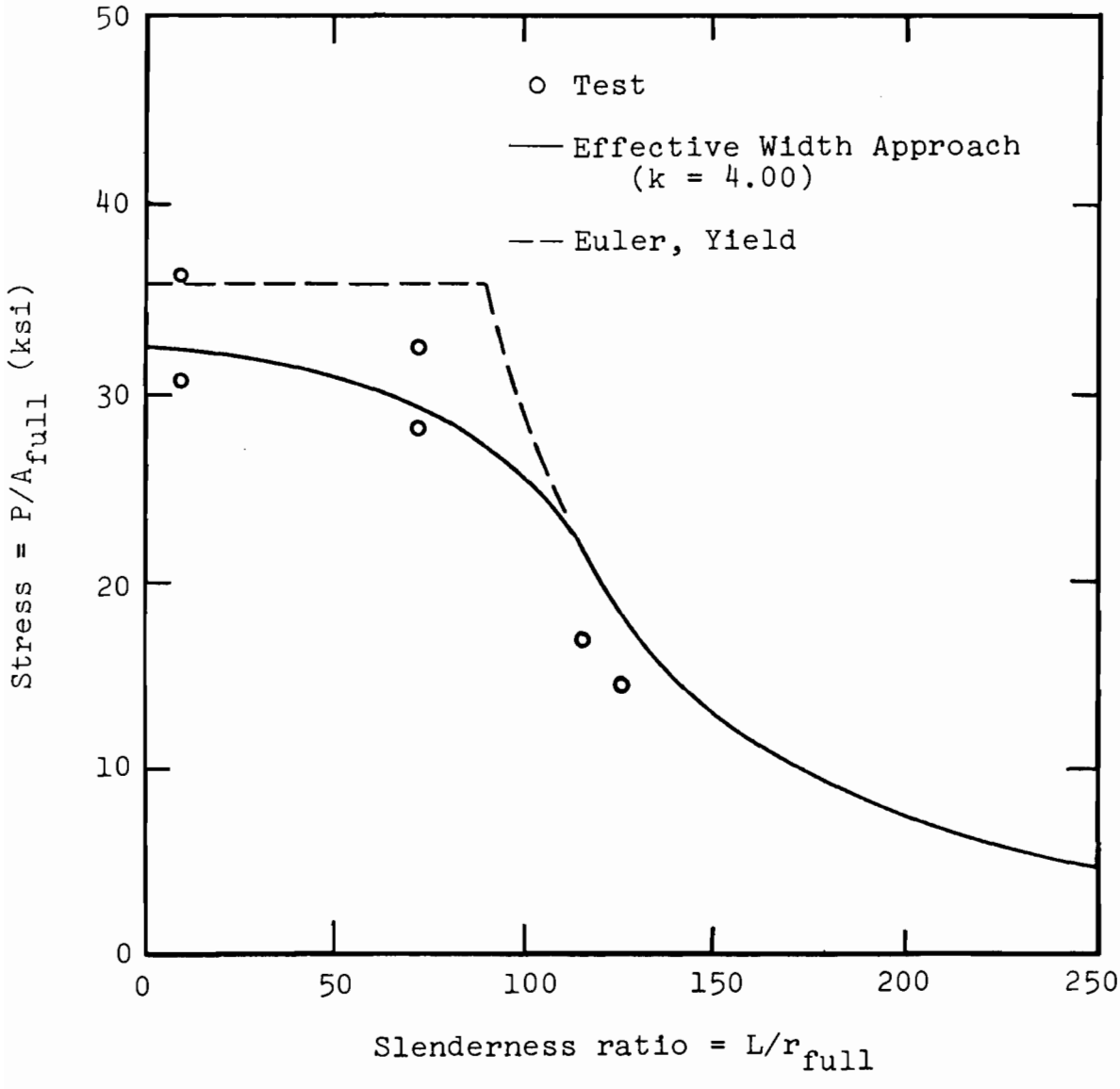

FIG. 6.29 COMPARISON OF EFFECTIVE WIDTH APPROACH AND EXPERIMENTAL RESULTS FOR SERIES A OF SKALOUD AND ZORNEROVA

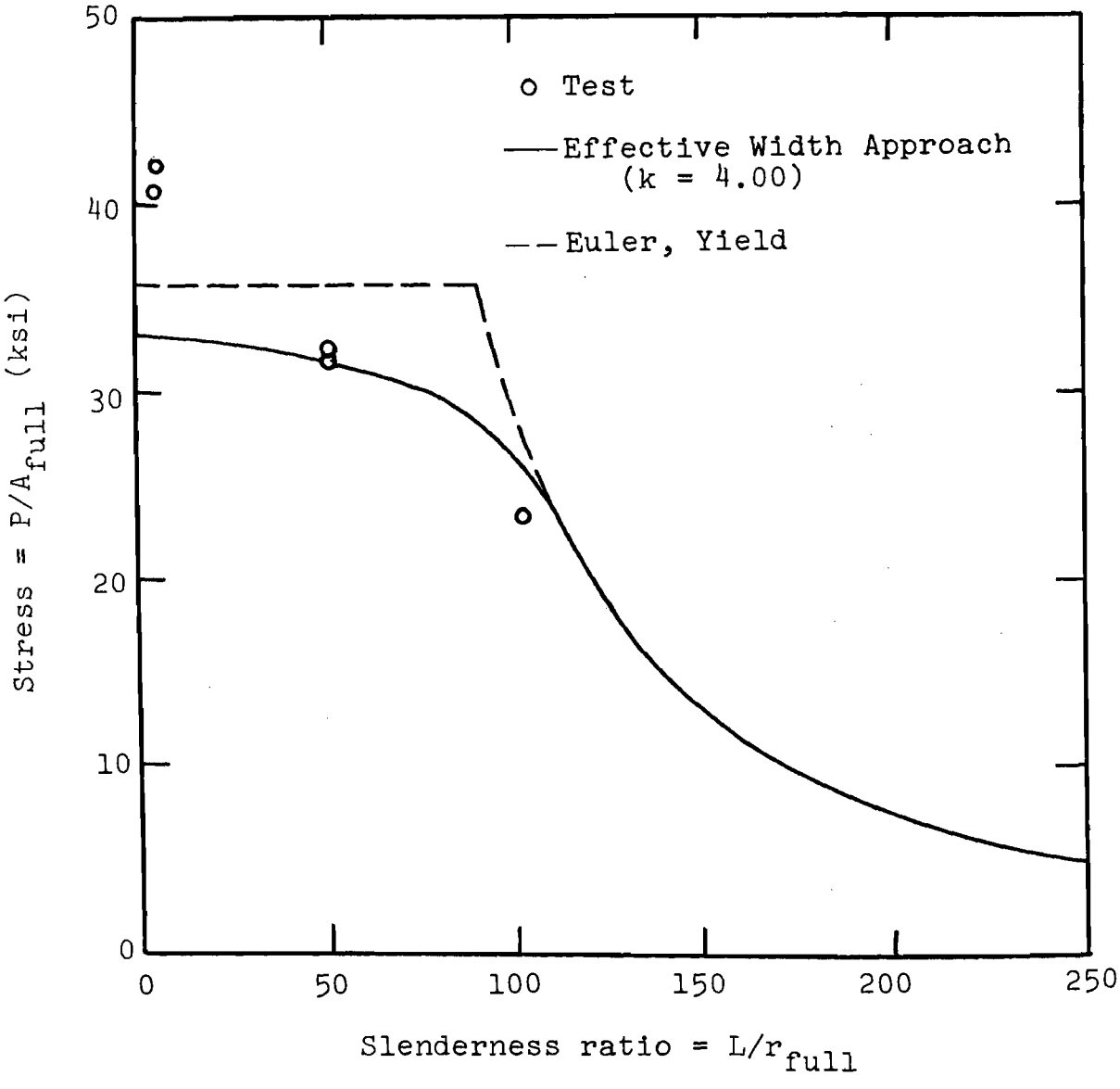

FIG. 6.30 COMPARISON OF EFFECTIVE WIDTH APPROACH AND EXPERIMENTAL RESULTS FOR SERIES B OF SKALOUD AND ZORNEROVA

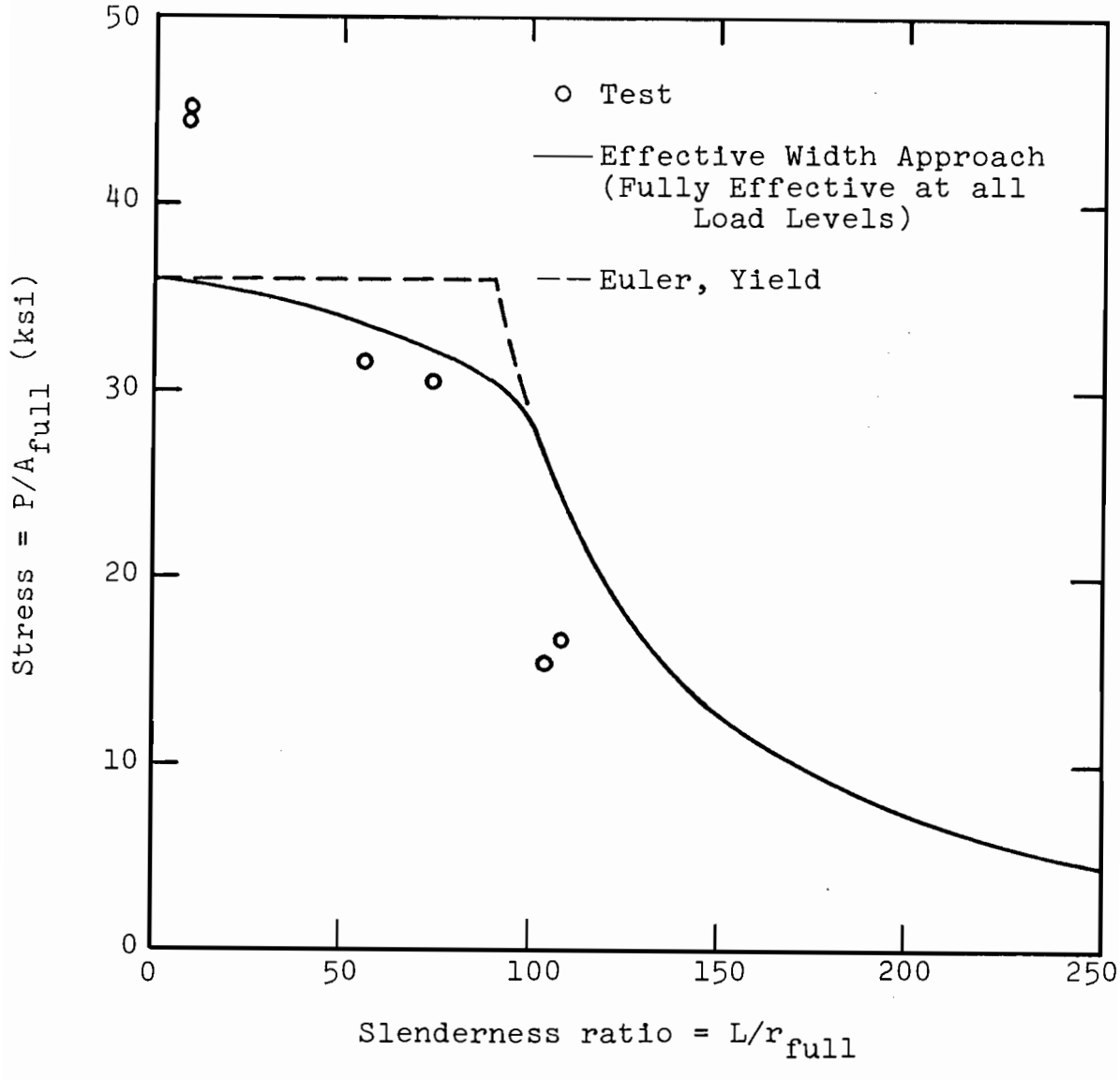

FIG. 6.31 COMPARISON OF EFFECTIVE WIDTH APPROACH AND EXPERIMENTAL RESULTS FOR SERIES C OF SKALOUD AND ZORNEROVA

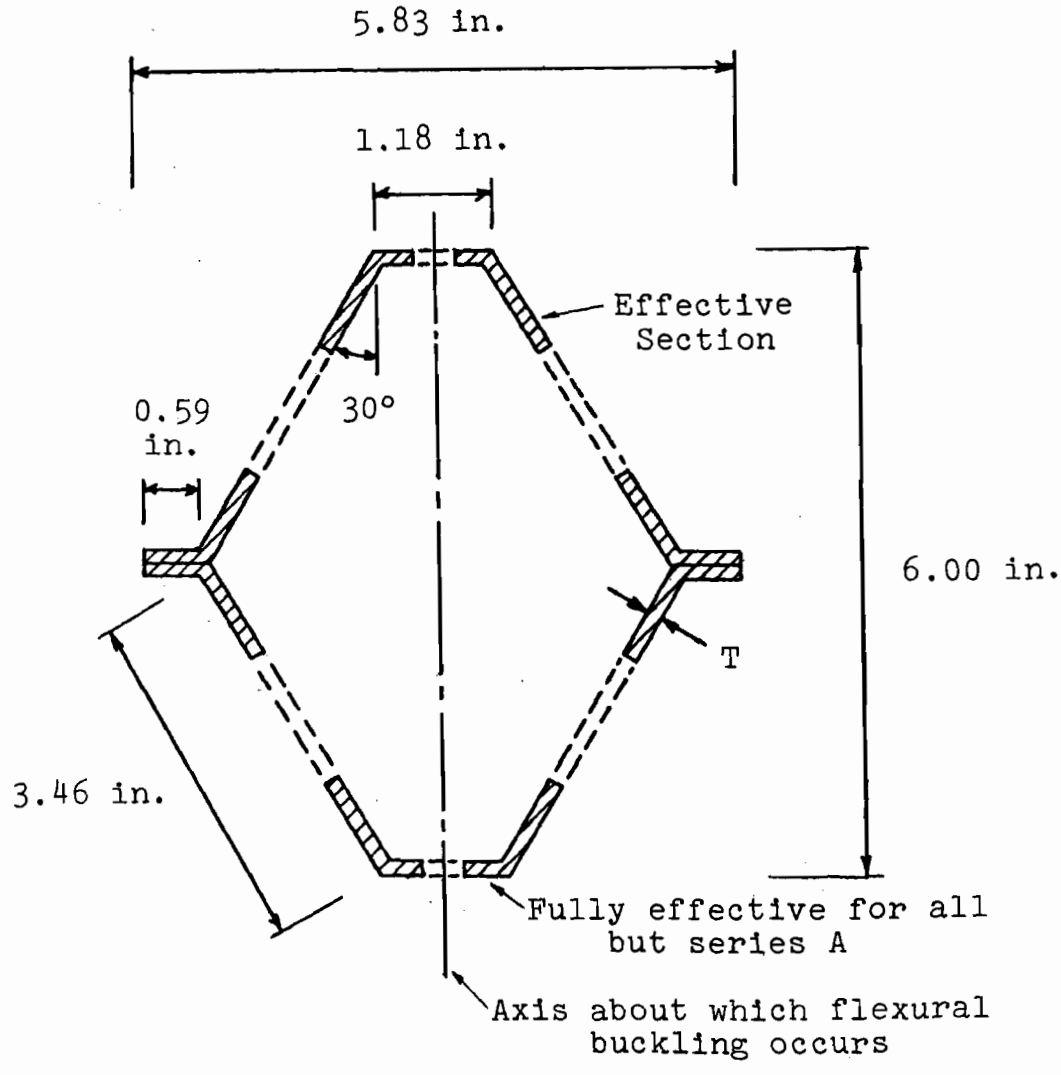

FIG. 6.32 COLUMN CROSS-SECTION FOR EXPERIMENTAL COLUMNS OF DELIEGE, BAAR, AND HICK

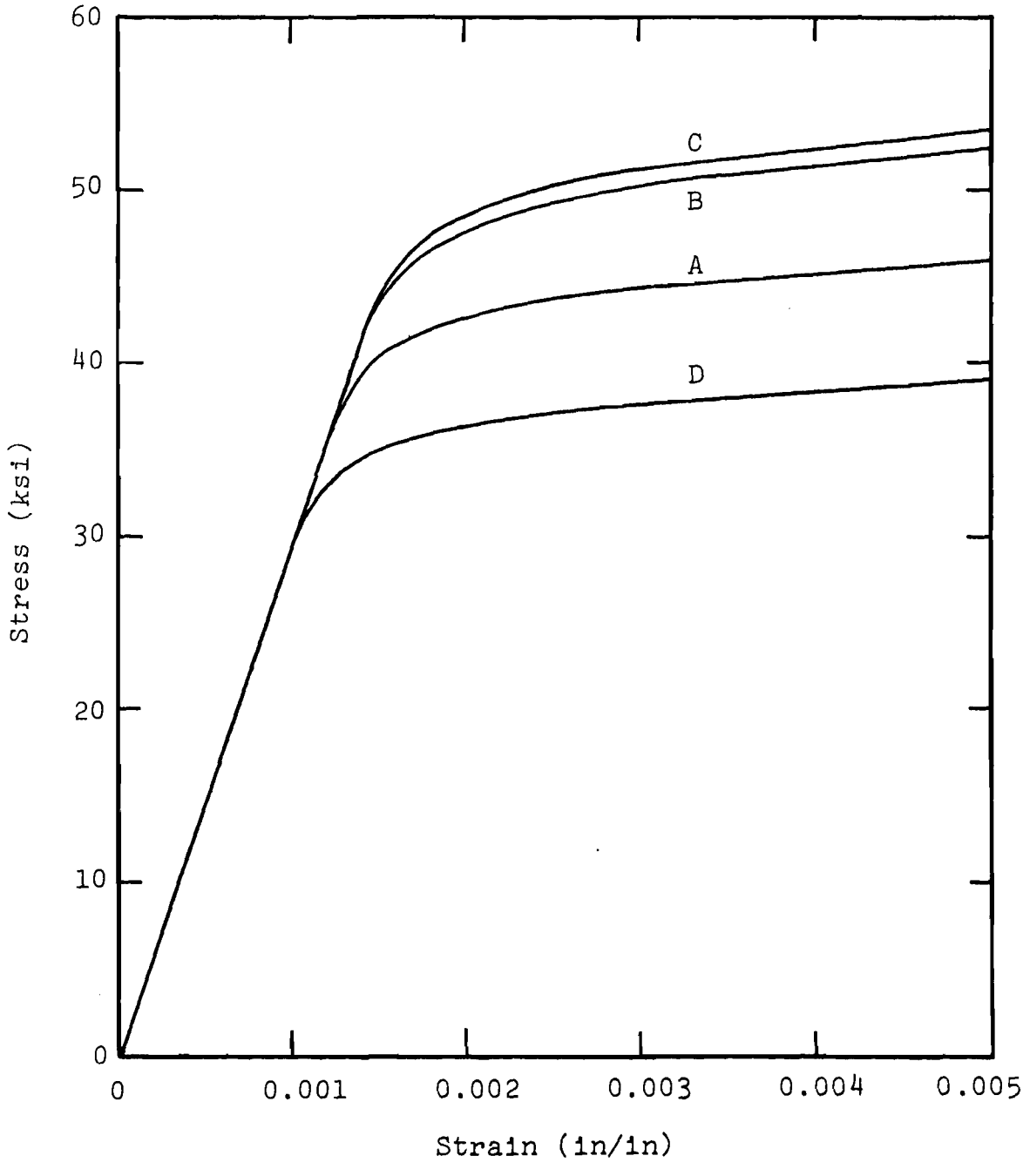

FIG. 6.33 ASSUMED STRESS-STRAIN CURVES FOR EXPERIMENTAL COLUMNS OF DELIEGE, BAAR, AND HICK

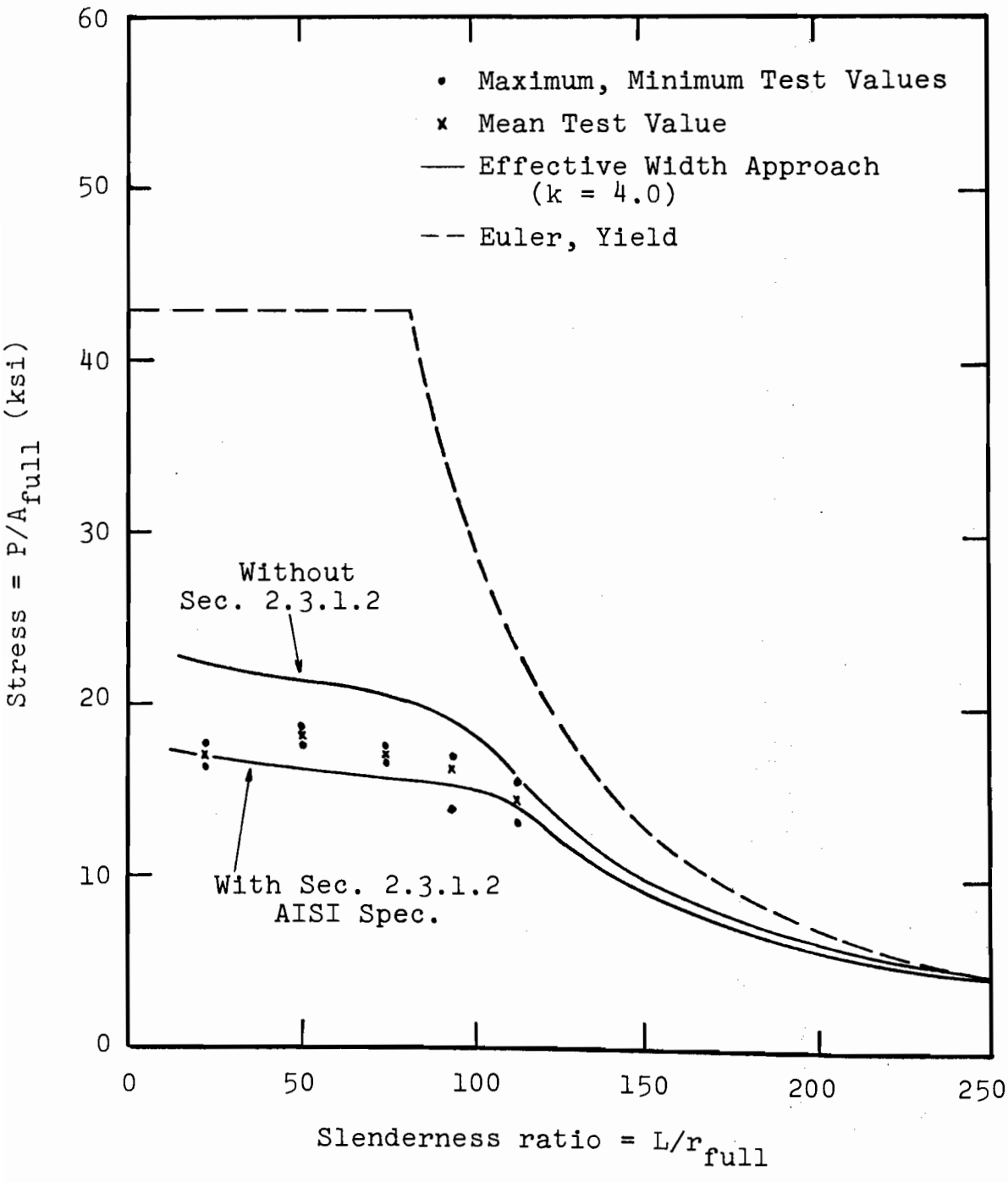

FIG. 6.34 COMPARISON OF EFFECTIVE WIDTH APPROACH AND EXPERIMENTAL RESULTS FOR SERIES A OF DELIEGE, BAAR, AND HICK

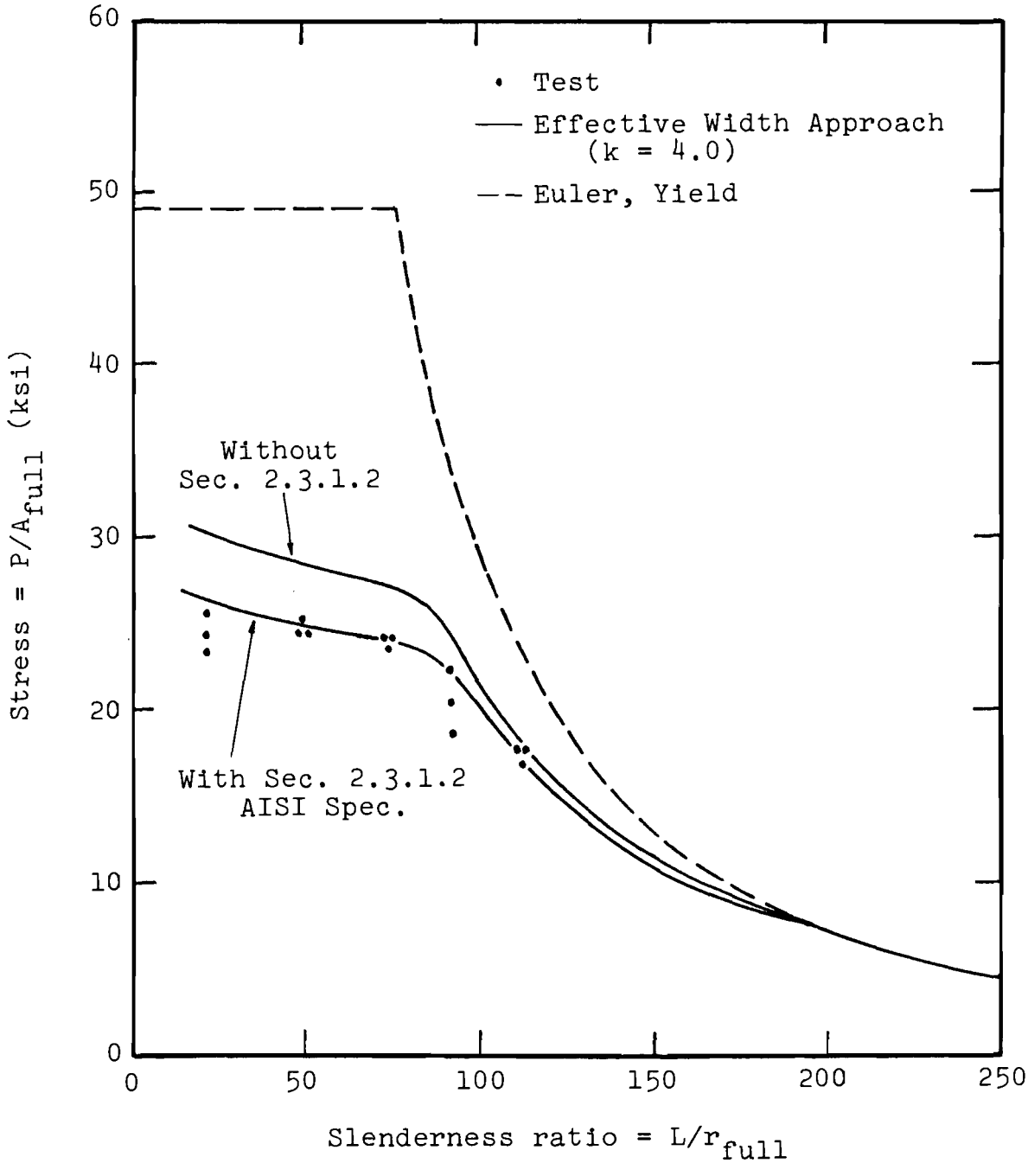

FIG. 6.35 COMPARISON OF EFFECTIVE WIDTH APPROACH AND EXPERIMENTAL RESULTS FOR SERIES B OF DELIEGE, BAAR, AND HICK

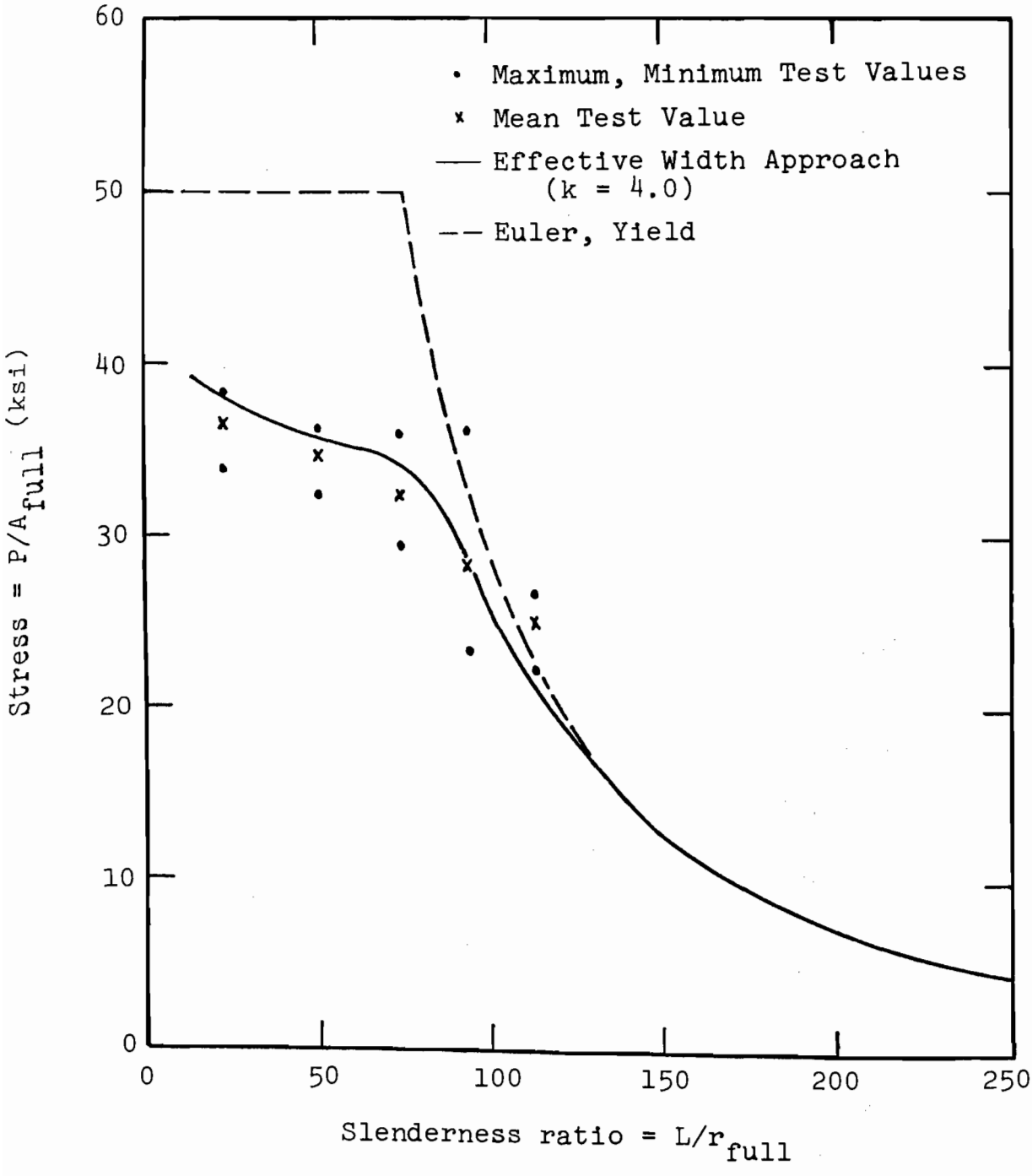

FIG. 6.36 COMPARISON OF EFFECTIVE WIDTH APPROACH AND EXPERIMENTAL RESULTS FOR SERIES C OF DELIEGE, BAAR, AND HICK

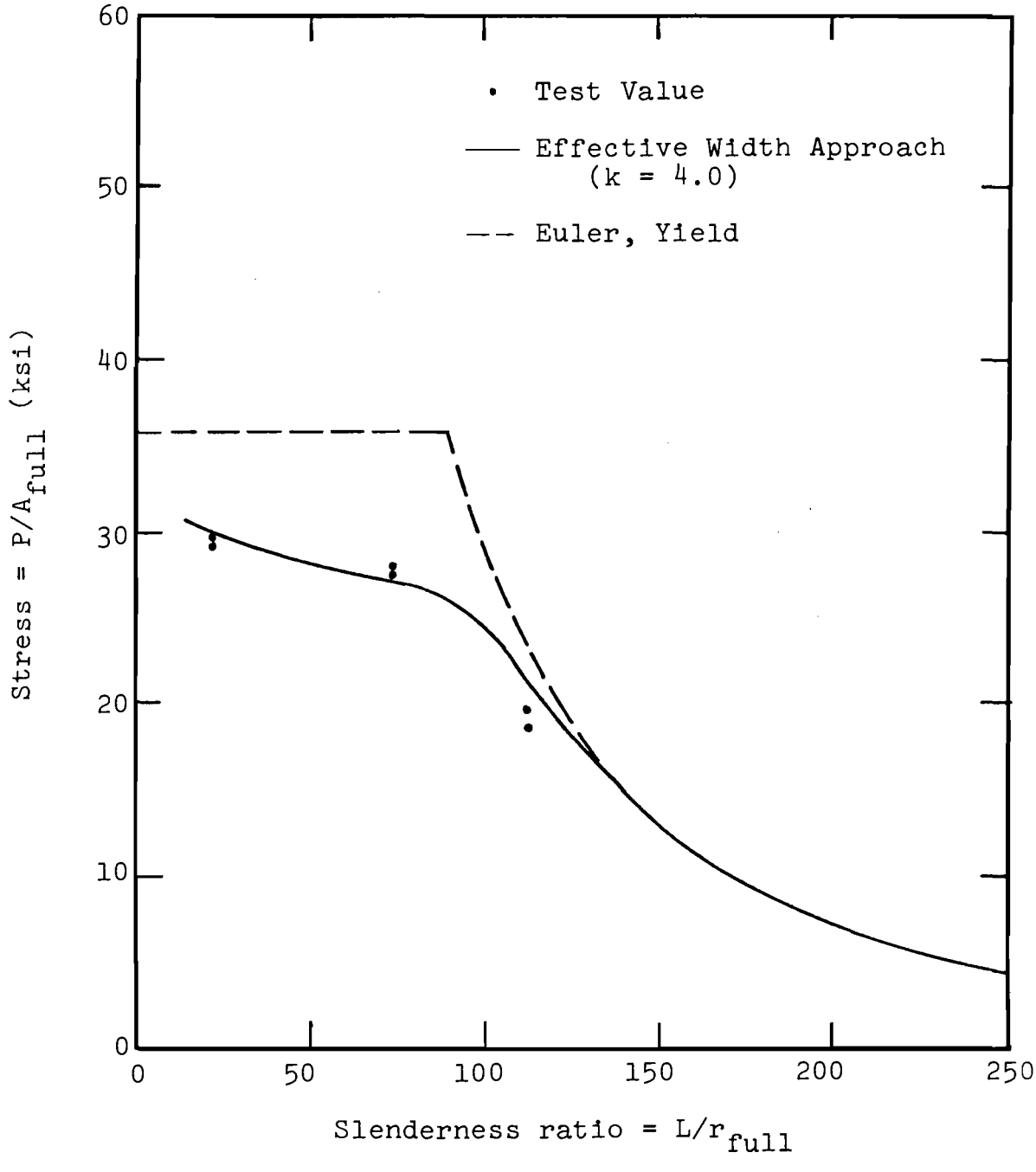

FIG. 6.37 COMPARISON OF EFFECTIVE WIDTH APPROACH AND EXPERIMENTAL RESULTS FOR SERIES D OF DELIEGE, BAAR, AND HICK

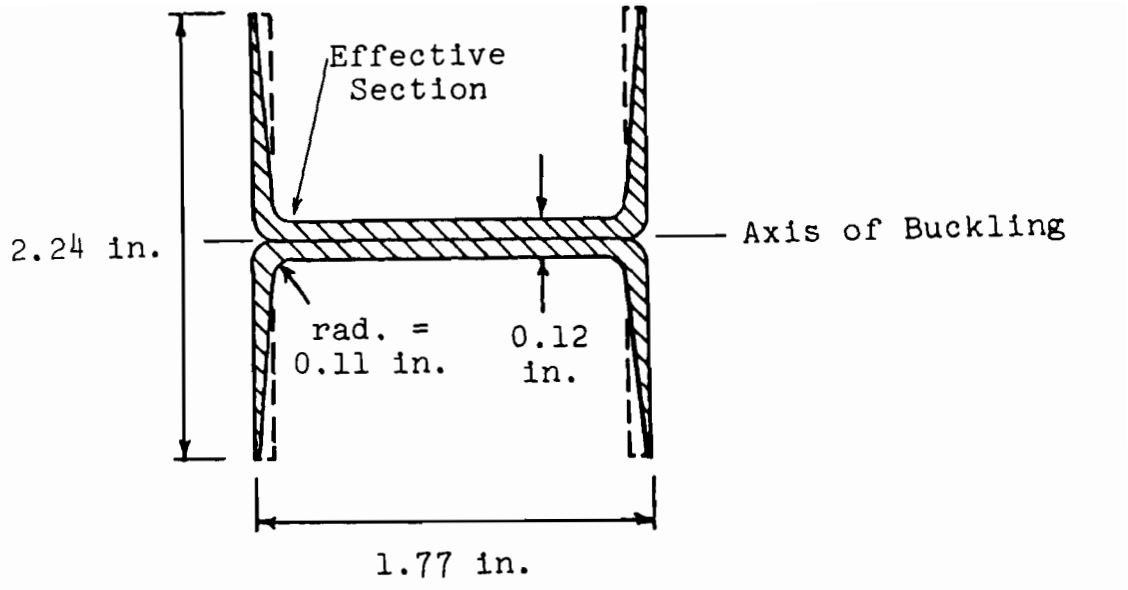

(a) Column UC-1

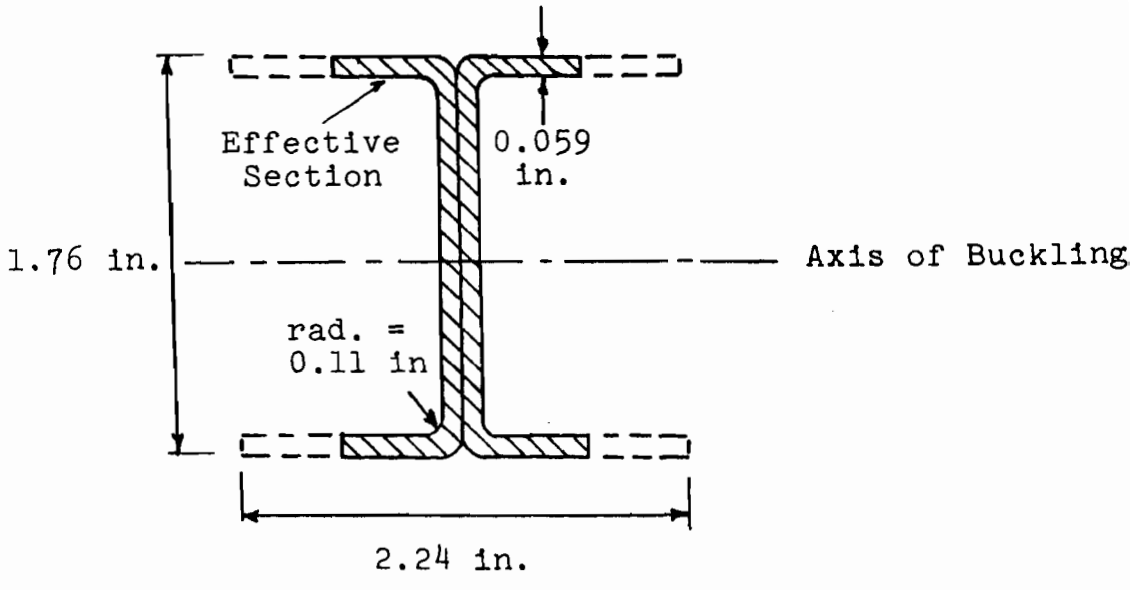

(b) Column UC-2

FIG. 6.38 COLUMN CROSS-SECTIONS FOR UNSTIFFENED EXPERIMENTAL COLUMNS OF URIBE

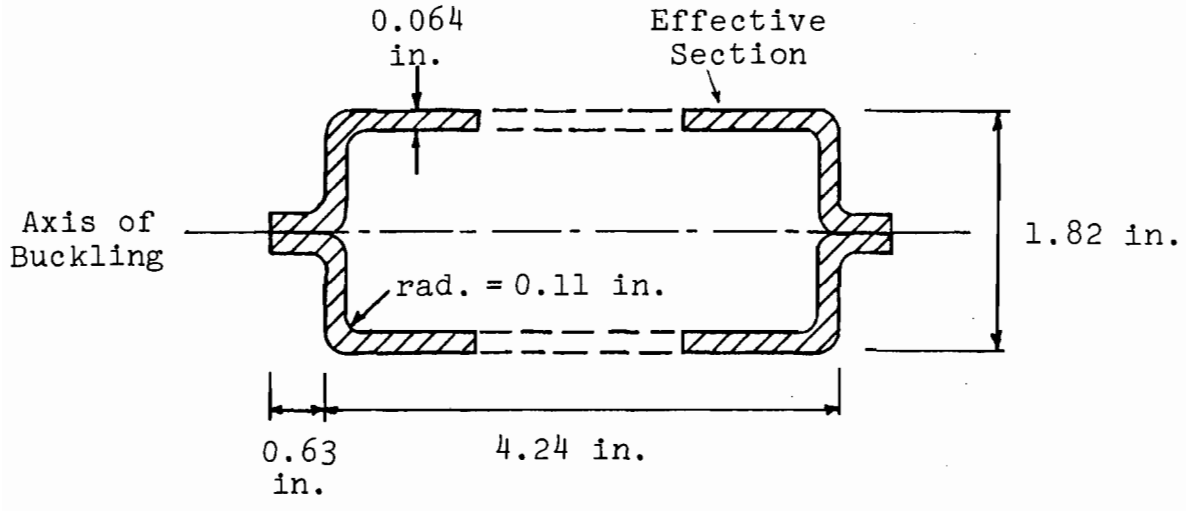

(a) Column SC-1

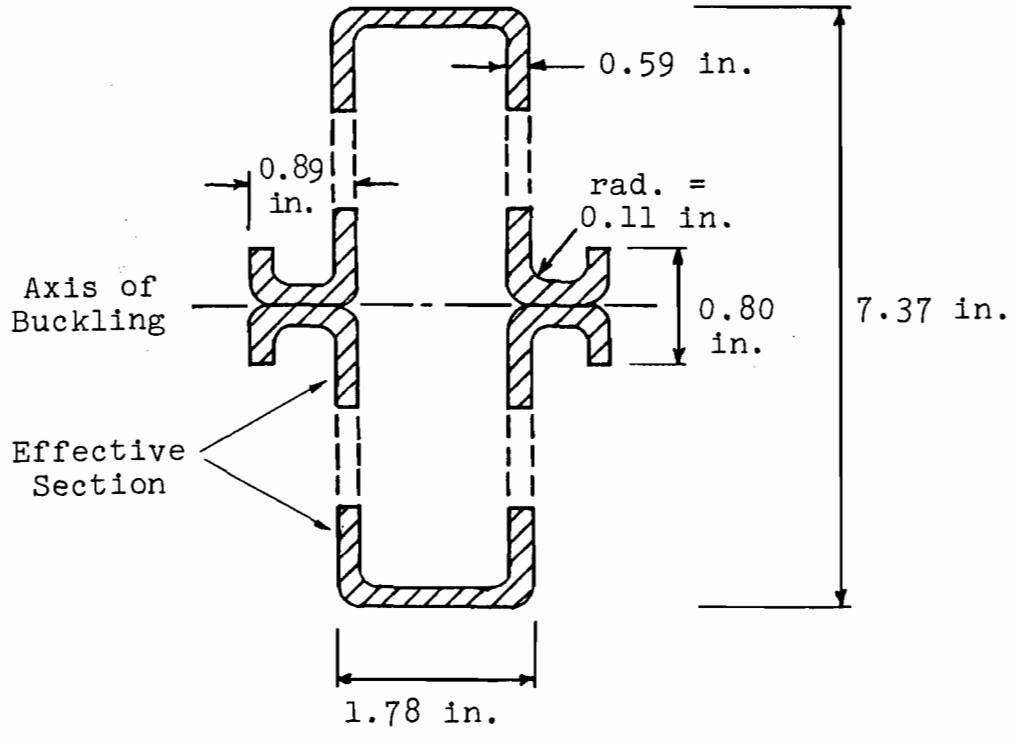

(b) Column SC-2

FIG. 6.39 COLUMN CROSS-SECTIONS FOR STIFFENED EXPERIMENTAL COLUMNS OF URIBE

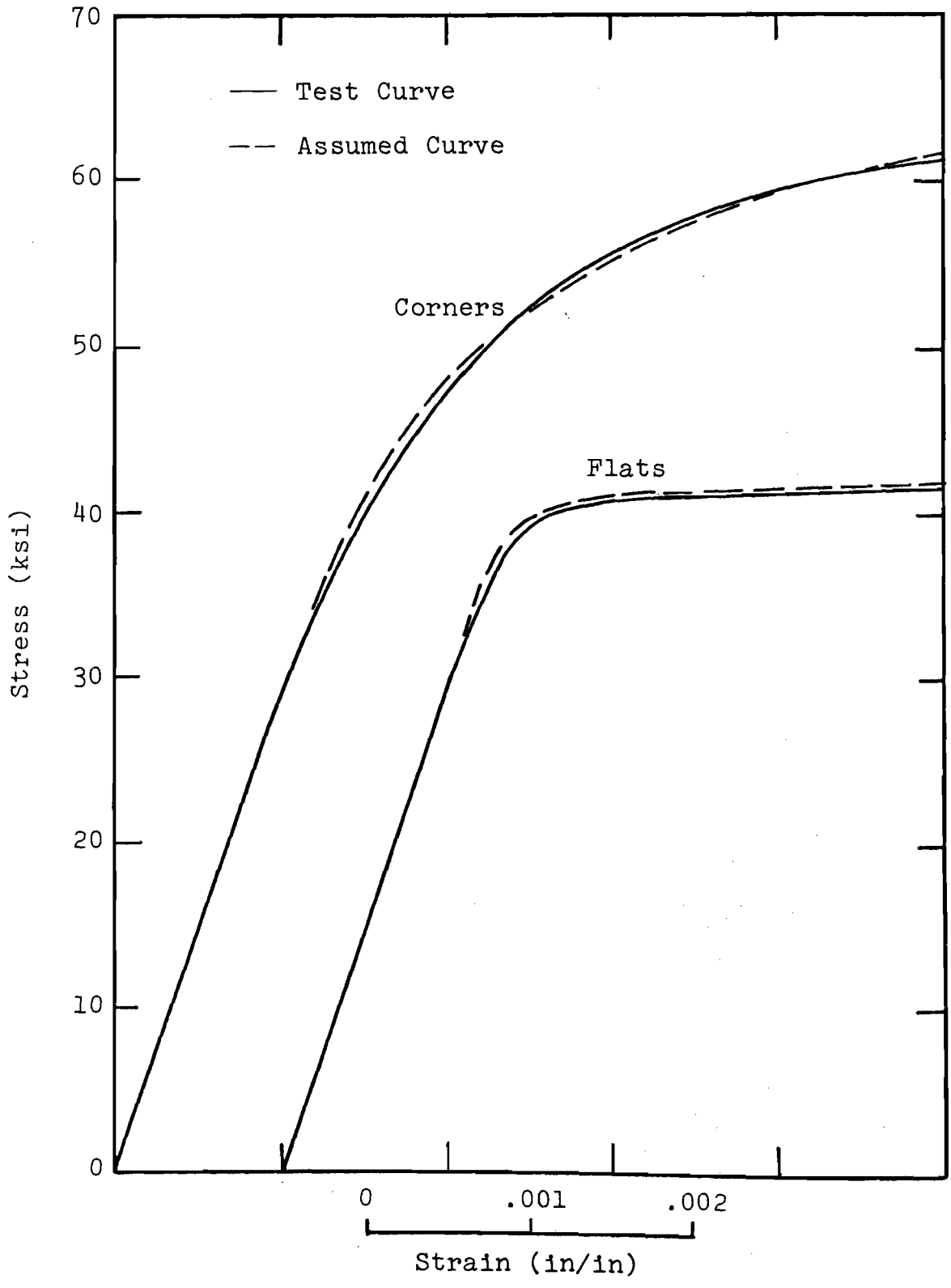

FIG. 6.40 TENSILE STRESS-STRAIN CURVES FOR COLUMNS UC-1 AND UC-2 OF URIBE

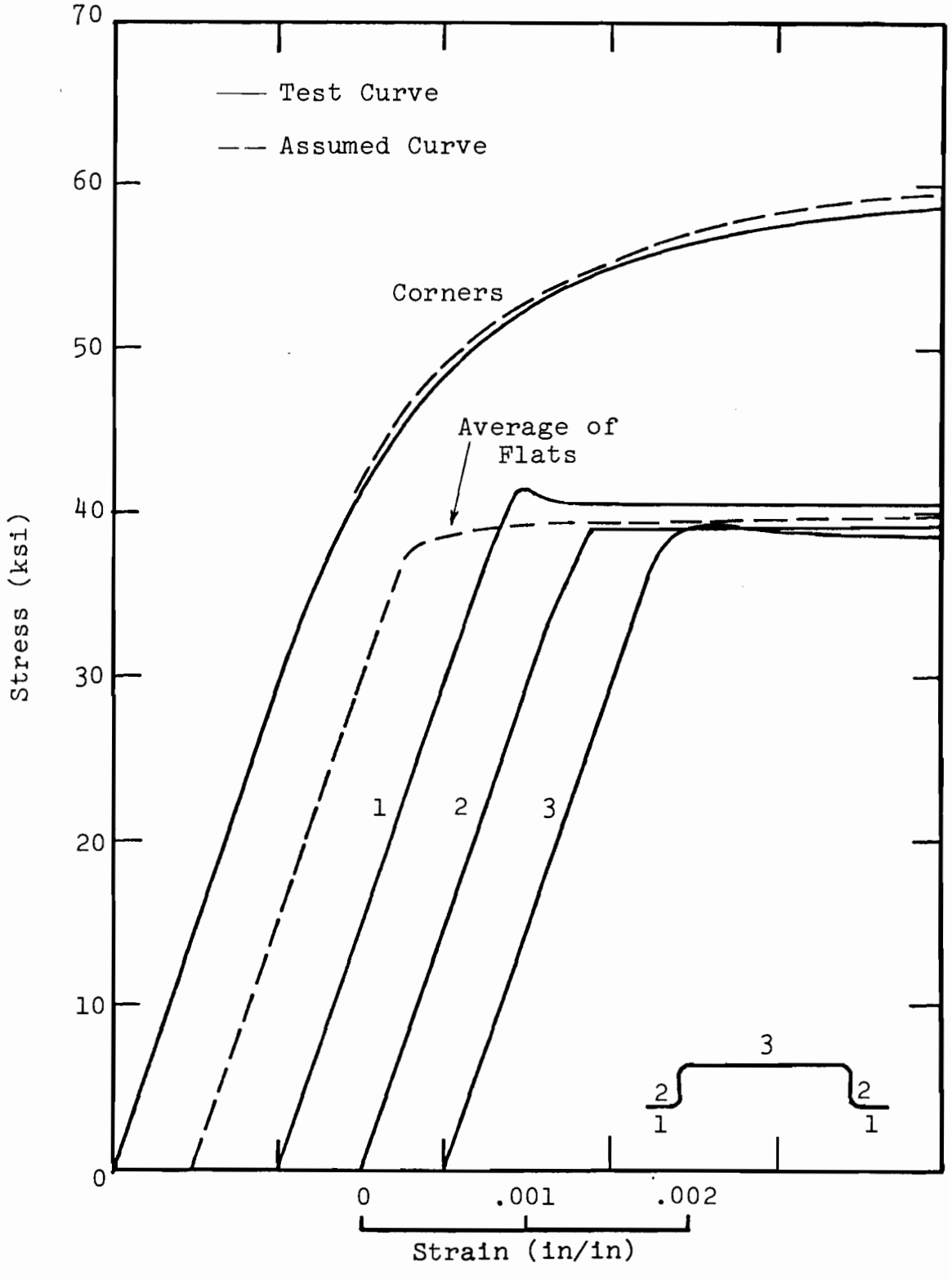

FIG. 6.41 TENSILE STRESS-STRAIN CURVES
FOR COLUMN SC-1 OF URIBE

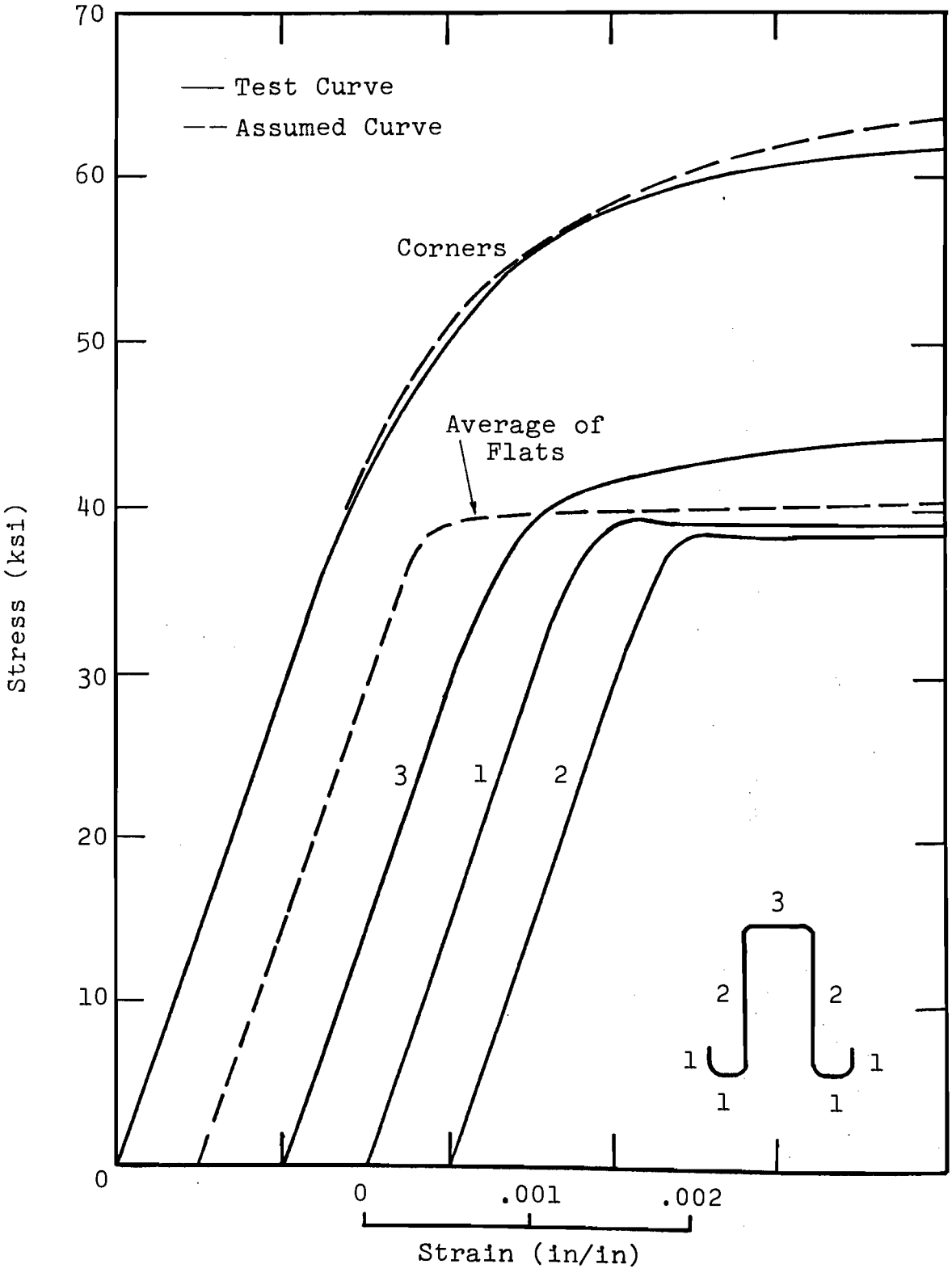

FIG. 6.42 TENSILE STRESS-STRAIN CURVES FOR COLUMN SC-2 OF URIBE

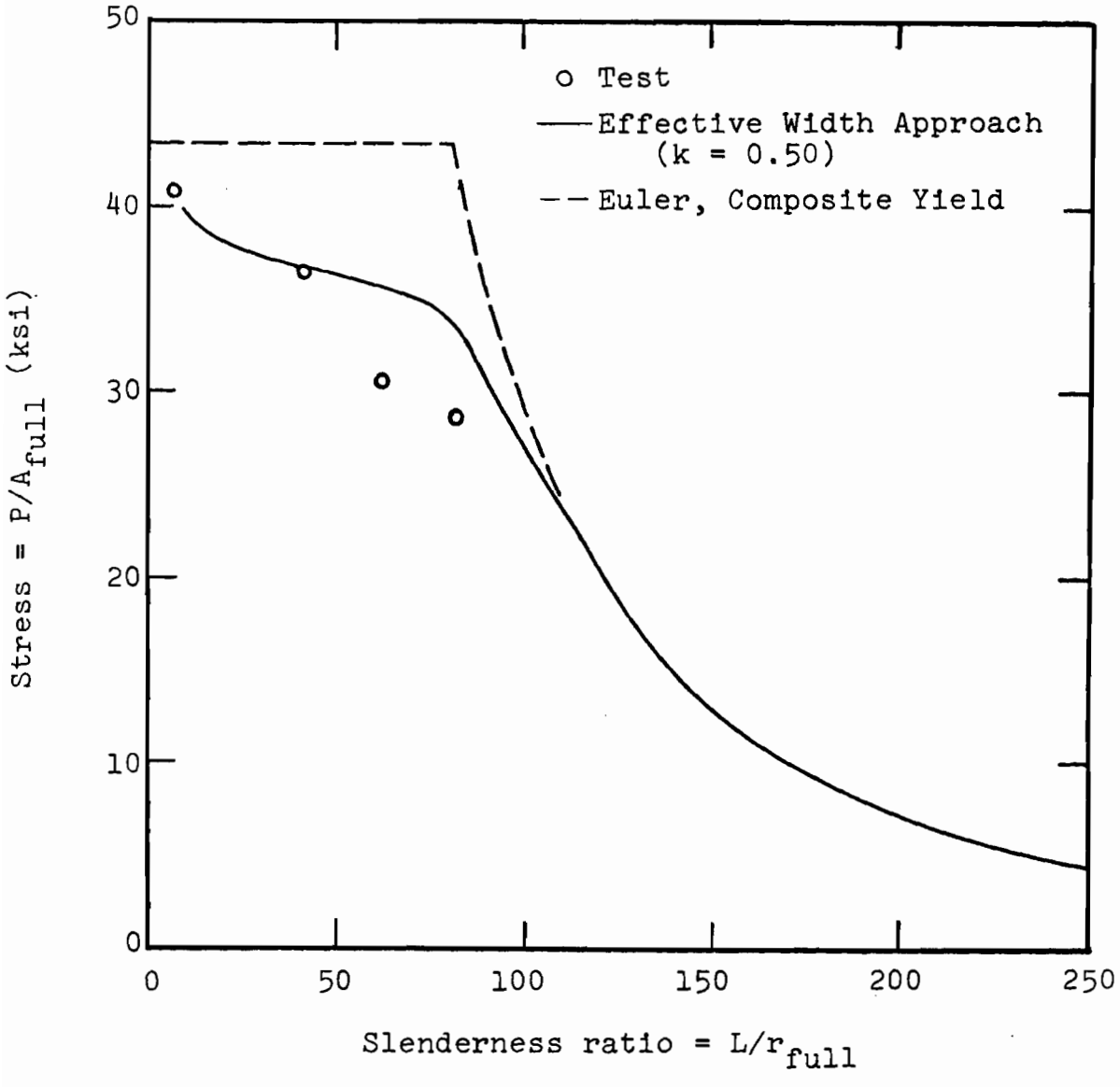

FIG. 6.43 COMPARISON OF EFFECTIVE WIDTH APPROACH AND EXPERIMENTAL RESULTS FOR SERIES UC-1 OF URIBE

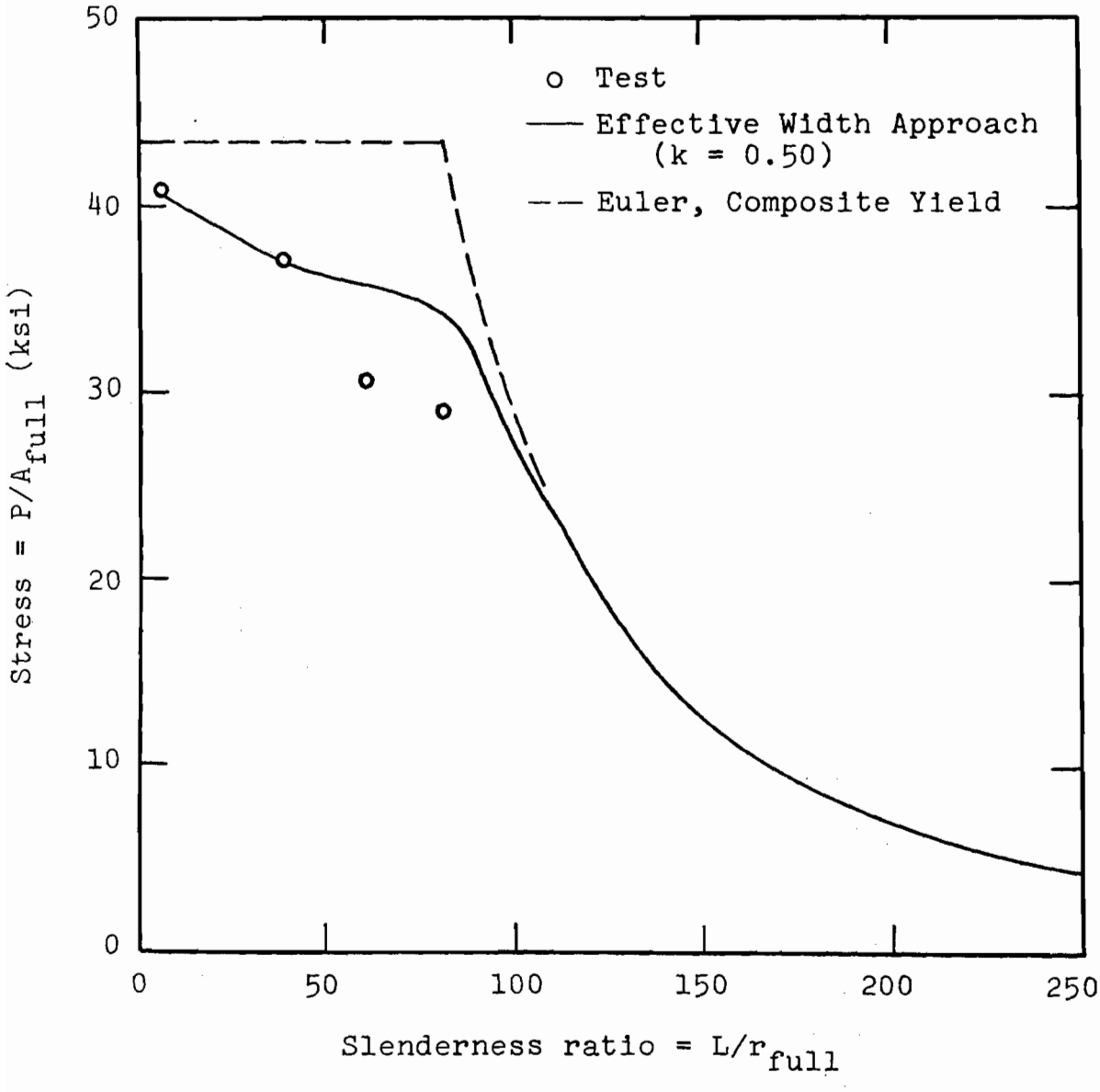

FIG. 6.44 COMPARISON OF EFFECTIVE WIDTH APPROACH AND EXPERIMENTAL RESULTS FOR SERIES UC-2 OF URIBE

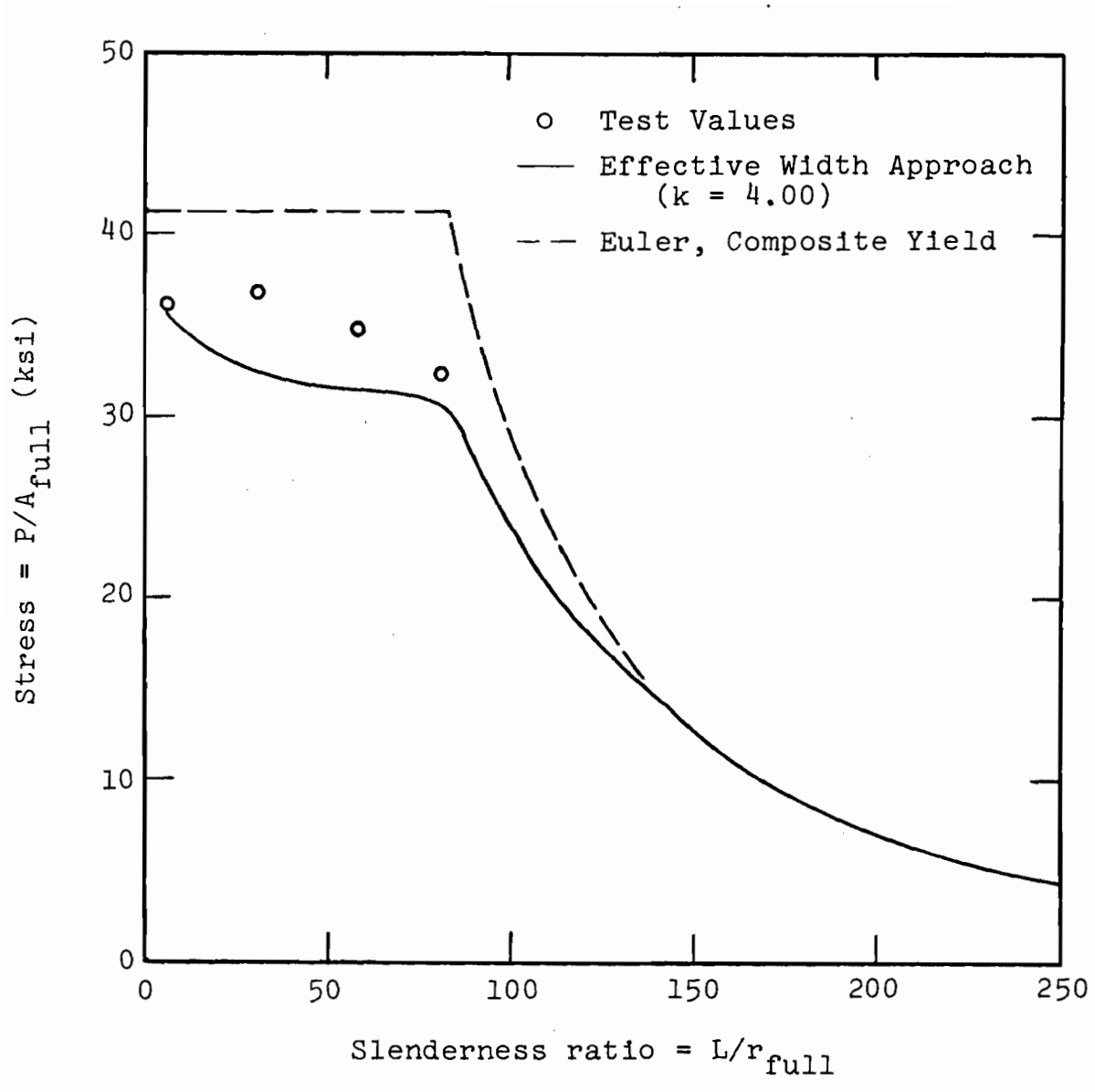

FIG. 6.45 COMPARISON OF EFFECTIVE WIDTH APPROACH AND EXPERIMENTAL RESULTS FOR SERIES SC-1 OF URIBE

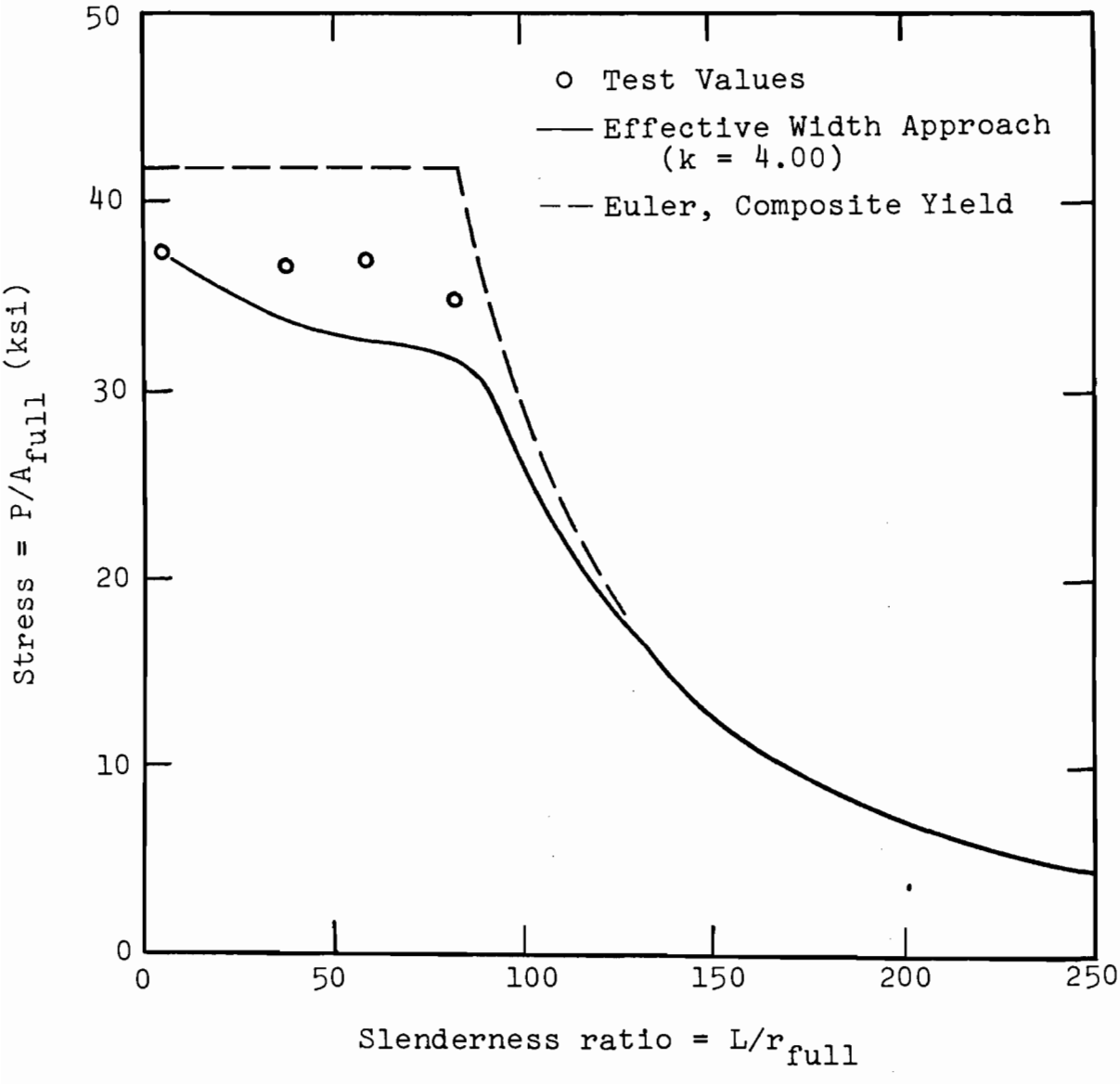

FIG. 6.46 COMPARISON OF EFFECTIVE WIDTH APPROACH AND EXPERIMENTAL RESULTS FOR SERIES SC-2 OF URIBE

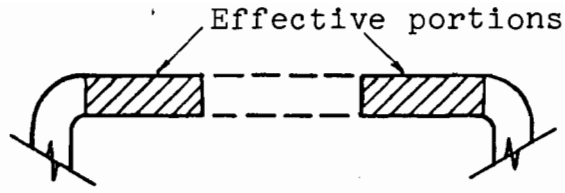

(a) Stiffened element, either parallel or perpendicular to principal axis

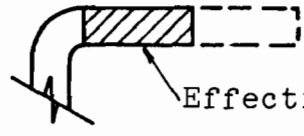

(b) Unstiffened element, parallel to principal axis

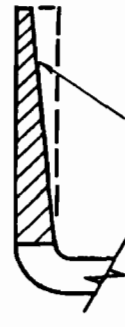

(c) Unstiffened element, perpendicular to principal axis, effective area equal or greater than half full element area

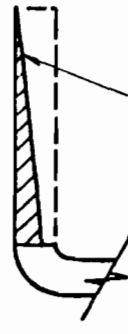

(d) Unstiffened element, perpendicular to principal axis, effective area less than half of full element area

FIG. 7.1 DISTRIBUTION OF EFFECTIVE AREAS

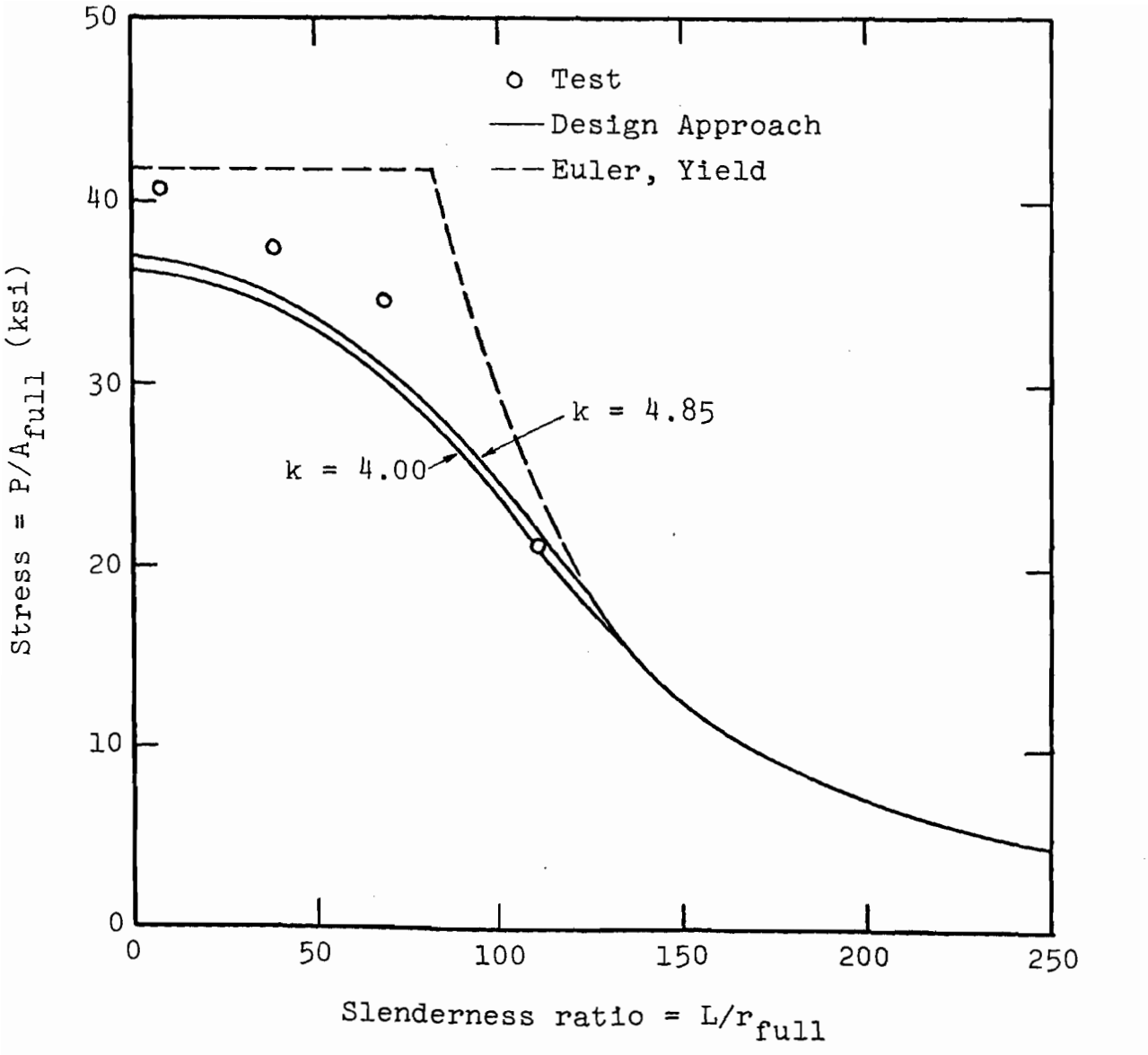

FIG. 7.2 COMPARISON OF DESIGN APPROACH AND TEST RESULTS FOR STIFFENED SECTION S-1

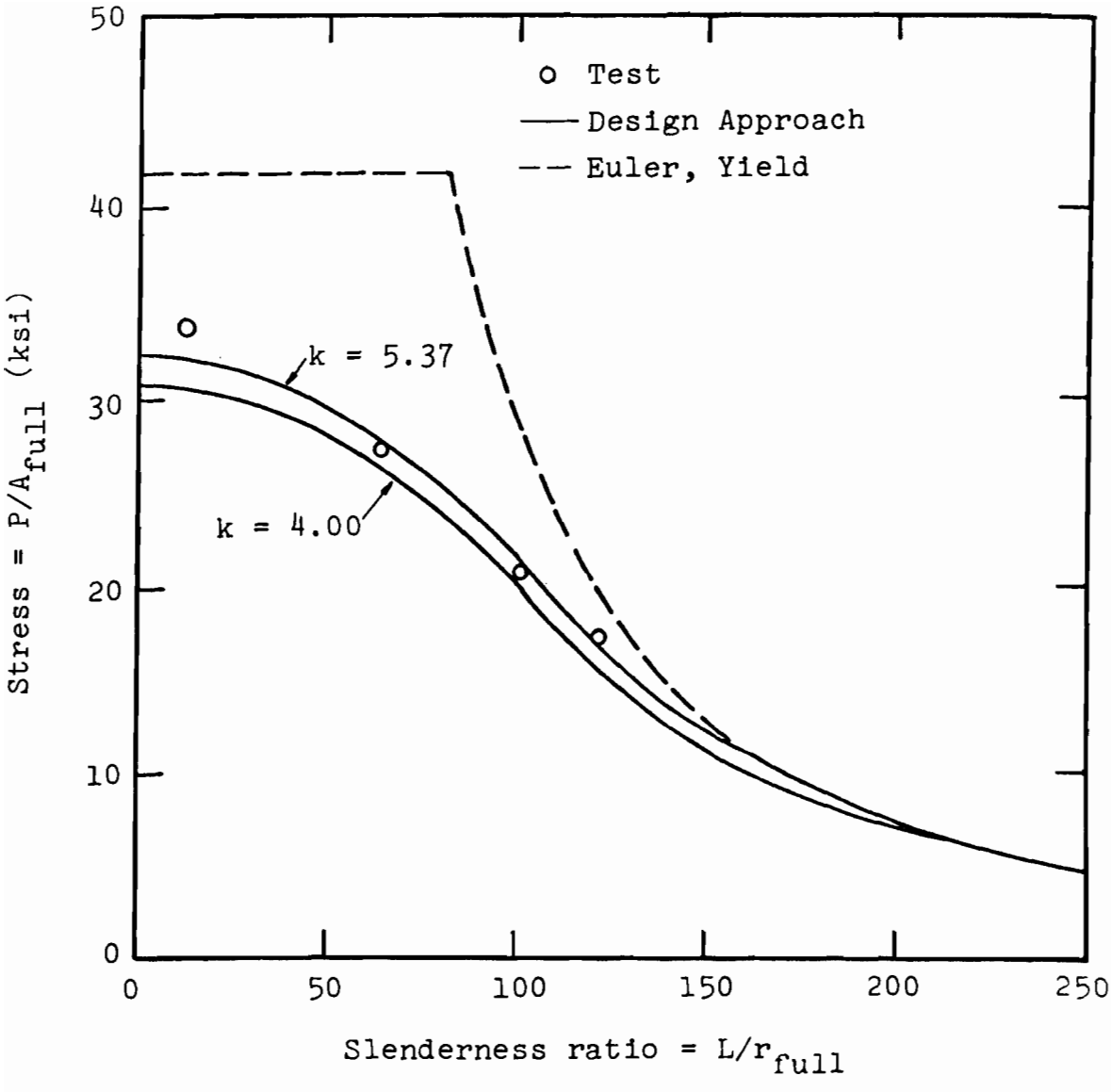

FIG. 7.3 COMPARISON OF DESIGN APPROACH AND TEST RESULTS FOR STIFFENED SECTION S-2

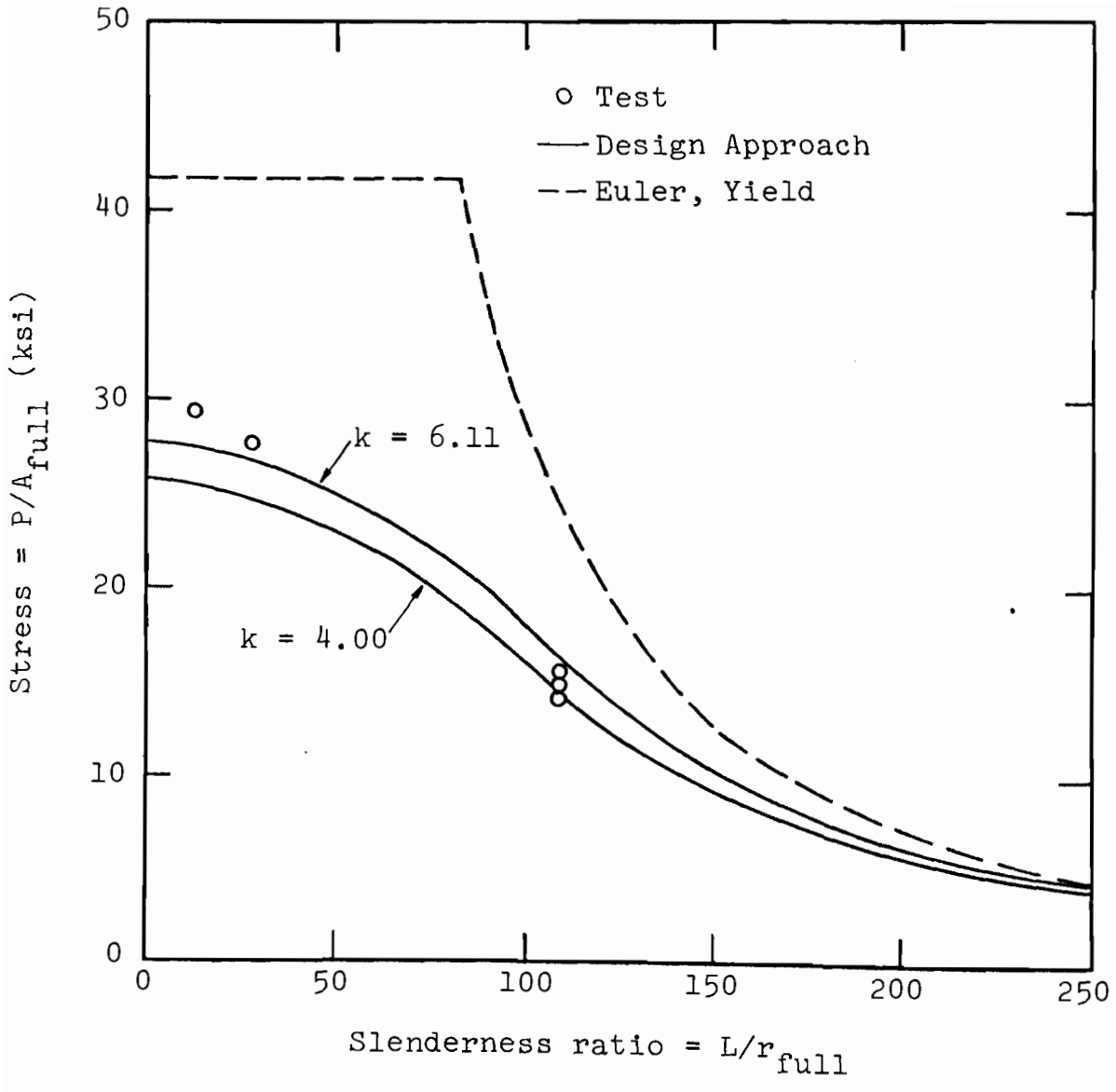

FIG. 7.4 COMPARISON OF DESIGN APPROACH AND TEST RESULTS FOR STIFFENED SECTION S-3

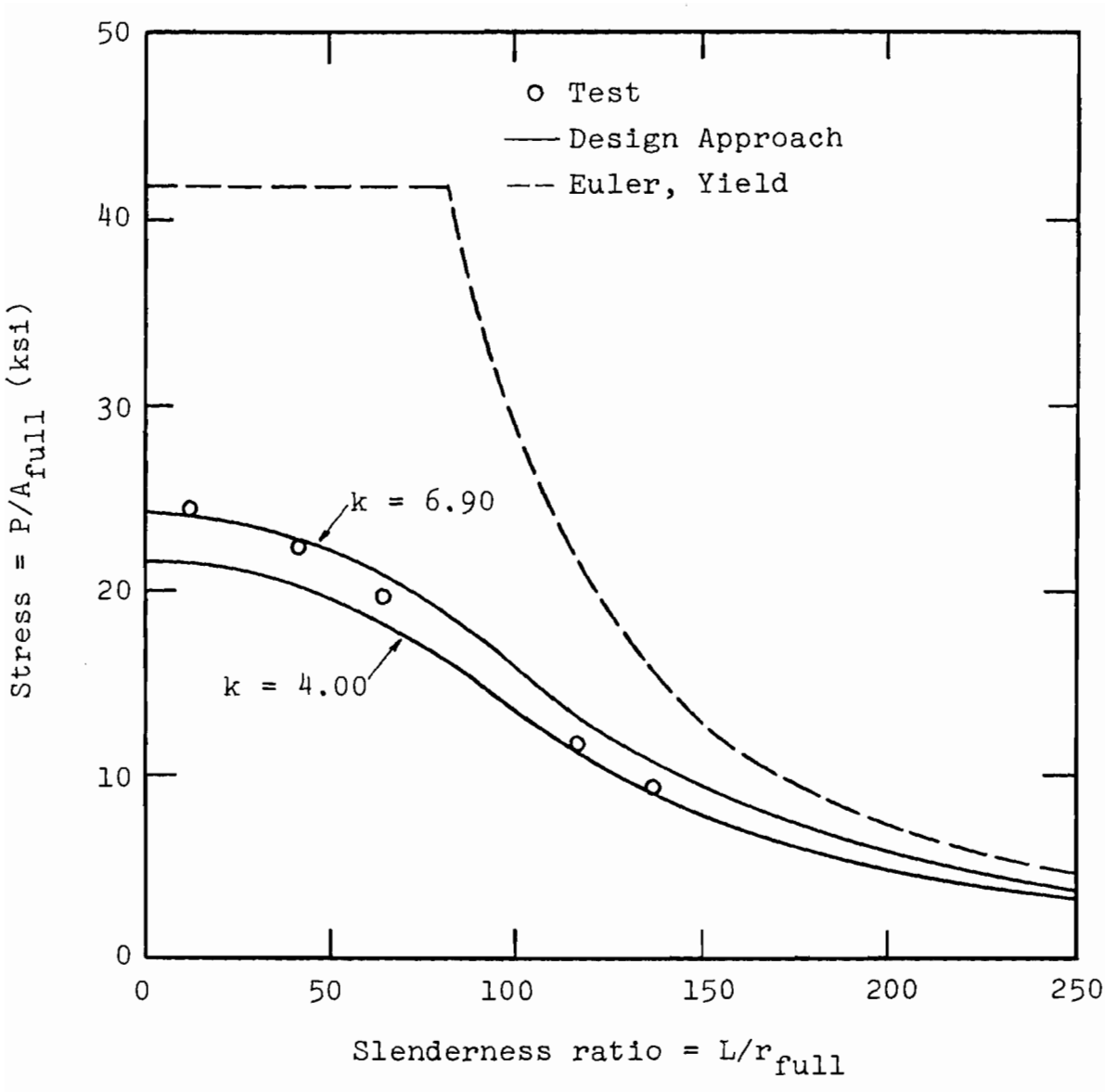

FIG. 7.5 COMPARISON OF DESIGN APPROACH AND TEST RESULTS FOR STIFFENED SECTION S-4

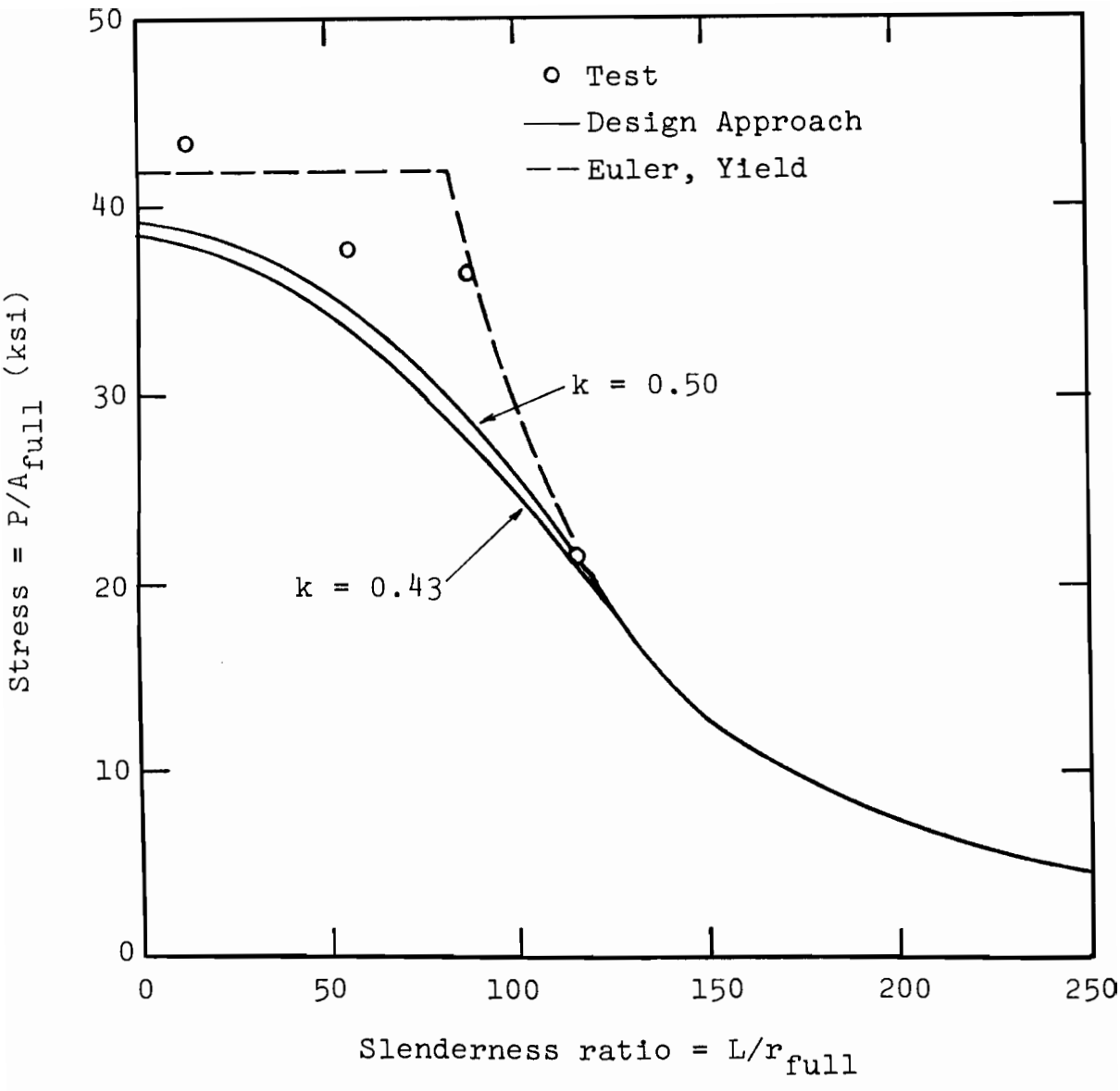

FIG. 7.6 COMPARISON OF DESIGN APPROACH AND TEST RESULTS FOR UNSTIFFENED SECTION U-1

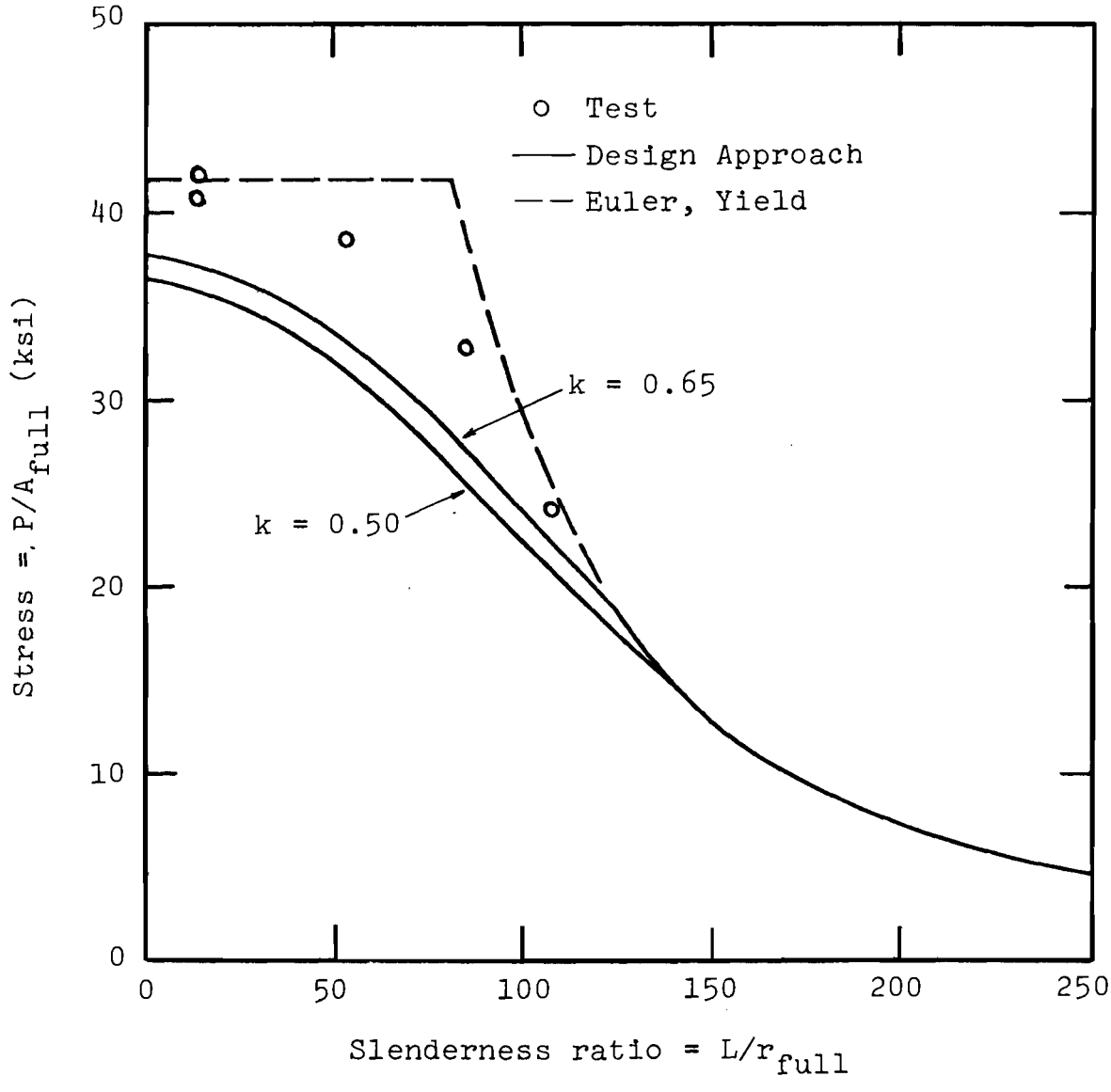

FIG. 7.7 COMPARISON OF DESIGN APPROACH AND TEST RESULTS FOR UNSTIFFENED SECTION U-2

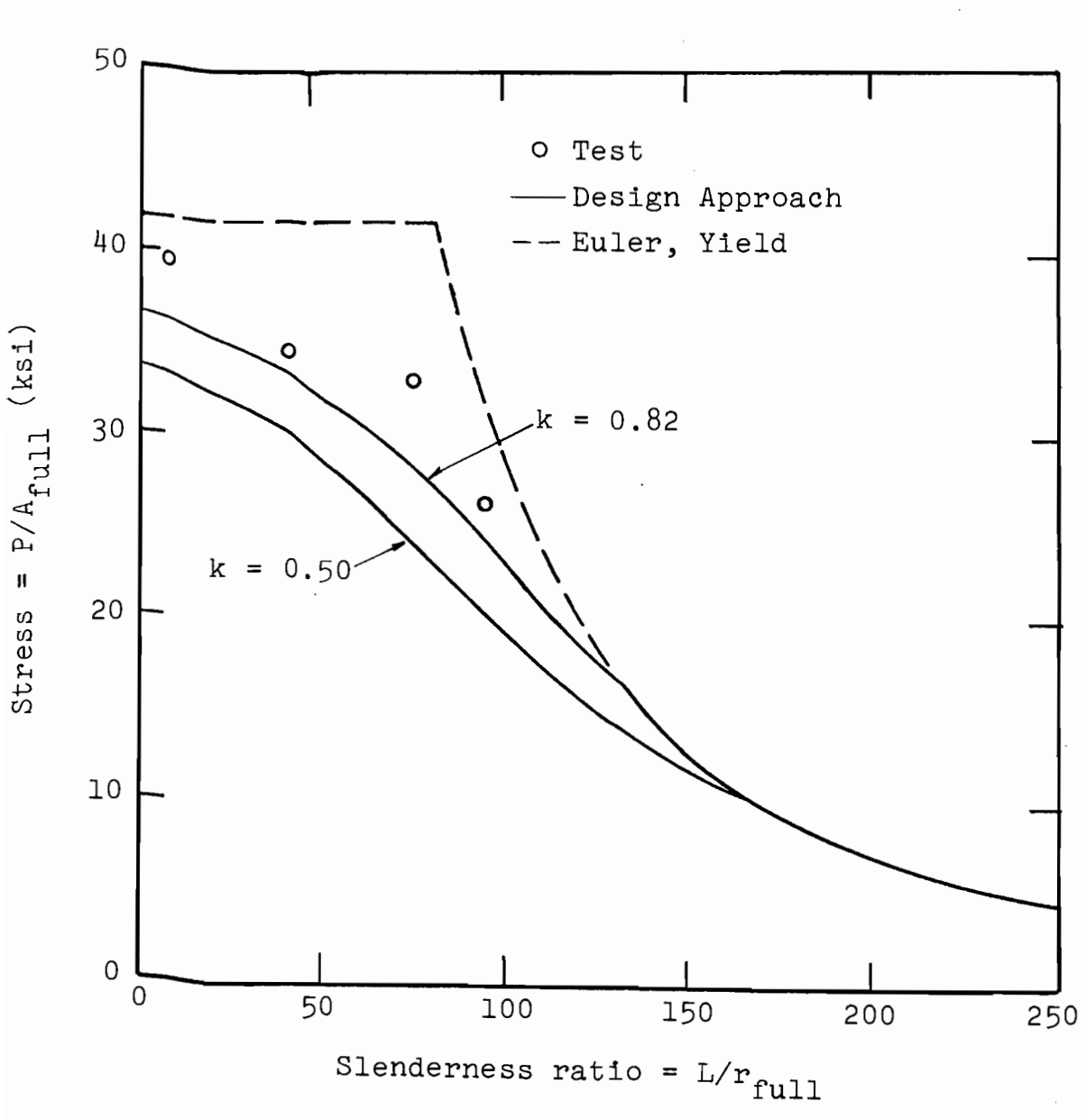

FIG. 7.8 COMPARISON OF DESIGN APPROACH AND TEST RESULTS FOR UNSTIFFENED SECTION U-3

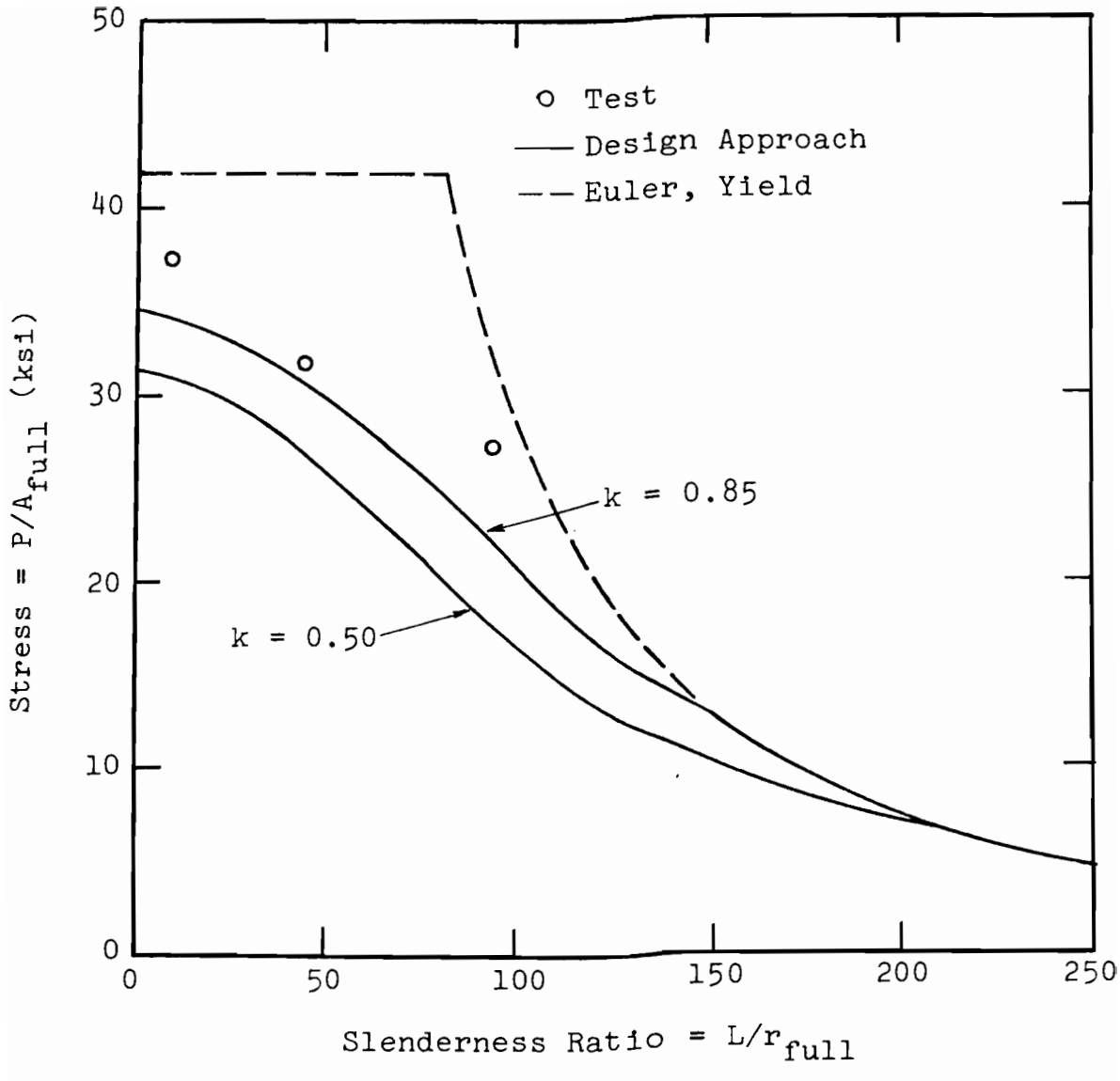

FIG. 7.9 COMPARISON OF DESIGN APPROACH AND TEST RESULTS FOR UNSTIFFENED SECTION U-4

Table 3.1

DIMENSIONS AND PROPERTIES OF SECTIONS

Specimen[a]	W (in)	D (in)	T (in)	Width-Thickness[b] Single Thickness Element	Width-Thickness Double Thickness Element	Area of Full Cross-Section (in^2)	Radius of Gyration About Weak Axis (in)	Q_{AISI}
(a) Stiffened Sections								
S-1	2.0	3.5	0.058	57.2	16.7	0.86	0.799	0.87
S-2	2.0	5.0	0.058	83.0	16.7	1.03	0.836	0.74
S-3	2.0	7.0	0.058	117.4	16.7	1.26	0.869	0.61
S-4	2.0	9.0	0.058	151.8	16.7	1.49	0.890	0.52
(b) Unstiffened Sections								
U-1	1.0	3.0	0.058	16.2	24.8	0.565	0.371	0.82
U-2	1.25	3.0	0.058	20.5	24.8	0.623	0.494	0.69
U-3	1.5	3.0	0.058	24.8	24.8	0.681	0.620	0.52
U-4	1.75	3.0	0.058	29.1	24.8	0.739	0.750	0.46

[a] Inside corner radii of all specimens were extremely small and may be considered as zero.

[b] Width based on distance to inside of adjoining element.

Table 3.2

ULTIMATE LOADS FOR STIFFENED SECTIONS

Specimen	Test Column Length (in)	Effective Length (in)	Slenderness Ratio = Eff. Length / Rad. of Gyration	Ultimate Load (kips)	Ultimate Stress = Ult. Load / Full Area (ksi)
S-1	10.5	6.8	8.5	34.6	40.5
	27.9	31.1	39.0	32.0	37.4
	52.0	55.2	69.1	29.6	34.6
	88.0	91.2	114.1	17.9	20.9
S-2	15.0	9.8	11.7	34.8	33.9
	52.0	55.2	66.0	28.0	27.2
	82.0	85.2	102.0	21.3	20.8
	99.9	103.1	123.5	17.7	17.2
S-3	18.1	11.8	13.6	37.0	29.3
	22.0	25.2	29.0	35.2	27.8
	92.0	95.2	109.8	19.6	15.5
	92.0	95.2	109.8	19.0	15.1
	92.0	95.2	109.8	18.2	14.4
S-4	18.9	12.3	13.8	36.7	24.6
	34.8	38.0	42.6	33.6	22.6
	55.0	58.2	65.5	29.3	19.6
	100.0	103.2	116.0	17.6	11.8
	119.9	123.1	138.2	13.75	9.2

Table 3.3

ULTIMATE LOADS FOR UNSTIFFENED SECTIONS

Specimen	Test Column Length (in)	Effective Length (in)	Slenderness Ratio = Eff. Length / Rad. of Gyration	Ultimate Load (kips)	Ultimate Stress = Ult. Load / Full Area (ksi)
U-1	7.4	4.8	12.9	24.7	43.8
	17.5	20.7	55.7	21.4	37.9
	19.9[a]	23.1	62.1	18.0	31.9
	29.9	33.1	89.1	20.4	36.2
	40.0	43.2	116.6	12.2	21.6
U-2	9.0	5.9	12.0	25.4	40.8
	9.0	5.9	12.0	26.1	42.0
	23.0	26.2	53.0	24.0	38.6
	39.0	42.2	85.6	20.4	32.8
	49.9	53.1	108.0	15.0	24.1
U-3	9.0	5.9	9.5	27.0	39.6
	23.0	26.2	42.2	23.6	34.6
	27.9[a]	31.1	50.1	20.6	30.2
	45.0	48.2	77.9	22.8	33.4
	55.9	59.1	95.5	18.0	26.4
U-4	9.0	5.9	7.9	27.4	37.2
	29.9	33.1	44.1	23.4	31.7
	50.0[a]	53.2	71.0	18.5	25.1
	65.9	69.1	92.4	20.1	27.2

[a]The loading was eccentric, and the results will not be included in the following Tables and Figures.

Table 4.1

COMPARISON OF Q VALUES AS DETERMINED

BY AISI SPECIFICATION AND TESTS

Specimen	$\frac{\text{Width}}{\text{Thickness}}$	Q_{AISI}	Q_{TEST}
(a) Stiffened Sections			
S-1	57.2	0.87	0.97
S-2	83.0	0.74	0.81
S-3	117.4	0.61	0.70
S-4	151.8	0.52	0.59
(b) Unstiffened Sections			
U-1	16.2	0.82	1.05
U-2	20.5	0.69	0.99[a]
U-3	24.8	0.52	0.95
U-4	29.1	0.46	0.89

[a]Based on average of two stub column tests.

Table 4.2

COMPARISON OF AISI SPECIFICATION ULTIMATE STRESSES AND TEST ULTIMATE STRESSES FOR STIFFENED SECTIONS

Specimen	Slenderness Ratio[a]	Test Ultimate Stress (ksi)[a]	AISI Ultimate Stress with Q_{AISI} (ksi)[a]	% Discrepancy from Test	AISI Ultimate Stress with Q_{TEST} (ksi)[a]	% Discrepancy from Test
S-1	8.5	40.5	36.3	10.4	40.5	0.0
	39.0	37.4	34.7	7.2	38.4	-2.7
	69.1	34.6	30.9	10.7	33.8	2.3
	114.1	20.9	21.4	-2.4[b]	22.1	-5.7
S-2	11.7	33.9	30.9	8.9	33.9	0.0
	66.0	27.2	27.4	-0.7	29.6	-8.8
	102.0	20.8	22.4	-7.7	23.6	-13.5
	123.5	17.2	18.4	-7.0	18.8	-9.3
S-3	13.6	29.3	25.6	12.6	29.3	0.0
	29.0	27.8	25.2	9.4	28.7	-3.2
	109.8	15.5	18.9	-22.0	20.4	-31.6
	109.8	15.1	18.9	-25.2	20.4	-35.1
	109.8	14.4	18.9	-31.2	20.4	-41.6
S-4	13.8	24.6	21.8	11.4	24.6	0.0
	42.6	22.6	21.2	6.2	23.7	-4.9
	65.5	19.6	20.1	-2.5	22.4	-14.3
	116.0	11.8	16.4	-39.0	17.6	-49.1
	138.2	9.2	14.0	-52.2	14.7	-59.8

[a]Slenderness ratios and stresses based on full section properties.

[b]Negative sign indicates predicted value above test value.

Table 4.3

COMPARISON OF AISI SPECIFICATION ULTIMATE STRESSES AND TEST ULTIMATE STRESSES FOR UNSTIFFENED SECTIONS

Specimen	Slenderness[a] Ratio	Test Ultimate[a] Stress (ksi)	AISI Ultimate[a] Stress with Q_{AISI} (ksi)	% Discrepancy from Test	AISI Ultimate[a] Stress with Q_{TEST} (ksi)	% Discrepancy from Test
U-1	12.9	43.8	34.0	22.4	41.6[c]	5.0
	55.7	37.9	31.1	18.0	37.2	1.8
	89.1	36.2	26.2	27.6	29.9	17.4
	116.6	21.6	20.5	5.1	20.5	5.1
U-2	12.0	42.0	28.9	31.2	41.3	1.7
	12.0	40.8	28.9	29.2	41.3	-1.2[b]
	53.0	38.6	27.0	30.0	37.4	3.1
	85.6	32.8	23.7	27.8	30.7	6.4
	108.0	24.1	20.6	14.5	24.3	-0.8
U-3	9.5	39.6	21.6	45.5	39.6	0.0
	42.2	34.6	20.9	39.6	37.4	-8.1
	77.9	33.4	19.2	42.5	31.6	5.4
	95.5	26.4	17.9	32.2	27.4	-3.8
U-4	7.9	37.2	19.4	47.9	37.2	0.0
	44.1	31.7	18.8	40.7	34.9	-10.1
	92.4	27.2	16.6	39.0	27.1	0.4

[a]Slenderness ratios and stresses based on full section properties.

[b]Negative sign indicates predicted value above test value.

[c]Use $Q_{TEST} = 1.00$.

Table 5.1

EFFECTIVE WIDTHS DETERMINED IN RIGOROUS ANALYTICAL APPROACH FOR SQUARE TUBE EXAMPLE

Strain (in/in)	Slenderness[a] Ratio	Average Stress[a] (ksi)	Effective Width (in)
0.0001	314.2	2.95	15.0[b]
0.0002	222.1	5.90	15.0
0.0003	181.4	8.84	15.0
0.0004	157.1	11.80	15.0
0.0005	140.5	14.73	15.0
0.0006	128.3	17.68	15.0
0.0007	118.7	20.60	15.0
0.0008	111.1	23.60	15.0
0.0009	104.7	26.55	15.0
0.0010	99.3	29.5	15.0
0.0011	94.1	31.55	14.16
0.0012	89.3	32.70	12.92
0.0013	85.3	33.95	11.96
0.0014	81.9	35.05	11.11
0.0015	79.0	35.95	10.31
0.0016	78.3	36.40	10.19
0.0017	78.0	36.60	10.06
0.0018	77.9	36.65[c]	9.92

[a]Slenderness ratios and areas are based on full section properties.

[b]Element width is 15.0 in.; local buckling stress is 30.8 ksi.

[c]Maximum load, beyond which load decreases.

Table 5.2

EFFECTIVE WIDTHS DETERMINED IN RIGOROUS ANALYTICAL APPROACH FOR RECTANGULAR TUBE EXAMPLE

Strain (in/in)	Slenderness[a] Ratio	Average[a] Stress (ksi)	Effective Width, Widest Element (in)	Effective Width, Narrowest Element (in)
0.0001	314.2	2.95	15.0[b]	7.5[b]
0.0002	222.1	5.90	15.0	7.5
0.0003	181.4	8.84	15.0	7.5
0.0004	157.1	11.80	15.0	7.5
0.0005	140.5	14.73	15.0	7.5
0.0006	128.3	17.68	15.0	7.5
0.0007	118.7	20.60	15.0	7.5
0.0008	111.1	23.60	15.0	7.5
0.0009	104.7	26.55	15.0	7.5
0.0010	99.3	29.50	15.0	7.5
0.0011	93.9	31.80	14.34	7.41
0.0012	88.8	33.55	13.39	7.28
0.0013	84.4	35.30	12.61	7.18
0.0014	80.5	37.00	11.88	7.09
0.0015	77.2	38.60	11.24	7.05
0.0016	74.5	39.90	10.70	7.08
0.0017	72.6	41.00	10.30	7.13[d]
0.0018	72.3	41.60	10.32	7.32[d]
0.0019	71.6	41.65[c]	10.02	7.47[d]

[a]Slenderness ratios and areas are based on full section properties.

[b]Element widths are 15.0 in. and 7.5 in.; local buckling stress is 30.7 ksi.

[c]Maximum load, beyond which load decreases.

[d]Error due to effects of plasticity; negligible effect on analytical column loads.

Table 5.3

COMPARISON OF RIGOROUS ANALYTICAL APPROACH ULTIMATE STRESSES AND TEST ULTIMATE STRESSES FOR STIFFENED SECTIONS

Specimen	Slenderness Ratio[a]	Test Ultimate Stress (ksi)[a]	Analytical Ultimate Stress (ksi)[a]	% Discrepancy From Test
S-1[b]	8.5	40.5	41.9	-3.5[c]
	39.0	37.4	41.9	-12.0
	69.1	34.6	41.9	-20.5
	114.1	20.9	22.3	-6.7
S-2	11.7	33.9	35.9	-5.9
	66.0	27.2	35.9	-32.0
	102.0	20.8	26.7	-28.4
	123.5	17.2	19.1	-11.0
S-3	13.6	29.3	31.8	-8.5
	29.0	27.8	31.8	-14.4
	109.8	15.5	19.1	-23.2
	109.8	15.1	19.1	-26.7
	109.8	14.4	19.1	-32.6
S-4	13.8	24.6	30.8	-25.2
	42.6	22.6	30.8	-36.3
	65.5	19.6	30.8	-57.1
	116.0	11.8	15.0	-27.1
	138.2	9.2	11.8	-28.3

[a]Slenderness ratios and stresses based on full section properties.

[b]Fully effective at all loads.

[c]Negative sign indicates predicted value above test value.

Table 5.4

EFFECTIVE WIDTHS DETERMINED IN RIGOROUS

ANALYTICAL APPROACH FOR SECTION S-2

Strain (in/in)	Slenderness[a] Ratio	Average Stress[a] (ksi)	Effective Width of Widest Element (in)
0.00014	265.5	4.13	4.94[b]
0.00026	194.8	7.67	4.94
0.00038	161.2	11.21	4.94
0.00050	140.5	14.75	4.94
0.00062	126.2	18.29	4.94
0.00074	115.5	21.83	4.94
0.00086	106.9	25.29	4.89
0.00098	98.8	27.83	4.51
0.00110	92.7	30.30	4.26
0.00122	87.7	32.50	4.03
0.00134	83.8	34.41	3.84
0.00146	81.4	35.88[c]	3.68

[a]Slenderness ratios and areas are based on full section properties.

[b]Element width is 4.94 in.; local buckling stress is 24.65 ksi.

[c]Maximum load, beyond which load decreases.

Table 5.5

EFFECTIVE WIDTHS DETERMINED IN RIGOROUS

ANALYTICAL APPROACH FOR SECTION S-3

Strain (in/in)	Slenderness[a] Ratio	Average Stress[a] (ksi)	Effective Width of Widest Element (in)
0.00014	265.5	4.13	6.94[b]
0.00026	194.8	7.67	6.94
0.00038	161.2	11.25	6.94
0.00050	138.5	14.16	6.36
0.00062	122.0	16.56	5.66
0.00074	110.2	18.97	5.20
0.00086	101.4	21.36	4.90
0.00098	94.9	23.74	4.72
0.00110	89.7	26.06	4.61
0.00122	85.2	28.28	4.48
0.00134	81.7	30.31	4.40
0.00146	80.1	31.78[c]	4.37

[a]Slenderness ratios and areas are based on full section properties.

[b]Element width is 6.94 in.; local buckling stress is 12.64 ksi.

[c]Maximum load, beyond which load decreases.

Table 5.6

EFFECTIVE WIDTHS DETERMINED IN RIGOROUS

ANALYTICAL APPROACH FOR SECTION S-4

Strain (in/in)	Slenderness[a] Ratio	Average Stress[a] (ksi)	Effective Width of Widest Element (in)
0.0001	314.2	2.99	8.94[b]
0.0003	179.1	8.52	8.26
0.0005	133.3	12.36	6.40
0.0007	110.5	16.20	5.63
0.0009	96.4	20.05	5.22
0.0011	87.2	23.87	5.05
0.0013	81.1	27.58	5.04
0.0015	76.9	30.84[c]	5.02

[a]Slenderness ratios and areas are based on full section properties.

[b]Element width is 8.94 in.; local buckling stress is 7.68 ksi.

[c]Maximum load, beyond which load decreases.

Table 5.7

COMPARISON OF EFFECTIVE WIDTHS AS DETERMINED BY RIGOROUS ANALYTICAL AND BY EMPIRICAL EFFECTIVE WIDTH EXPRESSION

Specimen	$\frac{L}{r}$[a]	b from Eq. 5-45 (in)	b from Eq. 6-7 with k=4.00 (in)	% Discrepancy from b using Eq. 5-45	b from Eq. 6-7 with k from Table 6.1 (in)	% Discrepancy from b using Eq. 5-45	b from Eq. 6-7 with k=6.97 (in)	% Discrepancy from b using Eq. 5-45
S-1	8.5	3.38	2.37	29.8	2.57	24.0	2.88	14.8
w = 3.38	39.0	3.38	2.39	29.3	2.59	23.4	2.91	13.9
$\frac{w}{t}$ = 57.2	69.1	3.38	2.43	28.1	2.63	22.2	2.96	12.4
	114.1	3.38	2.99	11.6	3.18	5.9	3.38	0.0
S-2	11.7	3.62[b]	2.55	29.6	2.88	20.4	3.19	11.9
w = 4.88	66.0	3.62[b]	2.62	27.6	2.96	18.2	3.27	9.7
$\frac{w}{t}$ = 83.0	102.0	4.59	3.14	31.6	3.48	24.2	3.80	17.2
	123.5	4.88	3.58	26.6	3.96	18.9	4.28	12.3
S-3	13.6	4.31[b]	2.66	15.0	3.22	25.2	3.40	21.1
w = 6.88	29.0	4.31[b]	2.68	14.6	3.24	24.8	3.42	20.6
$\frac{w}{t}$ = 117.4	109.8	5.13	3.60	29.8	4.23	17.5	4.46	13.1
S-4	13.8	4.96[b]	2.73	44.9	3.48	29.8	3.50	29.4
w = 8.88	42.6	4.96[b]	2.76	44.3	3.54	28.6	3.55	28.4
$\frac{w}{t}$ = 151.8	65.5	4.96[b]	2.81	43.3	3.59	27.6	3.60	27.4
	116.0	5.80	3.96	49.0	4.89	15.7	4.73	18.5
	138.2	6.54	4.54	30.6	5.57	14.8	5.61	14.2

[a]Slenderness ratios and areas are based on full section properties.

[b]Value at maximum load.

Table 6.1

DETERMINATION OF k VALUES FROM STUB COLUMN TESTS

Column	Strain at Local Buckling (in/in)	Stress at Local Buckling (ksi)	Value of k from Eq. 6-6
U-1	a	a	0.50[a]
U-2	b	40.3[b]	0.64
U-3	0.001205	35.6	0.82
U-4	0.000913	26.9	0.85
S-1	0.001340	39.5	4.85
S-2	0.000705	20.8	5.37
S-3	0.000308	9.1	6.11[c]
S-4	0.000270	8.0	6.90

[a]No local buckling was observed in the tests. The value of k chosen is based on the k values from the other unstiffened tests as discussed in Section 6.3.3.

[b]It was not possible to obtain the exact strain at local buckling from the tests; the stress was assumed as discussed in Section 6.3.3.

[c]This value is based not on the stub column but on the column with length equal to 22.0 in. as is discussed in Section 6.3.3.

Table 6.2

COMPARISON OF Q VALUES AS DETERMINED BY STUB COLUMN TESTS AND EFFECTIVE WIDTH APPROACH[a]

Specimen	$\frac{\text{Width}}{\text{Thickness}}$	$P_{ult,test}$ (kips)	Q_{TEST}	b from Eq. 6-7	$Q_{eff.width}$	Calculated $P_{ult} = A_{full} \times 41.9 \times Q_{eff.width}$ (kips)	$\frac{P_{ult,test}}{P_{ult,calc}}$
			(a) Stiffened Sections				
S-1	57.2	34.6	0.97	2.55	0.89	32.0	1.08
S-2	83.0	34.8	0.81	2.88	0.78	33.6	1.04
S-3	117.4	37.0	0.70	3.22	0.66	34.8	1.06
S-4	151.8	36.7	0.59	3.49	0.58	36.2	1.01
			(b) Unstiffened Sections				
U-1	16.2	24.7	1.05	0.79	0.94	22.2	1.11
U-2	20.5	25.8[b]	0.99[b]	0.93	0.90	23.5	1.10
U-3	24.8	27.0	0.95	1.06	0.87	24.8	1.09
U-4	29.1	27.4	0.89	1.12	0.82	25.4	1.08

[a]With k from Table 6.1.

[b]Based on average of two stub column tests.

Table 6.3

EFFECTIVE WIDTH APPROACH BASED ON EFFECTIVE MOMENT OF INERTIA

AS SHOWN IN FIG. 6.1 FOR SECTION S-1

Strain	k = 4.00			k = 4.97			k = 6.97		
	$\frac{L}{r}$[a]	σ_{Avg}[a] (ksi)	b from Eq. 6-7 (in)	$\frac{L}{r}$[a]	σ_{Avg}[a] (ksi)	b from Eq. 6-7 (in)	$\frac{L}{r}$[a]	σ_{Avg}[a] (ksi)	b from Eq. 6-7 (in)
0.0001	314.2	2.95	3.38[b]	314.2	2.95	3.38[b]	314.2	2.95	3.38[b]
0.0002	222.1	5.90	3.38	222.1	5.90	3.38	222.1	5.90	3.38
0.0003	181.4	8.85	3.38	181.4	8.85	3.38	181.4	8.85	3.38
0.0004	157.1	11.80	3.38	157.1	11.80	3.38	157.1	11.80	3.38
0.0005	140.3	14.69	3.35	140.5	14.75	3.38	140.5	14.75	3.38
0.0006	127.3	17.23	3.18	128.3	17.70	3.38	128.3	17.70	3.38
0.0007	117.1	19.69	3.04	118.1	20.26	3.24	118.8	20.65	3.38
0.0008	108.9	22.09	2.91	109.9	22.75	3.12	111.1	23.60	3.38
0.0009	102.1	24.44	2.80	103.1	25.19	3.00	104.5	26.33	3.32
0.0010	96.4	26.75	2.69	97.4	27.59	2.90	98.7	28.87	3.22
0.0011	91.5	29.03	2.60	92.5	29.94	2.81	93.8	31.37	3.13
0.0012	87.2	31.28	2.52	88.2	32.26	2.73	89.5	33.82	3.05
0.0013	81.7	33.48	2.45	82.6	34.54	2.65	83.9	36.23	2.98
0.0014	48.2	34.96	2.40	48.7	36.06	2.60	49.5	37.84	2.93
0.0015	30.4	35.44	2.39	30.7	36.56	2.59	31.2	38.36	2.91

[a] Slenderness ratio and average stress are based on full section properties.

[b] Element width w is 3.38 in.

Table 6.4

EFFECTIVE WIDTH APPROACH BASED ON EFFECTIVE MOMENT OF INERTIA

AS SHOWN IN FIG. 6.1 FOR SECTION S-2

Strain	k = 4.00			k = 5.37			k = 6.97		
	$\frac{L}{r}$[a]	σ_{Avg}[a] (ksi)	b from Eq. 6-7 (in)	$\frac{L}{r}$[a]	σ_{Avg}[a] (ksi)	b from Eq. 6-7 (in)	$\frac{L}{r}$[a]	σ_{Avg}[a] (ksi)	b from Eq. 6-7 (in)
0.0001	314.2	2.95	4.88[b]	314.2	2.95	4.88[b]	314.2	2.95	4.88[b]
0.0002	222.1	5.90	4.88	222.1	5.90	4.88	222.1	5.90	4.88
0.0003	179.8	8.51	4.54	181.4	8.85	4.88	181.4	8.85	4.88
0.0004	154.0	10.82	4.14	155.8	11.36	4.55	157.1	11.80	4.88
0.0005	136.4	13.01	3.84	138.1	13.69	4.24	139.5	14.28	4.60
0.0006	123.5	15.12	3.58	125.1	15.92	3.99	126.5	16.64	4.35
0.0007	113.4	17.16	3.38	115.1	18.08	3.78	116.4	18.92	4.14
0.0008	105.4	19.16	3.21	107.0	20.18	3.60	108.3	21.13	3.95
0.0009	98.8	21.11	3.07	100.3	22.24	3.44	101.5	23.29	3.79
0.0010	93.2	23.03	2.94	94.6	24.25	3.30	95.8	25.40	3.65
0.0011	88.4	24.93	2.83	89.8	26.23	3.18	91.0	27.47	3.52
0.0012	84.2	26.79	2.73	85.6	28.19	3.07	86.7	29.51	3.41
0.0013	78.8	28.62	2.64	80.1	30.10	2.98	81.2	31.50	3.30
0.0014	46.5	29.85	2.58	47.2	31.38	2.92	47.9	32.84	3.24
0.0015	29.3	30.25	2.56	29.8	31.80	2.90	30.2	33.28	3.22

[a] Slenderness ratio and average stress are based on full section properties.

[b] Element width w is 4.88 in.

Table 6.5

EFFECTIVE WIDTH APPROACH BASED ON EFFECTIVE MOMENT OF INERTIA

AS SHOWN IN FIG. 6.1 FOR SECTION S-3

Strain	k = 4.00			k = 6.11			k = 6.97		
	$\frac{L}{r}$[a]	σ_{Avg}[a] (ksi)	b from Eq. 6-7 (in)	$\frac{L}{r}$[a]	σ_{Avg}[a] (ksi)	b from Eq. 6-7 (in)	$\frac{L}{r}$[a]	σ_{Avg}[a] (ksi)	b from Eq. 6-7 (in)
0.0001	314.2	2.95	6.88[b]	314.2	2.95	6.88[b]	314.2	2.95	6.88[b]
0.0002	218.4	5.34	5.85	221.5	5.79	6.63	222.1	5.90	6.88
0.0003	175.4	7.38	5.07	178.4	8.05	5.90	179.2	8.25	6.15
0.0004	149.9	9.26	4.54	152.8	10.13	5.34	153.6	10.39	5.59
0.0005	132.6	11.05	4.15	135.4	12.08	4.92	136.1	12.41	5.16
0.0006	119.9	12.77	3.85	122.5	13.96	4.58	123.3	14.33	4.81
0.0007	110.1	14.44	3.61	112.6	15.77	4.31	113.3	16.19	4.53
0.0008	102.3	16.06	3.41	104.6	17.52	4.08	105.3	17.99	4.30
0.0009	95.8	17.66	3.24	98.1	19.24	3.89	98.7	19.75	4.10
0.0010	90.3	19.22	3.10	92.5	20.92	3.72	93.1	21.47	3.93
0.0011	85.6	20.77	2.98	87.7	22.58	3.58	88.3	23.17	3.77
0.0012	81.6	22.29	2.86	83.6	24.21	3.44	84.2	24.83	3.64
0.0013	76.4	23.78	2.76	78.3	25.80	3.33	78.8	26.46	3.52
0.0014	45.0	24.78	2.70	46.1	26.87	3.26	46.5	27.55	3.44
0.0015	28.4	25.11	2.68	29.1	27.22	3.24	29.3	27.90	3.42

[a]Slenderness ratio and average stress are based on full section properties.

[b]Element width w is 6.88 in.

Table 6.6

EFFECTIVE WIDTH APPROACH BASED ON EFFECTIVE MOMENT OF INERTIA

AS SHOWN IN FIG. 6.1 FOR SECTION S-4

Strain	k = 4.00			k = 6.90			k = 6.97		
	$\frac{L}{r}$[a]	σ_{Avg}[a] (ksi)	b from Eq. 6-7 (in)	$\frac{L}{r}$[a]	σ_{Avg}[a] (ksi)	b from Eq. 6-7 (in)	$\frac{L}{r}$[a]	σ_{Avg}[a] (ksi)	b from Eq. 6-7 (in)
0.0001	311.2	2.75	8.02[b]	314.2	2.95	8.88[b]	314.2	2.95	8.88[b]
0.0002	214.7	4.71	6.29	219.0	5.33	7.65	219.1	5.35	7.67
0.0003	172.2	6.43	5.36	176.3	7.30	6.63	176.4	7.32	6.66
0.0004	147.1	8.02	4.76	150.9	9.11	5.94	151.0	9.13	5.97
0.0005	130.1	9.53	4.33	133.6	10.80	5.44	133.1	10.83	5.46
0.0006	117.6	10.98	4.00	120.9	12.43	5.05	121.0	12.45	5.07
0.0007	107.9	12.39	3.74	111.1	13.99	4.73	117.2	14.02	4.75
0.0008	100.2	13.77	3.52	103.2	15.51	4.47	103.3	15.55	4.49
0.0009	93.8	15.11	3.34	96.7	16.99	4.25	96.8	17.03	4.27
0.0010	88.4	16.44	3.19	91.2	18.44	4.06	91.3	18.48	4.08
0.0011	83.8	17.74	3.05	86.5	19.87	3.89	86.6	19.91	3.91
0.0012	79.8	19.02	2.93	82.4	21.27	3.75	82.5	21.32	3.76
0.0013	74.7	20.28	2.83	77.2	22.64	3.62	77.2	22.69	3.63
0.0014	44.0	21.13	2.76	45.5	23.56	3.54	45.5	23.61	3.55
0.0015	27.8	21.41	2.74	28.7	23.86	3.51	28.7	23.91	3.53

[a]Slenderness ratio and average stress are based on full section properties.

[b]Element width w is 8.88 in.

Table 6.7

COMPARISON OF TEST ULTIMATE STRESSES AND EFFECTIVE WIDTH

APPROACH ULTIMATE STRESSES FOR STIFFENED SECTIONS

Specimen	$\frac{L}{r}$[a]	Test[a] σ_{Avg} (ksi)	Based on I_{full}		Based on I_{eff}		k
			σ_{Avg}[a] (ksi)	% Discrepancy from Test	σ_{Avg}[a] (ksi)	% Discrepancy from Test	
S-1	8.5	40.5	37.7	6.9	37.7	6.9	4.85
	39.0	37.4	36.3	2.9	36.3	2.9	
	69.1	34.6	36.0	-4.0[b]	35.9	-3.8[b]	
	114.1	20.9	22.5	-7.6	21.5	-2.9	
S-2	11.7	33.9	32.6	3.8	32.5	4.1	5.37
	66.0	27.2	31.2	-14.6	31.0	-14.0	
	102.0	20.8	28.0	-34.6	21.5	-3.4	
	123.5	17.2	19.5	-13.4	16.3	5.2	
S-3	13.6	29.3	27.9	4.8	27.7	5.5	6.11
	29.0	27.8	27.4	1.4	27.2	2.2	
	109.8	15.5	24.2	-56.0	16.2	-4.5	
	109.8	15.1	24.2	-60.2	16.2	-7.3	
	109.8	14.4	24.2	-68.0	16.2	-12.5	
S-4	13.8	24.6	24.5	0.4	24.3	1.2	6.90
	42.6	22.6	23.9	-5.8	23.6	-4.4	
	65.5	19.6	23.6	-20.4	23.1	-17.9	
	116.0	11.8	21.4	-81.3	13.0	-10.2	
	138.2	9.2	15.1	-64.0	10.2	-10.9	

[a]Slenderness ratios and areas are based on full section properties.

[b]Negative sign indicates predicted value above test value and therefore unconservative.

Table 6.8

COMPARISON OF TEST ULTIMATE STRESSES AND EFFECTIVE WIDTH APPROACH ULTIMATE STRESSES FOR STIFFENED SECTIONS

Specimen	$\frac{L}{r}$[a]	Test[a] σ_{Avg} (ksi)	Based on k = 4.00 and I_{eff}		Based on k = 6.97 and I_{eff}	
			σ_{Avg}[a] (ksi)	% Discrepancy from Test	σ_{Avg}[a] (ksi)	% Discrepancy from Test
S-1	8.5	40.5	36.5	9.9	39.5	2.5
	39.0	37.4	35.0	6.4	38.0	-1.6[b]
	69.1	34.6	34.4	0.6	37.4	-8.1
	114.1	20.9	20.5	1.9	22.3	-6.7
S-2	11.7	33.9	30.9	8.9	34.0	-0.3
	66.0	27.2	29.7	-9.2[b]	32.6	-19.8
	102.0	20.8	20.3	2.4	23.2	-11.5
	123.5	17.2	15.1	12.2	17.1	0.6
S-3	13.6	29.3	25.6	12.6	28.4	3.1
	29.0	27.8	25.1	9.7	27.9	-0.4
	109.8	15.5	14.4	7.1	17.0	-9.7
	109.8	15.1	14.4	4.6	17.0	-12.6
	109.8	14.4	14.4	0.0	17.0	-18.0
S-4	13.8	24.6	21.8	11.4	24.3	1.2
	42.6	22.6	21.1	6.6	23.6	-4.4
	65.5	19.6	21.0	-8.2	23.3	-18.9
	116.0	11.8	11.1	5.9	13.2	-11.9
	138.2	9.2	8.6	6.5	10.3	-12.0

[a]Slenderness ratios and areas are based on full section properties.

[b]Negative sign indicates predicted value above test value and therefore unconservative.

Table 6.9

EFFECTIVE WIDTH APPROACH BASED ON EFFECTIVE MOMENT OF INERTIA

AS SHOWN IN FIG. 6.2(b) FOR SECTION U-1

Strain	k = 0.425			k = 0.50			k = 1.277		
	$\frac{L}{r}$[a]	σ_{Avg}[a] (ksi)	b from Eq. 6-7 (in)	$\frac{L}{r}$[a]	σ_{Avg}[a] (ksi)	b from Eq. 6-7 (in)	$\frac{L}{r}$[a]	σ_{Avg}[a] (ksi)	b from Eq. 6-7 (in)
0.0001	314.2	2.95	0.94[b]	314.2	2.95	0.94[b]	314.2	2.95	0.94[b]
0.0002	222.1	5.90	0.94	222.1	5.90	0.94	222.1	5.90	0.94
0.0003	181.4	8.85	0.94	181.4	8.85	0.94	181.4	8.85	0.94
0.0004	157.1	11.80	0.94	157.1	11.80	0.94	157.1	11.80	0.94
0.0005	140.5	14.75	0.94	140.5	14.75	0.94	140.5	14.75	0.94
0.0006	128.3	17.70	0.94	128.3	17.70	0.94	128.3	17.70	0.94
0.0007	117.9	20.56	0.93	118.8	20.65	0.94	118.8	20.65	0.94
0.0008	107.9	23.17	0.90	110.6	23.53	0.93	111.1	23.60	0.94
0.0009	99.5	25.73	0.86	102.3	26.15	0.90	104.7	26.55	0.94
0.0010	92.4	28.25	0.84	95.2	28.13	0.88	99.4	29.50	0.94
0.0011	86.3	30.73	0.81	89.1	31.27	0.85	94.7	32.45	0.94
0.0012	81.0	33.18	0.79	83.8	33.77	0.83	90.7	35.40	0.94
0.0013	74.7	35.59	0.77	77.5	36.23	0.81	85.3	38.33	0.94
0.0014	43.6	37.21	0.75	45.3	37.88	0.79	50.4	40.31	0.94
0.0015	27.4	37.74	0.75	28.5	38.42	0.79	31.8	40.96	0.94

[a]Slenderness ratio and average stress are based on full section properties.

[b]Element width w is 0.94 in.

Table 6.10

EFFECTIVE WIDTH APPROACH BASED ON EFFECTIVE MOMENT OF INERTIA

AS SHOWN IN FIG. 6.2(b) FOR SECTION U-2

Strain	k = 0.425			k = 0.64			k = 1.277		
	$\frac{L}{r}$[a]	σ_{Avg}[a] (ksi)	b from Eq. 6-7 (in)	$\frac{L}{r}$[a]	σ_{Avg}[a] (ksi)	b from Eq. 6-7 (in)	$\frac{L}{r}$[a]	σ_{Avg}[a] (ksi)	b from Eq. 6-7 (in)
0.0001	314.2	2.95	1.19[b]	314.2	2.95	1.19[b]	314.2	2.95	1.19[b]
0.0002	222.1	5.90	1.19	222.1	5.90	1.19	222.1	5.90	1.19
0.0003	181.4	8.85	1.19	181.4	8.85	1.19	181.4	8.85	1.19
0.0004	157.1	11.80	1.19	157.1	11.80	1.19	157.1	11.80	1.19
0.0005	136.4	14.42	1.13	140.5	14.75	1.19	140.5	14.75	1.19
0.0006	120.4	16.90	1.07	128.3	17.70	1.19	128.3	17.70	1.19
0.0007	108.0	19.31	1.02	116.9	20.40	1.16	118.8	20.65	1.19
0.0008	98.0	21.68	1.96	107.0	22.94	1.11	111.1	23.60	1.19
0.0009	89.7	23.99	1.93	98.7	25.41	1.08	104.7	26.55	1.19
0.0010	82.7	26.27	1.90	91.7	27.85	1.04	99.4	29.50	1.19
0.0011	76.7	28.53	1.87	85.6	30.24	1.01	94.7	32.45	1.19
0.0012	71.5	30.75	1.84	80.4	32.60	0.98	90.7	35.40	1.19
0.0013	65.5	32.93	1.81	74.2	34.91	0.95	84.7	38.13	1.18
0.0014	38.1	34.39	1.80	43.3	36.47	0.93	49.7	39.86	1.15
0.0015	23.9	34.87	1.79	27.2	36.97	0.93	31.3	40.42	1.14

[a]Slenderness ratio and average stress are based on full section properties.

[b]Element width w is 1.19 in.

Table 6.11

EFFECTIVE WIDTH APPROACH BASED ON EFFECTIVE MOMENT OF INERTIA

AS SHOWN IN FIG. 6.2(b) FOR SECTION U-3

Strain	k = 0.425			k = 0.82			k = 1.277		
	$\frac{L}{r}$[a]	σ_{Avg}[a] (ksi)	b from Eq. 6-7 (in)	$\frac{L}{r}$[a]	σ_{Avg}[a] (ksi)	b from Eq. 6-7 (in)	$\frac{L}{r}$[a]	σ_{Avg}[a] (ksi)	b from Eq. 6-7 (in)
0.0001	314.2	2.95	1.44[b]	314.2	2.95	1.44[b]	314.2	2.95	1.44[b]
0.0002	222.1	5.90	1.44	222.1	5.90	1.44	222.2	5.90	1.44
0.0003	179.8	8.78	1.42	181.4	8.85	1.44	181.4	8.85	1.44
0.0004	148.6	11.25	1.30	157.1	11.80	1.44	157.1	11.80	1.44
0.0005	127.1	13.60	1.21	140.5	14.75	1.44	140.5	14.75	1.44
0.0006	111.3	15.87	1.14	126.5	17.48	1.40	128.3	17.70	1.44
0.0007	99.0	18.08	1.08	114.3	19.96	1.34	118.8	20.65	1.44
0.0008	89.1	20.24	1.02	104.4	22.38	1.29	111.1	23.60	1.44
0.0009	81.0	22.36	0.98	96.2	24.74	1.24	103.9	26.35	1.42
0.0010	74.1	24.45	0.94	89.2	27.06	1.20	97.0	28.87	1.38
0.0011	68.2	26.51	0.90	83.2	29.33	1.16	91.0	31.33	1.34
0.0012	63.1	28.54	0.87	78.0	31.57	1.12	85.8	33.76	1.30
0.0013	57.3	30.53	0.84	71.9	33.77	1.09	79.5	36.13	1.27
0.0014	33.1	31.88	0.83	41.9	35.24	1.07	46.5	37.71	1.25
0.0015	20.8	32.31	0.82	26.3	35.72	1.06	29.3	38.23	1.24

[a]Slenderness ratio and average stress are based on full section properties.

[b]Element width w is 1.44 in.

Table 6.12

EFFECTIVE WIDTH APPROACH BASED ON EFFECTIVE MOMENT OF INERTIA

AS SHOWN IN FIG. 6.2(b) FOR SECTION U-4

Strain	k = 0.425			k = 0.85			k = 1.277		
	$\frac{L}{r}$[a]	σ_{Avg}[a] (ksi)	b from Eq. 6-7 (in)	$\frac{L}{r}$[a]	σ_{Avg}[a] (ksi)	b from Eq. 6-7 (in)	$\frac{L}{r}$[a]	σ_{Avg}[a] (ksi)	b from Eq. 6-7 (in)
0.0001	314.2	2.95	1.69[b]	314.2	2.95	1.69[b]	314.2	2.95	1.69[b]
0.0002	222.1	5.90	1.69	222.1	5.90	1.69	222.1	5.90	1.69
0.0003	171.0	8.36	1.51	181.4	8.85	1.69	181.4	8.85	1.69
0.0004	139.8	10.64	1.38	157.1	11.80	1.69	157.1	11.80	1.69
0.0005	118.5	12.80	1.27	136.6	14.33	1.60	140.5	14.75	1.69
0.0006	102.8	14.90	1.19	120.9	16.72	1.51	128.3	17.70	1.69
0.0007	90.7	16.93	1.12	108.7	19.03	1.44	116.7	20.30	1.63
0.0008	80.9	18.92	1.06	98.9	21.27	1.38	106.9	22.72	1.61
0.0009	72.8	20.88	1.01	90.7	23.46	1.32	98.8	25.09	1.52
0.0010	66.0	22.80	0.97	83.8	25.61	1.27	91.9	27.41	1.46
0.0011	60.1	24.69	0.93	77.9	27.72	1.23	85.9	29.68	1.42
0.0012	55.0	26.57	0.90	72.7	29.79	1.19	80.7	31.92	1.38
0.0013	49.5	28.40	0.87	66.7	31.83	1.15	74.6	34.10	1.34
0.0014	28.3	29.64	0.85	38.8	33.19	1.13	43.6	35.56	1.32
0.0015	17.7	30.04	0.84	24.4	33.63	1.12	27.4	36.04	1.31

[a] Slenderness ratio and average stress are based on full section properties.

[b] Element width w is 1.69 in.

Table 6.13

COMPARISON OF TEST ULTIMATE STRESSES AND EFFECTIVE WIDTH

APPROACH ULTIMATE STRESSES FOR UNSTIFFENED SECTIONS

Specimen	$\frac{L}{r}$[a]	Test σ_{Avg}[a] (ksi)	Based on I_{full}		Based on I_{eff}, Fig. 6.2(a)		Based on I_{eff}, Fig. 6.2(b)		k
			σ_{Avg}[a] (ksi)	% Discrepancy from Test	σ_{Avg}[a] (ksi)	% Discrepancy from Test	σ_{Avg}[a] (ksi)	% Discrepancy from Test	
U-1	12.9	43.8	39.3	10.3	39.1	10.7	39.2	10.5	0.50
	55.7	37.9	37.6	0.8	37.4	1.3	37.3	1.6	
	89.1	36.2	35.8	1.1	29.4	18.8	31.3	13.5	
	116.6	21.6	21.4	0.9	21.4	0.9	21.4	0.9	
U-2	12.0	42.0	37.9	9.8	37.6	10.5	37.7	10.2	0.64
	12.0	40.8	37.9	7.1	37.6	7.9	37.7	7.6	
	53.0	38.6	36.5	5.4	35.5	8.0	36.0	6.7	
	85.6	32.8	35.8	-9.2[b]	27.5	16.2	30.2	7.9	
	108.0	24.1	25.0	-3.7	21.8	9.5	22.5	6.6	
U-3	9.5	39.6	36.8	7.1	36.5	7.8	36.6	7.6	0.82
	42.2	34.6	35.4	-2.3	35.0	-1.2[b]	35.2	-1.7[b]	
	77.9	33.4	35.2	-5.4	27.7	17.1	31.6	5.4	
	95.5	26.4	31.7	-20.1	22.8	13.6	24.8	6.1	
U-4	7.9	37.2	34.7	6.7	34.3	7.8	34.5	7.3	0.85
	44.1	31.7	33.4	-5.4	32.8	-3.5	33.0	-4.1	
	92.4	27.2	32.1	-18.0	20.3	25.4	23.2	14.7	

[a]Slenderness ratios and areas are based on full section properties.

[b]Negative sign indicates predicted value above test value and therefore unconservative.

Table 6.14

COMPARISON OF TEST ULTIMATE STRESSES AND EFFECTIVE WIDTH APPROACH ULTIMATE STRESSES FOR UNSTIFFENED SECTIONS

Specimen	$\frac{L}{r}$[a]	Test[a] σ_{Avg} (ksi)	Based on k = 0.425 and I_{eff}, Fig. 6.2(b)		Based on k = 1.277 and I_{eff}, Fig. 6.2(b)	
			σ_{Avg}[a] (ksi)	% Discrepancy from Test	σ_{Avg}[a] (ksi)	% Discrepancy from Test
U-1	12.9	43.8	38.5	12.1	41.1	6.2
	55.7	37.9	37.0	2.4	40.1	-5.8[b]
	89.1	36.2	29.4	18.8	36.5	-0.8
	116.6	21.6	21.0	2.8	21.4	0.9
U-2	12.0	42.0	35.5	15.5	41.4	1.4
	12.0	40.8	35.5	13.0	41.4	-1.5
	53.0	38.6	34.0	11.9	39.7	-2.9
	85.6	32.8	25.3	22.9	37.7	-14.9
	108.0	24.1	19.3	19.9	24.7	-2.5
U-3	9.5	39.6	32.9	16.9	39.3	0.8
	42.2	34.6	31.6	8.7	38.0	-9.8
	77.9	33.4	23.0	31.1	36.7	-9.9
	95.5	26.4	18.6	29.5	29.8	-12.9
U-4	7.9	37.2	30.7	17.5	37.1	0.3
	44.1	31.7	29.0	8.5	35.6	-12.3
	92.4	27.2	16.5	39.3	27.2	0.0

[a]Slenderness ratios and areas are based on full section properties.

[b]Negative sign indicates predicted value above test value and therefore unconservative.

Table 6.15

PROPERTIES FOR EXPERIMENTAL COLUMNS OF SKALOUD AND ZORNEROVA

Series[a]	T (in)	B (in)	D (in)	Maximum Width/Thickness[b]	Tensile Yield Str. (ksi)
A	.0788	1.97	3.94	48.0	35.8
B	.0788	3.15	3.94	48.0	35.8
C	.1182	1.97	3.94	31.4	35.8

[a]Redesignated for this report.

[b]Based on assuming width is clear distance between adjoining elements, i.e., the inside radius of the corners is 0.0.

Table 6.16

COMPARISON OF TEST ULTIMATE STRESSES AND EFFECTIVE WIDTH APPROACH

ULTIMATE STRESSES FOR COLUMNS OF SKALOUD AND ZORNEROVA

Specimen	$\frac{L}{r}$[a]	Test σ_{Avg}[a] (ksi)	Effective Width[a] σ_{Avg} with k = 4.00 and I_{eff} (ksi)	% Discrepancy from Test
A	9.7	30.8	32.5	-5.5[b]
	9.7	36.4	32.5	10.7
	72.8	32.9	29.4	10.6
	72.8	28.2	29.4	-4.3
	115.0	17.1	22.0	-28.6
	127.0	14.6	18.0	-23.3
B	6.3	42.1	33.0	21.6
	6.3	40.8	33.0	19.1
	51.0	32.2	31.4	2.5
	51.0	31.6	31.4	0.6
	102.0	23.5	25.9	-10.2
C	10.0	44.6	35.7	19.9
	10.0	45.0	35.7	20.6
	56.3	31.6	33.3	-5.4
	74.3	30.2	31.8	-5.3
	104.5	15.4	26.2	-70.0
	108.5	16.8	24.7	-47.0

[a]Slenderness ratios and areas are based on full section properties.

[b]Negative sign indicates predicted value above test value and therefore unconservative.

Table 6.17

PROPERTIES FOR EXPERIMENTAL COLUMNS OF DELIEGE, BAAR, AND HICK

Series[a]	Galvanized	Thickness[b] (in)	Maximum Width/Thickness[c]	Tensile Yield Stress (ksi)
A	Yes	0.0276	125.7	42.9
B	Yes	0.0394	88.0	48.9
C	Yes	0.0591	58.6	50.0
D	No	0.0591	58.6	35.8

[a]Redesignated for this report.

[b]All other dimensions are as shown in Fig. 6.32.

[c]Based on assuming width is clear distance between adjoining elements, i.e., the inside radius of the corners is 0.0.

Table 6.18

COMPARISON OF TEST ULTIMATE STRESSES AND EFFECTIVE WIDTH APPROACH ULTIMATE STRESSES FOR COLUMNS OF DELIEGE, BAAR, AND HICK

Specimen	$\frac{L}{r}$[a]	Mean[a] Test σ_{Avg} (ksi)	Without Section 2.3.1.2, AISI Spec.		With Section 2.3.1.2, AISI Spec.	
			Effective Width[a] σ_{Avg} with k = 4.00 and I_{eff} (ksi)	% Discrepancy from Test	Effective Width[a] σ_{Avg} with k = 4.00 and I_{eff} (ksi)	% Discrepancy from Test
A	22.2	17.2	22.5	-30.8[b]	16.9	1.7
	50.0	18.3	21.2	-15.8	16.1	12.0
	74.2	17.3	20.3	-17.3	15.7	9.2
	93.3	16.2	19.3	-19.1	15.2	6.2
	112.5	14.4	15.4	-6.9	14.0	2.8
B	22.2	24.5	30.4	-24.1	26.4	-7.8[b]
	50.0	24.8	28.6	-15.3	25.0	-0.8
	74.0	24.0	27.5	-14.6	24.0	0.0
	93.3	20.4	24.0	-17.6	22.3	-9.3
	112.5	17.4	18.1	-4.0	17.4	0.0
C	22.2	36.4	38.2	-4.9	(not applicable)	
	50.0	34.7	35.9	-3.5		
	74.3	32.4	33.9	-4.6		
	93.3	28.2	28.8	-2.1		
	113.0	25.2	21.4	15.1		
D	22.2	29.4	30.0	-2.0	(not applicable)	
	74.2	27.7	27.1	2.2		
	112.5	19.2	21.0	-9.4		

[a]Slenderness ratios and areas are based on full section properties.

[b]Negative sign indicates predicted value above test value and therefore unconservative.

Table 6.19

PROPERTIES FOR EXPERIMENTAL COLUMNS OF URIBE

Series	Maximum Width-Thickness	Tensile Yield Stress (ksi)	
		Corners	Flats-Average
UC-1	15.9	59.5	41.5
UC-2	16.2	59.5	41.5
SC-1	60.8	57.3	39.1
SC-2	56.8	60.9	39.6

Table 6.20

COMPARISON OF TEST ULTIMATE STRESSES AND EFFECTIVE WIDTH APPROACH ULTIMATE STRESSES FOR COLUMNS OF URIBE

(a) Columns containing unstiffened elements

Specimen	$\frac{L}{r}$[a]	Test σ_{Avg}[a] (ksi)	Effective width σ_{Avg}[a] with k = 0.5 and I_{eff} (ksi)	% Discrepancy from Test
UC-1	7.1	41.0	40.5	1.2
	40.3	36.5	36.6	-0.3[b]
	61.2	30.7	35.7	-16.3
	82.4	28.8	33.7	-17.0
UC-2	7.1	41.0	40.5	1.2
	39.2	37.3	37.0	0.8
	60.5	30.9	35.9	-16.2
	81.4	29.4	34.1	-16.0

(b) Columns containing stiffened elements

Specimen	$\frac{L}{r}$[a]	Test σ_{Avg}[a] (ksi)	Effective width σ_{Avg}[a] with k = 4.00 and I_{eff} (ksi)	% Discrepancy from Test
SC-1	5.7	36.0	36.0	0.0
	31.2	36.9	32.4	12.2
	59.8	35.0	31.4	10.3
	82.2	32.5	30.1	7.4
SC-2	5.9	37.4	37.3	0.3
	38.2	36.8	33.9	7.9
	59.6	37.2	33.0	11.3
	82.9	35.1	31.4	10.5

[a]Slenderness ratios and areas are based on full section properties.

[b]Negative sign indicates predicted value above test value and therefore unconservative.

Table 6.21

EXPERIMENTAL STUB COLUMNS OF DHALLA

(a) Cross-Section Dimensions[a]

Column	D (in)	W (in)	T (in)	Width-Thickness Ratio
UFC-1	1.497	0.596	0.061	7.76
UFC-2	1.523	0.820	0.061	11.40
UFC-3	1.539	1.046	0.060	15.40
UFC-4	1.540	1.365	0.060	20.75

(b) Results for Comparison of Tests with Effective Width Approach

Column	Test	Average Ultimate Stress (ksi)			
		Effective Width & Tensile Yield	% Discrepancy from Test	Effective Width & Compressive Yield	% Discrepancy from Test
UFC-1	82.36	88.2[b]	-7.1[c]	78.6[b]	4.6
UFC-2	75.96	80.4	-5.8	75.5	0.6
UFC-3	68.88	72.6	-5.4	65.5	4.9
UFC-4	62.98	62.5	0.8	56.9	9.7

[a]Inside radius of corners equals 0.12 in for all columns.

[b]Fully effective.

[c]Negative sign indicates predicted value above test value and therefore unconservative.

Table 7.1

COMPARISON OF TEST ULTIMATE STRESSES AND DESIGN APPROACH ULTIMATE STRESSES FOR STIFFENED SECTIONS

Specimen	$\frac{L}{r}$[a]	Test[a] σ_{Avg} (ksi)	Design Approach, k = 4.00		Design Approach, k from Table 6.1		
			σ_{Avg} (ksi)	% Discrepancy from Test	σ_{Avg} (ksi)	% Discrepancy from Test	k
S-1	8.5	40.5	36.0	11.1	37.1	8.4	4.85
	39.0	37.4	34.3	8.3	35.2	5.9	
	69.1	34.6	30.4	12.1	31.3	9.5	
	114.1	20.9	20.4	2.4	21.3	-1.9[b]	
S-2	11.7	33.9	30.7	9.4	32.2	5.0	5.37
	66.0	27.2	26.0	4.4	27.6	-1.5	
	102.0	20.8	19.6	5.8	21.2	-1.9	
	123.5	17.2	15.1	12.2	16.2	5.8	
S-3	13.6	29.3	25.4	13.3	27.5	6.1	6.11
	29.0	27.8	24.8	10.8	26.5	4.7	
	109.8	15.5	14.5	6.5	16.2	-4.5	
	109.8	15.1	14.5	4.0	16.2	-7.1	
	109.8	14.4	14.5	-0.7[b]	16.2	-12.5	
S-4	13.8	24.6	21.6	12.2	24.1	2.0	6.90
	42.6	22.6	20.3	10.2	22.7	-0.4	
	65.5	19.6	18.2	7.1	20.5	-4.6	
	116.0	11.8	11.1	5.9	13.1	-11.0	
	138.2	9.2	8.8	4.4	10.2	-10.9	

[a] Slenderness ratios and areas are based on full section properties.

[b] Negative sign indicates predicted value above test value and therefore unconservative.

Table 7.2

COMPARISON OF TEST ULTIMATE STRESSES AND DESIGN APPROACH ULTIMATE STRESSES FOR UNSTIFFENED SECTIONS

Specimen	$\frac{L}{r}$[a]	Test[a] σ_{Avg} (ksi)	Design Approach, k = 0.50		Design Approach, k from Table 6.1		
			σ_{Avg} (ksi)	% Discrepancy from Test	σ_{Avg} (ksi)	% Discrepancy from Test	k
U-1	12.9	43.8	38.9	11.2	38.2	12.8	0.43
	55.7	37.9	34.5	9.0	33.7	11.1	
	89.1	36.2	28.4	21.6	27.1	25.1	
	116.6	21.6	21.3	1.4	20.9	3.2	
U-2	12.0	42.0	36.1	14.0	37.4	11.0	0.64
	12.0	40.8	36.1	11.5	37.4	8.3	
	53.0	38.6	31.6	18.1	33.5	13.2	
	85.6	32.8	25.4	22.6	27.4	16.5	
	108.0	24.1	20.5	14.9	22.4	7.1	
U-3	9.5	39.6	33.5	15.4	36.3	8.3	0.82
	42.2	34.6	30.3	12.4	33.5	3.2	
	77.9	33.4	23.7	29.0	27.6	17.4	
	95.5	26.4	19.6	25.8	24.1	8.7	
U-4	7.9	37.2	31.3	15.9	34.2	8.1	0.85
	44.1	31.7	27.0	14.8	31.0	2.2	
	92.4	27.2	18.0	33.8	22.4	17.7	

[a] Slenderness ratios and areas are based on full section properties.

[b] Use 0.43 instead of 0.50 in Table 6.1 since 0.50 used in first column; in this way an indication of the possible ultimate load variation due to varying k values is obtained.